BULLETIN OF RUSSIAN STATE MEDICAL UNIVERSITY

BIOMEDICAL JOURNAL OF PIROGOV RUSSIAN NATIONAL RESEARCH MEDICAL UNIVERSITY

SUBMISSION http://vestnikrgmu.ru/login?lang=en
CORRESPONDENCE editor@vestnikrgmu.ru
COLLABORATION manager@vestnikrgmu.ru
ADDRESS ul. Ostrovityanova, d. 1, Moscow, Russia, 117997

Indexed in Scopus since 2017 — Scopus®
Indexed in WoS since 2018 — WEB OF SCIENCE™
Five-year h-index is 3 — Google scholar
Indexed in RSCI. IF 2017: 0,304 — НАУЧНАЯ ЭЛЕКТРОННАЯ БИБЛИОТЕКА eLIBRARY.RU
Listed in HAC 27.01.2016 (no. 1760) — ВЫСШАЯ АТТЕСТАЦИОННАЯ КОМИССИЯ (ВАК)
Open access to archive — CYBERLENINKA

Issue DOI: 10.24075/brsmu.2018–04
The mass media registration certificate no. 012769 issued on July 29, 1994
Founder and publisher is Pirogov Russian National Research Medical University (Moscow, Russia)

Approved for print 20.10.2018
Circulation: 100 copies. Printed by Print.Formula
www.print-formula.ru

ВЕСТНИК РОССИЙСКОГО ГОСУДАРСТВЕННОГО МЕДИЦИНСКОГО УНИВЕРСИТЕТА

НАУЧНЫЙ МЕДИЦИНСКИЙ ЖУРНАЛ РНИМУ ИМ. Н. И. ПИРОГОВА

ПОДАЧА РУКОПИСЕЙ http://vestnikrgmu.ru/login
ПЕРЕПИСКА С РЕДАКЦИЕЙ editor@vestnikrgmu.ru
СОТРУДНИЧЕСТВО manager@vestnikrgmu.ru
АДРЕС РЕДАКЦИИ ул. Островитянова, д. 1, г. Москва, 117997

Журнал включён в Scopus с 2017 года

Журнал включён в WoS с 2018 года

Индекс Хирша (h^5) журнала по оценке Google Scholar: 3

Журнал включён в РИНЦ. IF 2017: 0,304

Журнал включён в Перечень 27.01.2016 (№ 1760)

Здесь находится открытый архив журнала

DOI выпуска: 10.24075/vrgmu.2018–04

Свидетельство о регистрации средства массовой информации № 012769 от 29 июля 1994 г.

Учредитель и издатель — Российский национальный исследовательский медицинский университет имени Н. И. Пирогова (Москва, Россия)

Подписано в печать 20.10.2018
Тираж 100 экз. Отпечатано в типографии Print.Formula
www.print-formula.ru

BULLETIN OF RSMU 4, 2018
ВЕСТНИК РГМУ

Contents
Содержание

THE PROPER STRUCTURE OF A BIOSAFETY SYSTEM AS A WAY OF REDUCING THE VULNERABILITY OF A SOCIETY, ECONOMY OR STATE IN THE FACE OF A BIOGENIC THREAT

Gushchin VA[1,2] ✉, Manuilov VA[3], Makarov VV[4], Tkachuk AP[3]

[1] Laboratory of Population Variability Mechanisms in Pathogenic Microorganisms, Gamaleya Research Institute of Epidemiology and Microbiology, Moscow

[2] Department of Virology, Faculty of Biology, Lomonosov Moscow State University, Moscow

[3] Laboratory of Translational Medicine, Gamaleya Research Institute of Epidemiology and Microbiology, Moscow

[4] Center for Strategic Planning of the Ministry of Health of the Russian Federation, Moscow

To understand how vulnerable are a society, an economy and a state in the face of a biohazard, one should attempt to identify any potential holes in the national biosafety system, such as the lack of important components or technologies for biological monitoring and the inadequacy of existing analytical methods used to prevent or counteract biogenic threats. In Russia, biological monitoring is quite advanced. However, the agencies that ensure proper functioning of its components lack collaboration and do not form a well-coordinated network. Each of such agencies alone cannot provide comprehensive information on the subject. In the Russian Federation, there are at least 4 state-funded programs that collect epidemiological data and are quite efficient in performing the narrow task of monitoring infections. But because there is no central database where epidemiological data can be channeled and subsequently shared, these agencies do not complete each other. This leaves the Russian society, economy and state vulnerable to biogenic threats. We need an adequately organized, modern, fully functional and effective system for monitoring biohazards that will serve as a basis for the national biosafety system and also a tool for the identification and elimination of its weaknesses.

Keywords: biological safety, biological monitoring, pathogens

Funding: this work was supported by the Ministry of Health of the Russian Federation as part of the project *The National System for Chemical and Biological Security of the Russian Federation (2015-2020)* and by the Ministry of Education and Science as part of the project RFMEFI60117X0018.

✉ **Correspondence should be addressed:** Vladimir A. Gushchin
Gamalei 18, Moscow, 123098; wowaniada@gmail.com

Received: 30.09.2018 **Accepted:** 14.10.2018

DOI: 10.24075/brsmu.2018.054

НАДЛЕЖАЩАЯ ОРГАНИЗАЦИЯ СИСТЕМЫ БИОБЕЗОПАСНОСТИ КАК СРЕДСТВО СНИЖЕНИЯ УЯЗВИМОСТИ ОБЩЕСТВА, ЭКОНОМИКИ И ГОСУДАРСТВА ПЕРЕД БИОГЕННЫМИ УГРОЗАМИ

В. А. Гущин[1,2] ✉, В. А. Мануйлов[3], В. В. Макаров[4], А. П. Ткачук[3]

[1] Лаборатория механизмов популяционной изменчивости патогенных микроорганизмов, Национальный исследовательский центр эпидемиологии и микробиологии имени Н. Ф. Гамалеи, Москва

[2] Кафедра вирусологии, биологический факультет, Московский государственный университет имени М. В. Ломоносова, Москва

[3] Лаборатория трансляционной биомедицины, Национальный исследовательский центр эпидемиологии и микробиологии имени Н. Ф. Гамалеи, Москва

[4] ФГБУ Центр стратегического планирования Министерства здравоохранения России, Москва

Оценка потенциальной уязвимости общества, экономики и государства перед биогенными угрозами сводится прежде всего к поиску слабых звеньев существующей системы обеспечения биологической безопасности государства. К ним можно отнести как отсутствие отдельных элементов и технических средств мониторинга биологических рисков, так и недостаточность имеющихся аналитических средств для принятия своевременных мер по предупреждению биологических угроз или устранению их последствий. В целом действующие на сегодняшний день в России системы мониторинга биологических угроз достаточно хорошо развиты. Однако их отдельные элементы, во-первых, ведомственно разобщены, что не позволяет создать единую систему с общей координацией, а во-вторых, ни один из них по отдельности не дает результатов, соответствующих всем требованиям, предъявляемым к такой информации. Так, в России действуют, как минимум, четыре отдельные государственные системы сбора информации по эпидемической и эпидемиологической ситуации, которые с должной эффективностью решают узкие задачи по инфекционному мониторингу, но, к сожалению, не способны дополнять друг друга из-за отсутствия единого аналитического центра с доступом ко всем данным. На сегодняшний день отсутствие единого мониторингового центра в области биологической безопасности является фактором потенциально высокой уязвимости общества, экономики и государства перед лицом биогенных угроз. Необходима надлежащая организация современной полнофункциональной и эффективной национальной системы мониторинга биологических угроз как основа для функционирования общенациональной службы обеспечения биологической безопасности и одновременно как средство для идентификации и устранения собственных уязвимых элементов такой государственной структуры.

Ключевые слова: биологическая безопасность, мониторинг биологических угроз, патогенные микроорганизмы

Финансирование: статья подготовлена при поддержке Министерства здравоохранения Российской Федерации в рамках программы «Национальная система химической и биологической безопасности 2015–2020» и Министерства образования и науки РФ в рамках проекта RFMEFI60117X0018.

✉ **Для корреспонденции:** Владимир Алексеевич Гущин
ул. Гамалеи, д. 18, г. Москва, 123098; wowaniada@gmail.com

Статья получена: 30.09.2018 **Статья принята к печати:** 14.10.2018

DOI: 10.24075/vrgmu.2018.054

Importance of biological surveillance

The terms «biological security» and «biological safety» encompass the entire field of human epidemiological surveillance, animal, plant and environmental health control, and countermeasures to prevent and respond to biological emergencies. A situation is classified as an emergency when it has such a strong negative impact on the normal activities of the population that it can be likened to a national or international security threat [1, 2]. Another two important concepts used in this review are a biological (biogenic) risk, which is a probability of damage (of different severity or scope) to human health and/or the environment caused by a biohazard, and a biological threat defined as an unacceptable biological risk [1]. Therefore, a biological threat is an emergency.

Biohazards that pose a threat to national or international security are very diverse. Biological risks originate from an intrinsic ability of all biopathogens (BPs), i.e. bacteria, viruses, toxins, prions, and protozoa, to be virulent to humans, agricultural animals and plants. In spite of the advances in healthcare both in Russia and abroad, infectious diseases still remain the primary cause of disabilities and mortality. According to expert estimates, in 2017 the Russian economy suffered a loss of over 627 billion rubles caused by only 32 most common infections [3]. Importantly, it is not the extraordinary outbreaks of emerging or imported infections that contribute the most to morbidity and economic damage but traditional seasonal endemic diseases, including ARI, flu, acute intestinal infections, chickenpox, HIV, and viral hepatitis [3].

Infection control includes such well-known and actively exploited countermeasures as vaccination, timely diagnosis, antiviral and antibacterial therapies, wide promotion of hygiene awareness, update of antiseptic techniques, countering of epidemiological risk factors, and eventually improvement of the economic and social well-being of the population [4]. However, due to the biological nature of infections, the positive effect of such countermeasures rapidly declines as pathogens evolve and evade these new traps of natural selection [5]. This process has a few important consequences. Pathogenic strains responsible for seasonal and/or epidemic respiratory and alimentary infections regularly «update» their genotypes and serotypes; infections start to manifest through similar symptoms and epidemics unfold in similar patterns even if caused by the representatives of different taxa with different resistance to treatment and prophylaxis; pathogens acquire drug-resistance and spread undeterred by immunization and undetected by standard diagnostic techniques; new mutant strains that have never circulated in the human population before arrive from their natural reservoirs. In the backdrop of the varying efficacy and availability of vaccines depending on the area of residence, age or social status of the population, the evolution of pathogens can complicate the epidemiological situation. All factors of epidemiological risk need to be thoroughly studied and timely monitored to prevent epidemics, i.e. transformation of a biological risk into a real threat [6]. State-funded agencies that provide and oversee healthcare services must have an effective tool at their disposal to coordinate epidemiological surveillance and predict epidemiological trends.

The need for an integrated national center for biological surveillance aimed at preventing biological threats is articulated in the strategy documents of the Russian Government and current federal laws and regulations [1, 7–9]. Specifically, *the Basic Principles of the State Policy Ensuring Chemical and Biological Safety and Security in the Russian Federation until 2025 and beyond* [8] define biological surveillance and resource provision for its implementation as top-priority tasks faced by the national system of biosafety and biosecurity. The *National Security Strategy of the Russian Federation* published in 2015 [9] instructs state agencies and local authorities to cooperate with civil society organizations in order to promote and enhance biological surveillance in the Russian Federation.

The authors of this article consider it necessary to give recommendations regarding the organization of a joined coordinating center [10] for inter-agency cooperation in order to prevent duplication of the existing systems of national epidemiological surveillance today, since, as noted above, vulnerabilities in the biological security system can be directly equated to the vulnerabilities of the entire state and society.

Russia needs an integrated national system for biological surveillance

In Russia, federal agencies normally employ 4 major methods for collecting epidemiological and epidemic data. Each of them is used to solve a narrow range of tasks pertaining to biosurveillance, including:

– analysis of incidence of the most prevalent infections;

– investigation of disease outbreaks;

– control of infectious hazards posed by the environment and consumer goods;

– study of the local incidence of major diseases that have a significant impact on the society and the effects of epidemiological factors on the subpopulations at risk;

– study and prediction of seasonal and periodic strains of some epidemic infections.

Let us take a closer look at these methods.

1. *The incidence of the most common infections* is analyzed by Rospotrebnadzor (the Russian Federal Service for Surveillance of Consumer Rights Protection and Human Well-being) [11]. Information is collected by regional and municipal healthcare facilities (HCF). Once a patient has been diagnosed with an infection, the doctor fills out a report form and forwards it to a regional office of Rospotrebnadzor [12]. Rospotrebnadzor collects and processes the received data and then publishes an annual report. An undisputable advantage of this method of data collection is wide population coverage in all Russian regions: it keeps account of all infected patients who present to hospital. It also involves quite a few HCFs creating a stable network that continuously supplies new data to the head agency. The homogeneity of the collected data is ensured by the uniformity of reporting.

Considering the definition of incidence, which is a ratio of new cases of the disease to the annual average population size [13], this method of data collection accounts for only officially diagnosed cases of infection among self-referred patients. Individuals with asymptomatic chronic infections who choose not to consult a doctor or those misdiagnosed and therefore contagious are not reported. This renders the collected information somewhat irrelevant since it cannot be used to reliably estimate the prevalence of infection in the general population. In most cases, HCFs do not have the necessary equipment to identify a pathogen down to the strain level, especially when it comes to respiratory and acute intestinal infections. Therefore, etiologically, epidemiologically and biologically different infections that demand different prevention measures and different treatment regimens are reported as if they were the same, i.e. their incidence is estimated unreliably.

In this regard, the creation of a joined monitoring center will help overcome above mentioned shortcomings while observing the necessary principles for monitoring. At the same time,

such a center should not duplicate the functions of the listed agencies (such as morbidity analysis, outbreak investigation and product safety analysis, scientific epidemiological studies in risk groups) [6].

2. *At the state level, epidemiological surveillance and sanitary control* [14] are performed by the regional and federal centers for hygiene and epidemiology (CHE) of Rospotrebnadzor [11, 15]. Their duties include scheduled and surprise inspections of water, consumer goods, land reserves and other environmental objects for the presence of BPs included in the officially approved list, the majority of which persist in natural reservoirs, cause acute intestinal infections and helminthiases [16–18]. Another area of CHE expertise is investigation of infection outbreaks [13].

Control of animal infections including those posing a threat to humans is executed by regional and interregional veterinary laboratories of the Federal Service for Veterinary and Phytosanitary Surveillance. However, the agency does not share the obtained information with other healthcare services.

CHE owns an extensive network of laboratories across Russia equipped with state-of-the-art high-performance diagnostic tools for effective and continuous routine epidemiological surveillance, accurate identification of BP etiology, prompt reporting of imported BPs, causative agents of epidemic and highly dangerous infections or those persisting in natural reservoirs, and tracking their spread during the outbreak.

At the same time, routine duties of Rozpotrebnadzor normally include surveillance of a narrow range of BPs [16, 17] using specific tools for their detection [18] that covers only a few typical niches, preventing the real incidence of infections (even those from the list) from being unveiled and the actual vulnerability of the population in the face of these infections from being accurately estimated.

Executive bodies of Rospotrebnadzor have sufficient experience and efficient tools to detect causative agents of alimentary and zoonotic infections, as well as those persisting in natural reservoirs, and to investigate their outbreaks. Still, they hardly ever engage in the surveillance of parenteral and respiratory infections with epidemic potential although the economic and social damage caused by the latter exceeds the damage inflicted by the outbreaks of relatively rare infections [3].

On the whole, the existing system of epidemiological surveillance and sanitary control successfully solves vital yet narrow practical tasks that bear only partial relevance to the mission of epidemiological surveillance in Russia.

3. *Epidemiological research* into a narrow range of BPs afflicting some social groups or occurring in certain geographical locations is carried out by state research institutions supervised by Rospotrebnadzor, the Ministry of Health and the Ministry of Education and Science of the Russian Federation. These research studies are usually ordered by the state as part of what was formerly known as federal targeted programs or are initiated by the institution itself provided it has sufficient funds to sponsor the study. As a rule, research institutions are not expected to perform epidemiological surveillance and collect statistics on a regular basis. Still, some of them have transformed into centers for pathogen control, like the Federal Research and Methodological Center for AIDS Prevention and Control at the Central Research Institute of Epidemiology, WHO Collaborating Center for Influenza at the State Research Center of Virology and Biotechnology VECTOR, or the National Research and Methodological Center for Measles and Rubella at Gabrichevsky Institute for Epidemiology and Microbiology, and have their own diagnostic laboratories. Such centers share information about seasonal strains and serotypes of some BPs (including the influenza virus) essential for elaborating adequate prevention strategies.

These centers use advanced technologies in their work ensuring high sensitivity and specificity of detection and identification of various BPs and strictly adhere to the rules of good epidemiological practice. As a result, they can reliably estimate the actual incidence of a pathogen in a certain subpopulation at risk or in a reference group.

However, research institutions do not conduct large-scale epidemiological studies nor do they engage in small-scale studies on a regular basis in the absence of adequate funding. Besides, they only deal with their "specialty" pathogens. In addition, their findings are presented as articles in academic journals or similar literature sources, or as reports that do not comply with a format of a statistical report and therefore cannot be readily pasted into official papers, given the lack of interagency coordination.

4. *Healthcare and sanitary services* also gather data on disease incidence in different subpopulations, including information about the contamination of environmental objects. Among them are the Federal Security Service of the Russian Federation, the Ministry of Defense, the Federal Customs Service, the Federal Medical and Biological Agency (FMBA), the Ministry of Civil Defense, Emergencies and Disaster Relief, the Ministry of Transport, etc. However, the information they obtain is intended for internal use only and to our knowledge is not factored into public health strategies. So, these bodies do not participate in epidemiological surveillance (at least in times of peace).

To sum up, in Russia certain components of epidemiological surveillance of infectious diseases are relatively advanced (Fig. 1) but do not form a well-coordinated network due to the lack of collaboration between the involved agencies in the first place. Secondly, the collected information does not satisfy strict quality and quantity criteria: it cannot be extrapolated to the general population, it lacks important information about the etiology of pathogens and the rate of data collection is quite slow. The most important problem with these methods is that they do not complement each other in the absence of an integrated analytical center where all information could be dispatched.

The new integrated center is expected to be free of the drawbacks of the existing system while complying with the principles of biosurveillance [10]. The center should not take on functions already distributed between other agencies (analysis of disease incidence, investigation of outbreaks, control of consumer goods safety, epidemiological research in subpopulations at risk). The center is expected to estimate the prevalence of biopathogens in the population, identify their types and serological markers, contributing to the task of reducing the vulnerability of the society, the economy and the state in the face of biological threats.

This center must provide functional and organizational support to emergency responder agencies in the event of a biological threat and increase their efficiency by ensuring a more rapid response. The schematic of a network for biological surveillance is shown in Fig. 2.

At the same time, interagency coordination and data pooling are not the only activities that ensure efficient performance of the national system for biosecurity and safety. The vulnerability of the society largely depends on the properties of both BPs and tools for their detection.

Human component in screening tests. Low rate of pathogen detection

Arranging scattered sources of data into a network that continuously supplies information about current biological

risks to the integrated center for biological surveillance can significantly reduce response time in the event of a biological threat. At the same time, the lack of information sources or the lack of specificity, sensitivity, operational independence, or automation and low rates of pathogen detection are a threat of their own. Specifically, response to an alert about a potential biohazard reported by a common lab affiliated with an HCF or a center for hygiene and epidemiology (even if it is properly equipped) can be unacceptably imprompt, considering the time required for testing procedures, data transfer, and decision making and the time a patient needs to realize that he/she is sick, present to hospital, undergo tests, etc.

Therefore, a center for biological surveillance cannot solely rely on aggregating data from third parties but needs its own network of laboratories equipped with automated tools for real-time pathogen detection [19].

Advances in laboratory diagnostics have boosted the development of techniques for rapid automated pathogen detection that require little or no human participation and can be used along with traditional manually operated tools [19]. Being highly sensitive and specific, new automated tools reduce the time of the analysis down to a few hours or even minutes. Automated devices can keep on analyzing samples collected from the environment for the presence of pathogens almost non-stop.

Analysis of airborne aerosol particles facilitates detection of pathogens in the air before the latter can be contracted by humans, which, considering the incubation period, ensures early diagnosis and drastically reduces the number of individuals who can get infected, given that adequate measures are taken urgently. The saved time can be spent on launching large-scale immunization campaigns or promoting prevention immunoglobulin therapy.

So far, immuno- and nucleic acid assays remain the most reliable techniques for automated detection of various pathogens (bacteria, viruses and toxins) in the surrounding environment [19]. Immunoassays are capable of detecting intra- and extracellular BPs and the products of their metabolism. Nucleic acid assays exhibit higher sensitivity in smaller samples [19]. The use of both techniques in combination significantly reduces the risk of false-positive results [19, 20], whereas their ability to quantify the analyte in the sample increases their informative value.

At the same time, requirements for operational independence and automation impose certain limitations on these devices and assays. The number of stages in the procedure must be minimized. The assays are expected to retain acceptable sensitivity (at least 1,000 pathogens per one ml of the aerosol concentrate) and specificity; both sample preparation and the analysis itself must be quick. Given the scope of their application and requirements for portability, aerosol samplers and analyzers must be small in dimensions, tolerate transportation without demanding additional tuning upon arrival, provide unfailing performance under rough conditions, and be airtight to exclude the possibility of cross-contamination and contamination of the working chamber. Maintenance and cleaning must be safe for the laboratory personnel.

Indeed, air quality control is a pressing concern. But the real scope of application of aerosol samplers and analyzers will largely depend on the capacities of these devices: the rate of analysis, sensitivity and specificity, the ability to quantify pathogen concentrations in the sampled air, costs of reagents, assays and the device itself [6, 21, 22]. These factors must be accounted for when deploying a network of automated tools for pathogen detection in the integrated national center for biological surveillance.

Identification of previously unknown pathogens and pathogens with unknown characteristics

The number of drug-resistant bacteria has been rapidly growing in the past few years. New infections are springing up in all corners of the world, and the risk of bioterrorism or biological warfare is still high. In this light, development and routine use

Biological surveillance: current state

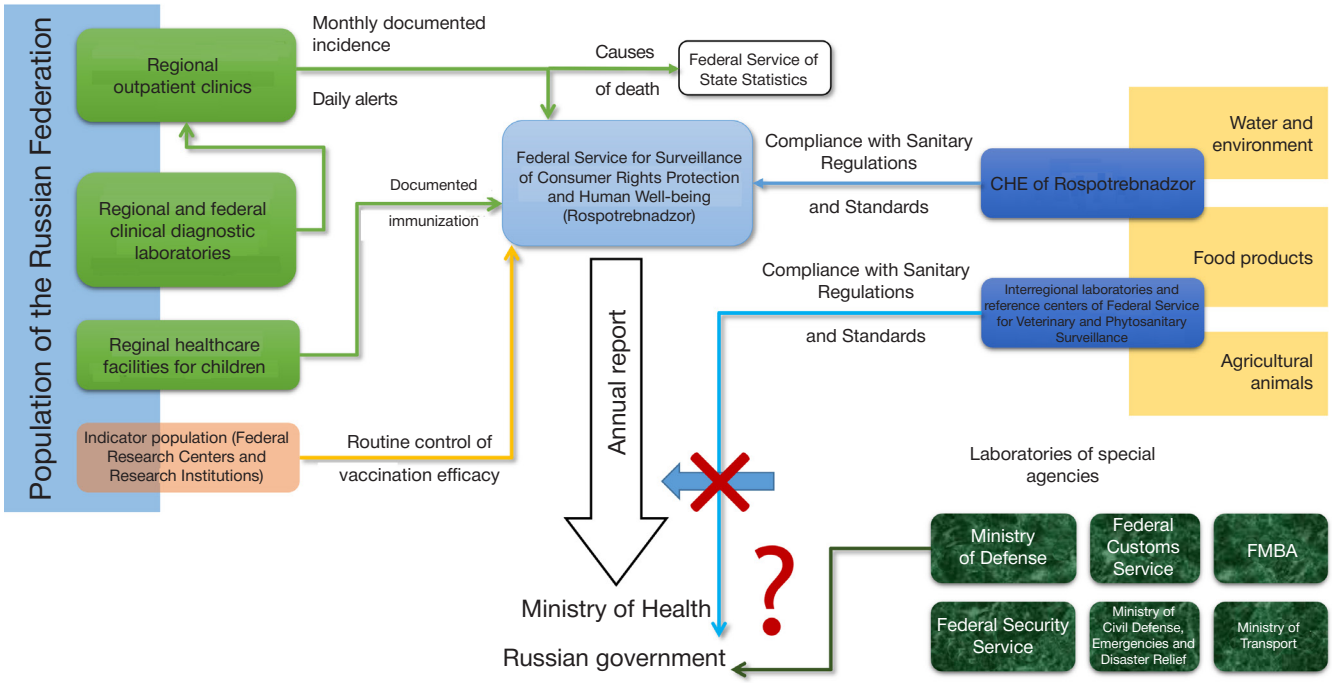

Fig. 1. The schematic representation of biological surveillance in its current state in Russia

of novel technologies for the detection of new pathogens with unknown properties are becoming critical.

The use of high-throughput sequencing by microbiologists and infectious disease physicians has driven medical progress. Commercial tools for next-generation sequencing (NGS), including Miseq and Hiseq (Illumina), GS (Roche-454), Ion Torrent (Life Technologies), Minion (Oxford Nanopore Technologies), and PacBio (Pacific Biosciences), capable of reading the entire BP genomes or shorter genomic regions have made a significant contribution to clinical microbiology and virology and inspired development of new diagnostic sequencing-based techniques [23]. By deciphering genome sequences of different strains, NGS offers a unique opportunity to estimate the virulence potential of pathogen isolates and to predict their drug resistance. Identification and characterization of virulence factors, especially toxins and antibiotic resistance markers, provide an insight into the pathogenesis of bacterial diseases and bacterial interactions with the host and drive the discovery of novel drugs, vaccines and molecular diagnostic tests [10, 24].

The use of next-generation sequencing in microbiology and epidemiology opens new horizons with regard to the detection of emerging pathogens and exploration of their properties (Fig. 3).

NGS-based methods are now available in some medical microbiological laboratories, such as the laboratory at the University Medical Center Groningen (UMCG), where they are employed to control outbreaks of infectious diseases, conduct molecular epidemiology studies, create pathogen profiles, study pathogen activity, rapidly identify bacteria by their 16S–23S rRNA region, and classify microorganisms. NGS is also exploited in metagenomic approaches to clinical samples and for tracking transmission of zoonotic infections from animals to humans.

The potential of whole genome sequencing (WGS) facilitates adoption of NGS into public health research [25–26]. Applied to investigate outbreaks of infections, WGS also yields data that can be used to elaborate strategies for combatting the spread of resistant bacterial clones. For example, the outbreak caused by colistin-resistant carbapenemase-producing *K. pneumonia* that invaded a few Dutch hospitals was handled by referring all patients infected with this pathogen to a special healthcare facility where they received adequate treatment from a team of experts [27].

WGS has also proved to be instrumental in preparing profiles of highly virulent bacteria, such as shiga-toxin-producing *Escherichia coli* (STEC) O104:H4 that caused an outbreak in Germany in 2011 [28].

Molecular identification of pathogens is part of the investigation of infection outbreaks. Retrospective analysis of data yielded by NGS and WGS may reveal the involvement of pathogens that were not identified by PCR or serological techniques at the time of the outbreak [29–30].

Routine preparation of pathogen profiles is impossible without using a combination of bacteriological, biochemical and molecular techniques, rendering it labor-intensive, time-consuming and expensive. NGS is a reliable and simple tool for exploring a variety of properties in a variety of pathogens [31–33]. Knowledge of their virulence profiles is critical for predicting the severity of the infection or treatment outcomes, as well as for risk assessment in the early stages of the disease. Because WGS covers the entire genome and not a single gene, its contribution to the detection of virulence factors may be substantial especially if assisted by special online tools [34, 35].

One of the large-scale cohort studies employed WGS to obtain a molecular profile of STEC in order to get a clear picture of the population structure and the genomic plasticity of this strain in the locations of Groningen and Rotterdam (Netherlands) [36]. Detailed information about a studied microbial strain related to its genotype, serotype, multilocus sequencing data, virulence and antibiotic resistance profiles, and phylogeny can be easily

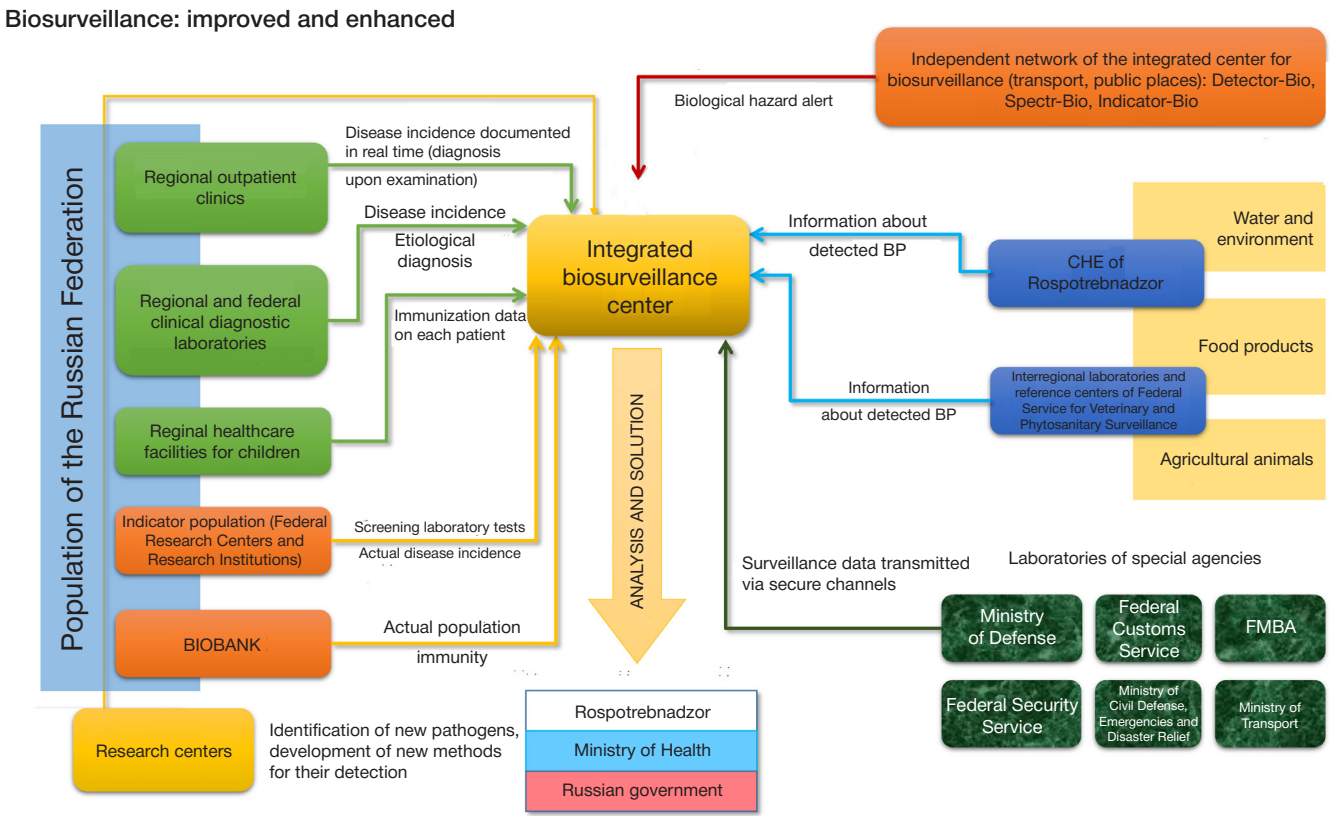

Fig. 2. Biological surveillance coordinated by the integrated national center

extracted from special databases by running a sequence search that selectively discriminates between closely related strains. Over a short period of time, many strains have been described and compared using NGS. The important role of WGS is indisputable in situations when a need arises for efficient molecular epidemiologic surveillance in separate regions and state-wide. NGS is also good at predicting new resistance genes, including those conferring antibiotic resistance, in both modern bacteria and their ancestors; further experiments can elucidate whether these genes are really responsible for the observed patterns of antibiotic resistance [37].

NGS-based techniques do not require culturing to detect a pathogen and are capable of identifying an infinite number of pathogens, enriching our knowledge of the entire microbiome. Some authors believe that in the future metagenomics will become an ultimate approach to the detection of all possible microorganisms [38]. However, large datasets require vast bioinformatic and computational resources to be processed that are not available in the majority of diagnostic microbiological laboratories. Besides, metagenomic approaches are time-consuming: the whole procedure takes up to 4 or 5 days.

To bridge the gap between traditional methods for the detection and identification of microorganisms (culturing, microbiological assays, PCR) and metagenomics, a culture-independent approach has been proposed based on targeted NGS (Fig. 3). In comparison with metagenomic approaches, it is faster, cheaper and simpler and has a potential to join the routinely used arsenal of diagnostic laboratories. It has been proved that the sequence of 16S rRNA gene is a reliable genetic marker of a bacterial genus (or even species or strain in some cases) as it is present in all bacteria and its function is fixed and stable [39]. This gene can be sequenced by NGS from a clinical sample without preparatory culturing. Culture-independent 16S rRNA sequencing has already been adopted in clinical routine as a valuable ancillary technique [40, 41]. However, it can produce ambiguous results as 16S rRNA sequences can be similar in different bacterial species [42].

Another innovative culture-independent 16S–23S rRNA NGS-based approach has been recently developed for the detection of bacteria in clinical samples. It has a few advantages over other analytical tools. It is capable of accurate pathogen identification in urine samples, as confirmed by conventional culturing techniques [43]. Moreover, it can simultaneous identify more than one pathogen in biological samples that were previously shown to be pathogen-free by conventional culturing techniques and PCR. Indeed, this novel approach will significantly contribute to the evolution of microbiology and optimize antibiotic therapies. Finally, it will prompt clinical microbiological laboratories to routinely use NGS in their work and drive the development of technologies and bioinformatic software necessary to adapt metagenomic methods to diagnostic tasks.

In terms of taxonomy, WGS yields more gene sequences to discriminate between species than classic DNA–DNA hybridization or 16S rRNA sequencing. Moreover, it can be used for phylogenetic reconstruction based on all gene sequences constituting a studied genome; conveniently, the clusters on the resulting dendrogram will be well-separated [44]. Some authors believe that profiles of new taxa should include genomic sequences with at least 20x coverage [45].

In the future NGS will help researchers to obtain more information about zoonotic transmission of BPs. Pioneer studies of this subject exploited low-selectivity techniques, such as serotyping [46]. It was not until very recently that attempts were made to use pulse-field gel electrophoresis and multiple locus variable number of tandem repeats analysis to detect specific bacterial clones in animals and humans [47]. Many aspects of biological mechanisms underlying zoonotic

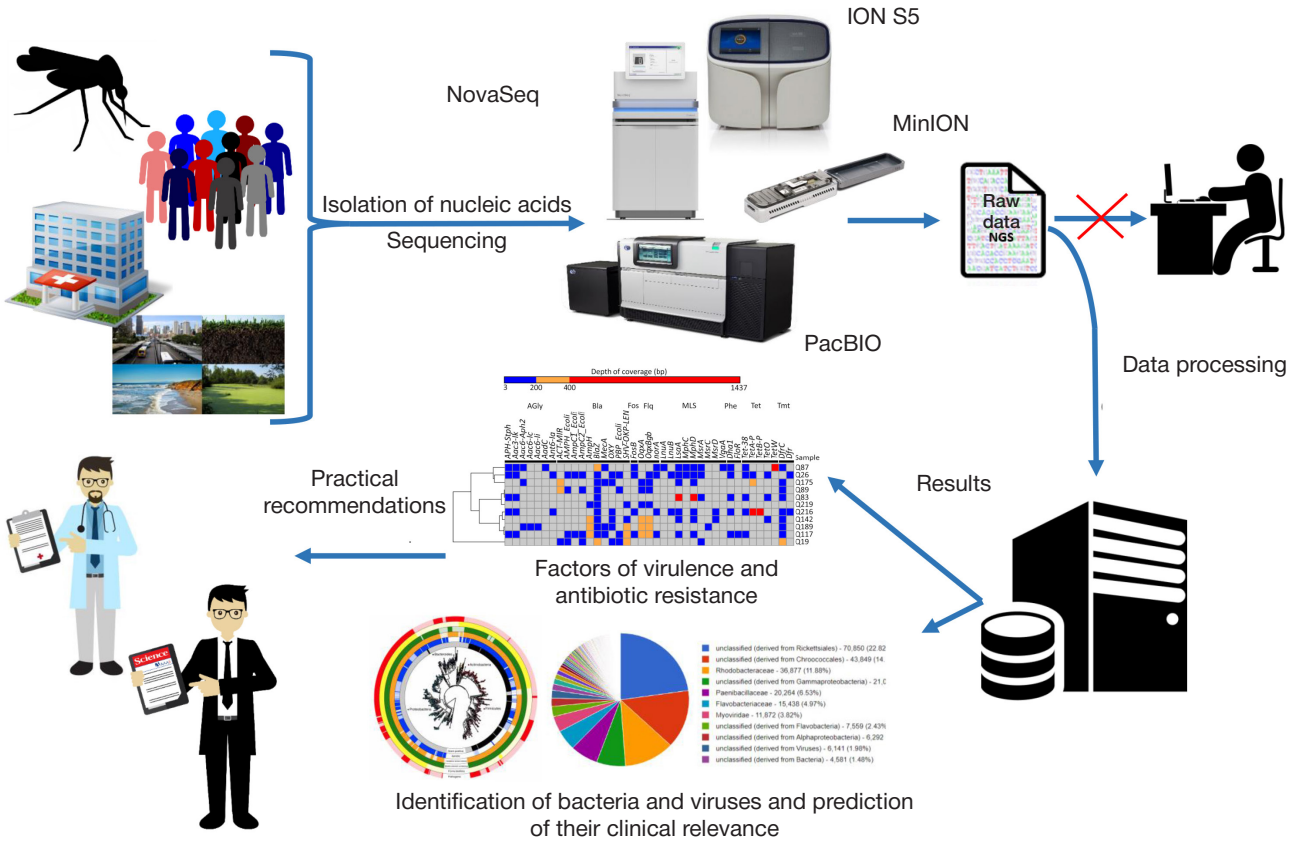

Fig. 3. Algorithm for the identification of emerging pathogens, virulence factors and antibiotic resistance of pathogenic bacteria

transmission of infections are yet to be elucidated, including its frequency (one or more contacts with animals or animal products), associated risk factors (close contact with animals or tasks involving processing of their feces) and the contribution of antibiotics used in agriculture. Here, NGS opens new horizons. Its high selectivity allows researchers to discriminate between previously undifferentiated bacterial strains infecting animals and humans. Combined with epidemiological data, this information will help to better locate and describe the potential sources of zoonotic infections [47–48].

Together, the metagenomic approach and NGS constitute a method for creating a comprehensive profile of a pathogen covering its antibiotic resistance, the ability to produce toxins and other pathogenic factors and the ability to pass these factors on between species. However, in spite of their good potential to identify previously unknown pathogens or those with new properties, the application of NGS and metagenomic approach in clinical practice is still limited to single cases.

Emergence of new biopathogens and acquisition of new pathogenic properties

Outbreaks of infectious diseases pose a continuous threat to the population. A lot of attention is paid to the problem of emerging pathogens, such as Middle East respiratory syndrome-related coronavirus and Zaire ebolavirus. But actually, epidemics are more often caused by well-known microbes, such as influenza virus, Dengue virus, causative agents of tuberculosis, and vibrio cholerae. The majority of epidemics are a direct consequence of external influences, climate changes or geographical factors. However, they can be anthropogenic. Every few years a new threat springs up following the emergence and spread of new pathogenic organisms. The literature reports new infectious agents discovered only recently, in the 21st century [49]. A good example of the human role in the emergence of new BPs or their new properties is the spread of antibiotic-resistant strains and genetic modification of BPs intended for bioterrorism.

Antibiotic resistance of human pathogens

Resistance of pathogenic microorganisms to antimicrobial drugs (including multidrug resistance) has become a common phenomenon and is the major factor affecting treatment outcomes in infected patients almost everywhere in the world. World Health Organization (WHO) defines it as a national security threat for many countries. It is a pressing concern highlighted in many research works [50–60].

Discovered in the late 1930s, antibiotics have saved millions of people from death of acute bacterial infections. For example, the use of penicillin G, the "magic bullet", led to a dramatic decline in streptococcus-associated mortality during World War II. By the time the first penicillin-resistant strains appeared, second-generation antibiotics had already been developed, such as methicillin, cephalothin, and imipenem. However, not many years passed before a methicillin-resistant strain of *Staphylococcus aureus* MRSA was isolated in 1961. The following years saw the arrival of other clinical strains resistant to streptomycin, chloramphenicol and tetracycline. It soon became clear that bacteria are capable of acquiring resistance to all known antibacterial drugs. As a rule, microorganisms become resistant to an antibiotic after a year or two of its use. Many pharmaceutical companies suspended or shut down antibiotic discovery projects because the drugs were no longer profitable due to their poor efficacy. Since 1987, not a single class of antibiotics has been discovered. Today, too few drugs addressing the problem of antibiotic resistance are being designed and tested [61]. Global healthcare achievements are at risk: antibiotic resistance is spreading across the world leaving patients vulnerable in the face of deadly infections and interfering with live-saving treatments, such as surgery and chemotherapy [62–65].

Resistance to antibiotics is largely a result of their mis- or overuse. Statistically, in about 75% of cases prescription of antibiotics is not justifiable [64]. Monoresistant strains gradually acquire multidrug and then pandrug resistance. A new concept of "problematic" microorganisms has emerged recently referring to pathogens with multidrug and extensive drug resistance, most of which are contracted in healthcare facilities where antibiotics and disinfectants are used in abundance. Among problematic bacteria are *Staphylococcus aureus*, *Pseudomonas aeruginosa*, *Klebsiella pneumoniae*, enterococci, pneumococci, and some others [66].

Bacterial resistance to antibiotics is determined genetically and supported by a number of well-known mechanisms, including inactivation of the antibiotic, modification of its target, increased efflux, reduced permeability of outer membranes, and bypass of metabolic pathways [67]. It means that antibiotic-resistant strains can be directly detected by PCR or sequencing, without prior culturing in the media supplemented with antibiotics and without the need to identify a species of the studied pathogen (antibiotic resistance genes are often transferred horizontally even between different taxa). In a word, there is an available arsenal of tools for routine detection of antibiotic-resistant strains posing a serious biological threat that can be used by the integrated center for biological surveillance.

Synthetic biology and bioterrorism

Although the Geneva protocol ratified in 1925 and so far signed by 65 states prohibits development, production and use of biological and chemical weapons, it was still thought justifiable that BPs could be used in a war as their components [68]. Biological and chemical weapons sprayed in Vietnam during the Vietnam war were reported by WHO and condemned by the 1967 UN resolution (XXI). In 1970 WHO released a report about the *Health aspects of chemical and biological weapons* revised in 2004 and re-published under the heading *Public health response to biological and chemical weapons* [69]. This document provides guidance for preparing to outbreaks of rare exotic infections. It also includes standard recommendations for public health surveillance and adequate medical help in the event of an emergency. WHO defines biological weapons as those that destroy the target by infecting it with disease-producing agents, such as viruses, infectious nucleic acids and prions.

A variety of available technologies makes production of biological weapons a relatively easy task, and the only reason why such weapons are not developed openly is a fear of sanctions or retaliation. Many countries can potentially use biological weapons. Since 1928 some states have been planning an offensive biological warfare and most likely have the resources to initiate it now [70]. The USA (until 1972) and the former USSR (until 1992) had very elaborate doctrines of biological warfare. Both states designed over 10 biological agents, including toxins, aimed at killing or seriously wounding people and destroying agriculture on enemy territory [71, 72]. At the same time, the military use of biological agents is forbidden by the Biological and Toxin Weapons Convention (BTWC). The states that joined the Convention cannot develop, produce or stockpile biological weapons. The Convention was signed and approved by 170 states. However, there are no real mechanisms to control how well the parties to this Convention

adhere to its terms. Development of biological weapons and its production can be easily "blended" into the biotechnological infrastructure of the state. Besides, the Convention does not demand the signees not to "develop, produce, stockpile or otherwise acquire or retain microbial or other biological agents, or toxins whatever their origin or method of production, of types and in quantities that have no justification for prophylactic, protective or other peaceful purposes". It means that the Convention does not specify what biological agents or toxins are banned and in what quantities. However, chances are that if a country takes a risk of developing or producing biological weapons regardless of whether it has joined the Convention or not, it can easily earn a reputation of a rouge state.

Bioterrorism attacks launched in non-belligerent states were first considered a local threat, and heir consequences were not thought to threaten national security. But after letters containing anthrax spores were sent through the US mail, the nightmare became a reality. The anthrax attack killed 5 and infected over 20 people. As many as a few thousands of people had to take strong antibiotics. The letters containing real or fake anthrax spores were also found in dozens of other countries, including Russia.

Bioterrorism is the deliberate dissemination of viruses, bacteria or other pathogenic agents that kill or infect people, animals and plants [73]. As a rule, terrorists seek to spark panic or fear and to cause social unrest or economic damage. Some of them are driven by ideological, religious, or political motives. Their primary tool is terror evoked by violence. Destructive doomsday cults like Aum Shinrikyo inflict mass casualties to achieve their own religious goals. However, terrorism is prosecuted by law. Counter-terrorism strategies and the lack of financial support and infrastructure obstruct implementation of successful large-scale attacks. On the other hand, for the majority of terrorists, success is probably determined by the amount of panic caused and does not need to be accompanied by a great number of casualties [74–76].

Another important phenomenon we would like to mention here is biocrime. A biocrime involves the use of a biological agent in order to kill one person or a small group of people and is largely motivated by hatred or financial gain and less by political, religious or ideological motives. For example, a situation in which ricin was used to get rid of an annoying partner or hospital staff were intentionally infected with *Shigella dysenteriae* by their colleague can be described as a biocrime [77]. The murder of the Bulgarian dissident writer Georgi Markov in London in 1978 by a ricin-containing pellet injected by an «umbrella gun» is another example of a biocrime.

The economic impact of bioterrorism against humans and agriculture can be truly devastating [75, 78–81].

So far bioterrorism has taken fewer lives than "traditional" attacks involving weapons and explosives. But the risk of mass casualties from infectious agents following an act of terror is real, though not so high. As a rule, the incubation period of biopathogens is long enough to detect and identify them before they start causing visible symptoms. Besides, effective antibiotic treatment is available for the majority of bacterial agents but for multidrug resistant strains.

There are two principal approaches to creating biological weapons:

a) a known pathogen is transferred from one host to another inducing severe symptoms in the latter due to the lack of adaptation of the new host;

b) a known biological agent acquires new properties, usually through horizontal gene transfer.

Before the advent of synthetic biology, creating novel biological weapons using the first approach was thought to be unlikely. Now, there is ongoing research into the mechanisms allowing prediction of mutations in the genome of a pathogen that entail the possibility of gene transfer. So, this approach is technically feasible [82–85].

Breakthroughs in synthetic biology are a fair reason to believe that in the nearest future we will witness the arrival of affordable methods for synthesizing new organisms with programmed properties that can be used in basic research and routine practice. Key discoveries in this field were made by Craig Venter, Daniel Gibson and their teams who were the first to demonstrate the possibility of synthesis of new organisms with a "designer" genome [82–85].

The potential of modern synthetic biology can be described by the following functions:

1 — combined chemical and enzymatic synthesis of long artificial DNA fragments;

2 — computer-aided design of individual genes and whole genomes with programmed metabolic functions;

3 — highly efficient assembly and editing of artificially synthesized genomes in simple biological systems (bacterial cells and single-celled eukaryotes);

4 — fully automated remote synthesis of DNA, RNA, proteins (toxins), viruses, and bacteria by robotic complexes from simple chemical compounds requiring zero human participation.

Therefore, synthetic biology can be employed to:

1) rapidly design vaccines and vaccine strains of any bacterium or virus, including known and unknown microorganisms of any nature, without using "raw" pathogenic material. The only thing one needs to have at their disposal is the genomic sequence of a pathogen that can be forwarded to a lab or an automated device as a digital message. It has been demonstrated experimentally that it takes as little as 2 months to create an influenza vaccine given that the only "raw" material available is information about the sequence of a new strain of type A flu;

2) carry out remote synthesis of bacterial cells to colonize other planets as part of space projects;

3) engineer ideal animal donors to transplant their organs to humans after introducing into their genome the loci responsible for histocompatibility;

4) design and synthesize viruses and bacteria with programmed properties that can be used in bioterrorism attacks and for military purposes.

Introduction of new pathogenic properties into known biological agents assisted by gene editing techniques and synthetic biology seems to be an easier task, as many of these organisms have already been well described. Besides, there are a lot of simple and affordable biotechnologies for horizontal gene transfer between both bacteria and viruses yielding pathogens with programmed properties. Open-access databases store information about sequences of virulence genes that can be synthesized *de novo* to create biological weapons even in the absence of a natural pathogen sample.

Of all currently existing approaches to pathogen engineering, genetic modification by introducing virulence genes into the genome of a pathogen is the simplest. Such modifications can include 1) incorporation of bacterial toxins into a biological target; 2) insertion of antibiotic resistance genes; 3) stimulation of excessive immune response of an infected host (cytokine storms); 4) synthesis of individual virulence genes and whole pathogenic organisms *de novo*.

Biological agents engineered as part of state military defense projects and pathogen repositories are another attractive target for bioterrorists. Civil wars, riots, and anarchy in the

countries that have biological weapons increase the risk their malicious use. At the same time, innovative technologies and rapid evolution of science have improved our understanding of interactions between pathogens and their hosts and stimulated development of medical countermeasures. In addition, they have expanded our arsenal of tools for the detection and identification of pathogens. Technological novelties, such as network cameras and intelligence gathering software, have become powerful tools for combatting terrorism and enhanced the efficacy of countermeasures to prevent attacks. Advances in forensics facilitate investigation of incidents and help to track down the biological agent. However, the risk of emergence of new genetically modified pathogens is very high and poses a serious challenge to the global community.

CONCLUSION

The analysis of the available literature reporting the emergence of new pathogens deliberately synthesized by humans leads us to conclude that biological risks can be mitigated only if new techniques for rapid detection of pathogens are introduced into routine practice. Fortunately, BPs modified by humans still retain their old known properties rendering their identification technically feasible. However, unknown pathogens that spontaneously acquire dangerous properties still pose a serious threat. Therefore, the integrated center for biological surveillance must have the tools for their identification.

Biosecurity and biosafety are serious issues faced by the state. The negative impact of currently existing biological hazards, the emergence of new and the re-emergence of previously known risks threaten the sanitary, epidemiological, veterinary, phytosanitary and ecological welfare of the society and undermine the security of the state that has to be well-prepared for any type of a biological threat.

Again, risks associated with the emergence of new pathogens or the spread of those with new properties can be mitigated only if novel detection techniques are adopted into clinical routine and environmental monitoring. Particular attention should be paid to the adoption of methods for the detection of previously unknown pathogens and the development of prevention measures and adequate treatment against those re-emerged.

In this review we aimed to comprehensively analyze biological threats to national security by identifying the vulnerabilities in the current system for biological surveillance. First, these threats are a natural product of pathogen evolution through which pathogens acquire new properties enabling them to overcome immunization barriers and become antibiotic-resistant. Second, the lack of technologies for the profound analysis and rapid response to alerts is a threat of its own addressed by some of the articles in the current issue of the journal. Third, the system for biological surveillance is vulnerable in its current state due to the lack of interagency coordination and slow response to alerts. All these factors urge creation of a national integrated center for biological surveillance to promptly aggregate, process and analyze information from different sources about all possible biological threats. The collected data can be used to model how the situation will unfold, predict its outcomes, keep the officials in charge informed, and facilitate decision making at the interagency level.

References

1. O biologicheskoj bezopasnosti. Proekt Federal'nogo zakona Rossijskoj Federacii. (red. ot avgusta 2016 g.). 30 s. Dostupno po ssylke: http://regulation.gov.ru/projects#npa=55658
2. Onishhenko GG, Popova AJu, Toporkov VP, Smolenskii VJu, Shherbakova SA, Kutyrev VV. Sovremennye ugrozy i vyzovy v oblasti biologicheskoj bezopasnosti i strategija protivodejstvija. Problemy osobo opasnyh infekcij. 2015; (3): 5–9.
3. O sostojanii sanitarno-jepidemiologicheskogo blagopoluchija naselenija v Rossijskoj Federacii v 2017 godu: Gosudarstvennyj doklad. M.: Federal'naja sluzhba po nadzoru v sfere zashhity prav potrebitelej i blagopoluchija cheloveka; 2018. 268 s.
4. Pokrovskij VI, Briko NI. Jepidemiologija. Uchebnik. M.: GJeOTAR-Media; 2016. 368 s.
5. Lobzin JuV, Belozerov ES, Beljaeva TV, Volzhanin VM. Virusnye bolezni cheloveka. SPb.: SpecLit; 2015. 400 s.
6. BioWatch and public health surveillance: Evaluating systems for the early detection of biological threats. Abbreviated version. Washington, DC: The National Academies Press. IOM and NRC. 2011. 252 p.
7. Onishhenko GG, Merkulov IV, Petrov EJu, Zhelobov VE, Shevchuk NA, Seledcova OV. O hode immunizacii naselenija v ramkah nacional'nogo kalendarja profilakticheskih privivok. Protokol selektornogo soveshhanija u rukovoditelja Federal'noj sluzhby po nadzoru v sfere zashhity prav potrebitelej i blagopoluchija cheloveka (Protokol #13 ot 20.07.2010). Dostupno po ssylke: http://41.rospotrebnadzor.ru/content/protokol-protokol-selektornogo-soveshchaniya-u-rukovoditelya-federalnoy-sluzhby-po-nadzoru-5
8. Osnovy gosudarstvennoj politiki v oblasti obespechenija himicheskoj i biologicheskoj bezopasnosti Rossijskoj Federacii na period do 2025 goda i dal'nejshuju perspektivu (utv. Prezidentom RF 1 nojabrja 2013 g. N Pr-2573). Dostupno po ssylke: http://www.garant.ru/products/ipo/prime/doc/70423098/
9. Ukaz Prezidenta RF ot 31.12.2015 N 683 «O Strategii nacional'noj bezopasnosti Rossijskoj Federacii». Dostupno po ssylke: http://www.consultant.ru/document/cons_doc_LAW_191669/
10. V Rossii sozdadut Centr po bor'be s biologicheskimi ugrozami. [Jelektronnyj resurs] Paper 16 matra 2015. Dostupno po ssylke: https://iz.ru/news/584008 (last accessed 12 September 2018).
11. Postanovlenie Pravitel'stva RF ot 30 ijunja 2004 g. N 322 «Ob utverzhdenii Polozhenija o Federal'noj sluzhbe po nadzoru v sfere zashhity prav potrebitelej i blagopoluchija cheloveka» (v red. ot 24 janvarja 2017 g.). Dostupno po ssylke: http://base.garant.ru/12136005/
12. Prikaz Federal'noj sluzhby gosudarstvennoj statistiki ot 28 janvarja 2014 g. N 52 «Ob utverzhdenii statisticheskogo instrumentarija dlja organizacii Federal'noj sluzhboj po nadzoru v sfere zashhity prav potrebitelej i blagopoluchija cheloveka federal'nogo statisticheskogo nabljudenija za zabolevaemost'ju naselenija infekcionnymi i parazitarnymi boleznjami i profilakticheskimi privivkami». Dostupno po ssylke: http://www.garant.ru/products/ipo/prime/doc/70479106/
13. Statisticheskij uchet i otchetnost' uchrezhdenij zdravoohranenija. M.: Ministerstvo zdravoohranenija i social'nogo razvitija Rossijskoj Federacii. 2006. 81 s.
14. Federal'nyj zakon ot 30.03.1999 N 52-FZ «O sanitarno-jepidemiologicheskom blagopoluchii naselenija» (v red. ot 03.07.2016). Dostupno po ssylke: http://www.consultant.ru/document/cons_doc_LAW_22481/

15. 15. Postanovlenie Pravitel'stva RF ot 2 fevralja 2006 g. N 60 «Ob utverzhdenii Polozhenija o provedenii social'no-gigienicheskogo monitoringa» (v red. ot 4 sentjabrja 2012 g.). Dostupno po ssylke: http://base.garant.ru/12144791/
16. SanPiN 2.3.2.1078-01. Gigienicheskie trebovanija bezopasnosti i pishhevoj cennosti pishhevyh produktov. Utverzhdeny glavnym gosudarstvennym sanitarnym vrachom Rossijskoj Federacii 06 nojabrja 2001 g. Dostupno po ssylke: http://base.garant.ru/4178234/
17. SanPiN 2.1.4.1074-01: Pit'evaja voda. Gigienicheskie trebovanija k kachestvu vody centralizovannyh sistem pit'evogo vodosnabzhenija. Kontrol' kachestva. Gigienicheskie trebovanija k obespecheniju bezopasnosti sistem gorjachego vodosnabzhenija. Utverzhdeny glavnym gosudarstvennym sanitarnym vrachom Rossijskoj Federacii 29 sentjabrja 2001 g. Dostupno po ssylke: http://docs.cntd.ru/document/901798042
18. Perechen' standartov, soderzhashhih pravila i metody ispytanij i izmerenij, v tom chisle pravila otbora obrazcov, neobhodimye dlja primenenija i ispolnenija trebovanij tehnicheskogo reglamenta Tamozhennogo sojuza «Trebovanija bezopasnosti pishhevyh dobavok, aromatizatorov i tehnologicheskih vspomogatel'nyh sredstv» i osushhestvlenija ocenki (podtverzhdenija) sootvetstvija. Prilozhenie k Edinym sanitarno-jepidemiologicheskim i gigienicheskim trebovanijam k tovaram, podlezhashhim sanitarno-jepidemiologicheskomu nadzoru (kontrolju). Utverzhdeny Resheniem Komissii Tamozhennogo sojuza ot 28 maja 2010 goda # 299. (v red. ot 09 dekabrja 2011 g.)
19. Dzenitis JM, Makarewicz AJ. The Autonomous Pathogen Detection System. The Microflow Cytometer. 2010: 263–84.
20. Hindson BJ, Makarewicz AJ, Setlur US, Henderer BD, McBride MT, Dzenitis JM. APDS: the autonomous pathogen detection system. Biosens Bioelectron. 2005; 20 (10): 1925–31.
21. Onishhenko GG, Kuzkin BP, Demina JuV. i dr. Obespechenie gotovnosti i organizacija raboty SPJeB FKUZ «Stavropol'skij protivochumnyj institut» Rospotrebnadzora v period provedenija XXII Olimpijskih i XI Paralimpijskih zimnih igr v Sochi. Problemy osobo opasnyh infekcij. 2015; (1): 58–62.
22. GAO-14-267T BIOSURVEILLANCE: Observations on the Cancellation of BioWatch Gen-3 and Future Considerations for the Program. GAO. Statement of Chris Currie, Acting Director, Homeland Security and Justice. Washington, D.C.: 2014.
23. Fournier PE, Raoult D. Prospects for the future using genomics and proteomics in clinical microbiology. Annu Rev Microbiol. 2011; (65): 169–188.
24. Diene SM, Bertelli C, Pillonel T, Schrenzel J, Greub G. Bacterial genomics and metagenomics: clinical applications and medical relevance. Rev Med Suisse. 2014; 10 (450): 2155–61.
25. Zhou K, Ferdous M, de Boer RF, Kooistra-Smid AM, Grundmann H, Friedrich AW, et al. The mosaic genome structure and phylogeny ofShiga toxin-producing Escherichia coli O104:H4 is driven by short-termadaptation. Clin Microbiol Infect. 2015; 21 (468): e467–18.
26. Zhou K, Lokate M, Deurenberg RH, Tepper M, Arends JP, Raangs EG, et al. Use ofwhole-genome sequencing to trace, control and characterize the regionalexpansion of extended-spectrum beta-lactamase producing ST15 Klebsiellapneumoniae. Sci Rep. 2016; (6): 20840.
27. Weterings V, Zhou K, Rossen JW, van Stenis D, Thewessen E, Kluytmans J, et al. An outbreak of colistin-resistant Klebsiella pneumoniaecarbapenemase-producing Klebsiella pneumoniae in the Netherlands (July–December 2013), with inter-institutional spread. Eur J Clin Microbiol Infect Dis. 2015; (34): 1647–55.
28. Ferdous M, Zhou K, de Boer RF, Friedrich AW, Kooistra-Smid AM, Rossen JW, Comprehensive characterization of Escherichia coli O104:H4isolated from patients in the Netherlands. Front Microbiol. 2015; (6): 1348.
29. Bathoorn E, Rossen JW, Lokate M, Friedrich AW, Hammerum AM. Isolation of an NDM-5-producing ST16 Klebsiella pneumoniae from a Dutchpatient without travel history abroad, August 2015. Euro Surveil. 2015; (20): 30040.
30. Falgenhauer L, Waezsada SE, Yao Y, Imirzalioglu C, Kasbohrer A, Chakraborty T. Colistin resistance gene mcr-1 in extended-spectrumbeta-lactamase-producing and carbapenemase-producing Gram-negativebacteria in Germany. Lancet Infect Dis. 2016; (16): 282–283.
31. Aanensen DM, Feil EJ, Holden MT, Dordel J, Yeats CA, Fedosejev A, et al. Whole-genome sequencing for routine pathogen surveillancein public health: a population snapshot of invasive Staphylococcus aureus in Europe. Mbio. 2016; 7 (3): e00444–16.
32. Fournier PE, Dubourg G, Raoult D. Clinical detection and characterizationof bacterial pathogens in the genomics era. Genome Med. 2014; (6): 114.
33. Hasman H, Saputra D, Sicheritz-Ponten T, Lund O, Svendsen CA, Frimodt-Moller N, et al. Rapid whole-genome sequencing fordetection and characterization of microorganisms directly from clinicalsamples. J Clin Microbiol. 2014; (52): 139–46.
34. Franz E, Delaquis P, Morabito S, Beutin L, Gobius K, Rasko DA, et al. Exploiting the explosion ofinformation associated with whole genome sequencing to tackle Shigatoxin-producing Escherichia coli (STEC) in global food production systems. Int J Food Microbiol. 2014; (187): 57–72.
35. Laabei M, Recker M, Rudkin JK, Aldeljawi M, Gulay Z, Sloan TJ, et al. Predicting the virulence of MRSA from its genome sequence. Genome Res. 2014; (24): 839–49.
36. Ferdous M, Friedrich AW, Grundmann H, de Boer RF, Croughs PD, Islam MA, et al. Molecular characterization and phylogeny of Shiga toxin-producingEscherichia coli isolates obtained from two Dutch regions using whole genomesequencing. Clin Microbiol Infect 2016; (22): 642.e1–642.e9.
37. Nijhuis RH, Oueslati S, Zhou K, Bosboom RW, Rossen JW, Naas T, et al. OXY-2-15, a novel variant showing increased ceftazidime hydrolytic activity. J Antimicrob Chemother. 2015; (70): 1429–33.
38. Hasman H, Saputra D, Sicheritz-Ponten T, Lund O, Svendsen CA, Frimodt-Moller N, et al. Rapid whole-genome sequencing fordetection and characterization of microorganisms directly from clinicalsamples. J Clin Microbiol 2014; (52): 139–46.
39. Patel JB. 16S rRNA gene sequencing for bacterial pathogen identification inthe clinical laboratory. Mol Diagn. 2001; (6): 313–21.
40. Schuurman T, de Boer RF, Kooistra-Smid AM, van Zwet AA. Prospectivestudy of use of PCR amplification and sequencing of 16S ribosomal DNA fromcerebrospinal fluid for diagnosis of bacterial meningitis in a clinical setting. J Clin Microbiol. 2004; (42): 734–40.
41. Srinivasan L, Pisapia JM, Shah SS, Halpern CH, Harris MC. Canbroad-range 16S ribosomal ribonucleic acid gene polymerase chain reactionsimprove the diagnosis of bacterial meningitis? A systematic review andmeta-analysis. Ann Emerg Med. 2012; (60): 609–20.
42. Kalia VC, Kumar R, Kumar P, Koul S. A genome-wide profiling strategy asan aid for searching unique identification biomarkers for Streptococcus. Indian J Microbiol. 2016; (56): 46–58.
43. Sabat AJ, van Zanten E, Akkerboom V, Wisselink G, van Slochteren K, de Boer RF. Targetedamplification for bacterial identification at the species-level usingnext-generation sequencing—increased discrimination of closely relatedspecies. ECCMID. 2016; E-poster EP0219.
44. Daubin V, Gouy M, Perriere G. Bacterial molecular phylogeny usingsupertree approach. Genome Inform. 2001; (12): 155–64.
45. Thompson CC, Chimetto L, Edwards RA, Swings J, Stackebrandt E, Thompson FL. Microbial genomic taxonomy. BMC Genom. 2013; (14): 913.
46. Tenover FC, Arbeit RD, Goering RV. How to select and interpretmolecular strain typing methods for epidemiological studies of bacterialinfections: a review for healthcare epidemiologists. Molecular Typing WorkingGroup of the Society for Healthcare Epidemiology of America. Infect Control Hosp Epidemiol. 1997; (18): 426–39.
47. Sabat AJ, Budimir A, Nashev D, Sa-Leao R, van Dijl J, Laurent F, et al. Overview of molecular typing methods for outbreakdetection and epidemiological surveillance. Euro Surveil. 2013; (18): 20380.

48. Harrison EM, Paterson GK, Holden MT, Larsen J, Stegger M, Larsen AR, et al. Whole genomesequencing identifies zoonotic transmission of MRSA isolates with the novelmecA homologue mecC. EMBO Mol Med. 2013; (5): 509–15.
49. Makarov VV, Hromov AV, Gushhin VA, Tkachuk AP. Vozniknovenie novyh infekcij v 21 veke i sposoby ih identifikacii s ispol'zovaniem vysokoproizvoditel'nogo sekvenirovanija (NGS). Vestnik RGMU. 2017; (1): 5–25.
50. Jakovlev SV, Suvorova MP, Beloborodov VB, Basin EE, Eliseeva EV, Kovelenov SV. i dr. Rasprostranennost' i klinicheskoe znachenie nozokomial'nyh infekcij v lechebnyh uchrezhdenijah Rossii: issledovanie JeRGINI. Antibiotiki i himioterapija 2016; 61 (5–6): 32–42.
51. Kozlov RS. Pnevmokokki: uroki proshlogo — vzgljad v budushhee. Smolensk: MAKMAH; 2010.
52. Paterson DL, Rossi F, Baquero F, et al. In vitro susceptibilities of aerobic and facultative Gram-negative bacilli isolated from patient with intra-abdominal infections worldwide: the 2003 Study for Monitoring Antimicrobial Resistance Trend (SMART). J Antimicrob Chemother. 2005; (55): 965–73.
53. Nauchnyj otchet o rezul'tatah issledovanija antibiotikorezistentnosti bakterial'nyh vozbuditelej nozokomial'nyh infekcij v otdelenijah s intensivnym ispol'zovaniem antibiotikov v stacionarah Rossii (ReVANSh). Smolensk: Nauchno-issledovatel'skij institut antimikrobnoj himioterapii; 2009.
54. Bonomo RA, Burd EM, Conly J, Limbago BM, Poirel L, Segre JA, Westblade LF. Carbapenemase-Producing Organisms: A Global Scourge. Clin Infect Dis. 2017 Oct 16.
55. Kohler PP, Volling C, Green K, Uleryk EM, Shah PS, McGeer A. Carbapenem Resistance, Initial Antibiotic Therapy, and Mortality in Klebsiella pneumoniae Bacteremia: A Systematic Review and Meta-Analysis. Infect Control Hosp Epidemiol. 2017 Nov; 38 (11): 1319–28.
56. Zavascki AP, Barth AL, Gaspareto PB, et al. Risk factors for nosocomial infections due to Pseudomonas aeruginosa producing metallo-beta-lactamase in two tertiary-care teaching hospitals. J Antimicrob Chemother. 2006; (58): 882–5.
57. Messadi AA, Lamia T, Kamel B, et al. Association between antibiotic use and changes in susceptibility patterns of P. aeruginosa in an intensive care unit: a 5-year study, 2000–2004. Burns. 2008; (34):1098–102.
58. Jakovlev SV, Procenko DN, Shahova TV. i dr. Antibiotikorezistentnost' v stacionare: kontroliruem li my situaciju? Antibiotiki i himioterapija. 2010; 55 (1–2): 50–58.
59. Tacconelli E, De Angelis G, Cataldo MA, et al. Does antibiotic exposure increase the risk of methicillinresistant Staphylococcus aureus (MRSA) isolation? A systematic review and meta-analysis. J Antimicrob Chemother. 2008; (61): 26–38.
60. Sarma JB, Ahmed GU. Characterisation of methicillin resistant S. aureus strains and risk factors for acquisition in a teaching hospital in northeast India. Indian J Med Microbiol. 2010; (28): 127–9.
61. Fair RJ, Tor Y. Antibiotics and bacterial resistance in the 21st century. Perspect Med Chem. 2014; (6): 25–64.
62. Curcio D. Multidrug-resistant Gram-negative bacterial infections: are you ready for the challenge? Curr Clin Pharmacol. 2014; (9): 27–38.
63. De Angelis GD, D'Inzeo T, Fiori B, et al. Burden of antibiotic resistant Gram-negative bacterial infections: evidence and limits. J Med Microbiol Diagn. 2014; (3): 132–37.
64. Global'nyj plan dejstvij po bor'be s ustojchivost'ju k protivomikrobnym preparatam. VOZ. 2016 g. 7 s. Dostupno po ssylke: http://apps.who.int/gb/ebwha/pdf_files/WHA69/A69_24-ru.pdf
65. Jakovlev SV, Procenko DN, Shahova TV. i dr. Antibiotikorezistentnost' v stacionare: kontroliruem li my situaciju? Antibiotiki i himioterapija. 2010; 55 (1–2): 50–8.
66. Jakovlev SV, Sidorenko SV, Rafal'skij VV, Spichak TV, redaktory. Strategija i taktika racional'nogo primenenija antimikrobnyh sredstv v ambulatornoj praktike. Rossijskie prakticheskie rekomendacii. M.: Izdatel'stvo «Pre100print»; 2014. 121 s.
67. Blair JM, Webber MA, Baylay AJ, et al. Molecular mechanisms of antibiotic resistance. Nat Rev Microbiol. 2015; (13): 42–51.
68. The Protocol for the Prohibition of the Use in War of Asphyxiating, Poisonous or Other Gases, and of Bacteriological Methods of Warfare. United Nations (1925). Available from: http://www.un.org/disarmament/WMD/Bio/1925GenevaProtocol.shtml (last accessed 12 December 2015).
69. World Health Organization. Public health response to biological and chemical weapons — WHO guidance, 2nd edn. Geneva: WHO, 2004.
70. Nuclear Threat Initiative. Available from: http://www.nti.org/country-profiles (last accessed 12 December 2015).
71. Atlas RM. The medical threat of biological weapons. Crit Rev Microbiol. 1998; (24): 157–68.
72. Leitenberg M, Zilinskas RA, editors. The Soviet biological weapons program: a history. Cambridge, MA: Harvard University Press; 2012.
73. Centers for Disease Control and Prevention. Webpage Emergency Preparedness and Response. Specific hazards: Bioterrorism. Available from: http://www.bt.cdc.gov/bioterrorism (last accessed 12 December 2015).
74. Carus WS. Bioterrorism and biocrimes: the illicit use of biological agents since 1900. February 2001 revision. Washington, DC: Center for Counterproliferation Research, National Defense University. 2001. Available from: http://www.fas.org/irp/threat/cbw/carus.pdf (last accessed 12 December 2015).
75. Ackermann GA, Moran KS. Bioterrorism and threat assessment. Weapons of Mass Destruction Commission. 2004. Available from: www.blixassociates.com/wp-content/uploads/2011/03/No22.pdf (last accessed 12 December 2015).
76. Dando M. Bioterrorism: what is the real threat? Science and Technology Report No. 3. UK Global Health Policy Programme. London: The Nuffield Trust, 2005.
77. Kolavic SA, Kimura A, Simons SL, et al. An outbreak of Shigella dysenteriae Type 2 among laboratory workers due to intentional food contamination. JAMA. 1997; (278): 396–8.
78. Wheelis M, Casagrande R, Madden LV. Biological attack on agriculture: low-tech, high-impact bioterrorism. Bioscience. 2002; (52): 569–76.
79. Bourn J. The 2001 Outbreak of Foot and Mouth Disease. Report by the Comptroller and Auditor General, HC 939 Session 2001–2002. London, UK, National Audit Office. 2002. Available from: www.nao.gov.uk (last accessed 12 December 2015).
80. Meuwissen MPM, Van Boven M, Hagenaars TJ, et al. Predicting future costs of high-pathogenicity avian influenza epidemics: large versus small uncertainties. NJAS. 2006; (52): 195–205.
81. Schmitt K, Zacchia NA. Total decontamination cost of the anthrax letter attacks. Biosecur Bioterror. 2012; (10): 1–10.
82. Gibson DG1, Glass JI, Lartigue C, Noskov VN, Chuang RY, Algire MA, et al. Creation of a bacterial cell controlled by a chemically synthesized genome. Science. 2010 Jul 2; 329 (5987): 52–6. DOI: 10.1126/science.1190719.
83. Gibson DG, Venter JC. Synthetic biology: Construction of a yeast chromosome. Nature. 2014 May 8; 509 (7499): 168–9. DOI: 10.1038/509168a.
84. Hutchison CA, Chuang RY, Noskov VN, Assad-Garcia N, Deerinck TJ, Ellisman MH, et al. Design and synthesis of a minimal bacterial genome. Science. 2016 Mar 25; 351 (6280): aad6253. DOI: 10.1126/science.aad6253.
85. Boles KS, Kannan K, Gill J, Felderman M, Gouvis H, Hubby B, et al. Digital-to-biological converter for on-demand production of biologics. Nature Biotechnology. 2017; (35): 672–5

Литература

1. О биологической безопасности. Проект Федерального закона Российской Федерации. (ред. от августа 2016 г.). 30 с. Доступно по ссылке: http://regulation.gov.ru/projects#npa=55658
2. Онищенко Г. Г., Попова А. Ю., Топорков В. П., Смоленский В. Ю., Щербакова С. А., Кутырев В. В. Современные угрозы и вызовы в области биологической безопасности и стратегия противодействия. Проблемы особо опасных инфекций. 2015; (3): 5–9.
3. О состоянии санитарно-эпидемиологического благополучия населения в Российской Федерации в 2017 году: Государственный доклад. М.: Федеральная служба по надзору в сфере защиты прав потребителей и благополучия человека; 2018. 268 с.
4. Покровский В .И., Брико Н. И. Эпидемиология. Учебник. М.: ГЭОТАР-Медиа; 2016. 368 с.
5. Лобзин Ю. В., Белозеров Е. С., Беляева Т. В, Волжанин В. М. Вирусные болезни человека. СПб.: СпецЛит; 2015. 400 с.
6. BioWatch and public health surveillance: Evaluating systems for the early detection of biological threats. Abbreviated version. Washington, DC: The National Academies Press. IOM and NRC. 2011. 252 p.
7. Онищенко Г. Г., Меркулов И. В., Петров Е. Ю., Желобов В. Е., Шевчук Н. А., Селедцова О. В. О ходе иммунизации населения в рамках национального календаря профилактических прививок. Протокол селекторного совещания у руководителя Федеральной службы по надзору в сфере защиты прав потребителей и благополучия человека (Протокол №13 от 20.07.2010). Доступно по ссылке: http://41.rospotrebnadzor.ru/content/protokol-protokol-selektornogo-soveshchaniya-u-rukovoditelya-federalnoy-sluzhby-po-nadzoru-5
8. Основы государственной политики в области обеспечения химической и биологической безопасности Российской Федерации на период до 2025 года и дальнейшую перспективу (утв. Президентом РФ 1 ноября 2013 г. N Пр-2573). Доступно по ссылке: http://www.garant.ru/products/ipo/prime/doc/70423098/
9. Указ Президента РФ от 31.12.2015 N 683 «О Стратегии национальной безопасности Российской Федерации». Доступно по ссылке: http://www.consultant.ru/document/cons_doc_LAW_191669/
10. В России создадут Центр по борьбе с биологическими угрозами. [Электронный ресурс] Paper 16 матра 2015. Доступно по ссылке: https://iz.ru/news/584008 (last accessed 12 September 2018).
11. Постановление Правительства РФ от 30 июня 2004 г. N 322 «Об утверждении Положения о Федеральной службе по надзору в сфере защиты прав потребителей и благополучия человека» (в ред. от 24 января 2017 г.). Доступно по ссылке: http://base.garant.ru/12136005/
12. Приказ Федеральной службы государственной статистики от 28 января 2014 г. N 52 «Об утверждении статистического инструментария для организации Федеральной службой по надзору в сфере защиты прав потребителей и благополучия человека федерального статистического наблюдения за заболеваемостью населения инфекционными и паразитарными болезнями и профилактическими прививками». Доступно по ссылке: http://www.garant.ru/products/ipo/prime/doc/70479106/
13. Статистический учет и отчетность учреждений здравоохранения. М.: Министерство здравоохранения и социального развития Российской Федерации. 2006. 81 с.
14. Федеральный закон от 30.03.1999 N 52-ФЗ «О санитарно-эпидемиологическом благополучии населения» (в ред. от 03.07.2016). Доступно по ссылке: http://www.consultant.ru/document/cons_doc_LAW_22481/
15. Постановление Правительства РФ от 2 февраля 2006 г. N 60 «Об утверждении Положения о проведении социально-гигиенического мониторинга» (в ред. от 4 сентября 2012 г.). Доступно по ссылке: http://base.garant.ru/12144791/
16. СанПиН 2.3.2.1078-01. Гигиенические требования безопасности и пищевой ценности пищевых продуктов. Утверждены главным государственным санитарным врачом Российской Федерации 06 ноября 2001 г. Доступно по ссылке: http://base.garant.ru/4178234/
17. СанПиН 2.1.4.1074-01: Питьевая вода. Гигиенические требования к качеству воды централизованных систем питьевого водоснабжения. Контроль качества. Гигиенические требования к обеспечению безопасности систем горячего водоснабжения. Утверждены главным государственным санитарным врачом Российской Федерации 29 сентября 2001 г. Доступно по ссылке: http://docs.cntd.ru/document/901798042
18. Перечень стандартов, содержащих правила и методы испытаний и измерений, в том числе правила отбора образцов, необходимые для применения и исполнения требований технического регламента Таможенного союза «Требования безопасности пищевых добавок, ароматизаторов и технологических вспомогательных средств» и осуществления оценки (подтверждения) соответствия. Приложение к Единым санитарно-эпидемиологическим и гигиеническим требованиям к товарам, подлежащим санитарно-эпидемиологическому надзору (контролю). Утверждены Решением Комиссии Таможенного союза от 28 мая 2010 года № 299. (в ред. от 09 декабря 2011 г.)
19. Dzenitis JM, Makarewicz AJ. The Autonomous Pathogen Detection System. The Microflow Cytometer. 2010: 263–84.
20. Hindson BJ, Makarewicz AJ, Setlur US, Henderer BD, McBride MT, Dzenitis JM. APDS: the autonomous pathogen detection system. Biosens Bioelectron. 2005; 20 (10): 1925–31.
21. Онищенко Г. Г., Кузькин Б. П., Демина Ю. В. и др. Обеспечение готовности и организация работы СПЭБ ФКУЗ «Ставропольский противочумный институт» Роспотребнадзора в период проведения XXII Олимпийских и XI Паралимпийских зимних игр в Сочи. Проблемы особо опасных инфекций. 2015; (1): 58–62.
22. GAO-14-267T BIOSURVEILLANCE: Observations on the Cancellation of BioWatch Gen-3 and Future Considerations for the Program. GAO. Statement of Chris Currie, Acting Director, Homeland Security and Justice. Washington, D.C.: 2014.
23. Fournier PE, Raoult D. Prospects for the future using genomics and proteomics in clinical microbiology. Annu Rev Microbiol. 2011; (65): 169–188.
24. Diene SM, Bertelli C, Pillonel T, Schrenzel J, Greub G. Bacterial genomics and metagenomics: clinical applications and medical relevance. Rev Med Suisse. 2014; 10 (450): 2155–61.
25. Zhou K, Ferdous M, de Boer RF, Kooistra-Smid AM, Grundmann H, Friedrich AW, et al. The mosaic genome structure and phylogeny ofShiga toxin-producing Escherichia coli O104:H4 is driven by short-termadaptation. Clin Microbiol Infect. 2015; 21 (468): e467–18.
26. Zhou K, Lokate M, Deurenberg RH, Tepper M, Arends JP, Raangs EG, et al. Use ofwhole-genome sequencing to trace, control and characterize the regionalexpansion of extended-spectrum beta-lactamase producing ST15 Klebsiellapneumoniae. Sci Rep. 2016; (6): 20840.
27. Weterings V, Zhou K, Rossen JW, van Stenis D, Thewessen E, Kluytmans J, et al. An outbreak of colistin-resistant Klebsiella pneumoniaecarbapenemase-producing Klebsiella pneumoniae in the Netherlands (July–December 2013), with inter-institutional spread. Eur J Clin Microbiol Infect Dis. 2015; (34): 1647–55.
28. Ferdous M, Zhou K, de Boer RF, Friedrich AW, Kooistra-Smid AM, Rossen JW, Comprehensive characterization of Escherichia coli O104:H4isolated from patients in the Netherlands. Front Microbiol. 2015; (6): 1348.
29. Bathoorn E, Rossen JW, Lokate M, Friedrich AW, Hammerum AM. Isolation of an NDM-5-producing ST16 Klebsiella pneumoniae from a Dutchpatient without travel history abroad, August

2015. Euro Surveil. 2015; (20): 30040.
30. Falgenhauer L, Waezsada SE, Yao Y, Imirzalioglu C, Kasbohrer A, Chakraborty T. Colistin resistance gene mcr-1 in extended-spectrumbeta-lactamase-producing and carbapenemase-producing Gram-negativebacteria in Germany. Lancet Infect Dis. 2016; (16): 282–283.
31. Aanensen DM, Feil EJ, Holden MT, Dordel J, Yeats CA, Fedosejev A, et al. Whole-genome sequencing for routine pathogen surveillancein public health: a population snapshot of invasive Staphylococcus aureus in Europe. Mbio. 2016; 7 (3): e00444–16.
32. Fournier PE, Dubourg G, Raoult D. Clinical detection and characterizationof bacterial pathogens in the genomics era. Genome Med. 2014; (6): 114.
33. Hasman H, Saputra D, Sicheritz-Ponten T, Lund O, Svendsen CA, Frimodt-Moller N, et al. Rapid whole-genome sequencing fordetection and characterization of microorganisms directly from clinicalsamples. J Clin Microbiol. 2014; (52): 139–46.
34. Franz E, Delaquis P, Morabito S, Beutin L, Gobius K, Rasko DA, et al. Exploiting the explosion ofinformation associated with whole genome sequencing to tackle Shigatoxin-producing Escherichia coli (STEC) in global food production systems. Int J Food Microbiol. 2014; (187): 57–72.
35. Laabei M, Recker M, Rudkin JK, Aldeljawi M, Gulay Z, Sloan TJ, et al. Predicting the virulence of MRSA from its genome sequence. Genome Res. 2014; (24): 839–49.
36. Ferdous M, Friedrich AW, Grundmann H, de Boer RF, Croughs PD, Islam MA, et al. Molecular characterization and phylogeny of Shiga toxin-producingEscherichia coli isolates obtained from two Dutch regions using whole genomesequencing. Clin Microbiol Infect 2016; (22): 642.e1–642.e9.
37. Nijhuis RH, Oueslati S, Zhou K, Bosboom RW, Rossen JW, Naas T, et al. OXY-2-15, a novel variant showing increased ceftazidime hydrolytic activity. J Antimicrob Chemother. 2015; (70): 1429–33.
38. Hasman H, Saputra D, Sicheritz-Ponten T, Lund O, Svendsen CA, Frimodt-Moller N, et al. Rapid whole-genome sequencing fordetection and characterization of microorganisms directly from clinicalsamples. J Clin Microbiol 2014; (52): 139–46.
39. Patel JB. 16S rRNA gene sequencing for bacterial pathogen identification inthe clinical laboratory. Mol Diagn. 2001; (6): 313–21.
40. Schuurman T, de Boer RF, Kooistra-Smid AM, van Zwet AA. Prospectivestudy of use of PCR amplification and sequencing of 16S ribosomal DNA fromcerebrospinal fluid for diagnosis of bacterial meningitis in a clinical setting. J Clin Microbiol. 2004; (42): 734–40.
41. Srinivasan L, Pisapia JM, Shah SS, Halpern CH, Harris MC. Canbroad-range 16S ribosomal ribonucleic acid gene polymerase chain reactionsimprove the diagnosis of bacterial meningitis? A systematic review andmeta-analysis. Ann Emerg Med. 2012; (60): 609–20.
42. Kalia VC, Kumar R, Kumar P, Koul S. A genome-wide profiling strategy asan aid for searching unique identification biomarkers for Streptococcus. Indian J Microbiol. 2016; (56): 46–58.
43. Sabat AJ, van Zanten E, Akkerboom V, Wisselink G, van Slochteren K, de Boer RF. Targetedamplification for bacterial identification at the species-level usingnext-generation sequencing—increased discrimination of closely relatedspecies. ECCMID. 2016; E-poster EP0219.
44. Daubin V, Gouy M, Perriere G. Bacterial molecular phylogeny usingsupertree approach. Genome Inform. 2001; (12): 155–64.
45. Thompson CC, Chimetto L, Edwards RA, Swings J, Stackebrandt E, Thompson FL. Microbial genomic taxonomy. BMC Genom. 2013; (14): 913.
46. Tenover FC, Arbeit RD, Goering RV. How to select and interpretmolecular strain typing methods for epidemiological studies of bacterialinfections: a review for healthcare epidemiologists. Molecular Typing WorkingGroup of the Society for Healthcare Epidemiology of America. Infect Control Hosp Epidemiol. 1997; (18): 426–39.
47. Sabat AJ, Budimir A, Nashev D, Sa-Leao R, van Dijl J, Laurent F, et al. Overview of molecular typing methods for outbreakdetection and epidemiological surveillance. Euro Surveil. 2013; (18): 20380.
48. Harrison EM, Paterson GK, Holden MT, Larsen J, Stegger M, Larsen AR, et al. Whole genomesequencing identifies zoonotic transmission of MRSA isolates with the novelmecA homologue mecC. EMBO Mol Med. 2013; (5): 509–15.
49. Макаров В. В., Хромов А. В., Гущин В. А., Ткачук А. П. Возникновение новых инфекций в 21 веке и способы их идентификации с использованием высокопроизводительного секвенирования (NGS). Вестник РГМУ. 2017; (1): 5–25.
50. Яковлев С. В., Суворова М. П. , Белобородов В. Б., Басин Е. Е., Елисеева Е. В., Ковеленов С. В. и др. Распространенность и клиническое значение нозокомиальных инфекций в лечебных учреждениях России: исследование ЭРГИНИ. Антибиотики и химиотерапия 2016; 61 (5–6): 32–42.
51. Козлов Р. С. Пневмококки: уроки прошлого — взгляд в будущее. Смоленск: МАКМАХ; 2010.
52. Paterson DL, Rossi F, Baquero F, et al. In vitro susceptibilities of aerobic and facultative Gram-negative bacilli isolated from patient with intra-abdominal infections worldwide: the 2003 Study for Monitoring Antimicrobial Resistance Trend (SMART). J Antimicrob Chemother. 2005; (55): 965–73.
53. Научный отчет о результатах исследования антибиотикорезистентности бактериальных возбудителей нозокомиальных инфекций в отделениях с интенсивным использованием антибиотиков в стационарах России (РеВАНШ). Смоленск: Научно-исследовательский институт антимикробной химиотерапии; 2009.
54. Bonomo RA, Burd EM, Conly J, Limbago BM, Poirel L, Segre JA, Westblade LF. Carbapenemase-Producing Organisms: A Global Scourge. Clin Infect Dis. 2017 Oct 16.
55. Kohler PP, Volling C, Green K, Uleryk EM, Shah PS, McGeer A. Carbapenem Resistance, Initial Antibiotic Therapy, and Mortality in Klebsiella pneumoniae Bacteremia: A Systematic Review and Meta-Analysis. Infect Control Hosp Epidemiol. 2017 Nov; 38 (11): 1319–28.
56. Zavascki AP, Barth AL, Gaspareto PB, et al. Risk factors for nosocomial infections due to Pseudomonas aeruginosa producing metallo-beta-lactamase in two tertiary-care teaching hospitals. J Antimicrob Chemother. 2006; (58): 882–5.
57. Messadi AA, Lamia T, Kamel B, et al. Association between antibiotic use and changes in susceptibility patterns of P. aeruginosa in an intensive care unit: a 5-year study, 2000–2004. Burns. 2008; (34):1098–102.
58. Яковлев С. В., Проценко Д. Н., Шахова Т. В. и др. Антибиотикорезистентность в стационаре: контролируем ли мы ситуацию? Антибиотики и химиотерапия. 2010; 55 (1–2): 50–58
59. Tacconelli E, De Angelis G, Cataldo MA, et al. Does antibiotic exposure increase the risk of methicillinresistant Staphylococcus aureus (MRSA) isolation? A systematic review and meta-analysis. J Antimicrob Chemother. 2008; (61): 26–38.
60. Sarma JB, Ahmed GU. Characterisation of methicillin resistant S. aureus strains and risk factors for acquisition in a teaching hospital in northeast India. Indian J Med Microbiol. 2010; (28): 127–9.
61. Fair RJ, Tor Y. Antibiotics and bacterial resistance in the 21st century. Perspect Med Chem. 2014; (6): 25–64.
62. Curcio D. Multidrug-resistant Gram-negative bacterial infections: are you ready for the challenge? Curr Clin Pharmacol. 2014; (9): 27–38.
63. De Angelis GD, D'Inzeo T, Fiori B, et al. Burden of antibiotic resistant Gram-negative bacterial infections: evidence and limits. J Med Microbiol Diagn. 2014; (3): 132–37.
64. Глобальный план действий по борьбе с устойчивостью к противомикробным препаратам. ВОЗ. 2016 г. 7 с. Доступно по ссылке: http://apps.who.int/gb/ebwha/pdf_files/WHA69/A69_24-ru.pdf
65. Яковлев С. В., Проценко Д. Н., Шахова Т. В. и др. Антибиотикорезистентность в стационаре: контролируем ли мы ситуацию? Антибиотики и химиотерапия. 2010; 55

(1–2): 50–8.
66. Яковлев С. В., Сидоренко С. В., Рафальский В. В., Спичак Т. В., редакторы. Стратегия и тактика рационального применения антимикробных средств в амбулаторной практике. Российские практические рекомендации. М.: Издательство «Пре100принт»; 2014. 121 с.
67. Blair JM, Webber MA, Baylay AJ, et al. Molecular mechanisms of antibiotic resistance. Nat Rev Microbiol. 2015; (13): 42–51.
68. The Protocol for the Prohibition of the Use in War of Asphyxiating, Poisonous or Other Gases, and of Bacteriological Methods of Warfare. United Nations (1925). Available from: http://www.un.org/disarmament/WMD/Bio/1925GenevaProtocol.shtml (last accessed 12 December 2015).
69. World Health Organization. Public health response to biological and chemical weapons — WHO guidance, 2nd edn. Geneva: WHO, 2004.
70. Nuclear Threat Initiative. Available from: http://www.nti.org/country-profiles (last accessed 12 December 2015).
71. Atlas RM. The medical threat of biological weapons. Crit Rev Microbiol. 1998; (24): 157–68.
72. Leitenberg M, Zilinskas RA, editors. The Soviet biological weapons program: a history. Cambridge, MA: Harvard University Press; 2012.
73. Centers for Disease Control and Prevention. Webpage Emergency Preparedness and Response. Specific hazards: Bioterrorism. Available from: http://www.bt.cdc.gov/bioterrorism (last accessed 12 December 2015).
74. Carus WS. Bioterrorism and biocrimes: the illicit use of biological agents since 1900. February 2001 revision. Washington, DC: Center for Counterproliferation Research, National Defense University. 2001. Available from: http://www.fas.org/irp/threat/cbw/carus.pdf (last accessed 12 December 2015).
75. Ackermann GA, Moran KS. Bioterrorism and threat assessment. Weapons of Mass Destruction Commission. 2004. Available from: www.blixassociates.com/wp-content/uploads/2011/03/No22.pdf (last accessed 12 December 2015).
76. Dando M. Bioterrorism: what is the real threat? Science and Technology Report No. 3. UK Global Health Policy Programme. London: The Nuffield Trust, 2005.
77. Kolavic SA, Kimura A, Simons SL, et al. An outbreak of Shigella dysenteriae Type 2 among laboratory workers due to intentional food contamination. JAMA. 1997; (278): 396–8.
78. Wheelis M, Casagrande R, Madden LV. Biological attack on agriculture: low-tech, high-impact bioterrorism. Bioscience. 2002; (52): 569–76.
79. Bourn J. The 2001 Outbreak of Foot and Mouth Disease. Report by the Comptroller and Auditor General, HC 939 Session 2001–2002. London, UK, National Audit Office. 2002. Available from: www.nao.gov.uk (last accessed 12 December 2015).
80. Meuwissen MPM, Van Boven M, Hagenaars TJ, et al. Predicting future costs of high-pathogenicity avian influenza epidemics: large versus small uncertainties. NJAS. 2006; (52): 195–205.
81. Schmitt K, Zacchia NA. Total decontamination cost of the anthrax letter attacks. Biosecur Bioterror. 2012; (10): 1–10.
82. Gibson DG1, Glass JI, Lartigue C, Noskov VN, Chuang RY, Algire MA, et al. Creation of a bacterial cell controlled by a chemically synthesized genome. Science. 2010 Jul 2; 329 (5987): 52–6. DOI: 10.1126/science.1190719.
83. Gibson DG, Venter JC. Synthetic biology: Construction of a yeast chromosome. Nature. 2014 May 8; 509 (7499): 168–9. DOI: 10.1038/509168a.
84. Hutchison CA, Chuang RY, Noskov VN, Assad-Garcia N, Deerinck TJ, Ellisman MH, et al. Design and synthesis of a minimal bacterial genome. Science. 2016 Mar 25; 351 (6280): aad6253. DOI: 10.1126/science.aad6253.
85. Boles KS, Kannan K, Gill J, Felderman M, Gouvis H, Hubby B, et al. Digital-to-biological converter for on-demand production of biologics. Nature Biotechnology. 2017; (35): 672–5.

MULTIPARAMETRIC DETECTION OF BACTERIAL CONTAMINATION BASED ON THE PHOTONIC CRYSTAL SURFACE MODE DETECTION

Petrova IO[1], Konopsky VN[2], Sukhanova AV[1], Nabiev IR[1] ✉

[1] Laboratory of Nano-Bioengineering, National Research Nuclear University MEPhI (Moscow Engineering Physics Institute), Moscow

[2] Laboratory of Spectroscopy of Condensed Matter, Institute for Spectroscopy, Russian Academy of Sciences, Troitsk

Conventional techniques for food and water quality control and environmental monitoring in general have a number of drawbacks. Below we propose a label-free highly accurate analytical technique for multiplex detection of biomarkers based on the analysis of propagation of Bloch waves on the surface of a photonic crystal. The technique can be used to measure molecular and cell affinity interactions in real time by recording critical and excitation angles of the surface wave on the surface of a photonic crystal. Based on the analysis of photonic crystal surface modes, we elaborated a protocol for the detection of the exotoxin A of *Pseudomonas aeruginosa* and the heat-labile toxin LT of *Escherichia coli*. The protocol exploits detection of affinity interactions between antigens pumped through a microfluidic cell and detector antibodies conjugated to the chemically activated silica chip. The proposed technique is highly sensitive, cheap and less time-consuming in comparison with surface plasmon resonance.

Keywords: photonic crystals, surface modes, bacterial toxins, real-time detection

Funding: this work was part of the Federal Targeted Program *The National system of Chemical and Biological Security of the Russian Federation (2015-2020)* supported by the Ministry of Healthcare of the Russian Federation (State grant No. K-27-НИР/144-5 dated December 24, 2015).

Acknowledgement: the authors wish to thank Tkachuk AP, Head of the Department of Translational Biomedicine (Gamaleya Research Institute of Epidemiology and Microbiology) for rabbit antibodies against the heat-labile toxin LT.

✉ **Correspondence should be addressed:** Igor R. Nabiev
Kashirskoe shosse 31, Moscow, 115529; igor.nabiev@gmail.com

Received: 28.07.2018 **Accepted:** 20.08.2018

DOI: 10.24075/brsmu.2018.047

МНОГОПАРАМЕТРИЧЕСКАЯ ДЕТЕКЦИЯ БАКТЕРИАЛЬНОГО ОБСЕМЕНЕНИЯ С ПОМОЩЬЮ АНАЛИЗА ИЗМЕНЕНИЙ РАСПРОСТРАНЕНИЯ ПОВЕРХНОСТНЫХ ВОЛН В ФОТОННЫХ КРИСТАЛЛАХ

И. О. Петрова[1], В. Н. Конопский[2], А. В. Суханова[1], И. Р. Набиев[1] ✉

[1] Лаборатория нано-биоинженерии, Национальный исследовательский ядерный университет «МИФИ» (Московский инженерно-физический институт), Москва

[2] Лаборатория спектроскопии конденсированных сред, Институт спектроскопии РАН, Троицк

Традиционные методы оценки качества продуктов питания, воды и других сред имеют ряд недостатков. Предлагается безметочный высокоточный аналитический метод многопараметрической детекции биомаркеров, основанный на анализе изменений параметров распространения поверхностных волн на поверхности фотонного кристалла (ПВФК). Метод позволяет проводить измерения молекулярных и клеточных аффинных взаимодействий в реальном времени путем независимой регистрации величин угла полного внутреннего отражения и угла возбуждения поверхностной волны на поверхности фотонного кристалла. На основании метода анализа ПВФК разработан протокол детекции экзотоксина А *Pseudomonas aeruginosa* и термолабильного токсина LT *Escherichia coli*. Протокол основан на детекции в реальном времени аффинного взаимодействия между антигенами, раствор которых прокачивается через микрофлюидную ячейку, и специфическими распознающими антителами, конъюгированными с химически активированной кремниевой подложкой каналов поверхности ФК. Показано, что метод ПВФК отличается более высокой чувствительностью, а также уменьшенным временем проведения анализа и сниженной материалозатратностью, по сравнению с методом поверхностного плазмонного резонанса.

Ключевые слова: фотонные кристаллы, поверхностные волны, бактериальные токсины, детекция в реальном времени

Финансирование: исследование поддержано Министерством здравоохранения Российской Федерации, в рамках Федеральной целевой программы «Национальная система химической и биологической безопасности Российской Федерации (2015–2020 годы)», государственный контракт № К-27-НИР/144-5 от 24.12.2015 г.

Благодарности: авторы благодарны заведующему лабораторией трансляционной биомедицины ФГБУ «НИЦЭМ им. Н. Ф. Гамалеи» Минздрава России А. П. Ткачуку за предоставление кроличьих антител против термолабильного токсина LT.

✉ **Для корреспонденции:** Игорь Руфаилович Набиев
Каширское шоссе, д. 31, г. Москва, 115529; igor.nabiev@gmail.com

Статья получена: 28.07.2018 **Статья принята к печати:** 20.08.2018

DOI: 10.24075/vrgmu.2018.047

Detection of pathogenic bacteria and their toxins in liquid samples is a critical component of food and water quality control and the environmental monitoring in general. Polymerase chain reaction (PCR), a well-established technique for pathogen detection, is highly sensitive yet lengthy, reagent-consuming and labor-intensive. Besides, it cannot recognize bacterial metabolites, including protein toxins (primary pathogenicity determinants), and other specific proteins, such as prions, since it is aimed at detecting nucleic acids.

At present, detection of proteins (e.g., protein toxins) in liquid samples is done by classic analytical techniques. Conventional western blotting and enzyme-linked immunosorbent assays (ELISA) are relatively user-friendly and cost-effective but at the same time low-throughput and time-consuming. They are

suitable for clinical diagnosis but require additional sample preparation involving the use of enzymatic and fluorescent labels to amplify the emitted signal, which increases costs and complicates the procedure.

Fortunately, novel techniques are emerging, including electrochemical immunoassays [1–2], chemiluminescence imaging [3], fluorescence flow immunoassays with activated silica beads [4], and electrochemical assays based on the use of affibodies [5]. Advantageously, all of them are multiplex, i.e. able to detect multiple analytes in one sample. Unlike traditional approaches, these techniques are high-throughput; however, they are expensive and the yielded results are difficult to interpret, which makes them unsuitable for routine use. The majority of these techniques rely on the use of additional labels, except for the label-free electrochemical assay, a sensitive and elegant approach, which, nevertheless, cannot be multiplexed [6].

Great promise is held by surface plasmon resonance [7] based on the excitation of surface plasmon polaritons at the metal/dielectric interface by incident light. This fast and sensitive label-free technique can go without complicated sample preparation. It exploits antibodies specific for a target protein that are conjugated to the surface of a thin gold film; soluble antigens present in the liquid sample bind to the antibodies, and the resulting mass transfer is manifested as a change in the refractive index value of the superficial layer of the liquid close to the surface of the golden film.

I. Design of the experiment

We propose a novel approach to the detection of bacterial contamination based on the use of photonic crystal surface modes (PCSMs). A photonic crystal is a structure in which the refractive index (RI) is periodically modulated on the scale of a light wavelength. Such structures maintain the far-reaching longitudinal propagation of optical waves across the external surface. PCSMs are exploited in optical sensors [8–10]. PCSM-based sensors are reported to be more sensitive than those relying on surface plasmon resonance [9]. PCSMs allow detection of both parallel and perpendicular polarization of the light wave, meaning that the thickness of the surface layer and the refractive index of the liquid phase can be measured separately and a change in the reflected signal is indicative of a mass transfer event (interaction of a soluble analyte with a functionalized crystal surface) regardless of the refractive index shifts occurring in close proximity to this surface.

Advantageously, this approach allows easy recovery of a chip surface by plasma cleaning. The chip can be reactivated and conjugated to another detector protein. This means that the PC chip can be used an infinite number of times and activated in advance before the actual experiment.

In this work we studied the interaction between the polymer microbeads coated with a layer of a polyelectrolyte (negatively charged polyacrylic acid) and the surface of a PCSM-based sensor coated with positively charged poly(sodium 4-styrenesulfonate). Because of their size (4.08 μm in diameter), microbeads can represent a bacterial cell model. Given that, our work demonstrates the feasibility of bacterial cell detection in a liquid sample using a PCSM-based biosensor.

Besides we show that a PCSM-based biosensor can detect bacterial toxins in a liquid sample using the exotoxin A of *Pseudomonas aeruginosa* and the heat-labile toxin LT of *Escherichia coli*.

Below we describe the main stages in the development of the proposed analytical technique for the multiplex detection of biomarkers and its application for the detection of bacterial toxins.

II. Preparation

1. Reagents

The following reagents were used: sodium chloride, > 99% (Sigma-Aldrich, S6191; USA); ethanol, 99.5% (Acros Organics, AC615090010; Belgium); acetone for high-performance liquid chromatography, 99.8% (Acros Organics, 268310010; Belgium); (3-aminopropyl)triethoxysilane (APTES), 99% (Sigma-Aldrich, 440140; USA); glutaraldehyde, grade I, 25% in H_2O (Sigma-Aldrich, G5882; USA); sodium phosphate dibasic heptahydrate, 98–102% (Sigma-Aldrich, S9390; USA); sodium phosphate monobasic monohydrate, ≥ 98% (Sigma-Aldrich, S9638; USA); phosphate buffered saline (PBS), tablets (Sigma-Aldrich, P4417; USA); protein A, United States Pharmacopeia (USP) Reference Standard (Sigma-Aldrich, 1578805; USA); poly(sodium 4-styrenesulfonate) (PSS), average Mw ~70,000 (Sigma-Aldrich, 243051; USA); poly(allylamine hydrochloride) (PAH), average Mw ~50,000 (Sigma-Aldrich, 283223; USA); poly(acrylic acid) (PAA), average Mw ~130,000 (Sigma-Aldrich, 181293; USA); rabbit antibodies to the exotoxin A of *Pseudomonas aeruginosa*, whole antiserum (Sigma-Aldrich, P2318; USA); the exotoxin A of *Pseudomonas aeruginosa*, lyophilized powder (Sigma-Aldrich, P0184; USA); the heat-labile recombinant toxin LT of *Escherichia coli*, subunit B, > 90%, lyophilized powder (Sigma-Aldrich, E8656; USA); crystalline bovine serum albumin (BSA), lyophilized powder, ≥ 98.0% (GE) (Sigma-Aldrich, 05470; USA).

The rabbit antibodies against the heat-labile toxin LT were courtesy of Tkachuk AP, Head of the Department of Translational Biomedicine, Gamaleya Research Institute of Epidemiology and Microbiology.

2. A biosensor based on the detection of surface modes in a photonic crystal

We used the PCSM-based biosensor EVA 2.0 described in [10] with the following one-dimensional PC structure: substrate/$(LH)_3L'$/water, where L is a SiO_2 layer with thickness d_1 = 186.4 nm, H is a Ta_2O_5 layer with thickness d_2 = 115.2 nm, and L' is a SiO_2 layer with thickness d_3 = 776.8 nm.

The 7-layer structure with the starting and finishing layers made of SiO_2 was created by magnetron sputtering. The prism and the glass plate were fabricated from BK-7 glass. Refractive indices of the substrate, SiO_2, Ta_2O_5 and water at λ = 632.8 nm were n_0 = 1.515, $n_1 = n_3$ = 1.47, n_2 = 2.07, and n_e = 1.332, respectively.

The obtained data were processed in Origin 8.1 (OriginLab; USA).

3. Microbeads

Latex microbeads of 4.08 μm in diameter (MF-COOH-AR421 Carboxyl-modified Melamine Resin-Research Particles, 10 ml 10% w/v aq. suspension (microParticles GmbH; Germany)) were coated with alternating layers of the oppositely charged polyelectrolytes PAH and PSS using the layer-by-layer deposition technique proposed in [11] following the pattern PAH/PSS/PAH/PSS/PAH; the coating was finished with a layer of PAA.

4. Preparation of the photonic crystal silica chip for the experiment with microbeads

Before the experiment, the silica PC chip was left in the UV cleaner box for at least 30 min.

The chip was mounted in the microfluidic flow cell for further measurements. To make the liquid flow through the cell, a peristaltic pump was used. After the flow cell was assembled, 1% aqueous APTES solution was pumped through it at 100 µl/min for 5 min to activate the surface of the PC by amino groups. Then 100 mg/ml solutions of PSS and PAH in 0.5 NaCl were pumped through the flow cell successively for 5 min each. Before changing the solution, the flow cell was washed with 0.5 NaCl. To ensure even coating of the chip, three bilayers of PSS/PHH were applied onto it in succession. After applying the finishing layer of PAH, the medium was replaced with 100 mM sodium phosphate buffer (pH 8.0) containing 0.5 M NaCl. The microbeads were suspended in the same buffer at a concentration of 10^6 beads per 1 ml. The microbead suspension was pumped through the flow cell at 100 µl/min for 10 min.

5. Preparation of the photonic crystal silica chip for the experiments with proteins

The PC chip was left in the UV cleaner box for 30 min to clean each side of the crystal and then washed once in acetone and once in ethanol successively followed by 3 washes in milliQ, with simultaneous exposure to UV light for 5 min. After that, the substrate was left to dry at 70 °C. The cleaned chip was incubated in 1% APTES solution in acetone for 16 h to functionalize its surface by amino groups and then calcinated at 120 °C for 90 min. Such aminized chips can be stored for at least one month without losing their properties. Before taking measurements, the chip was treated with 2.5% glutaraldehyde in the sodium-phosphate buffer (pH 7.4) under gentle stirring for 30 min. Dextran or other polymer frameworks were not used for chip preparation.

The flow cell was attached to the prepared chip. The flow speed was 30 µl/min. To functionalize the surface of the chip with detector antibodies, the solution of protein A (50 µg/ml) in PBS was pumped through the cell until the signal stabilized. Then the flow cell was washed in PBS for 2 min. After the monolayer of protein A bound to the surface of the chip, the antibody solution (50 µg/ml) was pumped through the flow cell again until the signal was stable. Protein A present on the surface of the PC chip bound the Fc fragment of the immunoglobulin ensuring a uniform orientation pattern of bound antibodies. The surface regions that did not react with the protein were neutralized with 2% solution of bovine serum albumin (BSA) in PBS, and the flow cell was washed with PBS until the signal reached the plateau. Finally, the studied sample was pumped though the cell at 30 µl/min.

III. Deposition of polyelectrolyte-coated microbeads on the chip coated with a layer of an oppositely charged polyelectrolyte

Layer-by-layer deposition of polyelectrolytes on the APTES-activated chip surface caused a stepwise increase in the thickness of the superficial layer (Fig. 1A). Thickness values observed for the first PSS and PAH layers were lower than those observed for the subsequent layers, suggesting that two first layers of polyelectrolytes covered the surface incompletely.

The binding of PAA-coated microbeads to the surface of the crystal caused the superficial layer to slowly grow in thickness. This phenomenon was not observed if the buffer solution pumped through the flow cell did not contain microbeads.

Notably, the kinetics of microbead binding was linear (R^2 = 0.996) and not dose dependent (Fig. 1B), possibly due to a low concentration of microbeads unable to saturate the chip surface (the area of the chip surface in contact with the solution was 1 cm^2, as determined by the flow cell architecture). The area on the chip surface occupied by one microbead did not exceed 13 μm^2, i.e. to fully cover the surface one would need ~10^7 microbeads. Therefore, the thickness of the microbead monolayer could be expected to be equal to the diameter of the microbead, i.e. 4.08 µm. Accordingly, the binding of 10^6 microbeads would correspond to a 400 nm thickness of the superficial layer. However, at low thickness values we can only measure the optical depth of a layer, that is its physical thickness multiplied by the refractive index. By taking the refractive index equal to 1.56 [10], we get the expected thickness of 624 nm consistent with the observed thickness. Knowing the flow rate, the rate of superficial thickness growth and the concentration of microbeads, we can estimate the number of the bound microbeads. As the microbeads are pumped through the cell for 10 min, the superficial layer increases in thickness by 0.57 nm, meaning that 1 × 10^3 microbeads (0.1% of the total number of pumped microbeads) have been bound.

IV. Detection of bacterial toxins

To attempt detection of protein toxins in a solution using the PCSW-based biosensor, we selected two toxins: the exotoxin of *Pseudomonas aeruginosa* and the heat-labile toxin of *Escherichia coli*.

Pseudomonas aeruginosa is a gram-negative motile rod-shaped bacterium sized 1–5 µm by 0.5–1 µm. It inhabits water and soil and causes opportunistic and nosocomial infections in humans. The exotoxin A of the bacteria consists of three domains: binding, transport and catalytic. Its cytotoxic activity is determined by the catalytic domain that inhibits synthesis of proteins by ATP-ribosylation of the elongation factor EF-2 [12–13]. Detection of this exotoxin is an important diagnostic problem normally solved by PCR which identifies the gene coding for it [14], ELISA which detects the presence of this toxin and a few other analytical techniques.

Escherichia coli is a gram-negative rod-shaped bacterium colonizing the lower intestinal tract of warm-blooded organisms. Enterotoxigenic strains of *Escherichia coli* can cause diarrhea by producing toxins such as the heat labile LT toxin. The latter consists of two subunits: the catalytically active subunit A and the subunit B responsible for the binding to the cell [15]. LT expression stimulates secretion and facilitates the binding of the bacteria to epithelial cells [16].

For toxin detection, we developed a system consisting of flow cells with 1, 2 or 4 channels. Briefly, the glass chamber with 1, 2 or 4 grooves is connected to a chemically activated sensitive surface of the silica chip functionalized with detector molecules. The amplitude of the signal recorded during antigen-antibody interactions on the sensor surface is directly proportional to the number of binding sites on the surface. The surface regions that have not reacted with the antigen are coated with BSA to avoid emission of a nonspecific signal.

If a cell has 2 or 4 channels, 1 of them can be used as a negative control; its surface is coated with BSA instead of antibodies.

In the experiment, the 50 µg/ml solution of the exotoxin A of *Pseudomonas aeruginosa* in PBS was pumped through the flow cell at 100 µl/min (Fig. 2). The obtained curve was similar to the SPR sensorgram and followed the same pattern of kinetics [17]. The binding of the protein to the sensor surface

caused a rapid increase in the thickness of the superficial layer, which reaches the plateau quite soon. The plateau represents the equilibrium between the absorption and desorption rates. The kinetic curve can be approximated using the Langmuir absorption model. It has been theorized that the detection limit allowed by PCSM is 70 fg/mm^2 of the studied sensor surface, which is well above the sensitivity of surface plasmon resonance [18]. But in practice, the lowest detectable concentration of exotoxin A in our experiment was 30 μg/ml, in spite of the low levels of the background noise. The sensorgram recorded during the detection of the heat-labile toxin LT (50 μg/ml in PBS) demonstrated that the detection limit was 10 μg/ml (Fig. 3).

Of note, in the experiment we used whole antiserum. The use of affinity purified antibodies will definitely improve the sensitivity of the biosensor allowing it to reach the anticipated value [18], which is way higher than the sensitivity of surface plasmon resonance.

V. Kinetics of bacterial cell binding to the surface of the sensor functionalized with antibodies

The upper limit of the binding rate for the microbeads was calculated using the Smoluchowski-Levich equation [19] and was 3.46 particles/cm^2; the working surface of the sensor was 1 cm^2, so the calculated value meant that 2,000 particles would be bound within 10 min. Here we can conclude that the binding rate of polyelectrolyte-coated microbeads to the surface of the biosensor coated with the oppositely charged polyelectrolyte in our system was close to the highest possible rate. Perhaps, it did not reach its maximum because the binding of microbeads to the surface is not instant and under real life conditions is determined not only by the diffusion of microparticles but also by their interaction with the surface. Therefore, we assume that the kinetics of bacterial cell binding to the sensor surface functionalized by antibodies

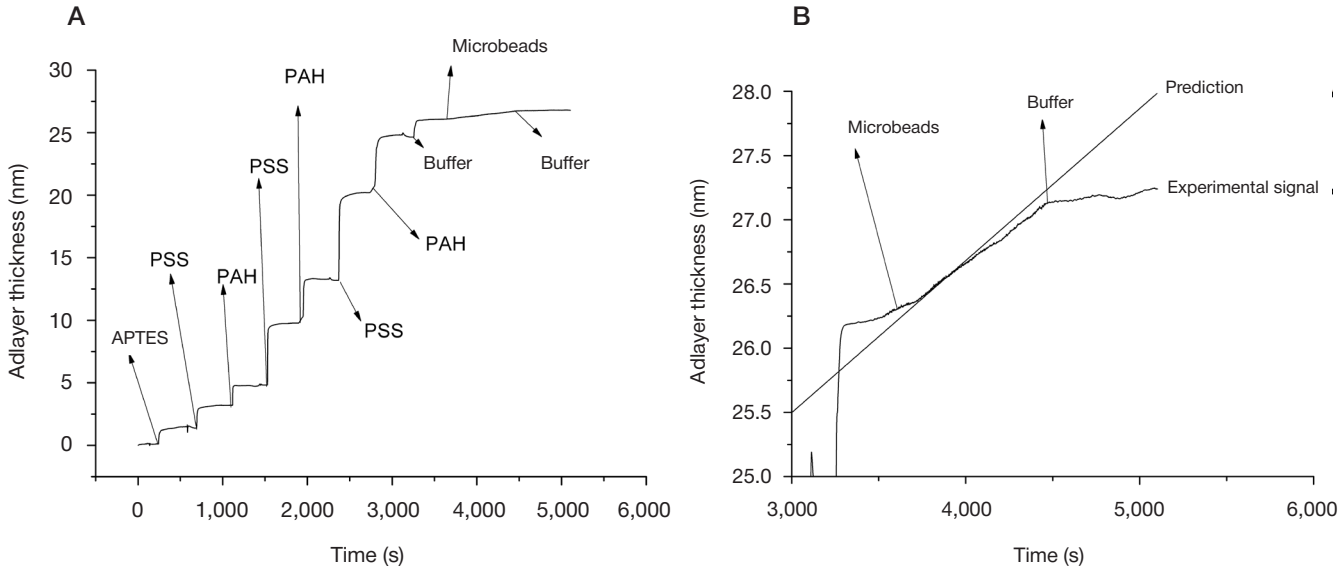

Fig. 1. Changes in the thickness of the superficial layer of the photonic crystal-based biosensor at the successive stages of surface preparation and the experiment studying the interaction between the polyelectrolyte-coated microbeads and the photonic crystal chip coated with an oppositely charged polyelectrolyte. Figure **A** shows how the adlayer on the surface of the photonic crystal changed in thickness when the crystal was treated with amino groups (APTES) and subjected to the deposition of layers of oppositely charged polyelectrolytes poly(sodium 4-styrenesulfonate) (PSS) and poly(allylamine hydrochloride) (PAH). The thickness of the surface increased with every applied layer of polyelectrolytes. The effect of the sodium phosphate buffer (pH 8.0) containing 0.5 M NaCl pumped through the microfluidic cell is marked with a «Buffer» arrow. The microbeads used as a bacterial model were resuspended in the same buffer; the effect of the microbead suspension pumped through the microfluidic cell is marked with a «Microbeads» arrow. Figure **B** shows how the thickness of the photonic crystal surface increased as the suspension of microbeads coated with poly(acrylic) acid (PAA) was pumped through the cell. The «Buffer» arrow represents a point at which the suspension of the microbeads was discontinued and the buffer was supplied to the flow cell. The figure also shows the results of theoretical modelling of microbeads binding to the surface of the photonic crystal (see the article)

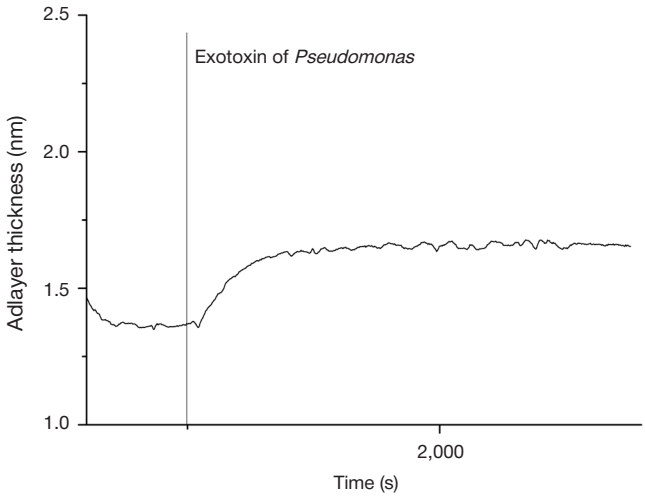

Fig. 2. Detection of the exotoxin A of *Pseudomonas aeruginosa* by the biosensor based on the photonic crystal surface mode detection

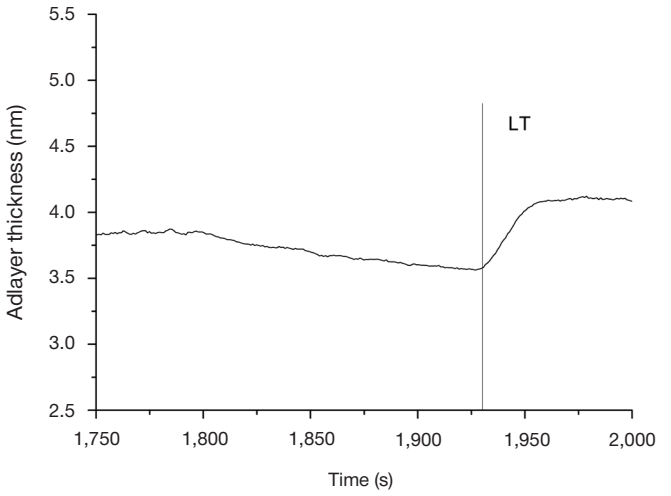

Fig. 3. Detection of the heat-labile toxin LT of *Escherichia coli* by the biosensor based on the photonic crystal surface mode detection

can differ from that demonstrated in our experiment involving microbeads.

It should be noted that changes in the composition of the microbeads-containing solution affected the binding kinetics only insignificantly.

VI. Optimization of detection of bacterial toxins

The results obtained in the experiment demonstrate the feasibility of multiplex detection of bacterial toxins using a PCSM-based biosensor. The detection limit can be lowered by (1) the use of affinity purified antibodies to the studied toxins; the antibody-antigen affinity is crucial because each molecule lacking it negatively affects the effective area of the sensor surface; (2) changing the parameters of the measuring flow cell [20]; (3) enhancing the signal by gold nanoparticles: the intensity of the signal from the crystal depends on mass transfer, so the use of specific antibodies recognizing a sterically distant epitope of the target protein and conjugated to colloid gold will increase the signal intensity at the same concentration of an analyte [21–22].

CONCLUSIONS

This work demonstrates the feasibility of PCSM-based detection of microparticles similar to bacterial cells in terms of their size in a liquid sample. We hope that the obtained results will assist development of protocols for real-time detection of bacteria in flow cells. The proposed technique is suitable for multiplex detection of protein toxins: the exotoxin A of *Pseudomonas aeruginosa* and the heat-labile toxin LT of *Escherichia coli*. Our findings could be used to design rapid and cheap tools for measuring bacterial contamination of water and food and establishing fast and accurate diagnosis of bacterial infections by detecting bacterial cells and their metabolites in the samples of biological fluids.

References

1. Wilson MS. Electrochemical Immunosensors for the Simultaneous Detection of Two Tumor Markers. Anal Chem. 2005; 77 (5): 1496–1502.
2. Xu T, Jia X, Chen X, Ma Z. Simultaneous electrochemical detection of multiple tumor markers using metal ions tagged immunocolloidal gold. Biosens Bioelectron. 2014; (56): 174–9.
3. Zong C, Wu J, Wang C, Ju H, Yan F. Chemiluminescence Imaging Immunoassay of Multiple Tumor Markers for Cancer Screening. Anal Chem. 2012; 84 (5): 2410–15.
4. Zhao Y, Zhao X, Pei X, et al. Multiplex detection of tumor markers with photonic suspension array. Anal Chim Acta. 2009; 633 (1): 103–8.
5. Ravalli A, Gomes C, Yamanaka H, Marrazza G. A label-free electrochemical affisensor for cancer marker detection : The case of HER2. Bioelectrochemistry. 2015; 106 (Pt B): 268–75.
6. Gomes RS, Moreira FTC, Fernandes R, Sales MGF. Sensing CA 15-3 in point-of-care by electropolymerizing O-phenylenediamine (oPDA) on Au-screen printed electrodes. PLoS One. 2018; 13(5): [about 1 p.]. Available from: http://journals.plos.org/plosone/article?id=10.1371/journal.pone.0196656
7. Nguyen HH, Park J, Kang S, Kim M. Surface Plasmon Resonance: A Versatile Technique for Biosensor Applications. Sensors (Switzerland). 2015; 15 (5): 10481–510.
8. Michelotti F, Sciacca B, Dominici L, Quaglio M. Fast optical vapour sensing by Bloch surface waves on porous silicon membranes. Phys Chem Chem Phys. 2010; (12): 502–6.
9. Khan MU, Corbett B. Bloch surface wave structures for high sensitivity detection and compact waveguiding. Sci Technol Adv Mater. 2016; 17 (1): 398–409
10. Konopsky V, Karakouz T, Alieva E, Vicario C, Sekatskii S, Dietler G. Photonic Crystal Biosensor Based on Optical Surface Waves. Sensors. 2013; 13 (3): 2566–78.
11. Bilan RS, Krivenkov VA, Berestovoy MA, et al. Engineering of Optically Encoded Microbeads with FRET-Free Spatially Separated Quantum-Dot Layers for Multiplexed Assays. Chem Phys Chem. 2017; 18 (8): 970–9.
12. Toren P, Ozgur E, Bayindir M. Label-Free Optical Biodetection of Pathogen Virulence Factors in Complex Media Using Microtoroids with Multifunctional Surface Functionality. ACS Sensors. 2018; 3 (2): 352–9.
13. Iglewski BH, Liu PV, Kabat D. Mechanism of Action of Pseudomonas aeruginosa Exotoxin A: Adenosine Diphosphate-Ribosylation of Mammalian Elongation Factor 2 In Vitro and In Vivo. 1977; 15 (1): 138–44.
14. Khan AA, Cerniglia CE. Detection of Pseudomonas aeruginosa from clinical and environmental samples by amplification of the exotoxin A gene using PCR. Appl Environ Microbiol. 1994; 60 (10): 3739–45.
15. Norton EB, Branco LM, Clements JD. Evaluating the A-Subunit of the Heat-Labile Toxin (LT) As an Immunogen and a Protective Antigen Against Enterotoxigenic Escherichia coli (ETEC). PLoS One. 2015; 10 (8): [about 1 p.]. Available from: https://www.ncbi.nlm.nih.gov/pmc/articles/PMC4549283/
16. Allen KP, Randolph MM, Fleckenstein JM. Importance of Heat-Labile Enterotoxin in Colonization of the Adult Mouse Small Intestine by Human Enterotoxigenic Escherichia coli Strains. Infect Immun. 2006; 74 (2): 869–75.
17. Schasfoort RBM, Tudos AJ, editors. Handbook of Surface Plasmon Resonance. Лондон: RSC Publisher; 2013. 524 c.
18. pcbiosensors.com [Internet]. Troitsk: PCbiosensors company. 2013 – [cited July 18, 2018.]. Available at: http://pcbiosensors.com/technology/technology.htm.
19. Myszka DG, He X, Dembo M, Morton TA, Goldstein B. Extending the Range of Rate Constants Available from BIACORE : Interpreting Mass Transport-Influenced Binding Data. Biophysical Journal. 1998; 75 (August): 583–94.
20. Lynn NS, Homola J. Biosensor Enhancement Using Grooved Micromixers: Part I, Numerical Studies. Anal Chem. 2015; 87 (11): 5524–30.
21. Springer T, Homola J. Biofunctionalized gold nanoparticles for SPR-biosensor-based detection of CEA in blood plasma. Anal Bioanal Chem. 2012; 404 (10): 2869-75.
22. Lee J, Cho H, Choi HK, Lee J-Y, Choi J-W. Application of Gold Nanoparticle to Plasmonic Biosensors. Int J Mol Sci. 2018; 19 (7): [about 14 p.]. Available from: http://www.mdpi.com/1422-0067/19/7/2021

Литература

1. Wilson MS. Electrochemical Immunosensors for the Simultaneous Detection of Two Tumor Markers. Anal Chem. 2005; 77 (5): 1496–1502.
2. Xu T, Jia X, Chen X, Ma Z. Simultaneous electrochemical detection of multiple tumor markers using metal ions tagged immunocolloidal gold. Biosens Bioelectron. 2014; (56): 174–9.
3. Zong C, Wu J, Wang C, Ju H, Yan F. Chemiluminescence Imaging Immunoassay of Multiple Tumor Markers for Cancer Screening. Anal Chem. 2012; 84 (5): 2410–15.
4. Zhao Y, Zhao X, Pei X, et al. Multiplex detection of tumor markers

with photonic suspension array. Anal Chim Acta. 2009; 633 (1): 103–8.
5. Ravalli A, Gomes C, Yamanaka H, Marrazza G. A label-free electrochemical affisensor for cancer marker detection : The case of HER2. Bioelectrochemistry. 2015; 106 (Pt B): 268–75.
6. Gomes RS, Moreira FTC, Fernandes R, Sales MGF. Sensing CA 15–3 in point-of-care by electropolymerizing O-phenylenediamine (oPDA) on Au-screen printed electrodes. PLoS One. 2018; 13(5): [about 1 p.]. Available from: http://journals.plos.org/plosone/article?id=10.1371/journal.pone.0196656
7. Nguyen HH, Park J, Kang S, Kim M. Surface Plasmon Resonance: A Versatile Technique for Biosensor Applications. Sensors (Switzerland). 2015; 15 (5): 10481–510.
8. Michelotti F, Sciacca B, Dominici L, Quaglio M. Fast optical vapour sensing by Bloch surface waves on porous silicon membranes. Phys Chem Chem Phys. 2010; (12): 502–6.
9. Khan MU, Corbett B. Bloch surface wave structures for high sensitivity detection and compact waveguiding. Sci Technol Adv Mater. 2016; 17 (1): 398–409
10. Konopsky V, Karakouz T, Alieva E, Vicario C, Sekatskii S, Dietler G. Photonic Crystal Biosensor Based on Optical Surface Waves. Sensors. 2013; 13 (3): 2566–78.
11. Bilan RS, Krivenkov VA, Berestovoy MA, et al. Engineering of Optically Encoded Microbeads with FRET-Free Spatially Separated Quantum-Dot Layers for Multiplexed Assays. Chem Phys Chem. 2017; 18 (8): 970–9.
12. Toren P, Ozgur E, Bayindir M. Label-Free Optical Biodetection of Pathogen Virulence Factors in Complex Media Using Microtoroids with Multifunctional Surface Functionality. ACS Sensors. 2018; 3 (2): 352–9.
13. Iglewski BH, Liu PV, Kabat D. Mechanism of Action of Pseudomonas aeruginosa Exotoxin A: Adenosine Diphosphate-Ribosylation of Mammalian Elongation Factor 2 In Vitro and In Vivo. 1977; 15 (1): 138–44.
14. Khan AA, Cerniglia CE. Detection of Pseudomonas aeruginosa from clinical and environmental samples by amplification of the exotoxin A gene using PCR. Appl Environ Microbiol. 1994; 60 (10): 3739–45.
15. Norton EB, Branco LM, Clements JD. Evaluating the A-Subunit of the Heat-Labile Toxin (LT) As an Immunogen and a Protective Antigen Against Enterotoxigenic Escherichia coli (ETEC). PLoS One. 2015; 10 (8): [about 1 p.]. Available from: https://www.ncbi.nlm.nih.gov/pmc/articles/PMC4549283/
16. Allen KP, Randolph MM, Fleckenstein JM. Importance of Heat-Labile Enterotoxin in Colonization of the Adult Mouse Small Intestine by Human Enterotoxigenic Escherichia coli Strains. Infect Immun. 2006; 74 (2): 869–75.
17. Schasfoort RBM, Tudos AJ, editors. Handbook of Surface Plasmon Resonance. Лондон: RSC Publisher; 2013. 524 c.
18. pcbiosensors.com [Internet]. Troitsk: PCbiosensors company. 2013 — [cited July 18, 2018.]. Available at: http://pcbiosensors.com/technology/technology.htm.
19. Myszka DG, He X, Dembo M, Morton TA, Goldstein B. Extending the Range of Rate Constants Available from BIACORE : Interpreting Mass Transport-Influenced Binding Data. Biophysical Journal. 1998; 75 (August): 583–94.
20. Lynn NS, Homola J. Biosensor Enhancement Using Grooved Micromixers: Part I, Numerical Studies. Anal Chem. 2015; 87 (11): 5524–30.
21. Springer T, Homola J. Biofunctionalized gold nanoparticles for SPR-biosensor-based detection of CEA in blood plasma. Anal Bioanal Chem. 2012; 404 (10): 2869-75.
22. Lee J, Cho H, Choi HK, Lee J-Y, Choi J-W. Application of Gold Nanoparticle to Plasmonic Biosensors. Int J Mol Sci. 2018; 19 (7): [about 14 p.]. Available from: http://www.mdpi.com/1422-0067/19/7/2021

HIGH-PERFORMANCE AEROSOL SAMPLER WITH LIQUID PHASE RECIRCULATION AND PRE-CONCENTRATION OF PARTICLES

Akmalov AE[1], Kotkovskii GE[1]✉, Stolyarov SV[1], Verdiev BI[2], Ovchinnikov RS[2], Pochtovyy AA[2], Tkachuk AP[2], Chistyakov AA[1]

[1] National Research Nuclear University MEPhI, Moscow

[2] Gamaleya Research Institute of Epidemiology and Microbiology, Moscow

Testing the surrounding environment for the presence of biogenic aerosols is crucial in ensuring its safety for the population. It is often necessary to collect aerosol samples from large areas in short time, which demands excellent particle collection efficiency, a sufficient incoming air flow rate and a capacity to maintain the viability of the collected samples. Below we present the aerosol sampler with a high volumetric flow rate based on a two-stage particle concentration algorithm and consisting of a virtual impactor and a cyclone concentrator with a recirculating liquid phase. We provide all necessary calculations and an algorithm for modeling impactor parameters. The sampler was tested using dry and liquid formulations dispersed into the particles of 0.5 to 5 μm in diameter. We demonstrate that at volumetric flow rates over 4,000 l/min efficiency of particle collection into the liquid phase at a volume of 10 ml makes over 20% of the total aerosol mass and at volumetric flow rates over 300 l/min this value is over 60%. The proposed device maintains viability of the collected microorganisms. The sampler is portable, with flexible settings for sampling and cleaning, and can be controlled remotely over the network.

Keywords: aerosols, pathogens, efficiency, sampler, impactor, volumetric flow rate, cyclone

Funding: this work was supported by the Federal Target Program *The National System for Chemical and Biological Security of the Russian Federation (2015-2020)*, the state contract No. K-27-НИР/148-2 signed by the Ministry of Healthcare of the Russian Federation and the National Research Nuclear University MEPhI.

✉ **Correspondence should be addressed:** Gennadii E. Kotkovskii
Kashirskoe shosse, 31, Moscow, 115409; geko@mail.ru

Received: 27.07.2018 **Accepted:** 23.08.2018

DOI: 10.24075/brsmu.2018.049

ВЫСОКОПРОИЗВОДИТЕЛЬНЫЙ АЭРОЗОЛЬНЫЙ ПРОБООТБОРНИК С РЕЦИРКУЛЯЦИЕЙ ЖИДКОЙ ФАЗЫ И ПРЕДВАРИТЕЛЬНЫМ КОНЦЕНТРИРОВАНИЕМ

А. Э. Акмалов[1], Г. Е. Котковский[1]✉, С. В. Столяров[1], Б. И. Вердиев[2], Р. С. Овчинников[2], А. А. Почтовый[2], А. П. Ткачук[2], А. А.Чистяков[1]

[1] Национальный исследовательский ядерный университет «МИФИ», Москва

[2] Национальный исследовательский центр эпидемиологии и микробиологии имени Н. Ф. Гамалеи, Москва

Обнаружение биогенных аэрозолей является важной задачей при обеспечении безопасности жизнедеятельности человека в современных условиях. На практике часто требуется собирать аэрозоли с больших площадей за малый промежуток времени, что накладывает жесткие ограничения на эффективность пробоотбора, величину прокачиваемого в единицу времени объема воздуха и жизнеспособность собранного биоматериала. В работе представлены результаты по разработке и испытанию устройства отбора аэрозольных проб с высокой объемной скоростью и двухступенчатым концентрированием аэрозольных частиц — виртуального импактора и циклонного коллектора с рециркулирующей жидкой фазой. Приведены алгоритм и результаты расчета параметров импактора, результаты испытаний устройства на модельных сухих и жидких тест-препаратах для частиц размерами 0,5–5 мкм. Подтверждено, что при объемных скоростях пробоотбора выше 4000 л/мин эффективность отбора в жидкую фазу объемом до 10 мл составляет более 20% массовой доли распыленного аэрозоля, а при объемных скоростях выше 300 л/мин — более 60% массовой доли. Показано, что устройство сохраняет жизнеспособность отобранного биоматериала. Прооотборник реализован в портативном варианте, обладает возможностью настройки всех параметров отбора и очистки, а также управления по сети.

Ключевые слова: аэрозоли, биопатогены, эффективность, пробоотборник, импактор, объемная скорость, циклон

Финансирование: Федеральная целевая программа «Национальная система химической и биологической безопасности Российской Федерации (2015–2020 г.)», государственный контракт №К-27-НИР/148-2 между Министерством здравоохранения Российской Федерации и Национальным исследовательским ядерным университетом «МИФИ».

✉ **Для корреспонденции:** Геннадий Евгеньевич Котковский
Каширское шоссе, 31, г. Москва, 115409; geko@mail.ru

Статья получена: 27.07.2018 **Статья принята к печати:** 23.08.2018

DOI: 10.24075/vrgmu.2018.049

Testing air for the presence of pathogenic, allergenic and immunogenic microorganisms is crucial in ensuring its safety for the population. Advances in biotechnology have added to the sources of contaminating aerosols, which now include genetically engineered microbial strains used in the production of pharmaceuticals, enzymes and synthetic foods [1]. Microbial concentrations in contaminated air can reach as high as 10^6 CFU/m^3 causing respiratory infections and

allergies in humans [2]. Another serious threat is posed by bioterrorism, which involves the intentional contamination of air with pathogens.

Traditionally, air sampling for bioaerosol detection and quantification is done using filters, impingers and impactors in which microorganisms go through a lot of stress caused by the sampling process itself and are unlikely to survive [3]. Microbial viability is critical when it comes to the sampling of microbiological flora. It is important to avoid applying unnecessary physical force on the collected microorganisms and to create conditions for maintaining their physiological properties. Here, great promise is held by liquid-based samplers [4] that separate microorganisms from their aerosol carriers and ensure accurate detection of individual microbial cells.

An air sampler for pathogen detection is expected to meet a number of elaborate requirements [5–8]. First, the volumetric air flow rate must be high enough to allow detection of low pathogen concentrations in reasonable time. Second, the capture of aerosol particles and the process of their concentration in a small liquid volume for further analysis must be efficient. Third, precipitation conditions must be gentle to allow survival of collected microorganisms and the sorption liquid must contain protective components. Finally, the aerodynamic drag has to be low, and the sampler is expected to produce little noise and have low energy consumption.

Devices for collecting aerosols from the surrounding air exploit different physical principles and have been around for quite a long time. They all have their drawbacks. Creating a sampler operating at a flow rate of over 3,000 l/min, with low levels of noise and energy consumption, capable of efficient pathogen capture and ensuring viability of captured microorganisms concentrated in small liquid volumes remains a challenge still awaiting a solution.

The aim of this work was to design a high-performance device for collecting and concentrating bioaerosols from the surrounding air and to test the obtained samples for pathogenic bacteria and viruses.

I. Design of the experiment

Our device exploits the principle of two-stage particle concentration and allows working with high volumetric flow rates. During the first stage, the captured particles are concentrated in the virtual impactor as the air flow coming through the inlet nozzle is forced to abruptly change its direction [9, 10]. The exiting air flow containing the concentrated particles follows the original direction of the incoming flow, but its rate is several times lower. During the second stage, the concentrated particles deposit on a recirculating liquid film of the cyclone [3, 11]. As the particles keep coming in, longer circulation time causes their concentration in the liquid to increase. The stages of the experiment are described below.

1. Creating a virtual impactor

A few preliminary calculations were done to compute the width and length of the impactor's inlet nozzle through which the air is sucked in and outlet nozzle through which the air containing concentrated particles is released at a decreased flow rate. In our calculations, the incoming flow rate ranged from 3,000 to 5,000 l/min, the size of the particles varied from 0.5 to 5 μm. According to [12], the Reynolds number and the ratio of the distance separating the inlet and the outlet nozzles to the width of the inlet nozzle determine the shape of the curve representing dependency of particle collection efficiency (expressed as percentage) on the aerodynamic diameter of the particles. The diameter corresponding to the collection efficiency of 50% is calculated according to the equation

$$d_{50} = \left(\sqrt{\frac{9\eta W}{\rho_p C_C U}} \right) \times \sqrt{Sk_{50}} \quad , (1)$$

where ρ_p is particle density; C_C is the Cunnigham slip correction factor accounting for the increase in the mobility of particles whose size is comparable to the gas mean free path; U is particle velocity; η is air/gas viscosity; W is nozzle width; S_{k50} is Stokes number corresponding to the diameter d_{50}. We aimed to select such nozzle widths that would ensure the Reynolds number

$$Re = \frac{\rho_{air} WU}{\eta}$$

in the range between 500 and 3,000 at a volumetric air flow below 5,000 l/min [12]. Based on the dependency of S_{k50} on Re calculated in [13], we determined the value of S_{k50} and then calculated the value of d_{50} according to the equation (1). This value cannot exceed the minimum required diameter of aerosols of 0.5 μm. In total, twenty different nozzle sizes were obtained with different values of the Reynolds number and d_{50}.

Next, we built a model of a virtual impactor body based on the calculated nozzle parameters and modelled the trajectory of aerosol particles in it. We also estimated distribution of particle velocities at each point of space in the impactor body covered by our calculations. For that, we used Solid Works 2014 (the system for automated modelling) and the Flow Simulation application.

During the third stage, we calculated the efficiency of particle collection at given parameters considering the obtained distribution of particle velocities. Calculations were done in the original software and the MathLab environment. The software estimated how a group of 100 aerosol particles relocated spatially as they travelled between the nozzles. Coordinates of every particle were calculated with due account of the centripetal acceleration. The centripetal acceleration is determined by the force (Stokes' law) resulting from the interaction between the aerosol particle and the air flow as it bends while traveling between the nozzles (Fig. 1). We assessed how well the particles "found" the outlet nozzle.

Finally, the joint performance of the virtual impactor and the cyclone concentrator was tested.

2. Creating a cyclone concentrator

To design a liquid-phase cyclone concentrator, we used calculations from [3]; they aid in measuring the efficiency of particle capture by the sorption liquid based on the height and radius of a cylinder in which the liquid circulates (Fig. 2). We hypothesized that for the cyclone the incoming flow rate would have the same value as the flow rate exiting from the virtual impactor. For liquid recirculation, a separate channel was introduced into the cyclone concentrator.

II. Testing the sampler

The fabricated virtual impactor and the cyclone were connected by a flexible air pipe and tested together and separately for the efficiency of aerosol collection. The tests were conducted at the facilities of the 48th Central Research Institute of the Ministry of Defense of the Russian Federation (Sergiev Posad), Gamaleya Research Institute of Epidemiology and Microbiology (Moscow) and in the Moscow Metro.

The tests conducted at the facilities of the 48th Central Research Institute for 10 days involved the use of a dry pathogen-free test formulation. The impactor was placed inside a static aerosol chamber; the cyclone was connected to the impactor by a flexible air pipe and placed outside the chamber. The concentration and size distribution of aerosol particles, as well as the total mass of the particles trapped in the sorption liquid, were measured by fluorescence and chemiluminescence. The efficiency of sampling was assessed relative to the KPK-3 sampler. Aerosol particles were generated in the static chamber from the dry pathogen-free test formulation by the pneumatic pulse generator. KPK-3 and May's 4-stage impactor were used to measure the integral mass concentration of aerosol and the distribution of particle sizes.

Another series of tests was conducted in the security check areas of Cherkizovskaya and Novokosino metro stations to compare the performance of our model with that of the SASS4000/2300 aerosol concentration device with a cyclone air sampler (Research International Inc.; USA). The collected samples were sent to the laboratory for the microbiological and biomolecular analyses to determine the composition of the captured microbial communities and to quantify them.

III. Microbiological analysis of the obtained samples

The following ready-to-use solid agar media were used: Columbia agar with defibrinated blood, Baird-Parker agar, Sabouraud dextrose agar w/ chloramphenicol, Endo agar, enterococci agar and lysogeny broth prepared on site (composition (g/l): 10 h g tryptone, 5 g yeast extract, 5 g NaCl, 17 g agar). Cultures were plated onto Petri dishes (CFGS; Russia). Each culture was plated onto 6 dishes containing different growth media. Before plating, the media were preheated to room temperature and dried in an incubator to remove condensed moisture.

Liquid samples were plated by pipetting (0.1 ml of the culture per Petri dish). The pipetted cultures were evenly spread across the medium surface with a sterile L-shaped spatula.

The cultures were incubated at 37 °C for 48 h. The cultures grown in Sabouraud agar were incubated at room temperature for up to 7 days when no visible culture growth was observed.

Grown colonies were counted in every dish and their morphological types (MTs) were described. Every MT received an identifier, and the colonies were photographed. Isolated colonies were reseeded onto fresh growth media for further identification and antibiotic susceptibility testing. Colonies with pronounced morphological features were preliminary identified to the genus level.

Sensitivity of the isolated cultures to antibiotics was determined by disc diffusion tests (Himedia; India). The panel of antibiotics included ampicillin, amoxiclav, cefoxitin, azithromycin, levofloxacin, gentamycin, amikacin, tetracycline, vancomycin, novobiocin, bacitracin, optochin and Mueller Hinton agar standardized for these purposes (CFGS; Russia).

Halos (zones of inhibition) around antibiotic discs were measured; their diameters were compared to the reference interval and assigned to one of three categories: r (resistant), s (susceptible) and i (moderately susceptible).

Tests were carried out at the facilities of Gamaleya Research Institute of Epidemiology and Microbiology in order to compare the performance of our system with that of the SASS4000/2300 aerosol concentration device with a cyclone air sampler (Research International Inc.; USA) using a test aerosol. Measurements were taken in the biosafety cabinet Laminar-S (Laminar systems; Russia). The liquid test formulation for aerosol generation was a 10% solution of saccharose in the carbonate buffer (pH 9.6) (C3041; Sigma; Germany) with fluorescein sodium taken at a final concentration of 1 μM. We compared the luminescence intensity of the sample collected for 5 min in the static chamber with the continuously generated test aerosol.

IV. Simulation of virtual impactor parameters and particle collection efficiency

We investigated the dependency of collection efficiency for the particles sized 0.5–5 μm in diameter on the parameters of the virtual impactor (Fig. 3–5). Collection efficiency was calculated as the ratio of the number of concentrated particles of a given size (the particles that made it to the outlet nozzle) (Fig. 1) to the number of particles present in the incoming air flow.

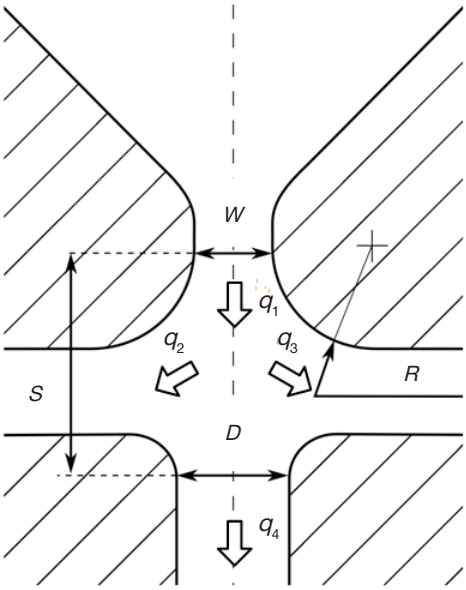

Fig. 1. The schematic of the virtual impactor (cross-section). *W* is the width of the inlet nozzle; *D* is the width of the outlet nozzle; *S* is the distance between the two nozzles; q_1 is the incoming air flow; q_4 is the exiting air flow containing concentrated aerosol particles; q_2 and q_3 represent the discarded flow

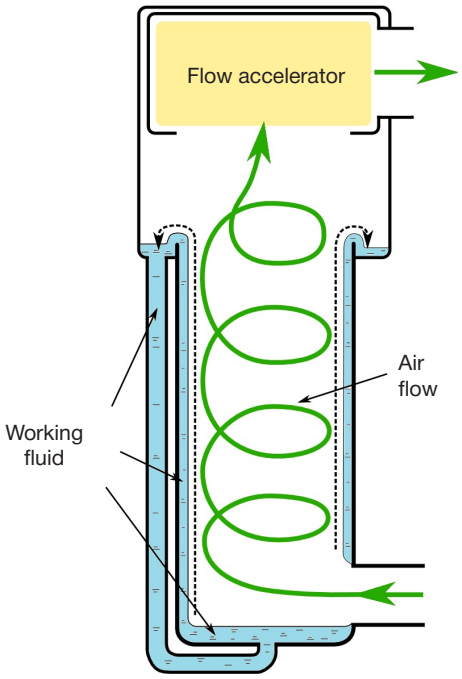

Fig. 2. The schematic of a liquid-phase cyclone concentrator

Collection efficiency rises from 18% to 37% for 0.5 μm-sized particles when the size of the inlet nozzle *W* goes down from 0.07 to 0.05 cm (Fig. 3). However, at *W* = 0.04 collection efficiency drops dramatically. This phenomenon was previously described in the literature [14] and means that the ratio of the inlet to the outlet nozzles should not be ignored: to achieve maximum effective collection, the inlet nozzle must be 30–40% smaller than the outlet nozzle.

At distances *S* between the inlet and outlet nozzles of 0.13 and 0.15 cm, collection efficiency reaches 27% for the particles

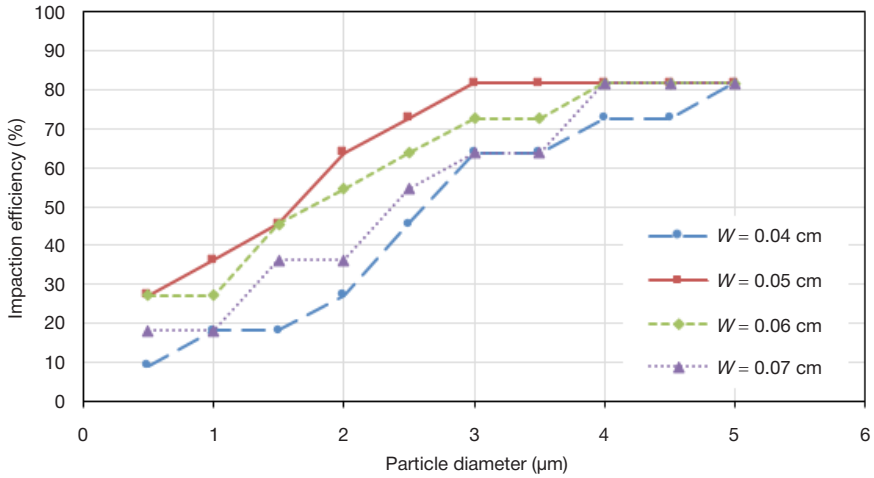

Fig. 3. Dependency of particle collection efficiency on aerosol particle size at various inlet nozzle widths *W* (Fig. 1) of the virtual impactor. The outlet width is 0.07 cm

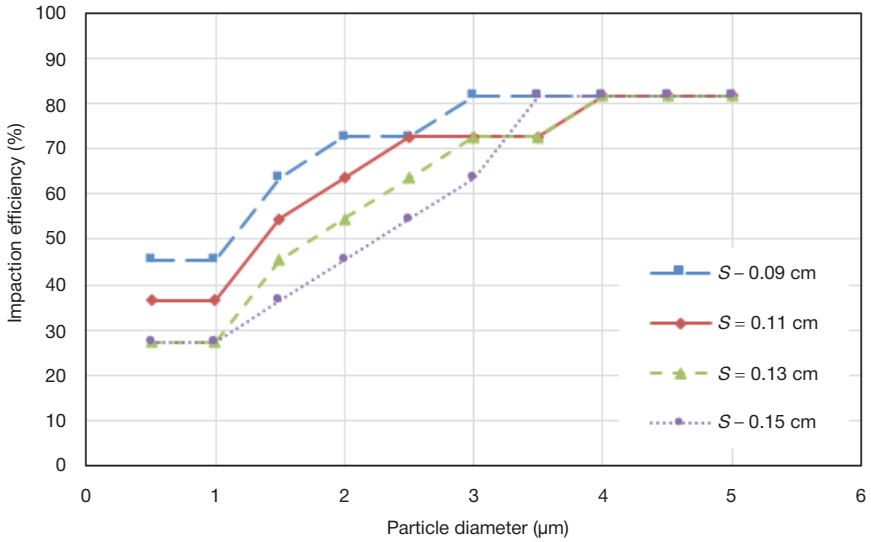

Fig. 4. Dependency of liquid collection efficiency on the aerosol particle size at various distances *S* between the inlet and outlet nozzles (Fig. 1) of the virtual impactor. The width of the inlet and outlet is 0.07 cm

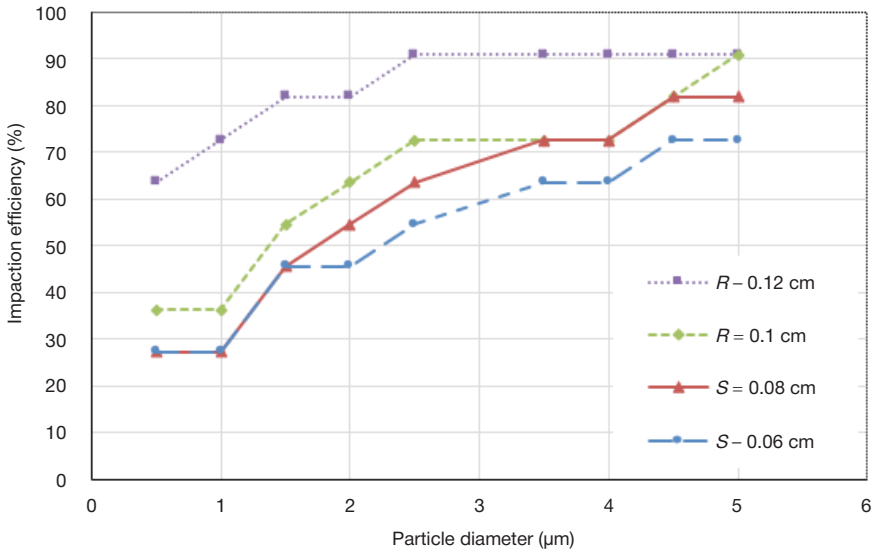

Fig. 5. Dependency of liquid collection efficiency on the corner radius *R* of the inlet nozzle. The width of the inlet and outlet nozzles is 0.07

sized from 0.5 to 1 μm (Fig. 4). When this distance shrinks to 0.09 cm, collection efficiency increases to 45%. Importantly, the anticipated efficiency for the particles over 4 μm in size at all possible *S* values does not exceed 82%.

As the corner radius *R* of the nozzle dips to 0.06 cm, particle collection efficiency drops for 1.5–5 μm-sized particles (Fig. 5). When the radius increases to 0.12 cm, 0.5 μm-sized particles are collected more efficiently (64%); for the particles of 2.5 μm in diameter and larger, collection efficiency is as high as 91%. However, one should be careful with the corner radius because of the risk of turbulence between the nozzles at high radius values.

Our calculations yielded a few parameters determining impaction efficiency (transfer of aerosol particles into the liquid phase), including the tube radius R = 42 mm, its height H = 100 mm, and the diameter of the inlet nozzle =15 mm at the volumetric flow rate Q = 350 l/min.

V. Simulation results and device tests

Fig. 6 demonstrates the schematic of the air sampler. The sampling device consists of a virtual impactor connected to a cyclone by an air pipe.

The cyclone is the control module of the device. Control is implemented via a sensor screen and is fully automated. Sampling occurs in a series of steps constituting a full cycle. The cycle includes supply of liquid from a tank into the cyclone, sampling by pumping air through the device, release of a liquid phase for the analysis, and washing of the cyclone. The duration of cycles and the values of volumetric flow rates can be regulated by an operator. The volume of the liquid phase returned by the device for further analysis ranges from 2.5 to 10 ml. The device can connect to a network via the RS-485 interface.

Table 1 demonstrates the results of the tests conducted at the facilities of the 48th Central Research Institute of the Ministry of Defense of the Russian Federation. Collection efficiency was measured for the dry test formulation and reached as high as 20% of the total mass of the generated aerosol particles. The volumetric flow rate of the device was estimated to be 100 times higher than that of the KPK-3 sampler ensuring 100% particle collection. The cyclone disconnected from the impactor collected up to 61% of the total mass of the particles at a flow rate 6 times higher than that of KPK-3.

Sixty-four samples collected in the Moscow metro were forwarded to the laboratory for the microbiological analysis. Forty-eight morphological types of microorganisms were isolated from the samples. Those microorganisms represented microbial communities inhabiting the air and surfaces of the metro stations. Our air sampler did not differ significantly from the SASS system and the control nanofilters (high-density filters) in terms of the number of microbial morphological types isolated from the collected samples (Fig. 7).

Four of five studied bacterial strains isolated from the samples collected in the Moscow metro were antibiotic-resistant. The strain *St. haemolyticus* MT22 demonstrated multiple drug resistance to macrolides and fluoroquinolones. The strain *Streptococcus viridans* MT8 was multidrug-resistant to macrolides, aminoglycosides, and inhibitor-protected ß-lactams (Table 2). These findings suggest that our device can be used to monitor the spread of antibiotic resistance in hospitals and the surrounding environment in general.

Quantification of total DNA isolated from the samples using the commercial PureLink™ Microbiome DNA Purification Kit (Invitrogen; USA) also showed the absence of any obvious advantage of the tested sampling systems over each other. Our device and SASS surpassed the performance of the nanofilter by two orders of magnitude.

The experiments involving the liquid test formulation conducted at the facilities of Gamaleya Research Institute of Epidemiology and Microbiology demonstrated that our sampling device ensures particle collection of 96% relative to the SASS system (5 tests were conducted; CI was 0.95).

VI. Optimization of the air sampler

Parameter simulation and device testing show that the main challenge is posed by the concentration of aerosol particles < 1 μm in diameter. Collection efficiency of 50% (d50) for such particles requires narrow inlet nozzles. Narrowing the nozzle from 0.5 to 0.4 mm causes a 1.5-fold decline in the incoming flow rate and therefore negatively affects collection efficiency. To maintain the sufficient incoming air flow rate, pressure difference generated by the fan needs to be increased accordingly, which will increase energy consumption and the size of the device. It is reasonable to assume that the real achievable linear flow rate of the incoming air cannot be more than 100 cm/s for small particles < 1 μm in size and that the width of the nozzle cannot be less than 0.5 μm. In our device the volumetric flow rate does not exceed 4,500 l/min when the device operates at maximum power.

Efficiency of particle collection into the liquid phase by the cyclone can be increased by spraying finely dispersed water droplets in the inlet. Optimization is also required for the balance between the aerodynamic drag in the outlet of the virtual impactor and the inlet of the cyclone concentrator, which we did not attempt in the course of our experiment. Remote control of the device and its settings may also be a useful feature.

CONCLUSION

This work presents calculations for the fabrication of an aerosol sampler for the particles of 0.5 to 5 μm in diameter, operating at a high volumetric air flow and ensuring efficient particle collection in the liquid phase. The device that successfully passed a series of tests can reach the volumetric flow rate of 4,500 l/min, demonstrates the particle collection efficiency of 20% (of the total particulate mass) at the flow rate over 4,000 l/min and the particle collection efficiency of up to 61% at the volumetric flow rate over 300 l/min. The device can collect

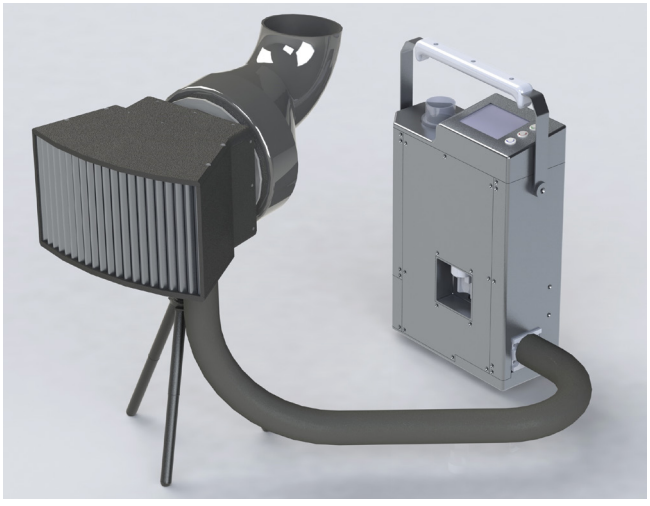

Fig. 6. The Cyclon-Bio device assembled. *On the left*: the impactor. *On the right*: the cyclone concentrator

Table 1. Test of the sampler performance using a test formulation (Central Research Institute of the Ministry of Defense of the Russian Federation)

Device	Integral concentration of the test formulation, mg/l (5 test, CI of 0.95)	Duration of sample collection, min	Volumetric flow rate, 1/min	Collection efficiency, %
Aerosol sampler	$(1.91 \pm 0.18) \cdot 10^{-3}$	2	4325	16 ± 1.5
	$(1.70 \pm 0.16) \cdot 10^{-3}$	2	4325	20 ± 2.1
Cyclone concentrator of the aerosol sampler	$(3.75 \pm 0.35) \cdot 10^{-3}$	2	325	61 ± 14
	$(2.91 \pm 0.27) \cdot 10^{-2}$	2	325	48 ± 125
KPK-3 sampler, collection efficiency control	$(3.75 \pm 0.36) \cdot 10^{-3}$	2	50	100.0
	$(2.91 \pm 0.28) \cdot 10^{-2}$	2	50	100.0

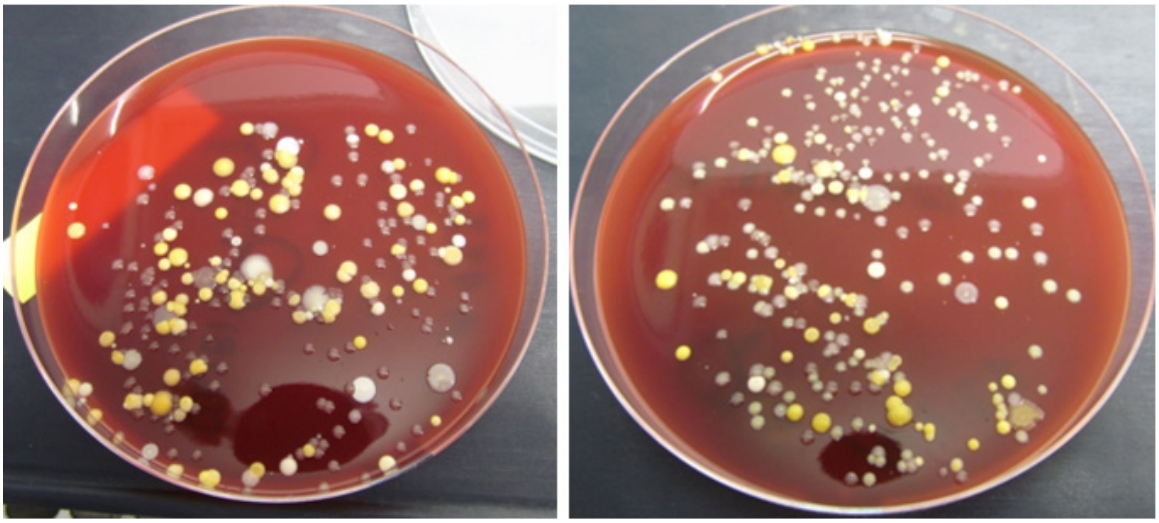

Fig. 7. Overnight culture of the samples collected at Novokosino metro station during the morning rush hour and plated onto blood agar. *On the left*: sample A123 collected by the SASS sampler. *On the right*: sample A223, Cyclon sampler (MEPhI)

Table 2. Testing antibiotic susceptibility of the collected strains

Antibiotic	MT 11 (*Staphylococcus haemolyticus*)	MT 12 (*Staphylococcus saprophyticus*)	MT 22 (*Staphylococcus haemolyticus*)	MT 24 (*Staphylococcus aureus*)	MT 8 (*Streptococcus viridans?*)
Ampicillin	**R**	S	S	S	I
Amoxiclav	n/a	n/a	n/a	n/a	**R**
Cefoxitin*	S	S	S	S	n/a
Azithromycin	S	**R**	**R**	S	R
Levofloxacin	S	S	**R**	S	S
Gentamycin	S	S	S	S	**R**
Amikacin	S	S	S	S	**R**
Tetracycline	S	S	S	S	S
Vancomycin	S	S	S	S	S
Novobiocin	S	R	S	S	n/a
Bacitracin	n/a	n/a	n/a	n/a	R
Optochin	n/a	n/a	n/a	n/a	R

particles in the range between 0.5 and 5 μm. The virtual impactor weighs 7.2 kg, and the cyclone concentrator weighs 5.6 kg. The device operates at 220 Volts AC and 24 and 12 Volts DC. The device is dust- and water-proof. Its performance is no inferior to that of the world's best air samplers. Over 90% of its components are made in Russia. The device can be used in public transport, at customs, border checkpoints or other public places to test the air for possible contamination and carry out environmental monitoring. It can also be installed in healthcare facilities and research institutions of the Ministry of Healthcare and the Ministry of Defense of the Russian Federation.

References

1. Lacey J, Dutkiewicz J. Bioaerosols and Occupational Lung Desease. J Aerosol Sci. 1994; 25 (8): 1371–1404.
2. Omelianetz G. Biological Hazards as Risks Factors in Microbial Industry. Pharmacol Toxicolog Suppl. 1997; (80): 141–145.
3. Sigaev G, et al. Development of a Cyclone-based Aerosol Sampler with Recirculating Liquid Film: Theory and Experiment. Aerosol Sci and Tech. 2006; 40 (5): 293–308.
4. Henningson EW, Ahlberg MS. Evaluation of Microbiological Aerosol Samplers. A Review. J Aerosol Sci. 1994; (25): 1459–1492.
5. Baron PA, Willeke K. Aerosol Fundamentals. In: Baron PA, Willeke K, editors. Aerosol measurement: principles, techniques and applications. 2nd ed. New York: Wiley-Interscience; 2001. p. 55–60.
6. McFarlandAR, HYPERLINK "https://www.researchgate.net/profile/Maria_King4" King MD, HYPERLINK "https://www.researchgate.net/profile/John_Haglund2" Haglund JS, HYPERLINK "https://www.researchgate.net/scientific-contributions/21610210_Youngjin_Seo" Seo Y.Wetted Wall Cyclones for Bioaerosol Sampling. Aerosol sampling and technology. 2010; 44 (4): 241–252. DOI: 10.1080/02786820903555552.
7. Marple V, Olson B, Rubow K. Inertial gtavitational, centrifugal and thermal collection techniques. In: Baron PA, Willeke K, editors. Aerosol measurement: principles, techniques and applications. 2nd ed. New York: Wiley-Interscience; 2001. p. 229–39.
8. Sigaev VI. Novel liquid sampler for aerosols. Abstracts of the 20th annual AAAR Conference; Portland, Oregon. 2001. Abstract 11PG5:406.
9. Solomon PA, HYPERLINK "https://www.researchgate.net/profile/Matthew_Landis" Landi MS, HYPERLINK "https://www.researchgate.net/scientific-contributions/71734146_Gary_Norris" Norris G, HYPERLINK "https://www.researchgate.net/scientific-contributions/10776481_Michael_P_Tolocka" Tolocka MP. Chemical analyses methods for atmospheric aerosol components. In: Baron PA, Willeke K, editors. Aerosol measurements: principles, techniques and applications. 2nd ed. New York: Wiley-Interscience; 2001. p. 261–93
10. Saaski E, et al. Concentrator. US Patent 9791353B2. October 2017.
11. Saaski E, et al. Liquid particulate extraction device. US Patent 7846228B1. December 2010.
12. Marple VA, Liu BYH. Characteristics of laminar jet impactors. Envir Sci Technol. 1974; (7): 648–54.
13. Marple V. A fundamental study of inertial impactors [dissertation]. Minneapolis (MN): University of Minnesota; 1970.
14. Chen BT, Yeh HC. An improved virtual reactor: design and performance. J Aerosol Sci. 1987; 18 (2): 203–14.

Литература

1. Lacey J, Dutkiewicz J. Bioaerosols and Occupational Lung Desease. J Aerosol Sci. 1994; 25 (8): 1371–1404.
2. Omelianetz G. Biological Hazards as Risks Factors in Microbial Industry. Pharmacol Toxicolog Suppl. 1997; (80): 141–145.
3. Sigaev G, et al. Development of a Cyclone-based Aerosol Sampler with Recirculating Liquid Film: Theory and Experiment. Aerosol Sci and Tech. 2006; 40 (5): 293–308.
4. Henningson EW, Ahlberg MS. Evaluation of Microbiological Aerosol Samplers. A Review. J Aerosol Sci. 1994; (25): 1459–1492.
5. Baron PA, Willeke K. Aerosol Fundamentals. In: Baron PA, Willeke K, editors. Aerosol measurement: principles, techniques and applications. 2nd ed. New York: Wiley-Interscience; 2001. p. 55–60.
6. McFarlandAR, HYPERLINK "https://www.researchgate.net/profile/Maria_King4" King MD, HYPERLINK "https://www.researchgate.net/profile/John_Haglund2" Haglund JS, HYPERLINK "https://www.researchgate.net/scientific-contributions/21610210_Youngjin_Seo" Seo Y. Wetted Wall Cyclones for Bioaerosol Sampling. Aerosol sampling and technology. 2010; 44 (4): 241–252. DOI: 10.1080/02786820903555552.
7. Marple V, Olson B, Rubow K. Inertial gtavitational, centrifugal and thermal collection techniques. In: Baron PA, Willeke K, editors. Aerosol measurement: principles, techniques and applications. 2nd ed. New York: Wiley-Interscience; 2001. p. 229–39.
8. Sigaev VI. Novel liquid sampler for aerosols. Abstracts of the 20th annual AAAR Conference; Portland, Oregon. 2001. Abstract 11PG5:406.
9. Solomon PA, HYPERLINK "https://www.researchgate.net/profile/Matthew_Landis" Landis MS, HYPERLINK "https://www.researchgate.net/scientific-contributions/71734146_Gary_Norris" Norris G, HYPERLINK "https://www.researchgate.net/scientific-contributions/10776481_Michael_P_Tolocka" Tolocka MP. Chemical analyses methods for atmospheric aerosol components. In: Baron PA, Willeke K, editors. Aerosol measurements: principles, techniques and applications. 2nd ed. New York: Wiley-Interscience; 2001. p. 261-93
10. Saaski E, et al. Concentrator. US Patent 9791353B2. October 2017.
11. Saaski E, et al. Liquid particulate extraction device. US Patent 7846228B1. December 2010.
12. Marple VA, Liu BYH. Characteristics of laminar jet impactors. Envir Sci Technol. 1974; (7): 648-54.
13. Marple V. A fundamental study of inertial impactors [dissertation]. Minneapolis (MN): University of Minnesota; 1970.
14. Chen BT, Yeh HC. An improved virtual reactor: design and performance. J Aerosol Sci. 1987; 18 (2): 203–14.

PERFORMANCE OF THE ORIGINAL WORKSTATION FOR AEROSOL TESTS UNDER CONTROLLED CONDITIONS

Kleymenov DA[1] ✉, Verdiev BI[1], Enenko AA[2], Gushchin VA[1,3,4], Tkachuk AP[1]

[1] Laboratory of Translational Biomedicine,
Gamaleya Research Institute of Epidemiology and Microbiology, Moscow

[2] ZAO Laminar Systems, Miass, Chelyabinsk oblast

[3] Laboratory of Population Variability Mechanisms in Pathogenic Microorganisms,
Gamaleya Research Institute of Epidemiology and Microbiology, Moscow

[4] Department of Virology, Faculty of Biology, Lomonosov Moscow State University, Moscow

Air quality monitoring is essential when it comes to protecting the urban population, especially that of big metropolises, from biohazards including biopathogens (BPs). This process is aided by different samplers and analyzers of aerosol pollutants, filters and disinfection systems. Their performance is tested using experimental aerosol formulations with a predetermined composition. Unfortunately, the majority of such systems available in Russia are only able to process a few hundred liters of air per time unit, which is too little. Big aerosol chambers (10 to 20 m^3) are very expensive and may not fit into a lab, necessitating an extensive overhaul. In this work we present a workstation for the detection of BP markers under controlled conditions based on the microbiological safety box MSB-III-Laminar-C-1.5 (380.150.01) that was originally designed to test the performance of samplers and analyzers of experimental aerosol formulations. Our workstation can handle the majority of BSL-1-2 BPs and, given the chamber volume that satisfies the requirements of aerosol experiments (> 4 m^3), can be installed in a lab with an area of >10 m^2.

Keywords: infection, aerosol, aerosol sampling, aerosol chamber

Funding: this work was supported by the Ministry of Health of the Russian Federation as part of the project *The National System for Chemical and Biological Security of the Russian Federation (2015-2020)* and by the Ministry of Education and Science as part of the project RFMEFI60117X0018.

✉ **Correspondence should be addressed:** Denis A. Kleymenov
Gamalei 18, Moscow, 123098; 10000let@rambler.ru, denis.a.kleymenov@gamaleya.org

Received: 06.08.2018 **Accepted:** 31.08.2018

DOI: 10.24075/brsmu.2018.053

ОПЫТ ИСПОЛЬЗОВАНИЯ АНАЛИТИЧЕСКОГО СТЕНДА ДЛЯ ПРОВЕДЕНИЯ АЭРОЗОЛЬНЫХ ИСПЫТАНИЙ В КОНТРОЛИРУЕМЫХ УСЛОВИЯХ

Д. А. Клейменов[1] ✉, Б. И. Вердиев[1], А. А. Ененко[2], В. А. Гущин[1,3,4], А. П. Ткачук[1]

[1] Лаборатория трансляционной биомедицины,
Национальный исследовательский центр эпидемиологии и микробиологии имени Н. Ф. Гамалеи Минздрава России, Москва

[2] ЗАО Ламинарные системы, Миасс, Челябинская обл.

[3] Лаборатория механизмов популяционной изменчивости патогенных микроорганизмов,
Национальный исследовательский центр эпидемиологии и микробиологии имени Н. Ф. Гамалеи Минздрава России, Москва

[4] Кафедра вирусологии, биологический факультет, Московский государственный университет имени М. В. Ломоносова, Москва

Для обеспечения безопасности проживающих в условиях города людей необходимо контролировать воздушную среду населенных пунктов и прежде всего мегаполисов на наличие патогенных биологических агентов (ПБА). Разрабатываются различные системы контроля биологического состава воздушной среды (сбор и анализ аэрозоля) и ее очистки (фильтрация, дезинфекция). Возможность экспериментального создания аэрозолей заданного состава является необходимым условием разработки любых подобных устройств. Рабочий объем большинства установок для работы с аэрозолями, имеющихся в России, достигает нескольких сотен литров, что недостаточно. Специальные аэрозольные камеры с большим рабочим объемом (10–20 $м^3$) характеризуются высокой стоимостью и требуют проведения капитального строительства/реконструкции помещений для их установки. В настоящей работе представлен аналитический стенд для индикации маркеров ПБА в контролируемых условиях, разработанный на основе специального варианта бокса БМБ-III-«Ламинар-С»-1,5 (380.150.01), главным назначением которого является проведение тестов и испытаний приборов для сбора и/или анализа аэрозолей модельных биопатогенов. Устройство предназначено для проведения исследований начального и среднего уровня с большинством ПБА III группы патогенности внутри отдельной лаборатории. Внешние размеры позволяют устанавливать его в помещениях площадью от 10 $м^2$ при достаточном внутреннем объеме камеры для проведения испытаний (более 4 $м^3$).

Ключевые слова: инфекционные заболевания, аэрозольные инфекции, сбор аэрозоля, аэрозольный стенд

Финансирование: статья подготовлена при поддержке Министерства здравоохранения Российской Федерации в рамках программы «Национальная система химической и биологической безопасности 2015–2020» и Министерства образования и науки РФ в рамках проекта RFMEFI60117X0018.

✉ **Для корреспонденции:** Денис Александрович Клейменов
ул. Гамалеи, д. 18, г. Москва, 123098; 10000let@rambler.ru, denis.a.kleymenov@gamaleya.org

Статья получена: 06.08.2018 **Статья принята к печати:** 31.08.2018

DOI: 10.24075/vrgmu.2018.053

In the modern world, air quality monitoring is becoming increasingly important. The evolution of biotechnologies has largely contributed to the natural diversity of biopathogens: genetically engineered microbial strains used in the pharmaceutical industry have turned into an additional source of environmental contamination [1]. Urban areas and agroindustrial zones provide a favorable environment for bacteria and viruses to thrive. Microorganisms settle in public places (clinics, maternity hospitals, metro systems) and utility networks (vent shafts, water supply systems, sewage networks). Some colonize animals and conquer their natural habitat. High density of the urban population, as well as its mobility, prepare

the ground for the spread of airborne infectious aerosols [2]. In addition, bioterrorism still poses a serious threat [3, 4].

Fortunately, we have an extensive arsenal of tools for monitoring air contamination at our disposal capable of sampling aerosol particles, estimating their concentration and size, and identifying biopathogens contained in the sample. Obviously, adaptation of these devices to a specific task and improvement of their performance are impossible without proper testing involving the use of experimental aerosol formulations that model the behavior of the actual particulate matter. In an enclosed indoor aerosol test chamber, protection from hazardous bioaerosols can be ensured by state-of-the-art high-performance filters [5, 6].

Among the most important parameters the chamber has to meet are sufficient space to accommodate the equipment; easy access inside; reasonable dimensions compatible with the size of the room it will be installed in; the inbuilt system of incoming and exiting air filtration; even distribution of aerosol particles throughout the chamber volume; simplicity of cleaning and decontamination procedures. Modern class III biological safety cabinets (BSC-III) meet the majority of these requirements but one for the inner volume of the chamber [6].

I. Design of the experiment

Our bioaerosol test chamber devised for the detection of biopathogens in the controlled environment is a modernized version of the BSC-III Laminar-C-1.5 (380.150.01) designed to test samplers and analyzers of model bioaerosols.

A prototype of an aerosol sampler with liquid phase recirculation and preconcentration of particles was developed at the National Research Nuclear University MEPhI. The sampler can operate at a volumetric air flow of 4,000 l/min collecting particles of >0.5 μm in size. Its performance was compared to that of the SASS 4000/2300 aerosol concentration device with a cyclone air sampler (Research International Inc.; USA).

The main stages of chamber development and testing procedures are described below.

II. Preparation

1. Equipment

1.1. Chamber for the detection of hazardous bioaerosols in the controlled environment

BSC-III Laminar-C-1.5 (380.150.01) by ZAO Laminar Systems, Russia, is a class III biological safety enclosure (GOST R EN 12469-2010) with chamber dimensions of 1.5 × 1.5 × 1.9 m (Fig. 1). Before entering the chamber, the continuously supplied air passes through a high-efficiency class H-14 inlet HEPA filter. The filter maintains a clean environment in the chamber corresponding to ISO class 5 of air cleanliness for 0.5 μm particles (GOST 14644-1-2002). The air exits through a cascade of 2 consecutive class H14 exhaust HEPA filters. In the chamber, the negative pressure of at least 250 Pa (relative to the outside pressure) is created by exhaust fans, forcing the air to circulate in the chamber. The maximum air flow rate through the chamber is 800 m^3/h but it can be reduced or terminated by adjusting the rotation speed of the exhaust fans and the position of a gate valve that changes the aerodynamic drag in the inlet air duct. The air containing aerosol particles generated in the chamber goes through a cascade of exhaust filters for decontamination and exits into the room where the workstation is installed. The negative pressure of 250 Pa maintained in the chamber minimizes the risk of aerosol leakage, which depends solely on the efficiency of HEPA filters cascade. This chamber is not equipped with separate air pipes for the aerosol-contaminated air, so the exiting air just travels straight into the first exhaust HEPA filter.

The equipment that needs to be tested is loaded into the chamber through a full-sized leak-tight door. The biaxial hinge mechanism and 4 handles allow the glass surface of the door to fit tightly against the door seal.

Inside the chamber, the environment is controlled by the monitoring equipment connected to a feedthrough panel. Another panel has all necessary airpipe fittings and electrical connectors to connect diagnostic and measuring equipment to the computer.

The operating mode is selected using a control sensor panel. The system can automatically maintain a preset air flow rate and negative pressure in the chamber and signal any abnormal situation or equipment failure. It also reports clogged HEPA- and prefilters and adjusts the fan speed and the position of the gate valve to compensate for a change in their aerodynamic drag.

Disinfection is performed according to standard protocols considering the specifics of the conducted tests. The chamber is equipped with a pair of UV lamps for primary disinfection. Terminal decontamination can be performed using formaldehyde or hydrogen peroxide vapor phases. The equipment required for decontamination can be plugged into 38-mm feedthroughs.

1.2. Aerosol sampling device (National Research Nuclear University MEPhI; Russia)

The aerosol sampler used for our tests consists of a virtual impactor connected to a cyclone by an air pipe (Fig. 2). The device exploits the idea of two-stage particle concentration, allowing to achieve high volumetric air flow rates of up to 4,000 l/min. First, air is sucked into the nozzle of the virtual impactor where captured particles are concentrated. Then the air containing concentrated particles exits the impactor at 300 l/min and enters the cyclone collector where the captured particles precipitate in the sorption liquid circulating in the cyclone. The longer the circulation time, the higher the concentration of the incoming particles in the liquid phase. The volume of the released liquid sample is 7–8 ml.

1.3 Air sampling device SASS 4000/2300 (Research International Inc.; USA)

The air sampler SASS 4000/2300 utilizes a similar principle of action. In the first stage, the air flows into the impactor nozzle at 3,600 l/min. In the second stage, the cyclone collector ensures the flow rate of 325 l/min and releases 4-5 ml of the liquid sample.

1.4. Portable aerosol particle counter SOLAIR 3100 (Lighthouse Worldwide Solutions; USA)

This device is used to test the integrity of inlet and exhaust HEPA filters. In our experiment, we took measurements using 6 particle channels: 0.3, 0.5, 1.0, 3.0, 5.0, and 10.0 μm.

1.5. Aerosol counter of submicron particles 4705 (AeroNanoTech; Russia)

This portable aerosol counter of submicron particles is intended for measuring the concentration of particles and their size

distribution in the submicronic range. Five particle channels (1, 2, 3, 5, and 10 μm) were used in our experiment.

III. Tests

1. Integrity of HEPA filters (Test 1)

The integrity of the filters was checked before the chamber was put into operation, as recommended by GOST R ISO 14644-3-2007 [7]. The filters were challenged with a control aerosol formulation. Filter surfaces and holding frames were scanned using the SOLAIR 3100 particle counter; alternatively, particle count was performed in the samples of the filtered air collected from the air pipe.

2. Rate and efficiency of air decontamination (Test 2). Efficiency test of the aerosol sampler designed at the National Research Nuclear University MEPhI

Decontamination tests were conducted in 3 different operating modes. Before the tests, the fans installed in the chamber to set the air in motion and to ensure even distribution of aerosol particles throughout the chamber volume (Fig. 1) and the filtration system were switched on. Upon reaching the air cleanliness of 0-353 particles per m^3 (or 0–1 particle sized 1, 3, 5, or 10 μm as detected by the particle counter), the filters were inactivated, but the fans continued working. Fig. 3 features data obtained starting from this point of the experiment. After the filtration system was switched off, aerosol was generated from a 10% saccharose solution in distilled water for 5 min by the Comp Air NE-C28 compressor nebulizer (Omron Healthcare Co., Ltd.; Japan) placed inside the chamber. Particles sized 1, 3 and 5 μm were counted inside the chamber using the counter of submicron particles 4705. The counter reported an average number of particles per 1 min for 16 minutes in a row. In the first operating mode (precipitation of unstirred aerosol) the fans were turned off, the filtration system inactivated, and aerosol particles counted for 11 minutes. In the second operating mode (precipitation of stirred aerosol) the fans were turned on, filtration switched off, and particles counted for 11 min. Additionally, at this stage of the experiment we introduced the aerosol sampler designed at MEPhI and counted aerosol particles while the device was working. In the third mode (air decontamination from stirred aerosol) the fans were turned off, filtration inactivated, and particles counted for 11 minutes.

3. Comparing the efficiency of aerosol collection of the two aerosol samplers (Test 3)

To evaluate the efficiency of polydisperse aerosol collection, we prepared 100 ml of a 10% saccharose solution in distilled water containing fluorescein sodium salt at a final concentration

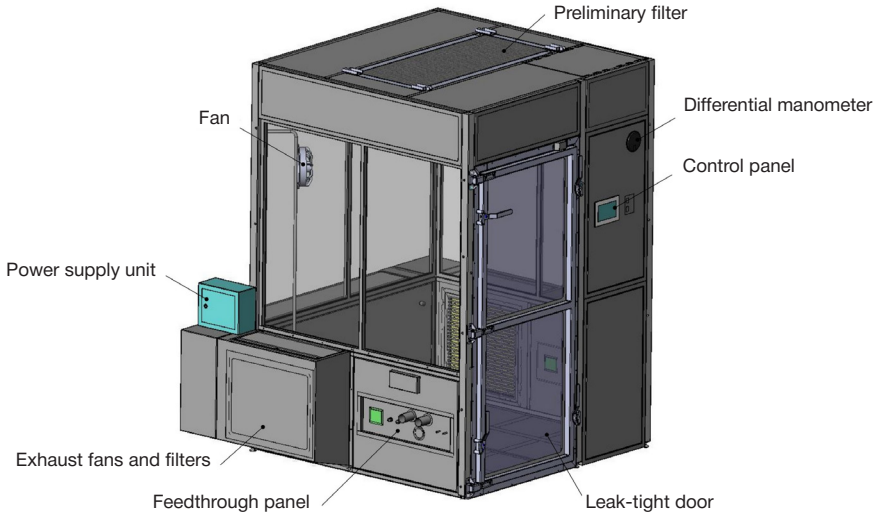

Fig. 1. Laminar-C-1.5 Class III Biosafety Enclosure (380.150.01)

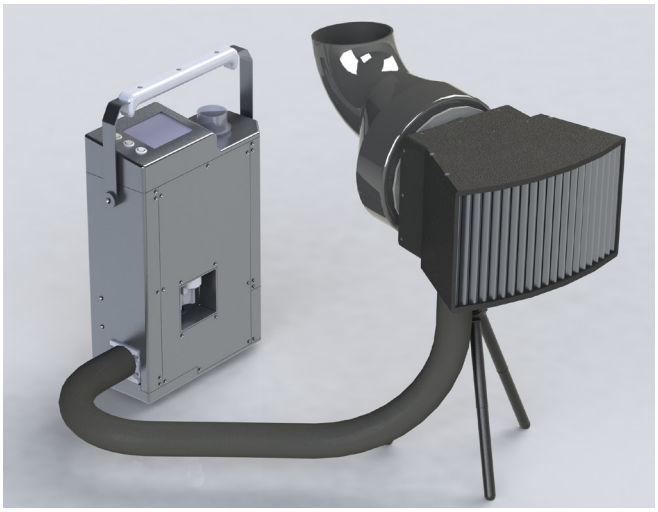

Fig. 2. The aerosol sampling device (National Research Nuclear University MEPhI)

of 1 μM. This amount was sufficient to run all the tests we planned. Fluorescence intensity of the collected tracer was measured on the Qubit 3.0 Fluorometer (Invitrogen; USA) in relative fluorescence units at 470 nm excitation and 510–580 nm emission wavelengths in 0.6 ml test tubes (SSI; USA) containing carbonate buffer (pH 9.6) (C3041; Sigma; Germany).

All tests were carried out with the fans switched on. Prior to each test, the air inside the chamber was decontaminated. Briefly, the ventilation system was left to work for 15 minutes. Then the cyclone collector was washed automatically with the impactor turned on. After that, control air samples were collected for 6 minutes. For the analysis, we took 270 μl of the sample, mixed them with 30 μl 10x carbonate buffer (pH 9.6) (C3041; Sigma; Germany) and measured fluorescence intensity. If the measured value exceeded the background fluorescence of empty test tubes, the cyclone collector was washed again. Once the anticipated fluorescence intensity was reached, the ventilation system was turned off.

Aerosol was generated inside the chamber by the compressor nebulizer Comp Air NE-C28 for 5 minutes. Prior to each test the device was washed and wiped dry with a lint-free cloth. Then 4 ml of the saccharose solution containing sodium fluorescein were loaded into the nebulizer. The aerosol sampler was turned on simultaneously with the nebulizer and collected aerosol particles for 6 min, i.e. the sampling process continued for another minute after aerosol generation was terminated. After samples were taken to the lab for the analysis, the cyclone collector was washed as described above.

For each aerosol sampler the tests were done in five replicates.

IV. Analysis of workstation performance

The equipment was commissioned as recommended by GOST R ISO 14644-3-2007. As part of the procedure, the integrity of HEPA filters was evaluated [7].

The conducted tests (Table 1) confirmed that the integrity and efficiency of the installed filters meet the requirements for class H14 filters.

The rate and efficiency of air decontamination in the chamber is shown in Fig. 3. All graphs demonstrate the contribution of the ventilation system to the dynamics of air decontamination. In figures A, C, and E the Y-axis is linear, while in B, D, and F it is logarithmic. The 3 latter graphs do not include the data obtained in the third operating mode. The number of aerosol particles sized 1 to 5 μm decreased to only a few within 3 to 6 minutes of the 11-min-long test when all components of the air purification system were in operation. When the filters were inactivated, decontamination was much slower, especially when the fans were turned off. Most likely, in this operating mode aerosol precipitates on the internal surfaces of the chamber. When the system of air purification is in full operation, it takes only 10 minutes to completely decontaminate the air in the chamber from the generated particles sized 1 to 5 μm.

The aerosol sampler developed at MEPhI was able to collect 92–99% of dust (relative to the number of particles measured before collection) within 7 minutes in the ventilated chamber with inactivated air filtration. However, we did not account for the size of the particles present in the air before collection (tens of millions 1 μm particles and millions of 3 and 5 μm particles) (Table 2).

Table 1. Integrity tests of HEPA filters installed in the chamber

HEPA filter	Number of 0.3 μm particles (N_c) before air filtration	Concentration of aerosol particles per cm^3 (C_c) before air filtration $C_c = \frac{N_c}{q_{vs} \cdot T_{stat}} \cdot dil$	Number of particles sized 0.3 μm or larger after air filtration	The highest detected number of particles sized 0.3 μm or larger exiting the filter scan (N_{scan}) $N_{scan} \le C_c \cdot P_{int} \cdot q_{vs} \cdot T_{scan}$	Threshold
Inlet filter	50109	1061	130	≤ 18779	Not exceeded
First stage exhaust filter	91343	1935	4493	≤ 13701	Not exceeded
Second stage exhaust filter	49624	1051	281	≤ 18602	Not exceeded
q_{vs}	Claimed sampling rate of the particle counter = 472 cm^3/s				
dil	Claimed dilution factor = 100				
T_{stat}	Recommended time for stationary measurements = 10 s				
P_{int}	Tolerated local penetration of HEPA filters (GOST R ISO 14644-3-2007) = 0.00025				
T_{scan}	Sampling time = 150 s, 60 s, and 150 s, respectively				

Table 2. Rate of dust particle collection by the aerosol sampler (National Research Nuclear University MEPhI)

Time elapsed from the start of the test (min)	1 μm particles		3 μm particles		5 μm particles	
5	56829268	100%	6700900	100%	1289540	100%
7	41036585	72%	3322200	50%	555680	43%
8	21097561	37%	1062200	16%	160966	12%
10	11707317	21%	497200	7%	51038	4%
11	6951220	12%	265550	4%	17032.8	1%
12	4512195	8%	172890	3%	6402.4	0.5%

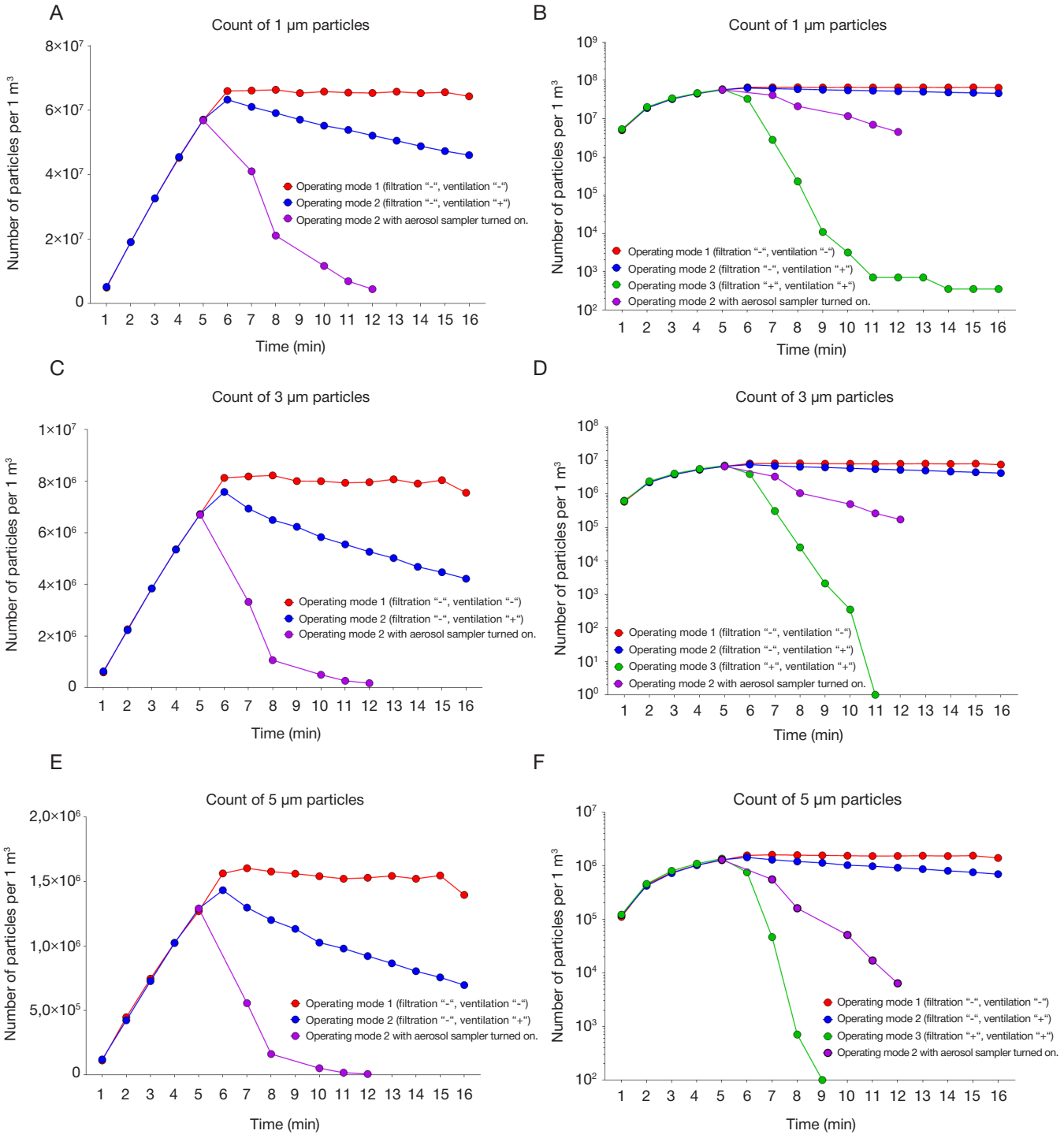

Fig. 3. Dynamics of air decontamination from 1 to 10 μm particles (**A**–**F**) in the Laminar-C-1.5 Class III Biosafety Enclosure after 5 minutes of aerosol generation in different operating modes

Table 3 demonstrates the efficiency of polydisperse aerosol collection evaluated from the fluorescence intensity of the tracer. Fluorescence expressed in relative fluorescence units was normalized to the volume of the released liquid sample for each device. The prototype of the aerosol sampler developed at the National Research Nuclear University MEPhI has an average rate of collection similar to that of SASS; based on the results of 5 measurements, the difference is insignificant ($p > 0.05$; Student's T-test applied). For each of the compared aerosol samplers 4 washes in the ventilated environment were enough to remove the fluorescent tracer and reach the level of background fluorescence.

V. Discussion of the results

There are a few factors complicating the study of properties exhibited by biopathogens in ambient air. First, bioaerosols must be generated in enclosed laboratory spaces to prevent damage to the environment and people. Seconds, such enclosures must have an inbuilt system for rapid and efficient air decontamination and disinfection after the experiment. Third, they must satisfy the strict sanitation and safety requirements set by state agencies. Finally, our high-tech age demands that such chambers should be made from cutting-edge environment-friendly materials and equipped with sensors to

Table 3. Efficiency of polydisperse aerosol collection

Aerosol sampler	Average sample volume, ml	Average RFU/ml considering error of measurement	Relative to SASS, %
MEPhI	7.5	1441 ± 98	97.7
SASS	4.5	1475 ± 122	100

monitor pressure, temperature, air flow rate, air cleanliness, and other parameters inside the chamber and have electronic panels for control and data input [8–10].

All of these factors have to be accounted for in the design of the end product. Given that it is not intended for mass production, the final price can be really formidable.

In Russia, such workstations are available in the shared facilities of big research institutions. A good example is an enclosure for static and dynamic aerosol measurements designed at the State Research Institute for Biological Instrumentation to test the technical parameters of biosafety systems in the controlled environment at temperatures ranging from - 20 to + 40 °C and relative humidity of 30 to 95% [11]. This huge enclosure (static chamber sizes are 8 and 26 m^3) is a perfect space to experiment with pathogenic aerosols and airborne microorganisms. Sadly, for technical reasons the Institute cannot work with pathogens included in the hazard groups 3 and 4 which seriously limits the range of tested bioaerosols to their simulators. Although a series of minor experiments can be conveniently conducted here, the situation does not favor long-term extensive research, which is very unfortunate given construction costs.

Class III biosafety cabinets are cheaper and, therefore, more available. They protect the operator and the environment from contamination by hazardous aerosols resulting from manipulations with pathogenic agents and also protect the agents inside the chamber from external contamination. Cabinets are intended for one or two operators and their internal working space is quite small (> 1 m^3).

The experimental workstation described and successfully tested in this study is a trade-off between the two. This Laminar-C-1.5 Class III Biosafety Enclosure (380.150.01) was designed to test the devices for testing and analyzing model pathogenic bioaerosols. Class H14 HEPA filters installed in the chamber capture over 99.995 % of generated particles sized > 0.3 μm [12]. The primary application of these filters is air decontamination from radioactive particulate matter with 99.97 % efficiency. They have a few drawbacks. The majority of (but not all) bacteria are from 0.4 (*Proteus mirabilis*) to 10 μm (*Clostridium perfringens*) in size; pathogenic fungi vary in size from 1 (*Pneumocystis jirovecii*) to 20 μm (*Fusarium sp.*). Viruses fall into the range from 0.02 (*Rhinovirus*) to 0.3 (*Mumps virus*) μm [13]. In addition, for some pathogens the infective dose is really tiny, such as <10 bacterial cells for *Coxiella burnetii that* causes Q fever. These 10 cells may well be part of those 0.005 % of the particles that are not retained by the filter in the experiment where the number of the sprayed bacteria is 10^7 CFU or higher [14]. Studies of HEPA filters involving the MS2 phage have shown that filtration efficiency is directly dependent on the air flow rate [15]. Thus, the choice of filters is largely determined by the task set for the researcher. Our Laminar-C-1.5 Class III Biosafety Enclosure is equipped with two consecutive exhaust HEPA filters (the calculated particle penetration value is 3×10^{-9}%) and is capable of maintaining the optimal air flow rate, ensuring sufficient protection in the experiments involving high concentrations of biopathogens (up to 10^6–10^7 CFU/m^3). The conducted tests (Table 1) prove that the filters satisfy the state requirements for integrity and efficiency and that the chamber can be used for the majority of standard tasks.

Tests of the rate and efficiency of air decontamination from 1, 3 and 5 μm particles have shown that aerosol concentration remains more or less stable for quite a long time (11 minutes) if the systems of filtration and ventilation are turned off. When the fans inducing air circulation in the chamber are turned off, the concentration of particles of all three sizes slightly decreases within the same time interval. The system of air decontamination has demonstrated high rate and efficiency by removing all particulate admixtures from the air in 3 to 6 minutes depending on the size and number of the particles generated in the chamber. In test 3 some parameters of the aerosol sampler developed at the National Research Nuclear University MEPhI were compared to those of its foreign counterpart.

CONCLUSION

Laminar-C-1.5 Class III Biosafety Enclosure (380.150.01) is a high-quality workstation for aerosol tests that can be installed inside a lab. The volume of the work chamber is 4.275 m^3, which is sufficient for the first- and second-level tests involving the majority of biopathogens. The workstation can be used to test aerosol samplers and study bioaerosol behavior at various concentrations in static and dynamic modes.

References

1. Lacey J, Dutkiewicz J. Bioaerosols and Occupational Lung Desease. J Aerosol Sci. 1994; 25 (8): 1371–404.
2. Li Y, Leung GM, Tang JW, et al. Role of Ventilation in Airborne Transmission of Infectious Agents in the Built Environment — a Multidisciplinary Systematic Review. Indoor Air. 2007; (17): 2–18.
3. Tu AT. Aum Shinrikyo's Chemical and Biological Weapons: More Than Sarin. Forensic Sci Rev. 2014; 26 (2): 115–20.
4. Schep LJ, Temple WA, Butt GA, Beasley MD. Ricin as a weapon of mass terror--separating fact from fiction. Environ Int. 2009; 35 (8): 1267–71.
5. SP 1.3.1285-2003. Bezopasnost' raboty s mikroorganizmami I–II grupp patogennosti (opasnosti). Minjust RF. Reg. nom. 4545 (15 maja 2003).
6. GOST R EN 12469-2010. Biotehnologija. Tehnicheskie trebovanija k boksam mikrobiologicheskoj bezopasnosti. Rosstandart. Reg. nom. 1144-st (29 dekabrja 2010).
7. GOST R ISO 14644-3-2007. Chistye pomeshhenija i svjazannye s nimi kontroliruemye sredy. Chast' 3. Metody ispytanij. Rosstandart. Reg. nom. 616-st (27 dekabrja 2007).
8. Bezopasnost' raboty s mikroorganizmami I–II grupp patogennosti (opasnosti): Sanitarno-jepidemiologicheskie pravila SP 1.3.3118-13. M.: Federal'nyj centr gigieny i jepidemiologii Rospotrebnadzora; 2014. 195 s.
9. Bezopasnost' raboty s mikroorganizmami III–IV grupp patogennosti (opasnosti) i vozbuditeljami parazitarnyh boleznej: Sanitarno-jepidemiologicheskie pravila SP 1.3.2322-08 (s izmenenijami na 29 ijunja 2011 g). Dostupno po ssylke: http://docs.cntd.ru/document/902091086

10. Bezopasnost' raboty s mikroorganizmami III–IV grupp patogennosti (opasnosti) i vozbuditeljami parazitarnyh boleznej. Dopolnenija i izmenenija N 1 k SP 1.3.2322-08. Sanitarno-jepidemiologicheskie pravila SP 1.3.2518-09. M.: Federal'nyj centr gigieny i jepidemiologii Rospotrebnadzora; 2009. 8 s.
11. Nauchno-tehnologicheskaja infrastruktura Rossijskoj Federacii. Centry kollektivnogo pol'zovanija nauchnym oborudovaniem i unikal'nye nauchnye ustanovki. Dostupno po ssylke: http://ckp-rf.ru/usu/73550/
12. lamsys.ru [internet]. ZAO "Laminarnye sistemy" Dostupno po ssylke: http://www.lamsys.ru/nera.php
13. Kowalski W. Hospital Airborne Infection Control. CRC Press. 2012; p. 42–48.
14. EJ van Schaik, C. Chen, K. Mertens, MM Weber, JE Samuel. Molecular pathogenesis of the obligate intracellular bacterium Coxiella burnetii. Nat Rev Microbiol. 2013; 11 (8): 561–73.
15. Heimbuch BK, Hodge JE, Wander JD. Viral Penetration of High Efficiency Particulate Air (HEPA) Filters. 5th ASM Biodefense and Emerging Diseases Research Meeting; 2007 27 Feb–2 Mar; Washington DC. Available from: https://www.researchgate.net/publication/235151297_Viral_Penetration_of_High_Efficiency_Particulate_Air_HEPA_Filters

Литература

1. Lacey J, Dutkiewicz J. Bioaerosols and Occupational Lung Desease. J Aerosol Sci. 1994; 25 (8): 1371–404.
2. Li Y, Leung GM, Tang JW, et al. Role of Ventilation in Airborne Transmission of Infectious Agents in the Built Environment — a Multidisciplinary Systematic Review. Indoor Air. 2007; (17): 2–18.
3. Tu AT. Aum Shinrikyo's Chemical and Biological Weapons: More Than Sarin. Forensic Sci Rev. 2014; 26 (2): 115–20.
4. Schep LJ, Temple WA, Butt GA, Beasley MD. Ricin as a weapon of mass terror--separating fact from fiction. Environ Int. 2009; 35 (8): 1267–71.
5. СП 1.3.1285-2003. Безопасность работы с микроорганизмами I–II групп патогенности (опасности). Минюст РФ. Рег. ном. 4545 (15 мая 2003).
6. ГОСТ Р ЕН 12469-2010. Биотехнология. Технические требования к боксам микробиологической безопасности. Росстандарт. Рег. ном. 1144-ст (29 декабря 2010).
7. ГОСТ Р ИСО 14644-3-2007. Чистые помещения и связанные с ними контролируемые среды. Часть 3. Методы испытаний. Росстандарт. Рег. ном. 616-ст (27 декабря 2007).
8. Безопасность работы с микроорганизмами I–II групп патогенности (опасности): Санитарно-эпидемиологические правила СП 1.3.3118-13. М.: Федеральный центр гигиены и эпидемиологии Роспотребнадзора; 2014. 195 с.
9. Безопасность работы с микроорганизмами III–IV групп патогенности (опасности) и возбудителями паразитарных болезней: Санитарно-эпидемиологические правила СП 1.3.2322-08 (с изменениями на 29 июня 2011 года). Доступно по ссылке: http://docs.cntd.ru/document/902091086
10. Безопасность работы с микроорганизмами III–IV групп патогенности (опасности) и возбудителями паразитарных болезней. Дополнения и изменения N 1 к СП 1.3.2322-08. Санитарно-эпидемиологические правила СП 1.3.2518-09. М.: Федеральный центр гигиены и эпидемиологии Роспотребнадзора; 2009. 8 с.
11. Научно-технологическая инфраструктура Российской Федерации. Центры коллективного пользования научным оборудованием и уникальные научные установки. Доступно по ссылке: http://ckp-rf.ru/usu/73550/
12. lamsys.ru [internet]. ЗАО "Ламинарные системы" Доступно по ссылке: http://www.lamsys.ru/nera.php
13. Kowalski W. Hospital Airborne Infection Control. CRC Press. 2012; p. 42–48.
14. EJ van Schaik, C. Chen, K. Mertens, MM Weber, JE Samuel. Molecular pathogenesis of the obligate intracellular bacterium Coxiella burnetii. Nat Rev Microbiol. 2013; 11 (8): 561–73.
15. Heimbuch BK, Hodge JE, Wander JD. Viral Penetration of High Efficiency Particulate Air (HEPA) Filters. 5th ASM Biodefense and Emerging Diseases Research Meeting; 2007 27 Feb – 2 Mar; Washington DC. Available from: https://www.researchgate.net/publication/235151297_Viral_Penetration_of_High_Efficiency_Particulate_Air_HEPA_Filters

COMPARISON OF FLUORESCENCE EXCITATION MODES FOR CDSE SEMI-CONDUCTOR QUANTUM DOTS USED IN MEDICAL RESEARCH

Kuzishchin YA[1] ✉, Martynov IL[1], Osipov EV[1], Samokhvalov PS[2], Chistyakov AA[1], Nabiev IR[2]

[1] Department of Physics of Micro- and Nanosystems,
National Research Nuclear University MEPhI, Moscow

[2] Laboratory of Nano-Bioengineering,
National Research Nuclear University MEPhI, Moscow

Fluorescence spectroscopy is a powerful tool used in applied biological and medical research. Colloid semi-conductor quantum dots are promising fluorescent tags for simultaneous detection of different biopathogens. The techniques employing these tags can be improved by selecting the optimal modes for signal excitation and detection. The aim of the present work was to derive a mathematical expression to describe the signal-to-noise ratios in the pulsed and modulated excitation modes. Below, we compare these two modes of fluorescence excitation in ultralow quantities of quantum dots. We demonstrate that modulated excitation should be preferred for CdSe/ZnS quantum dots given that signal accumulation time is over 100 mc and the photosensor is exposed to background light of > 1 μW.

Keywords: quantum dots, CdSe/ZnS, luminescence, excitation, photodetection

Funding: this work was supported by the Federal Target Program *The National System for Chemical and Biological Security of the Russian Federation (2015–2020)* and carried out under the state contract No. K-27-НИР/146-2 dated December 28, 2015.

✉ **Correspondence should be addressed:** Yuri A. Kuzishchin
Kashirskoe shosse, 31, Moscow, 115409; yriy.kuzishchin@gmail.com

Received: 29.07.2018 **Accepted:** 25.08.2018

DOI: 10.24075/brsmu.2018.050

СРАВНЕНИЕ РЕЖИМОВ ВОЗБУЖДЕНИЯ ФЛУОРЕСЦЕНЦИИ ПОЛУПРОВОДНИКОВЫХ КВАНТОВЫХ ТОЧЕК НА ОСНОВЕ СЕЛЕНИДА КАДМИЯ ДЛЯ БИОМЕДИЦИНСКИХ ПРИЛОЖЕНИЙ

Ю. А. Кузищин[1] ✉, И. Л. Мартынов[1], Е. В. Осипов[1], П. С. Самохвалов[2], А. А. Чистяков[1], И. Р. Набиев[2]

[1] Кафедра физики микро- и наносистем,
Национальный исследовательский ядерный университет «МИФИ» (Московский инженерно-физический институт), Москва

[2] Лаборатория нано-бионженерии,
Национальный исследовательский ядерный университет «МИФИ» (Московский инженерно-физический институт), Москва

В настоящее время, флуоресцентная спектроскопия — это мощный инструмент, используемый в биологических и медицинских прикладных исследованиях. Одним из перспективных типов люминесцентных меток для одновременного обнаружения различных биологических агентов в одной пробе являются коллоидные полупроводниковые квантовые точки. Важным направлением совершенствования методики их применения является подбор оптимального режима возбуждения и регистрации флуоресцентного сигнала. Таким образом, целью настоящей работы было получение математического выражения для оценки отношения сигнал/шум в случае импульсного и модуляциоонго режимов возбуждения. Представлены результаты теоретического сравнения данных режимов возбуждения для регистрации флуоресцентного сигнала от ультра-малых количеств квантовых точек. Показано, что в случае применения квантовых точек CdSe/ZnS в условиях фоновой засветки с мощностью свыше 1 мкВт и временем накопления полезного сигнала свыше 100 мс для достижения высокой обнаружительной способности предпочтительнее использовать модуляционный режим возбуждения.

Ключевые слова: квантовые точки, CdSe/ZnS, люминесценция, возбуждение, фотодетекция

Финансирование: исследование поддержано Министерством здравоохранения Российской Федерации, в рамках Федеральной целевой программы «Национальная система химической и биологической безопасности Российской Федерации (2015–2020 годы)», государственный контракт К-27-НИР/146-2 от 28.12.15.

✉ **Для корреспонденции:** Юрий Александрович Кузищин
Каширское ш., д. 31, г. Москва, 115409; yriy.kuzishchin@gmail.com

Статья получена: 29.07.2018 **Статья принята к печати:** 25.08.2018

DOI: 10.24075/vrgmu.2018.050

Today, fluorescence-based analytical techniques are widely used in applied biological and medical research to study protein structures [1–3], diagnose cancer [4–8] and autoimmune disorders [9], detect and classify biopathogens and toxins [10]. The majority of these techniques rely on fluorescence tags, among which semi-conductor quantum dots hold the highest potential [8, 11–13]. Unlike conventional organic dyes, quantum dots have broad absorption spectra [14, 15], exhibit high quantum yield [16] and record-breaking photostability [17]. Besides, the wavelength of the fluorescence emitted from quantum dots depends on their size, so one can «tune» the fluorescence spectra by varying the size of nanocrystals [16, 18].

Sometimes, as is the case with detecting low pathogen concentrations or screening for cancer and autoimmune

disorders, it is necessary to record ultralow-intensity fluorescence [10]. Indeed, the best state-of-the-art photosensors sensitive to the visible light spectrum are capable of detecting single photons [10]. Such devices, however, only operate at very low temperatures [19, 20] and are ultrasensitive to background light [20]. These factors combined with high costs limit the use of photodetectors to specific laboratory equipment or commercial premium-quality machines [21–25]. Still, applied research cannot do without highly sensitive, small, cheap, background-noise-resistant photodetectors for fluorescence-based assays involving multiple measurements of the same type.

Such photodetectors can be constructed from standard silicon PIN photodiodes. To reduce background light interfering with their performance, pulsed [26, 27] and modulated [28–30] excitation modes can be used for luminophore excitation. In the first approach, luminescence induced by pulsed excitation is detected over a short time interval comparable to the excited-state lifetime of the luminophore. If the intensity of the excitation pulse is chosen properly, the amplitude peak of the luminescence signal will significantly exceed the level of background light. This approach, however, has a drawback: it relies on the use of broadband photodetectors, broadband recording units and expensive laser sources of excitation radiation with a pulse duration ranging from 10 ns to tens of picoseconds, depending on the selected fluorophore.

In the second approach, the effect of background light is neutralized by reaching a high modulation frequency of excitation light that exceeds a typical fluctuation frequency of background light. Usually, the modulation frequency falls within a range of 10 to 100 kHz [31, 32]. By applying the Fourier transform at the modulation frequency during signal processing, one can isolate and discard the signal resulting from low-frequency power fluctuations of background light.

To create a photosensor exploiting the principle of modulated excitation, narrowband or lock-in amplifiers, the Fourier transform of the emitted luminescence signal or their combination are employed [31, 32]. Each of these approaches has its own specifics. Although the use of a broadband amplifier necessitates a broad dynamic range and a good ADC (analog-to-digital converter) resolution for the Fourier transform to be applied, the latter is instrumental in eliciting a plethora of information about the recorded signal as possible. Narrowband amplifiers do not impose such strict requirements on the ADC but their architecture is more complex.

On the whole, the technique based on the modulation of excitation light requires a simpler laser source than the pulsed-based one. Still, it is not perfect: one of the most obvious downsides to it is long signal accumulation time not needed for pulsed excitation.

Considering the above said, the optimal choice of a technique for detecting low-intensity luminescence is determined by the photo- and physical properties of the selected luminophore and the level of background light. Devices for luminescence analysis must be fast, cheap and have low power consumption.

The aim of this work was to carry out a comprehensive comparison of techniques exploiting pulsed and modulated signals to excite low-intensity luminescence in the visible part of the light spectrum and detect it using PIN photodiode photosensors. The average power of excitation light was selected as a reference condition. We hope that the obtained data will aid in selecting the optimal system for a luminescence assay based on the excited-state lifetime of the luminophore and the level of background light. In this work we also talk about the choice of optimal modulation frequency of excitation light.

METHODS

In this section we derive mathematical expressions to describe the signal-to-noise ratio using a standard noise model, write them in a convenient form for further comparison and use them for the analysis of different fluorophore excitation modes. The average power of excitation light was selected as a reference condition allowing us to compare the pulsed and modulated excitation modes.

The output of the majority of Si PIN photodiode photosensors is voltage [33–36], whereas the photodiode itself is a source of current [37]. To convert current to voltage, such photodetectors are equipped with a transimpedance amplifier [38] set up for a particular task.

The main characteristics of a transimpedance amplifier are transimpedance resistance R_T and the upper bound frequency f_p. The following statement is true for the signal with a frequency below f_p:

$$U_s = P_s \cdot S \cdot R_T ,$$

where U_s is the output voltage, P_s is the power of the fluorescence signal, S is the sensitivity of the photodiode. The noise of the amplifier can be described in terms of the output voltage noise density of the amplifier u_{na}. However, in practice NEP (the noise equivalent power of the optical signal) is often used for this purpose [37]:

$$NEP = \frac{u_{na}}{R_T \cdot S}\left[\frac{W}{\sqrt{Hz}}\right]. \quad (1)$$

Clearly, both NEP and the detection threshold of the photosensor are directly dependent on the noise characteristics of the amplifier and the operating mode.

Of note, the noise of a multistage amplifier is determined by the noise of the first stage [39]; the subsequent stages only proportionally increase the amplitude of both signal and noise and do not affect their ratio. This phenomenon allows us to use a single-stage amplifier as a model for analyzing noise characteristics. In transimpedance amplifiers the primary source of noise is the thermal noise of feedback resistance R_f which corresponds to transimpedance resistance R_T. Using the standard equation for thermal noise [40], one can write:

$$NEP = \frac{1}{S} \cdot \sqrt{\frac{4kT}{R_T}} \sim \frac{1}{\sqrt{R_T}}, \quad (2)$$

where k is the Boltzmann constant and T is resistance temperature.

From the expression (2) we can deduce that an increase in feedback resistance improves noise characteristics of the photosensor, but because of the parasitic capacitance C_p of the photodiode [37] the upper bound frequency f_p decreases. Considering the relationship between R_T and C_p, the NEP equation can be rewritten as follows:

$$NEP = \frac{1}{S} \cdot \sqrt{8\pi\kappa T C_p f_p} \quad . \quad (3)$$

The equation (3) means that the simplest way to detect an ultralow-intensity fluorescence signal is to continuously excite the studied sample and use a photosensor equipped with a direct current amplifier. This approach, however, is hardly ever implemented because of the sources of additional low-frequency noise $\Delta NEP(f)$, such as flicker noise [29, 40, 41], popcorn noise [40] and power fluctuations of external light sources [42–45]. At frequencies below ~1 kHz, the contribution of these noise sources can considerably exceed thermal noise density and outweigh the advantages of a low-frequency photosensor [29,

46]. Therefore, pulsed and modulated excitation modes are used instead, reducing the effect of additional noise sources [29]. Each of these approaches, however, has its own specifics.

For a broadband amplifier unexposed to background light and a signal induced by modulated excitation, the signal-to-noise ratio can be described by the following equation:

$$S/N = \frac{P_{lum}}{P_n} = \frac{<P_{lum}> \cdot 2}{\left(\int_0^{fm} \left(\frac{8\pi\kappa TC_p f_p}{S^2} + \Delta NEP^2(f)\right) df\right)^{0.5}}, \quad (4)$$

where $<P_{lum}>$ is the average power of the fluorescence signal, P_n is the noise power, f_m is the modulation frequency of excitation light. Presumably, the inverse duty ratio of excitation pulses equals 2 and the upper bound frequency of the amplifier fp equals the modulation frequency or slightly exceeds it.

At the same time, the photosensor operating in the modulated excitation mode can only have a narrow gain bandwidth Δf_p near the modulation frequency f_p. So, to use modulated excitation, physical or programmable lock-in amplification [32], narrowband amplifiers [47] or filters [47] are required; alternatively, multiple measurements can be taken to average the signal [47]. These measures can help to avoid the contribution of $\Delta NEP(f)$ to the total noise. If $f_m = n \cdot \Delta fp$, where n represents the number of periods needed to average the signal, a photodetector with a narrowband amplifier can be described by the following equation:

$$S/N = \frac{P_{lum}}{P_n} = \frac{<P_{lum}> \cdot S \cdot \sqrt{n}}{f_m \sqrt{2\pi\kappa TC_p}} = \frac{<P_{lum}> \cdot S}{\Delta f_p \sqrt{2\pi\kappa TC_p n}}, \quad (5)$$

Another challenge of this approach is the choice of an optimal modulation frequency of excitation light. From (5) it is clear that one should use the lowest frequency possible allowed by the operational speed of the device. At frequencies below ~1 kHz the contribution of additional noises increases, rendering work in this mode useless. The presence of background light necessitates additional analysis with due account of the spectral density of external light fluctuations at various frequencies.

The pulsed excitation mode relies on the phenomenon of the peak power of the fluorescence signal $P_{lum} = <P_{lum}> \cdot d$,

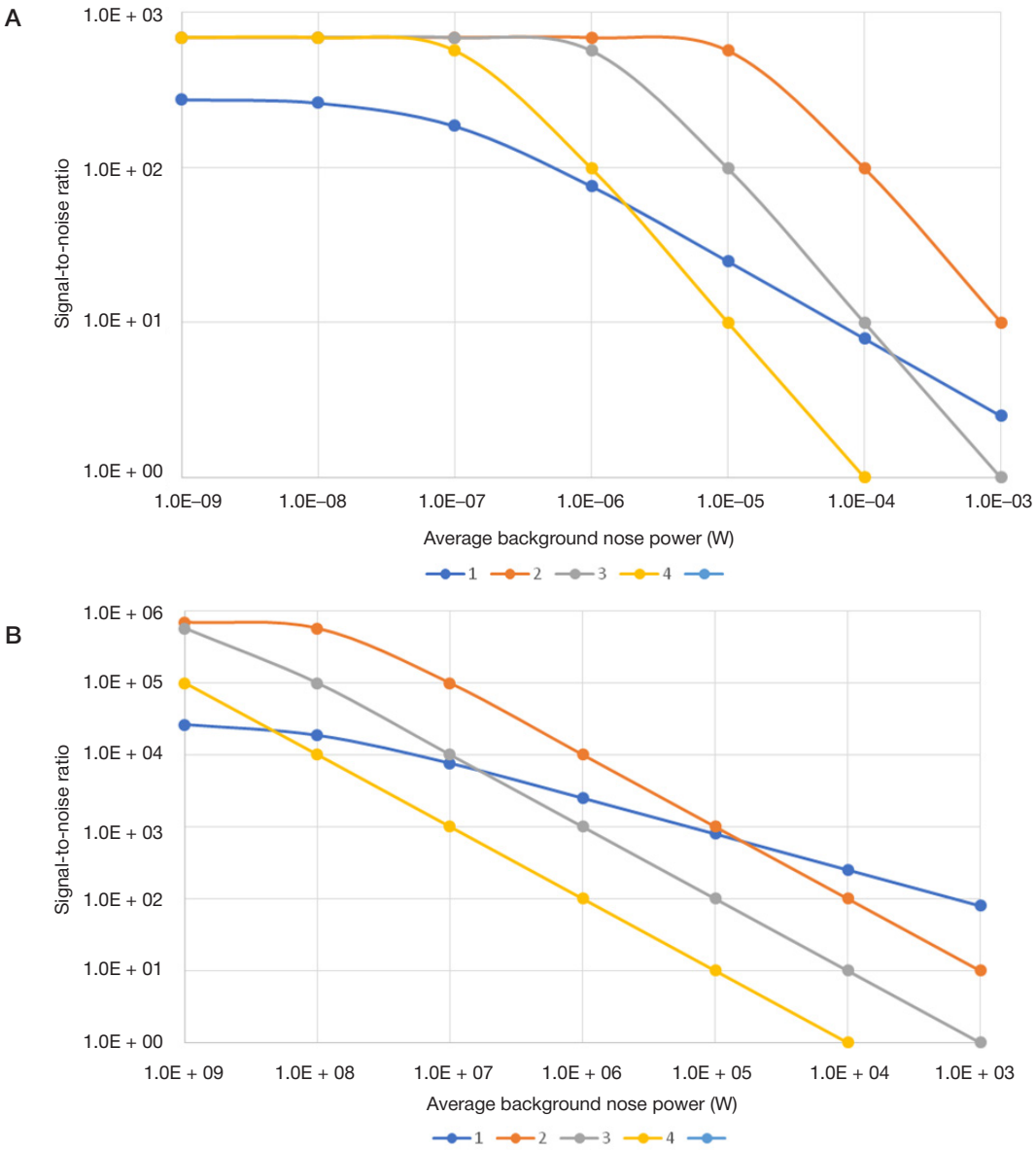

Fig. 1. Dependency of the signal-to-noise ratio of the receiver on the background noise power in the modulated excitation mode (1) and pulsed excitation mode (2) for a luminophore with an excited-state lifetime of 1 ns (2), 10 ns (3), and 100 ns (4). **A**. Signal accumulation times is 1 ms, the average power of the fluorescent signal is 1 nW, the typical frequency of background fluctuations is 100 Hz. **B**. Signal accumulation times is 1,000 ms, the average power of the fluorescent signal is 1 nW, the typical frequency of background fluctuations is 100 Hz

where d is the inverse duty cycle of excitation pulses. The pulse repetition rate f_{ex} is determined by the requirements for the operational speed of the device and is limited by the excited-state lifetime τ_{lum} of the used fluorophore. If the task is to obtain information about τ_{lum}, then the duration of the excitation pulse τ_{ex} must be significantly lower than τ_{lum}. But generally, it can be comparable to τ_{lum}, mitigating requirements for the upper bound frequency, which in this case is $f_p \approx 1/\tau_{lum}$ or $f_p = d \cdot f_{ex}$.

The excited-state lifetime of such fluorophores as organic dyes and quantum dots normally varies from 1 to 100 ns [48, 49]. Therefore, the upper bound frequency of the photosensor must fall within an interval between ~0.01 and 1 GHz. Under such conditions, the contribution of additional low-frequency noises $\Delta NEP(f)$ is negligible in comparison with the total thermal noise of the amplifier. With that in mind, NEP and the signal-to-noise ratio of the photosensor operating in the pulsed-modulation mode can be described by the following equations:

$$S/N = \frac{P_{lum}}{P_n} = \frac{<P_{lum}> \cdot S \cdot d}{\sqrt{8\pi\kappa T C_p f_p} \cdot \sqrt{f_p}} = \frac{<P_{lum}> \cdot S}{\sqrt{8\pi\kappa T C_p} \cdot f_{ex}}. \quad (6)$$

To account for the effects of background light with the average power P_{bg}, the obtained formulas have to be corrected. In the modulated excitation mode, the effect of background light is indirect and manifests as an increase in shot noise. In the pulsed-excitation mode, the effect of background light shows as fluctuations of external illumination with the typical borderline frequency f_{bg}. Considering that, the signal-to-noise ratio in both excitation modes can be written as

$$S/N = \frac{<P_{lum}>}{\left[2\pi\kappa T C_p \Delta f_p^2 n / S^2 + eP_{bg}\Delta f_p / 2S\right]^{0.5}}, \quad (7)$$

$$S/N = \frac{<P_{lum}>}{\left[8\pi\kappa T C_p f_{ex}^2 / S^2 + (P_{bg}\tau_{lum} f_{bg})^2\right]^{0.5}}. \quad (8)$$

The formulas (7) and (8) allow adequate comparison of signal-to-noise ratios in pulsed and modulated excitation modes at the same operational speed of the device and the same average power of the fluorescence signal (and, therefore, the same average power of excitation light).

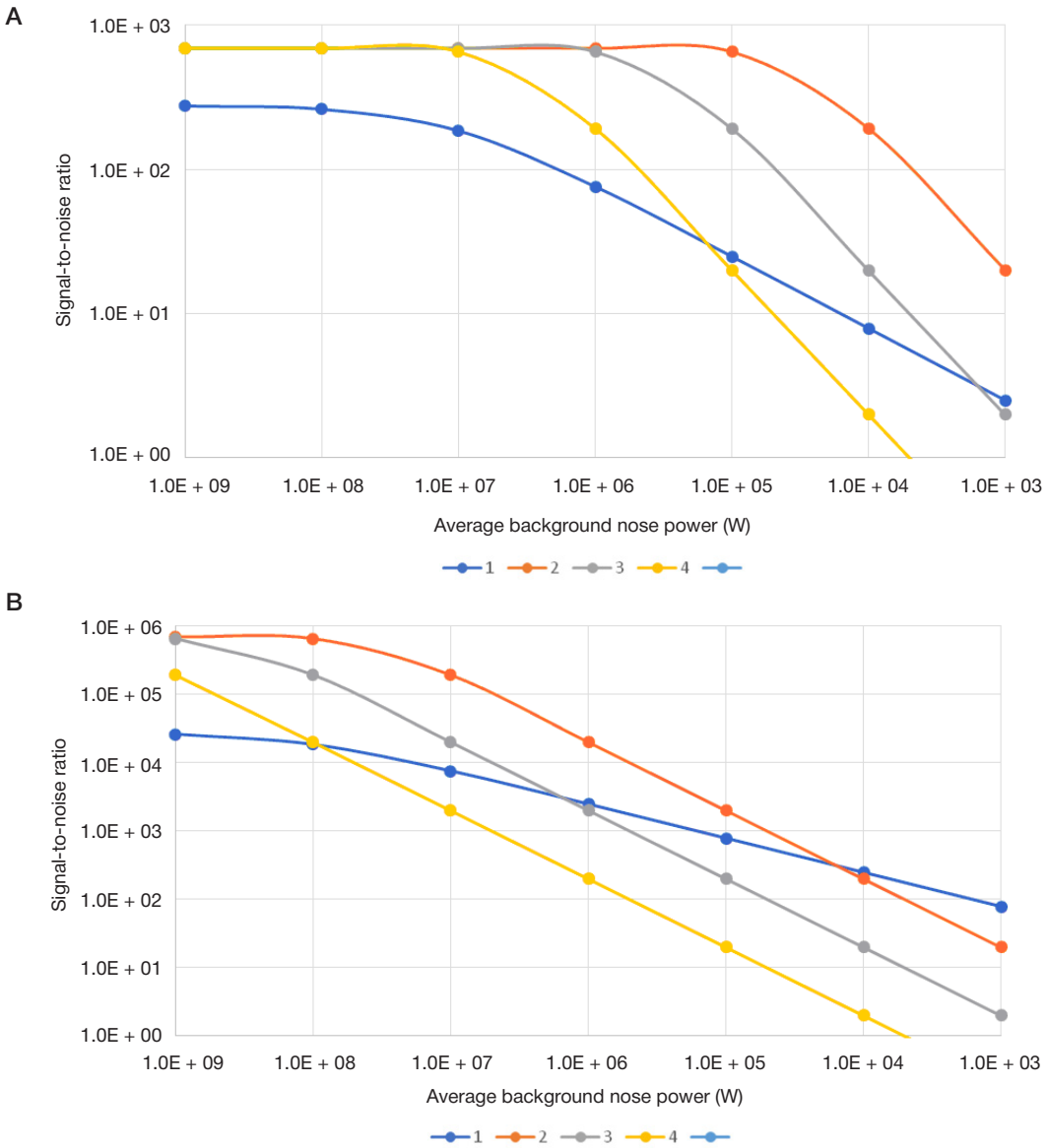

Fig. 2. Dependency of the signal-to-noise ratio of the receiver on the background noise power in the modulated excitation mode (1) and pulsed excitation mode (2) at typical frequencies of the background power fluctuation of 10 Hz (1), 100 Hz (2), and 1,000 Hz (4). **A**. Signal accumulation times is 1 ms, the average power of the fluorescent signal is 1 nW, the excited-state lifetime of the luminophore is 5 ns. **B**. Signal accumulation times is 1,000 ms, the average power of the fluorescent signal is 1 nW, the excited-state lifetime of the luminophore is 5 ns

RESULTS

Using the equations (7) and (8), we have analyzed the dependencies of the signal-to-noise ratio on different parameters, including the power and frequency of background light fluctuations, the operational speed of the photodetector and the excited-state lifetime of the fluorophore. For convenience, we constructed the curves shown in the figures below. Fig. 1A and 1B feature curves representing dependencies of the signal-to-noise ratio on the power of background light for luminophores with different excited-state lifetimes. Figures 2A and 2B show curves representing dependencies of the signal-to-noise ratio on the power of background light at various typical frequencies of its fluctuations.

DISCUSSION

In the absence of background light, pulsed excitation of the fluorophore is preferable (Fig. 1A and 1B). In the presence of background light, pulsed excitation still should be opted for when fast results are needed and the selected fluorophore has an excited-state lifetime of less than 1 ns.

At the same time, as the power of background light increases, the signal-to-noise ratio declines more slowly if pulse excitation is applied. Also, it is important to remember that the signal-to- noise ratio depends both on the excited-state lifetime of the fluorophore and the typical fluctuation frequencies of the background light power. Thus, for pulsed excitation the signal-to-noise ratio is lower than for modulated excitation if the excited-state lifetime of the luminophore is over 100 ns. A similar situation is observed when the average background light power exceeds ~ 1 μW and its typical fluctuation frequency is over 100 Hz. Such conditions occur when scanning systems or artificial light sources are used [42, 43, 50], especially LED lamps [46]. The detection threshold of a photosensor operating in the modulated excitation mode at a properly selected modulation frequency will not depend on the excited-state lifetime of the selected luminophore or fluctuation frequencies of the background light power (Fig. 2A and 2B).

The excited-state lifetime of quantum dots normally falls within the range from 10 to 100 ns. Thus, modulated excitation is a better choice if the task is to detect the ultralow quantities of semi-conductor quantum dots in the presence of background light with an average power of > 1 μW given that signal accumulation time is least 100 ms. Moreover, the sources of excitation light for the modulation-based method are cheaper and simpler in architecture than those generating very short (nano/pico) pulsed signals.

CONCLUSIONS

We have derived a mathematical expression for computing the signal-to-noise ratio for Si PIN photodiode photosensors operating in the pulsed and modulated excitation modes used for the induction of luminescence in the visible light spectra in the presence of background light. We have demonstrated that modulated excitation is preferable for luminescent CdSe/ZnS semi-conductor quantum dots given that signal accumulation time is at least 100 ms and the device is exposed to background light > 1 μW.

References

1. Moulick R, Udgaonkar JB. Identification and structural characterization of the precursor conformation of the prion protein which directly initiates misfolding and oligomerization. J Mol Biol. 2017; 429 (6): 886–899.
2. Chen H, Rhoades E. Fluorescence characterization of denatured proteins. Curr Opin Struct Biol. 2008;18 (4): 516–524.
3. Hevekerl H, Tornmalm J, Widengren J. Fluorescence-based characterization of non-fluorescent transient states of tryptophan — prospects for protein conformation and interaction studies. Sci Rep. 2016; 6 (1): 35052.
4. Dramićanin T, Dramićanin M. Using fluorescence spectroscopy to diagnose breast cancer. Appl Mol Spectrosc to Curr Res Chem Biol Sci. 2016.
5. Sukhanova A, Even-Desrumeaux K, Kisserli A, et al. Oriented conjugates of single-domain antibodies and quantum dots: toward a new generation of ultrasmall diagnostic nanoprobes. Nanomedicine: NBM. 2012; 8 (4): 516–25.
6. Bilan R, Ametzazurra A, Brazhnik K, et al. Quantum-dot-based suspension microarray for multiplex detection of lung cancer markers: preclinical validation and comparison with the Luminex xMAP® system. Sci Rep. 2017; (7): 44668.
7. Brazhnik K, Sokolova Z, Baryshnikova M, et al. Quantum dot-based lab-on-a-bead system for multiplexed detection of free and total prostate-specific antigens in clinical human serum samples. Nanomedicine: NBM. 2015; 11 (5): 1065–75.
8. Hafian H, Sukhanova A, Turini M, et al. Multiphoton imaging of tumor biomarkers with conjugates of single-domain antibodies and quantum dots. Nanomedicine: NBM. 2014; 10 (8): 1701–9.
9. Sukhanova A, Susha AS, Bek A, et al. Nanocrystal-encoded fluorescent microbeads for proteomics: Antibody profiling and diagnostics of autoimmune diseases. Nano Lett. 2007; 7 (8): 2322–7.
10. Wessels L, Raad H. Recent advances in point of care diagnostic tools: a review. Am J Eng Appl Sci. 2016; 9 (4): 1088–1095.
11. Samokhvalov P, Artemyev M, Nabiev I. Basic principles and current trends in colloidal synthesis of highly luminescent semiconductor nanocrystals. Chem – A Eur J. 2013; 19 (5): 1534–1546.
12. Vokhmintcev KV, Samokhvalov PS, Nabiev I. Charge transfer and separation in photoexcited quantum dot-based systems. Nano Today. 2016; 11 (2): 189–211.
13. Resch-Genger U, Grabolle M, Cavaliere-Jaricot S, Nitschke R, Nann T. Quantum dots versus organic dyes as fluorescent labels. Nat Methods. 2008; 5 (9): 763–775.
14. Yu WW, Qu L, Guo W, Peng X. Experimental determination of the extinction coefficient of CdTe, CdSe, and CdS nanocrystals. Chem Mater. 2003; 15 (14): 2854–60.
15. Jasieniak J, Smith L, Van Embden J, Mulvaney P, Califano M. Re-examination of the size-dependent absorption properties of CdSe quantum dots. J Phys Chem C. 2009; 113 (45): 19468–74.
16. Krivenkov V, Samokhvalov P, Zvaigzne M, et al. Ligand-mediated photobrightening and photodarkening of CdSe/ZnS quantum dot ensembles. J Phys Chem C. 2018; DOI: 10.1021/acs.jpcc.8b04544.
17. Ramos-Gomes, F, Bode J, Sukhanova A et al. Single- and two-photon imaging of human micrometastases and disseminated tumour cells with conjugates of nanobodies and quantum dots. Sci Rep. 2018; (8): 4595.
18. Bonilla JC, Bozkurt F, Ansari S, Sozer N, Kokini JL. Applications of quantum dots in food Science and biology. Trends Food Sci Technol. 2016; (53): 75–89.
19. Collazuol G, Bisogni MG, Marcatili S, Piemonte C, Del Guerra A. Studies of silicon photomultipliers at cryogenic temperatures. Nucl Instruments Methods Phys Res Sect A Accel Spectrometers, Detect Assoc Equip. 2011; 628 (1): 389–92.
20. Takeuchi S, Kim J, Yamamoto Y, Hogue HH. Development of a high-quantum-efficiency single-photon counting system. Appl Phys Lett. 1999; 74 (8): 1063–5.
21. Moon S, Kim DY. Analog single-photon counter for high-speed

scanning microscopy. Opt Express. 2008; 16 (18): 13990–14003.
22. Benninger RKP, Ashby WJ, Ring E a., Piston DW. A single-photon counting detector for increased sensitivity in two-photon laser scanning microscopy. Opt Lett. 2008; 33 (24): 2895–7.
23. Du B, Pang C, Wu D, et al. High-speed photon-counting laser ranging for broad range of distances. Sci Rep. 2018; 8 (1): 1–6.
24. Jang JY, Cho M. Image visualization of photon counting confocal microscopy using statistical estimation. Optik (Stuttg). 2016; 127 (2): 844–7.
25. Chen W, Wang X, Wang B, et al. Lock-in-photon-counting-based highly-sensitive and large-dynamic imaging system for continuous-wave diffuse optical tomography. Biomed Opt Express. 2016; 7 (2): 499.
26. Boscher ND, Choquet P, Duday D, Verdier S. Advantages of a pulsed electrical excitation mode on the corrosion performance of organosilicon thin films deposited on aluminium foil by atmospheric pressure dielectric barrier discharge. Plasma Process Polym. 2010; 7 (2): 163–71.
27. Steen HB, Sqrensen OI. Pulse Modulation of the excitation light source boosts the sensitivity of an arc lamp-based flow cytometer. Cytometry. 1993; (14): 115–22.
28. Huang C, Lu X, Jiang Y, Wang X, Qiao Z, Fan W. Real-time characterization of FM-AM modulation in a high-power laser facility using an RF-photonics system and a denoising algorithm. Appl Opt. 2017; 56 (6): 1610–15.
29. Gak J, Miguez M, Bremermann M, Arnaud A. On the reduction of thermal and flicker noise in ENG signal recording amplifiers. Analog Integr Circuits Signal Process. 2008; 57 (1–2): 39–48.
30. De Marcellis A, Palange E, Giuliani R, Janneh M. Very high sensitivity electrically modulated Si-photodiode in photovoltaic-mode as phase-sensitive detector of light power. Proc IEEE Sensors. 2014; 2014 December: 1115–7.
31. Ayat M, Karami MA, Mirzakuchaki S, Beheshti-Shirazi A. Design of multiple modulated frequency lock-in amplifier for tapping-mode atomic force microscopy systems. IEEE Trans Instrum Meas. 2016; 65 (10): 2284–92.
32. Bhattacharyya S, Ahmed RN, Purkayastha BB, Bhattacharyya K. Implementation of digital lock-in amplifier. J Phys Conf Ser. 2016; 759 (1).
33. Datta S, Rajagopalan S, Lemke S, Joshi A. Balanced PIN-TIA photoreceiver with integrated 3 dB fiber coupler for distributed fiber optic sensors. 2014; 9098: 90980Y.
34. Angelini P, Blache F, Caillaud C, et al. High sensitivity SOA-PIN/TIA photoreceiver for 40 Gb/s applications and beyond. Int J Microw Wirel Technol. 2016; 8 (03): 437–445.
35. Rahman SN, Hall D, Mei Z, Lo Y-H. Integrated 1550 nm photoreceiver with built-in amplification and feedback mechanisms. Opt Lett. 2013; 38 (20): 4166–9.
36. Cervantes FG, Livas J, Silverberg R, Buchanan E, Stebbins R. Characterization of photoreceivers for LISA. Class Quantum Gravity. 2011; 28 (9).
37. M A, Gregory H. Photodetection. In: Michael Bass, editor. Handbook of Optics. McGraw-Hill , Inc.; 1994. 1664 p.
38. Lin TY, Green RJ, O'Connor PB. A low noise single-transistor transimpedance preamplifier for Fourier-transform mass spectrometry using a T feedback network. Rev Sci Instrum. 2012;83(9).
39. Jaquay JW. Designers Guide to: Instrumentation amplifiers. Exp Tech. 1977;2(2):40–43.
40. Wai Chen. The Electrical Engineering Handbook. Elsevier Academic Press; 2004. 1228 p.
41. Vernotte F, Lantz E. Metrology and 1/f noise: Linear regressions and confidence intervals in flicker noise context. Metrologia. 2015; 52 (2): 222–37.
42. Sindhubala K, Vijayalakshmi B. Review jn impact of ambient light noise sources and applications in optical wireless communication using LED. International Journal of Applied Engineering Research. 2015; 10 (12): 31115–30.
43. Pham Q, Rachim V, An J, Chung W-Y. Ambient light rejection using a novel average voltage tracking in visible light communication system. Appl Sci. 2017; 7 (7): 670.
44. Shen Z, Thomas JJ, Siuzdak G, Blackledge RD. A case study on forensic polymer analysis by DIOS-MS: the suspect who gave us the SLIP. J Forensic Sci. 2004; 49 (5): 1028–35.
45. Cletus B, Olds W, Fredericks PM, Jaatinen E, Izake EL. Real-time detection of concealed chemical hazards under ambient light conditions using raman spectroscopy. J Forensic Sci. 2013; 58 (4): 1008–14.
46. Kim T, Rylander M, Powers EJ, Grady WM, Arapostathis A. LED lamp flicker caused by interharmonics. Conf Rec - IEEE Instrum Meas Technol Conf. 2008: 1920–5.
47. Zumbahlen H, editor. Linear Circuit Design Handbook. Newnes/Elsevier; 2008. 960 p
48. Gong K, Martin JE, Shea-Rohwer LE, Lu P, Kelley DF. Radiative lifetimes of zincblende CdSe/CdS quantum dots. J Phys Chem C. 2015; 119 (4): 2231–8.
49. Berezin MMY, Achilefu S. Fluorescence lifetime measurements and biological imaging. Chem Rev. 2011; 110 (5): 2641–84.
50. Kovalenko B, Roskosky M, Freedman BA, Shuler MS. Effect of ambient light on near infrared spectroscopy. Trauma Treat. 2015; 911–6.

Литература

1. Moulick R, Udgaonkar JB. Identification and structural characterization of the precursor conformation of the prion protein which directly initiates misfolding and oligomerization. J Mol Biol. 2017; 429 (6): 886–899.
2. Chen H, Rhoades E. Fluorescence characterization of denatured proteins. Curr Opin Struct Biol. 2008;18 (4): 516–524.
3. Hevekerl H, Tornmalm J, Widengren J. Fluorescence-based characterization of non-fluorescent transient states of tryptophan — prospects for protein conformation and interaction studies. Sci Rep. 2016; 6 (1): 35052.
4. Dramićanin T, Dramićanin M. Using fluorescence spectroscopy to diagnose breast cancer. Appl Mol Spectrosc to Curr Res Chem Biol Sci. 2016.
5. Sukhanova A, Even-Desrumeaux K, Kisserli A, et al. Oriented conjugates of single-domain antibodies and quantum dots: toward a new generation of ultrasmall diagnostic nanoprobes. Nanomedicine: NBM. 2012; 8 (4): 516–25.
6. Bilan R, Ametzazurra A, Brazhnik K, et al. Quantum-dot-based suspension microarray for multiplex detection of lung cancer markers: preclinical validation and comparison with the Luminex xMAP® system. Sci Rep. 2017; (7): 44668.
7. Brazhnik K, Sokolova Z, Baryshnikova M, et al. Quantum dot-based lab-on-a-bead system for multiplexed detection of free and total prostate-specific antigens in clinical human serum samples. Nanomedicine: NBM. 2015; 11 (5): 1065–75.
8. Hafian H, Sukhanova A, Turini M, et al. Multiphoton imaging of tumor biomarkers with conjugates of single-domain antibodies and quantum dots. Nanomedicine: NBM. 2014; 10 (8): 1701–9.
9. Sukhanova A, Susha AS, Bek A, et al. Nanocrystal-encoded fluorescent microbeads for proteomics: Antibody profiling and diagnostics of autoimmune diseases. Nano Lett. 2007; 7 (8): 2322–7.
10. Wessels L, Raad H. Recent advances in point of care diagnostic tools: a review. Am J Eng Appl Sci. 2016; 9 (4): 1088–1095.
11. Samokhvalov P, Artemyev M, Nabiev I. Basic principles and current trends in colloidal synthesis of highly luminescent semiconductor nanocrystals. Chem – A Eur J. 2013; 19 (5): 1534–1546.
12. Vokhmintcev KV, Samokhvalov PS, Nabiev I. Charge transfer and separation in photoexcited quantum dot-based systems. Nano Today. 2016; 11 (2): 189–211.
13. Resch-Genger U, Grabolle M, Cavaliere-Jaricot S, Nitschke R, Nann T. Quantum dots versus organic dyes as fluorescent labels. Nat Methods. 2008; 5 (9): 763–775.
14. Yu WW, Qu L, Guo W, Peng X. Experimental determination of

the extinction coefficient of CdTe, CdSe, and CdS nanocrystals. Chem Mater. 2003; 15 (14): 2854–60.
15. Jasieniak J, Smith L, Van Embden J, Mulvaney P, Califano M. Re-examination of the size-dependent absorption properties of CdSe quantum dots. J Phys Chem C. 2009; 113 (45): 19468–74.
16. Krivenkov V, Samokhvalov P, Zvaigzne M, et al. Ligand-mediated photobrightening and photodarkening of CdSe/ZnS quantum dot ensembles. J Phys Chem C. 2018; DOI: 10.1021/acs.jpcc.8b04544.
17. Ramos-Gomes, F, Bode J, Sukhanova A et al. Single- and two-photon imaging of human micrometastases and disseminated tumour cells with conjugates of nanobodies and quantum dots. Sci Rep. 2018; (8): 4595.
18. Bonilla JC, Bozkurt F, Ansari S, Sozer N, Kokini JL. Applications of quantum dots in food Science and biology. Trends Food Sci Technol. 2016; (53): 75–89.
19. Collazuol G, Bisogni MG, Marcatili S, Piemonte C, Del Guerra A. Studies of silicon photomultipliers at cryogenic temperatures. Nucl Instruments Methods Phys Res Sect A Accel Spectrometers, Detect Assoc Equip. 2011; 628 (1): 389–92.
20. Takeuchi S, Kim J, Yamamoto Y, Hogue HH. Development of a high-quantum-efficiency single-photon counting system. Appl Phys Lett. 1999; 74 (8): 1063–5.
21. Moon S, Kim DY. Analog single-photon counter for high-speed scanning microscopy. Opt Express. 2008; 16 (18): 13990–14003.
22. Benninger RKP, Ashby WJ, Ring E a., Piston DW. A single-photon counting detector for increased sensitivity in two-photon laser scanning microscopy. Opt Lett. 2008; 33 (24): 2895–7.
23. Du B, Pang C, Wu D, et al. High-speed photon-counting laser ranging for broad range of distances. Sci Rep. 2018; 8 (1): 1–6.
24. Jang JY, Cho M. Image visualization of photon counting confocal microscopy using statistical estimation. Optik (Stuttg). 2016; 127 (2): 844–7.
25. Chen W, Wang X, Wang B, et al. Lock-in-photon-counting-based highly-sensitive and large-dynamic imaging system for continuous-wave diffuse optical tomography. Biomed Opt Express. 2016; 7 (2): 499.
26. Boscher ND, Choquet P, Duday D, Verdier S. Advantages of a pulsed electrical excitation mode on the corrosion performance of organosilicon thin films deposited on aluminium foil by atmospheric pressure dielectric barrier discharge. Plasma Process Polym. 2010; 7 (2): 163–71.
27. Steen HB, Sqrensen OI. Pulse Modulation of the excitation light source boosts the sensitivity of an arc lamp-based flow cytometer. Cytometry. 1993; (14): 115–22.
28. Huang C, Lu X, Jiang Y, Wang X, Qiao Z, Fan W. Real-time characterization of FM-AM modulation in a high-power laser facility using an RF-photonics system and a denoising algorithm. Appl Opt. 2017; 56 (6): 1610–15.
29. Gak J, Miguez M, Bremermann M, Arnaud A. On the reduction of thermal and flicker noise in ENG signal recording amplifiers. Analog Integr Circuits Signal Process. 2008; 57 (1–2): 39–48.
30. De Marcellis A, Palange E, Giuliani R, Janneh M. Very high sensitivity electrically modulated Si-photodiode in photovoltaic-mode as phase-sensitive detector of light power. Proc IEEE Sensors. 2014; 2014 December: 1115–7.
31. Ayat M, Karami MA, Mirzakuchaki S, Beheshti-Shirazi A. Design of multiple modulated frequency lock-in amplifier for tapping-mode atomic force microscopy systems. IEEE Trans Instrum Meas. 2016; 65 (10): 2284–92.
32. Bhattacharyya S, Ahmed RN, Purkayastha BB, Bhattacharyya K. Implementation of digital lock-in amplifier. J Phys Conf Ser. 2016; 759 (1).
33. Datta S, Rajagopalan S, Lemke S, Joshi A. Balanced PIN-TIA photoreceiver with integrated 3 dB fiber coupler for distributed fiber optic sensors. 2014; 9098: 90980Y.
34. Angelini P, Blache F, Caillaud C, et al. High sensitivity SOA-PIN/TIA photoreceiver for 40 Gb/s applications and beyond. Int J Microw Wirel Technol. 2016; 8 (03): 437–445.
35. Rahman SN, Hall D, Mei Z, Lo Y-H. Integrated 1550 nm photoreceiver with built-in amplification and feedback mechanisms. Opt Lett. 2013; 38 (20): 4166–9.
36. Cervantes FG, Livas J, Silverberg R, Buchanan E, Stebbins R. Characterization of photoreceivers for LISA. Class Quantum Gravity. 2011; 28 (9).
37. M A, Gregory H. Photodetection. In: Michael Bass, editor. Handbook of Optics. McGraw-Hill , Inc.; 1994. 1664 p.
38. Lin TY, Green RJ, O'Connor PB. A low noise single-transistor transimpedance preamplifier for Fourier-transform mass spectrometry using a T feedback network. Rev Sci Instrum. 2012;83(9).
39. Jaquay JW. Designers Guide to: Instrumentation amplifiers. Exp Tech. 1977;2(2):40–43.
40. Wai Chen. The Electrical Engineering Handbook. Elsevier Academic Press; 2004. 1228 p.
41. Vernotte F, Lantz E. Metrology and 1/f noise: Linear regressions and confidence intervals in flicker noise context. Metrologia. 2015; 52 (2): 222–37.
42. Sindhubala K, Vijayalakshmi B. Review jn impact of ambient light noise sources and applications in optical wireless communication using LED. International Journal of Applied Engineering Research. 2015; 10 (12): 31115–30.
43. Pham Q, Rachim V, An J, Chung W-Y. Ambient light rejection using a novel average voltage tracking in visible light communication system. Appl Sci. 2017; 7 (7): 670.
44. Shen Z, Thomas JJ, Siuzdak G, Blackledge RD. A case study on forensic polymer analysis by DIOS-MS: the suspect who gave us the SLIP. J Forensic Sci. 2004; 49 (5): 1028–35.
45. Cletus B, Olds W, Fredericks PM, Jaatinen E, Izake EL. Real-time detection of concealed chemical hazards under ambient light conditions using raman spectroscopy. J Forensic Sci. 2013; 58 (4): 1008–14.
46. Kim T, Rylander M, Powers EJ, Grady WM, Arapostathis A. LED lamp flicker caused by interharmonics. Conf Rec - IEEE Instrum Meas Technol Conf. 2008: 1920–5.
47. Zumbahlen H, editor. Linear Circuit Design Handbook. Newnes/Elsevier; 2008. 960 p
48. Gong K, Martin JE, Shea-Rohwer LE, Lu P, Kelley DF. Radiative lifetimes of zincblende CdSe/CdS quantum dots. J Phys Chem C. 2015; 119 (4): 2231–8.
49. Berezin MMY, Achilefu S. Fluorescence lifetime measurements and biological imaging. Chem Rev. 2011; 110 (5): 2641–84.
50. Kovalenko B, Roskosky M, Freedman BA, Shuler MS. Effect of ambient light on near infrared spectroscopy. Trauma Treat. 2015; 911–6.

A STUDY OF ANTIMICROBIAL ACTIVITY OF POLYPHENOLS DERIVED FROM WOOD

Shevelev AB[1] ✉, Isakova EP[2], Trubnikova EV[3], La Porta N[4], Martens S[4], Medvedeva OA[5], Trubnikov DV[6], Akbaev RM[7], Biryukova YK[8], Zylkova MV[8], Lebedeva AA[1], Smirnova MS[1], Deryabina YI[2]

[1] Vavilov Institute of General Genetics, Russian Academy of Sciences, Moscow
[2] Bakh Institute of Biochemistry, Research Center of Biotechnology of the Russian Academy of Sciences, Moscow
[3] Kursk State University, Kursk
[4] Fondazione Edmund Mach, San Michele all'Adige, Italy
[5] Kursk State Medical University, Kursk
[6] Prof. Ivanov Kursk State Agricultural Academy, Kursk
[7] Skryabin Moscow State Academy of Veterinary Medicine and Biotechnology, Moscow
[8] Chumakov Federal Scientific Center for Research and Development of Immune and Biological Products of the Russian Academy of Sciences, Moscow

Due to the spreading and increasing drug resistance of pathogens, the search for novel antibiotics is becoming ever more important. Plant-derived polyphenols are a vast and promising class of compounds with a potential to fight infectious diseases. Still, they are not routinely used in clinical practice. No reports on the *in vivo* studies of these compounds have been presented. The aim of our work was to compare the antimicrobial activity of resveratrol (stilbene), dihydroquercetin and dihydromyricetin (flavonols) extracted from the bark and wood of conifers against the dermatophytes *Staphylococcus aureus*, *Pseudomonas aeruginosa* and *Candida albicans*. Using the radial diffusion assay, we established that dihydroquercetin, resveratrol and dihydromyricetin exhibit high activity against *S. aureus* even at the smallest possible concentrations of 0.22, 0.15, and 0.15 mM, respectively. In contrast, the highest achievable concentrations of these compounds in the solutions (21.5, 15.5 and 15.0 mM for dihydroquercetin, resveratrol and dihydromyricetin, respectively) have no effect on the growth of *P. aeruginosa* and *C. albicans*. These findings suggest that polyphenols derived from conifers could have a potential to be used as a medicine for topical application to treat bacterial infections of the skin caused by *S. aureus*.

Keywords: polyphenols, flavonoid, stilbene, antimicrobial agents, resveratrol, antimicrobial activity, antioxidants, wood

Funding: this work was supported by the Ministry of Education and Science of the Russian Federation (Subsidy Contract No 14.616.21.0083 since July 17, 2017; ID RFMEFI61617X0083).

✉ **Correspondence should be addressed:** Alexei B. Shevelev
Gubkina 3, Moscow, 119991; shevel_a@hotmail.com

Received: 13.06.2018 **Accepted:** 20.07.2018

DOI: 10.24075/brsmu.2018.040

ИССЛЕДОВАНИЕ АНТИМИКРОБНОЙ АКТИВНОСТИ ПОЛИФЕНОЛОВ ИЗ ДРЕВЕСНОГО СЫРЬЯ

А. Б. Шевелев[1] ✉, Е. П. Исакова[2], Е. В. Трубникова[3], Н. Ла Порта[4], Ш. Мартенс[4], О. А. Медведева[5], Д. В. Трубников[6], Р. М. Акбаев[7], Ю. К. Бирюкова[8], М. В. Зылькова[8], А. А. Лебедева[1], М. С. Смирнова[1], Ю. И. Дерябина[2]

[1] Институт общей генетики имени Н. И. Вавилова РАН, Москва
[2] Институт биохимии имени А. Н. Баха, ФИЦ Биотехнологии РАН, Москва
[3] Курский государственный университет, Курск
[4] Фонд имени Э. Маха, С. Микеле аль Адидже, Италия
[5] Курский государственный медицинский университет, Курск
[6] Курская государственная сельскохозяйственная академия имени И. И. Иванова, Курск
[7] Московская государственная академия ветеринарной медицины и биотехнологии — МВА имени К. И. Скрябина, Москва
[8] Федеральный научный центр исследований и разработки иммунобиологических препаратов имени М. П. Чумакова РАН, Москва

В связи с выработкой патогенами лекарственной устойчивости к используемым антибиотикам поиск антимикробных агентов нового типа приобретает все большую актуальность. Растительные полифенолы — обширный и перспективный в борьбе с инфекционными заболеваниями класс соединений. Однако они почти не используются в медицинской практике, а результаты их биологических испытаний *in vivo* в литературе отсутствуют. Целью работы было провести сравнительное исследование антимикробной активности препаратов полифенолов ресвератрола (стильбен), дигидрокверцетина и дигидромерицетина (флавонолы), выделенных из коры и древесины хвойных пород, в отношении дерматофитов: *Staphylococcus aureus*, *Pseudomonas aeruginosa* и *Candida albicans*. В тесте на подавление роста газона индикаторных культур в условиях радиальной диффузии из лунки установлено, что все три соединения проявляют высокую активность в отношении *S. aureus*: концентрации 0,22 мМ для дигидрокверцетина, 0,15 мМ для ресвератрола и 0,15 мМ для дигидромерицетина превышают предел эффективности. Напротив, в отношении *P. aeruginosa* и *C. albicans* даже максимально возможные с учетом растворимости концентрации полифенольных соединений 21,5 мМ, 15,5 мМ и 15,0 мМ не оказывают какого-либо эффекта на рост культур. Полученные данные позволяют рассматривать полифенолы из хвойных растений в качестве перспективного наружного средства для лечения бактериальных инфекций кожи, вызываемых *S. aureus*.

Ключевые слова: полифенолы, флавоноиды, стильбены, антимикробные средства, ресвератрол, антимикробная активность, антиоксиданты, древесное сырье

Финансирование: исследование поддержано Министерством образования и науки Российской Федерации (Соглашения о представлении субсидии № 14.616.21.0083 от 17.07.2017, уникальный идентификатор RFMEFI61617X0083).

✉ **Для корреспонденции:** Алексей Борисович Шевелев
ул. Губкина, д. 3, г. Москва, 119991; shevel_a@hotmail.com

Статья получена: 13.06.2018 **Статья принята к печати:** 20.07.2018

DOI: 10.24075/vrgmu.2018.043

Polyphenols are secondary metabolites massively produced by plants. They have found wide application in the pharmaceutical industry and are routinely used as basic ingredients in complementary medicine. So far, over 8,000 phenolic compounds of plant origin have been identified. They are classified into simple phenols, derivatives of hydroxy cinnamyl and hydroxy benzyl alcohols, flavonoids, stilbenes, and lignans [1]. The largest class of polyphenols is constituted by flavonoids. Their core is formed by a flavan nucleus: a structure consisting of two aromatic rings linked by a chain of three carbon atoms [2]. Flavonoids (chalcones, catechins, anthocyanins, leuco-anthocyanins, flavones, flavanones, and flavonols) are found in abundance in bark, flowers, seeds and fruits. Stilbenes, another group of polyphenols, have two benzene rings and are related to flavonoids.

Stilbenes exert antioxidant and antimicrobial activity protecting plants from the harmful effects of phytopathogens, ozone and ultraviolet light. Stilbenes are found in various phyla and in conifers in particular [3]. The most famous representative of stilbenes is resveratrol. Other stilbenes, including pterostilbene, pinosylvin and rhaponticin, have also exhibited a similar type of activity [2].

Functionally, stilbenes and flavonoids belong to a class of phytoalexins, natural antibiotics of plants that protect the latter against infectious diseases and are synthesized in response to bacterial or fungal infections. It is reasonable to assume that phytoalexins will also demonstrate their bactericidal activity *in vitro*. As a rule, the extracts of herbs rich in flavonoids, such as chamomile, St. John's wort, plantain, and marigold, have a marked antibacterial effect [4]. In recent years, there has been growing interest in phytoalexins stimulated by the challenge of drug resistance and the ability of bacteria to form biofilms normally studied in such important model pathogens as *Mycobacterium tuberculosis*, *Streptococcus pneumoniae*, *Neisseria gonorrhoeae*, and *Streptococcus mutans* [5]. The most promising polyphenols capable of neutralizing these bacteria are a group of red wine polyphenols responsible for the "French paradox", such as quercetin, kaempferol, resveratrol, and some others [6]. However, despite a surge of interest in this problem, the mechanisms of antibacterial activity of stilbenes and flavonoids remain obscure, although it is known that all subclasses of flavonoids have bactericidal and fungicidal effects [7]. For example, resveratrol inhibits growth of *Helicobacter pylori*, a pathogen that causes peptic ulcer, in vitro [8], enhances phagocytosis of *C. albicans* [9] and suppresses phagocytosis of *S. aureus* and *E. coli*; this effect is mediated by the TLR-2 receptors of the innate immunity.

Although there is a huge body of evidence about the antimicrobial activity of plant-derived polyphenols, their use in clinical practice is limited to herbal extracts with unknown or only roughly estimated concentrations of active ingredients. As of today, a few companies and organizations, including TransMIT Gesellschaft für Technologietransfer mbH (Germany) and Favorsky Irkutsk Institute of Chemistry, have launched production of purified polyphenols derived from the bark and wood of conifers. These formulations could be a good option in the treatment of pyogenic and inflammatory conditions caused by infection, considering a rapid spread of multidrug-resistant bacteria.

In this study, we aimed to measure the antimicrobial activity of commercial polyphenols produced from the available raw materials against dermatophytes *S. aureus*, *P. aeruginosa* and *C. albicans* and to compare it between the studied compounds and with the activity of the antimicrobial ointments for topical application routinely used to treat similar infections.

METHODS

Resveratrol and dihydromyricetin extracted from conifer wood were courtesy of TransMIT Gesellschaft für Technologietransfer mbH (Germany). Dihydroquercetin was provided by the laboratory of Favorsky Irkutsk Institute of Chemistry. Quality control by ^{1}H-nuclear magnetic resonance spectrometry was performed on the Bruker AM-300 spectrometer (Bruker Daltonics GmbH; Germany). Resveratrol used in the study was a homogenous 100% trans-isomer.

The studied compounds were dissolved in nonpyrogenic injection-grade normal saline (Escom; Moscow) and passed though Sterile Minisart® syringe filters with polyether sulfone membranes (Sartorius; Germany). Solutions of polyphenolic compounds were stored in 50-ml polypropylene screw-cap tubes at +4 °C for 1 month away from direct sunlight.

Levomecol (Nizhfarm; Nizhny Novgorod) is an ointment for topical application used to treat purulent wounds, venous ulcers, inflammation of the skin, and burns. Its active substances are dioxymethyltetrahydropyrimidine (4.0%) and chloramphenicol (0.75%). For our experiments, the ointment was weighted in sterile Eppendorf tubes and diluted tenfold in 96% ethanol.

Clotrimazole (Glaxo-Wellcome Poznan; Poland) formulated as an ointment containing 1% of the active substance was diluted in 96% ethanol in the same way as levomecol was.

Strains of human pathogens

Pathogenic *S. aureus* (ATCC 25923), *P. aeruginosa* (ATCC 27853), and *C. albicans* (NCTC 2625) were provided by Tarasevich State Institute of Standardization and Control (Moscow). The strains were cultured for 18–20 hours in an agarized meat-peptone broth supplemented with 0.1% glucose (for bacteria) and 1% glucose (for *C. albicans*).

Twenty milliliters of the meat-peptone agar were applied onto 9-cm sterile plastic Petri dishes. The plates were then slightly air-dried at room temperature and heated in an air incubator to +37 °C.

The prepared 1% agarose was poured into 2-ml glass tubes and cooled down to 40 °C in the water bath. The melted agarose from each tube was combined with 5×10^{5} CFU of each pathogenic culture, mixed, transferred to a culture plate containing the corresponding growth medium, and the upper layer of the mix was evenly distributed on the plate surface.

One hour after the first layer of the culture was applied, 4-mm wells were made in the agar using a sterile stainless-steel puncher.

Solutions of polyphenolic compounds with concentrations close to the solubility limit were prepared using 96% ethanol as a solvent: 0.43 M for resveratrol, 0.31 M for dihydromyricetin, and 0.3 M for dihydroquercetin. These solutions, as well as stock solutions of levomecol and clotrimazole, were then diluted 10-, 100- and 1000-fold in 96% ethanol. Aliquots of each dilution (5 µl) were mixed with 15 µl of sterile deionized water. Twenty microliters of the obtained mix were introduced into the wells. Each dilution was tested in three replicates in different culture plates. After the dilutions in the wells were air-dried, the plates were placed in the incubator preheated to +37 °C and incubated for 40 hours. Clear areas (zones of inhibition) formed in the bacterial and fungal lawns were measured using a pair of calipers.

Statistical processing

The diameter of a halo in the bacterial/fungal lawn was measured with calipers with an accuracy of 0.5 mm. Every

Table. Evaluation of *in vitro* antimicrobial activity of resveratrol, dihydromyricetin and dihydroquercetin against *S. aureus*, *P. aeruginosa*, and *C. albicans* by radial diffusion

Compound	Dilution	The diameter of the inhibition zone (mm)		
		S. aureus	*P. aeruginosa*	*C. albicans*
Dihydroquercetin	1/10	9.7 ± 0.4	0	0
	1/100	8.3 ± 0.4	0	0
	1/1000	7.7 ± 0.4	0	0
Resveratrol	1/10	10.0 ± 0.0	0	0
	1/100	8.3 ± 0.4	0	0
	1/1000	7.3 ± 0.4	0	0
Dihydromyricetin	1/10	11.7 ± 0.4	0	0
	1/100	10.0 ± 0.0	0	0
	1/1000	8.7 ± 0.4	0	0
Levomecol	1/10	9.3 ± 0.4	6.3 ± 0.4	0
	1/100	6.3 ± 0.4	0	0
	1/1000	0	0	0
Clotrimazole	1/10	5.7 ± 0.4	0	12.3 ± 0.4
	1/100	0	0	8.3 ± 0.4
	1/1000	0	0	6.0 ± 0.0

measurement was done in three replicates in different culture dishes. For a series of 3 measurements, an arithmetic mean and a mean square error were calculated.

RESULTS

Sizes of the zones of inhibition in the bacterial and fungal lawns are shown in the Table.

Even the highest possible concentrations of the polyphenols tested in our experiment (21.5, 15.5 and 15.0 mM, respectively) exhibited zero antimicrobial activity against the gram-negative bacterium *P. aeruginosa* and fungus *C. albicans*. In contrast, the lowest possible concentrations of these polyphenolic compounds (0.22, 0.15, and 0.15 mM, respectively) were effective against the gram-positive *S. aureus*. *In vitro* activity of dihydromyricetin against *S. aureus* was slightly higher than that of resveratrol and dihydroquercetin.

Levomecol was active against *S. aureus* at the minimal concentration of 24.2 mM and against *P. aeruginosa* at 242.3 mM. The lowest active concentration of clotrimazole against *C. albicans* was below 3.4 mM.

DISCUSSION

The *in vitro* antimicrobial and antifungal activity of resveratrol and other polyphenols has been reported in several studies [10–12]. Some authors have tested the activity of phenolic compounds against human dermatophytes [13]. The study [14] demonstrates that resveratrol inhibits bacterial phagocytosis by macrophages through the interaction with the TLR2 receptor and the nuclear factor NF-κβ. There is evidence suggesting that resveratrol is capable of inhibiting retinal inflammation experimentally induced by *S. aureus* [15]. However, so far polyphenols have not been used as an alternative to antibiotics, which raises the question whether research should be continued to obtain a comprehensive description of their specific biological activity.

Our experiments demonstrate that the molar antimicrobial activity of flavonol (dihydromyricetin and dihydroquercetin) and stilbene (resveratrol) against the gram-positive human pathogen *S. aureus* is high: it is even higher than the molar activity of some antibiotics traditionally used for topical application.

In contrast, the activity of those polyphenols against gram-negative *P. aeruginosa* and the pathogenic yeast *C. albicans* is so low that it could not be detected by the assay used in the study. This observation is, however, not consistent with the literature [13] reporting marked resveratrol activity against *S. aureus* and *P. aeruginosa* (in the range between 171 and 342 μg/ml, i.e. 39–78 mM) and the microscopic fungi *Trichophyton mentagrophytes*, *Trichophyton tonsurans*, *Trichophyton rubrum*, *Epidermophyton floccosum*, and *Microsporum gypseum* (25–50 μg/ml, i.e. 5.7–11.4 mM).

The obtained data suggest that plant-derived polyphenols, such as dihydromyricetin, have a potential to be used as a medicine for topical application to treat skin infections caused by staphylococci, including their drug-resistant strains. Therefore, further research is needed to investigate the antimicrobial activity of polyphenols using animal models and to assess the toxicity of these compounds towards animal cells, as well as their immunostimulatory and immunosuppressive effects [14, 15].

CONCLUSIONS

Our study has confirmed the marked antimicrobial activity of resveratrol, dihydromyricetin and dihydroquercetin exerted *in vitro* at concentrations of 0.15 mM and above. The most pronounced effect was observed for dihydromyricetin. The study suggests a significantly higher bactericidal activity of polyphenols in comparison with the traditionally used levomecol ointment active against *S. aureus* at 24.2 mM.

References

1. Teplova VV, Isakova EP, Klein OI, Dergacheva DI, Gessler NN, Deryabina Y. I. Natural Polyphenols: Biological Activity, Pharmacological Potential, Means of Metabolic Engineering (Review). Applied Biochemistry and Microbiology, 2018, Vol. 54, No. 3, pp. 221–237
2. Gudkov SV, Bruskov VI, Kulikov AV, Bobyljov AG, Kulikov DA, Molochkov AV. Biooksidanty. Al'manah klinicheskoj mediciny. 2014; 61 (31): 61–5.
3. Reinisalo M, et al. Polyphenol Stilbenes: Molecular Mechanisms of Defence against Oxidative Stress and Aging-Related Diseases. Oxid Med Cell Longev. 2015: 340520.
4. Mishra A, et al. Bauhinia variegata leaf extracts exhibit considerable antibacterial, antioxidant, and anticancer activities. Biomed Res Int. 2013: 915436.
5. Quave CL, et al. Ellagic acid derivatives from Rubus ulmifolius inhibit Staphylococcus aureus biofilm formation and improve response to antibiotics. PLoS One. 2012; 7 (1): e28737.
6. Slobodnikova L, et al. Antibiofilm Activity of Plant Polyphenols. Molecules. 2016; 21 (12): 1717.
7. Andrae-Marobela K, et al. Polyphenols: a diverse class of multi-target anti-HIV-1 agents. Curr Drug Metab. 2013; 14 (4): 392–413.
8. Mahady G.B, Pendland SL, Chadwick LR. Resveratrol and red wine extracts inhibit the growth of CagA+ strains of Helicobacter pylori in vitro. Am J Gastroenterol. 2003; 98 (6): 1440–1.
9. Roupe KA, et al. Pharmacometrics of stilbenes: seguing towards the clinic. Curr Clin Pharmacol. 2006; 1 (1): 81–101.
10. Erlejman AG, Verstraeten SV, Fraga CG, Oteiza PI. The interaction of flavonoids with membranes: potential determinant of flavonoid antioxidant effects. Free Radic Res. 2004; 38 (12): 1311–20.
11. Volynec AP. Novoobrazovanie zashhitnyh fenol'nyh soedinenij pri infekcionnom stresse. V sbornike: Zagoskina NV, Burlakova EB, redaktory. Fenol'nye soedinenija: fundamental'nye i prikladnye aspekty. M.: Nauchnyj mir, 2010. S. 168–196.
12. Mishra A, Kumar S, Pandey AK., Scientific validation of the medicinal efficacy of Tinospora cordifolia. The Scientific World Journal. 2013; 2013; ID 292934.
13. Chan MM. Antimicrobial effect of resveratrol on dermatophytes and bacterial pathogens of the skin. Biochem Pharmacol. 2002; 63 (2): 99–104.
14. Iyori M, et al. Resveratrol modulates phagocytosis of bacteria through an NF-kappaB-dependent gene program. Antimicrob Agents Chemother. 2008; 52 (1): 121–7.
15. Marino A, et al. Resveratrol role in Staphylococcus aureus-induced corneal inflammation. Pathog Dis. 2013; 68 (2): 61–4.

Литература

1. Теплова В. В., Исакова Е. П., Кляйн О. И., Дергачева Д. И., Гесслер Н. Н., Дерябина Ю. И. Природные полифенолы: биологическая активность, фармакологический потенциал, пути метаболической инженерии (обзор). Прикладная биохимия и микробиология. 2018; 54 (3): 1–21.
2. Гудков С. В., Брусков В. И., Куликов А. В., Бобылев А. Г., Куликов Д. А., Молочков А. В. Биооксиданты. Альманах клинической медицины. 2014; 61 (31): 61–5.
3. Reinisalo M, et al. Polyphenol Stilbenes: Molecular Mechanisms of Defence against Oxidative Stress and Aging-Related Diseases. Oxid Med Cell Longev. 2015: 340520.
4. Mishra A, et al. Bauhinia variegata leaf extracts exhibit considerable antibacterial, antioxidant, and anticancer activities. Biomed Res Int. 2013: 915436.
5. Quave CL, et al. Ellagic acid derivatives from Rubus ulmifolius inhibit Staphylococcus aureus biofilm formation and improve response to antibiotics. PLoS One. 2012; 7 (1): e28737.
6. Slobodnikova L, et al. Antibiofilm Activity of Plant Polyphenols. Molecules. 2016; 21 (12): 1717.
7. Andrae-Marobela K, et al. Polyphenols: a diverse class of multi-target anti-HIV-1 agents. Curr Drug Metab. 2013; 14 (4): 392–413.
8. Mahady G.B, Pendland SL, Chadwick LR. Resveratrol and red wine extracts inhibit the growth of CagA+ strains of Helicobacter pylori in vitro. Am J Gastroenterol. 2003; 98 (6): 1440–1.
9. Roupe KA, et al. Pharmacometrics of stilbenes: seguing towards the clinic. Curr Clin Pharmacol. 2006; 1 (1): 81–101.
10. Erlejman AG, Verstraeten SV, Fraga CG, Oteiza PI. The interaction of flavonoids with membranes: potential determinant of flavonoid antioxidant effects. Free Radic Res. 2004; 38 (12): 1311–20.
11. Волынец А. П. Новообразование защитных фенольных соединений при инфекционном стрессе. В сборнике: Загоскина Н. В., Бурлакова Е. Б., редакторы. Фенольные соединения: фундаментальные и прикладные аспекты. М.: Научный мир, 2010. С. 168–196.
12. Mishra A, Kumar S, Pandey AK., Scientific validation of the medicinal efficacy of Tinospora cordifolia. The Scientific World Journal. 2013; 2013; ID 292934.
13. Chan MM. Antimicrobial effect of resveratrol on dermatophytes and bacterial pathogens of the skin. Biochem Pharmacol. 2002; 63 (2): 99–104.
14. Iyori M, et al. Resveratrol modulates phagocytosis of bacteria through an NF-kappaB-dependent gene program. Antimicrob Agents Chemother. 2008; 52 (1): 121–7.
15. Marino A, et al. Resveratrol role in Staphylococcus aureus-induced corneal inflammation. Pathog Dis. 2013; 68 (2): 61–4.

IDENTIFICATION OF MICROORGANISMS BY FOURIER-TRANSFORM INFRARED SPECTROSCOPY

Suntsova AYu[1], Guliev RR[1], Popov DA[2], Vostrikova TYu[2], Dubodelov DV[3], Shchegolikhin AN[1], Laypanov BK[5], Priputnevich TV[3], Shevelev AB[1,4] ✉, Kurochkin IN[1]

[1] Emanuel Institute of Biochemical Physics, Moscow

[2] Bakulev National Medical Research Center of Cardiovascular Surgery, Moscow

[3] Kulakov National Medical Research Center for Obstetrics, Gynecology and Perinatology, Moscow

[4] Vavilov Institute of General Genetics, Moscow

[5] Skryabin Moscow State Academy of Veterinary Medicine and Biotechnology, Moscow

The need for novel techniques of rapid identification of pathogenic microorganisms arises from the massive spread of drug-resistant nosocomial strains and the emergence of centers for biohazard control. Fourier-transform infrared spectroscopy is a promising alternative to mass spectrometry as it is cost-effective, fast and suitable for field use. The aim of this work was to propose an algorithm for the identification of microorganisms in pure cultures based on the analysis of their Fourier transform infrared spectra. The algorithm is based on the automated principal component analysis of infrared spectra. Unlike its analogues described in the literature, the algorithm is capable of identifying bacteria regardless of the culture medium or growth phase. The training sample included the most prevalent causative agents of infections and sepsis in humans: *Staphylococcus aureus* (*n* = 67), *Enterococcus faecalis* (*n* = 10), *Enterococcus faecium* (*n* = 10), *Klebsiella pneumoniae* (*n* = 10), *Escherichia coli* (*n* = 10), *Serratia marcescens* (*n* = 10), *Enterobacter cloacae* (*n* = 10), *Acinetobacter baumannii* (*n* = 10), *Pseudomonas aeruginosa* (*n* = 10), and *Candida albicans* (*n* = 10). The model we built successfully passed a series of blind tests involving clinical isolates of 10 methicillin-resistant (MRSA) and 10 methicillin-sensitive (MSSA) *Staphylococcus aureus* strains as well as pair mixes of these cultures with clinical isolates of *Pseudomonas aeruginosa*, *Escherichia coli*, and *Klebsiella pneumoniae*.

Keywords: spectroscopy, Fourier, IR, principal component analysis, identification, bacteria, yeasts

✉ **Correspondence should be addressed:** Alexei B. Shevelev
Kosygina 4, Moscow, 119334; shevel_a@hotmail.com

Received: 01.08.2018 **Accepted:** 25.08.2018

DOI: 10.24075/brsmu.2018.046

ИДЕНТИФИКАЦИЯ МИКРООРГАНИЗМОВ С ПОМОЩЬЮ ИНФРАКРАСНЫХ ФУРЬЕ-СПЕКТРОВ

А. Ю. Сунцова[1], Р. Р. Гулиев[1], Д. А. Попов[2], Т. Ю. Вострикова[2], Д. В. Дубоделов[3], А. Н. Щеголихин[1], Б. К. Лайпанов[5], Т. В. Припутневич[3], А. Б. Шевелев[1,4] ✉, И. Н. Курочкин[1]

[1] Институт биохимической физики имени Н. М. Эмануэля, Москва

[2] Национальный медицинский исследовательский центр сердечно-сосудистой хирургии имени А. Н. Бакулева, Москва

[3] Национальный медицинский исследовательский центр акушерства, гинекологии и перинатологии имени В. И. Кулакова, Москва

[4] Институт общей генетики имени Н. И. Вавилова, Москва

[5] Московская государственная академия ветеринарной медицины и биотехнологии имени К. И. Скрябина, Москва

Актуальность развития быстрых методов идентификации патогенных биологических объектов растет в связи с массовым распространением в лечебных учреждениях микроорганизмов с лекарственной устойчивостью и в связи с развертыванием центров мониторинга биологических угроз. Инфракрасная Фурье-спектроскопия является эффективной альтернативой масс-спектрометрии с точки зрения стоимости и портативности оборудования, экспрессности анализа. Целью работы было описать алгоритм идентификации микроорганизмов в чистых культурах, основанный на анализе колебательных инфракрасных Фурье-спектров культур (Fourier transform infrared, FTIR). Алгоритм основан на автоматизированном анализе спектров методом главных компонент. В отличие от известных в литературе, он позволяет идентифицировать бактерии вне зависимости от стадии роста культуры и состава среды. Обучающая база данных включала наиболее распространенные возбудители гнойно-септических инфекций человека: *Staphylococcus aureus* (*n* = 67), *Enterococcus faecalis* (*n* = 10), *Enterococcus faecium* (*n* = 10), *Klebsiella pneumoniae* (*n* = 10), *Escherichia coli* (*n* = 10), *Serratia marcescens* (*n* = 10), *Enterobacter cloacae* (*n* = 10), *Acinetobacter baumannii* (*n* = 10), *Pseudomonas aeruginosa* (*n* = 10) и *Candida albicans* (*n* = 10). Построенная модель успешно апробирована на серии клинических изолятов *Staphylococcus aureus*: в слепых испытаниях участвовало 10 штаммов с фенотипом лекарственной устойчивости MRSA (methicillin-resistant *Staphylococcus aureus*) и 10 чувствительных штаммов, а также смесь культур этих штаммов с клиническими изолятами *Pseudomonas aeruginosa*, *Escherichia coli* и *Klebsiella pneumoniae*.

Ключевые слова: спектроскопия, Фурье, ИК-спектр, метод главных компонент, идентификация, бактерии, дрожжи

✉ **Для корреспонденции:** Шевелев Алексей Борисович
ул. Косыгина, д. 4, г. Москва, 119334; shevel_a@hotmail.com

Статья получена: 01.08.2018 **Статья принята к печати:** 25.08.2018

DOI: 10.24075/vrgmu.2018.046

Identification of microbial species is a routine task for clinical microbiology laboratories. Rapid identification of pathogens in patients with infections or sepsis is essential in prescribing an adequate antibiotic treatment. Efficient therapy for these aggressively progressing conditions is important since they are a common cause of postoperative morbidity and mortality in cardiac surgery [1] and maternal and neonatal death after childbirth [2].

Pathogens can be identified by both traditional microbiological tests and modern techniques now available worldwide, such as matrix-assisted laser desorption/ionization time-of-flight mass spectrometry (MALDI-ToF MS). The most popular spectrometers are MALDI BioTyper (Bruker; Germany) and Vitek MS (Biomerieux; France). They deliver fast and reliable results but are quite expensive and cannot be afforded by many hospitals. Besides, these devices are too bulky and, therefore, unsuitable for field use by biosafety agencies.

An alternative technique for the identification of microorganisms is Fourier transform infrared (FTIR) spectroscopy. It can determine the chemical composition of a studied culture and identify any type of macromolecule or low molecular weight compound. Similar to MALDI ToF MS, sample preparation for FTIR spectroscopy is easy: the culture sample simply needs to be mounted on a surface transparent to infrared light and left there to dry. Although FTIR spectroscopy ensures a quick diagnosis, its application in clinical microbiology is limited because the FTIR-spectra of a studied culture vary depending on the composition of the growth medium and culture growth phase. The aim of this work was to develop an algorithm for the reliable identification of microorganisms in pure cultures regardless of the growth medium or growth phase based on the analysis of their FTIR spectra.

METHODS

Strains of human pathogens

In this work, we used the strains of the most common causative agents of infections and sepsis in humans, including *S. aureus* (20 MRSA and 47 MSSA isolates), *E. faecalis* (*n* = 10), *E. faecium* (*n* = 10), *K. pneumoniae* (*n* = 10), *E. coli* (*n* = 10), *S. marcescens* (*n* = 10), *E. cloacae* (*n* = 10), *A. baumannii* (*n* = 10), *P. aeruginosa* (*n* = 10), *S. epidermidis* (*n* = 10), and *C. albicans* (*n* = 10).

The pathogens were isolated from patients of Bakulev National Medical Research Center of Cardiovascular Surgery and Kulakov National Medical Research Center for Obstetrics, Gynecology and Perinatology. Isolation and identification were carried out according to the standard technique [3]. Differential diagnostic media included mannitol salt agar selective for staphylococci, Enterococcus agar, Endo agar with fish hydrolysate for culturing gram-negative rods (*Enterobacterales*, *A. baumannii*, and *P. aeruginosa*), Sabouraud agar and meat-peptone broth supplemented with 1% glucose for *C. albicans*. Confirmatory identification of isolates was performed on the MALDI BioTyper mass spectrometer (Bruker; Germany).

Isolates deposited in the Cryobank were plated onto blood agar plates under aerobic conditions at 37 °C and cultured overnight.

Each isolate was grown in 4 different types of culture media: agarized or liquid, with or without blood. The bloodless media included egg-yolk salt, meat-peptone and Endo broths and Sabouraud agar. For FTIR spectroscopy, the samples were harvested 12, 24 and 48 hours after plating.

To protect the operator of the FTIR spectrometer from the risk of infection and to prepare the cultures for short-term storage, they were inactivated in 70% alcohol before spectroscopy. Thirty microliter aliquots of fresh liquid cultures were collected into polypropylene microtubes, supplemented with 70 µl of 96% ethanol and carefully mixed by pipetting. Samples of the cultures grown on solid agar were collected using the inoculation loop and then suspended in 70% aqueous ethanol (30 mg of the biomass per 100 µl of the alcohol solution).

Recording IR spectra of isolates

IR spectra were recorded from the suspensions of pathogen cultures fixed in 70% aqueous ethanol. To prepare individual samples for transmission IR spectroscopy, 5 to 19 µl of the suspension were micropipetted onto standard (12.5 mm long and 2 mm thick) ZnSe surfaces (Elektrosteklo; Moscow) and left to dry until complete evaporation of the ethanol (5–15 min). The spectra were recorded by the FTIR spectrometer Spectrum Two (Perkin-Elmer; USA) over the wavenumber range of 4000–600 cm^{-1} at 4 cm^{-1} optical resolution and 1 cm^{-1} digital resolution. The ZnSe surface with an applied pathogen sample was positioned vertically in the Microfocus holder (Perkin-Elmer; USA) and placed in the way of a horizontal probe beam generated by the IR source; 16 individual averaged scans were accumulated for about 2 min. The background spectrum of the spectrometer was recorded under the same conditions but with the clean ZnSe surface and updated before recording the IR spectrum of every new incoming sample.

Data analysis

After discarding the abnormal spectra, the number of spectra ready for further analysis totalled 347, including 188 spectra obtained from *S. aureus* (39 from these had MRSA phenotype; 48 had MSSA phenotype; and 101 were not characterized in terms of their drug-resistance) and 169 spectra obtained from other pathogens (14 from *A. baumannii*, 32 from *C. albicans*, 8 from *E. cloacae*, 21 from *E. faecalis*, 20 from *E. faecium*, 11 from *E. coli*, 17 from *K. pneumoniae*, 18 from *P. aeruginosa*, 8 from *S. marcescens*, 10 from *S. epidermidis*); 10 spectra represented mixed cultures: 2 were obtained from *S. aureus* (MRSA) + *E. coli*; 2 from *S. aureus* (MSSA) + *E. coli*; 2 from *S. aureus* (MRSA) + *K. pneumoniae*, 2 from *S. aureus* (MSSA) + *K. pneumoniae*, and another 2 from *S. aureus* (MSSA) + *P. aeruginosa*. Fig. 1 illustrates the initial spectra used in the analysis.

Using routine spectroscopy algorithms, the initial spectra were preprocessed for unification; artifacts caused by drifts in the baseline or atmospheric carbon dioxide and water vapor fluctuations were eliminated. Briefly, the initial spectra were normalized to the average transmission, and the first derivative of the envelope was calculated; the relevant wavenumber ranges were narrowed down to 600–1800 cm^{-1} and 2800–3000 cm^{-1}. Because the initial spectra were of good quality and did not require any extra smoothing, the derivative was calculated using the symmetric difference formula at two points for numerical differentiation. Fig. 2 shows the preprocessed spectra.

The preprocessed spectra were used to build a mathematical model for the identification of *S. aureus* in a culture sample. Another model capable of discriminating between MRSA and MSSA strains was constructed based on the spectra of MRSA and MSSA phenotypes of *S. aureus*. Both models exploited

the spectra of pure cultures. The spectra of culture mixes were used for model validation.

Both models were built by applying the principal component analysis (PCA) and the linear discriminant analysis (LDA) [4]. LDA [5] allows selecting a line or a hyperplane effectively separating two or more classes of the data. The ratio of between-class to within-class variances shows reliability of classification. However, matrix calculations in LDA do not allow direct application of the spectral data. Datasets must be characterized by a high number of correlated features and regions of poor informative value must be identified. LDA should be preceded by PCA to extract the most informative and uncorrelated spectral data from the dataset. The informative value of the method is assessed by variance: if the latter is low at a given wavenumber, almost all spectra here are expected to behave identically; therefore, such regions cannot provide any valuable information. In PCA, informative and uncorrelated data are extracted by projecting onto corresponding vectors (principal components). In fact, a model constructed with PCA-LDA is a projection of spectral data onto a new vector. In practice, it entails calculation of a linear combination with certain coefficients.

The built models were cross-validated [6]. Cross-validation is a series of blind tests: the initial dataset is randomly partitioned into k subsets; one of the resulting subsets (the test dataset) is discarded, others $k - 1$ training sets are analyzed by PCA-LDA. The obtained model predicts the values for the test dataset as if they were initially unknown. This procedure is repeated for each of k subsets. Once the values predicted for all test subsets are averaged, one can make predictions about new unknown spectra. When splitting the spectra into the subsets, all spectra from the same isolate must fall within one subset only. Otherwise, predicted values will be higher than the actual ones. Cross-validation of our model for *S. aureus* identification was performed at $k = 20$, i.e. the total set of spectra was divided into 20 subsets so that the spectra of one and the same isolate always fell into one subset only. For the model discriminating between MSSA and MRSA strains, each strain was represented by an equal number of isolates ($k = 40$). Thus, each subset represented only one isolate.

Preprocessing and the analysis of the obtained spectral data were done in R [7] and the RStudio environment. Spectral data were handled by hyperSpec [8]; the models were built and validated using caret [9] and MASS [10]. Images were created in ggplot2 [11].

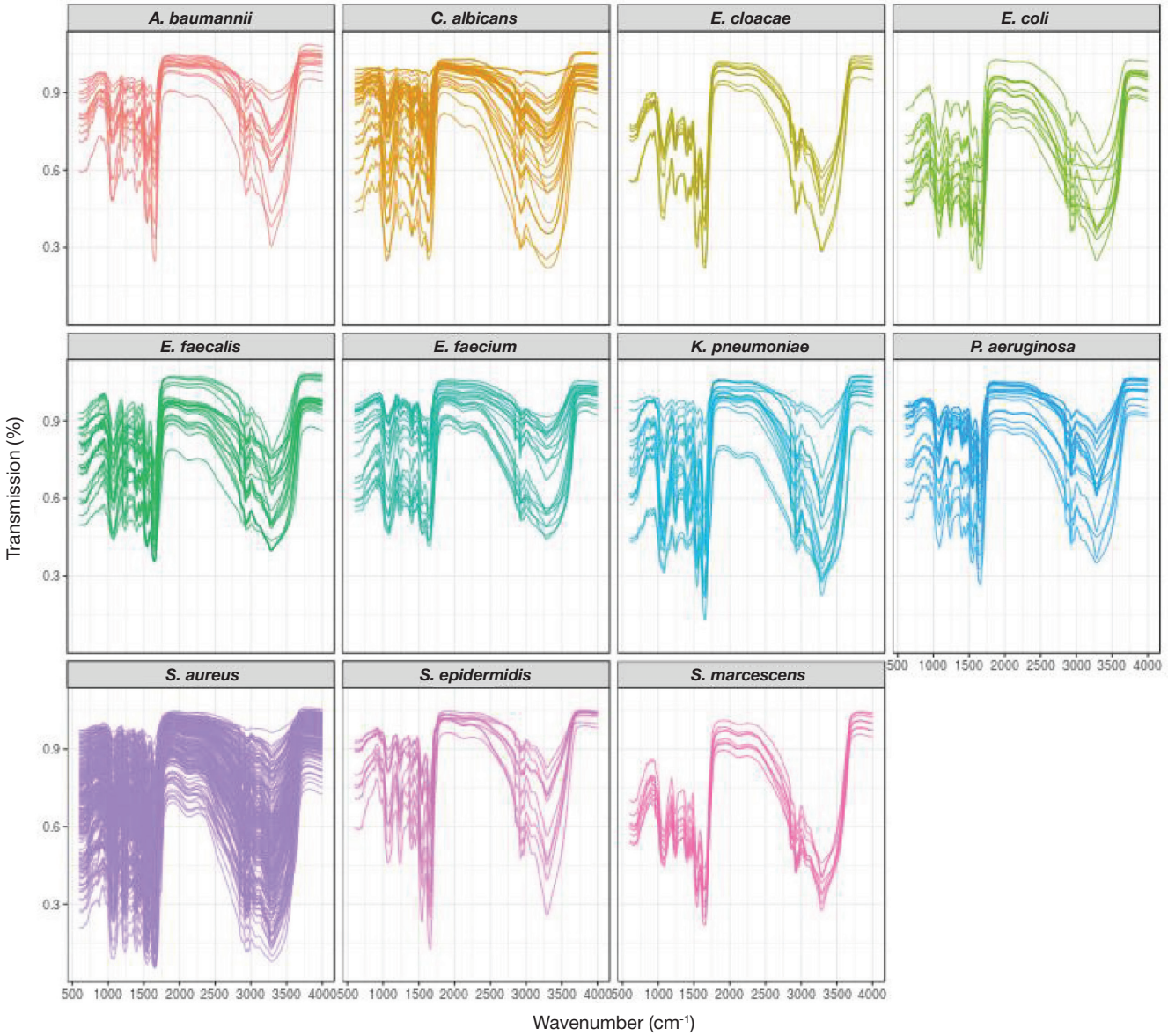

Fig. 1. The raw Fourier transform infrared spectra of pathogenic bacteria. Left to right and top to bottom are the spectra of *A. baumannii*, *C. albicans*, *E. cloacae*, *E. coli*, *E. faecalis*, *E. faecium*, *K. pneumoniae*, *P. aeruginosa*, *S. aureus*, *S. epidermidis*, and *S. marcescens* expressed in the units of light transmission

RESULTS

Identification of *S. aureus*

Based on the spectra obtained from 11 species that are the most common causative agents of infections and sepsis in humans (*S. aureus*, *S. epidermidis*, *E. faecalis*, *E. faecium*, *K. pneumoniae*, *E. coli*, *S. marcescens*, *E. cloacae*, *A. baumannii*, *P. aeruginosa*, and *C. albicans*), we built a mathematical model for *S. aureus* identification. The accuracy of the model was assessed by cross-validation on 20 subsets (the spectra of one and the same isolate got into one subset only) and reached 98.4% (± 4%). However, further in-depth analysis of cross-validation results revealed that almost all errors arose from the *S. epidermidis* isolate getting into the test sample. This means that at the genus level the model performs well considering the size and composition of the training dataset. The spectra of other staphylococci (two *S. epidermidis* isolates) were too poorly represented in the training dataset to let the model make accurate predictions at the species level. The worst accuracy (81%) observed during cross-validation represented the case when the test dataset included the spectra of *S. epidermidis* leaving the training set with insufficient data to establish a reliable difference between *S. epidermis* and *S. aureus*.

From that, one might conclude that these two related species cannot be discriminated using our approach. But the final model that aggregated all obtained data and was built without cross-validation demonstrated an ability to discriminate between these 2 species with 100% accuracy. This ability is visually represented as the projection of the spectral data onto the linear discriminant (the separating axis in the PCA-LDA method; Fig. 3)

This projection is basically a result of multiplication of each spectrum by a coefficient vector: if a preprocessed spectrum is a vector (a set of values), then the linear discriminant is a result of a linear combination. Model tuning is all about the choice of optimal coefficients. Their values for the obtained model are presented as a graph in Fig. 4.

The visual representation of the coefficients serves to roughly interpret the obtained model: the higher is the coefficient expressed in absolute figures, the more significant is the corresponding spectral range. Higher coefficient values expressed in absolute figures (with due account of preprocessing and computation of the derivative) in the zone of

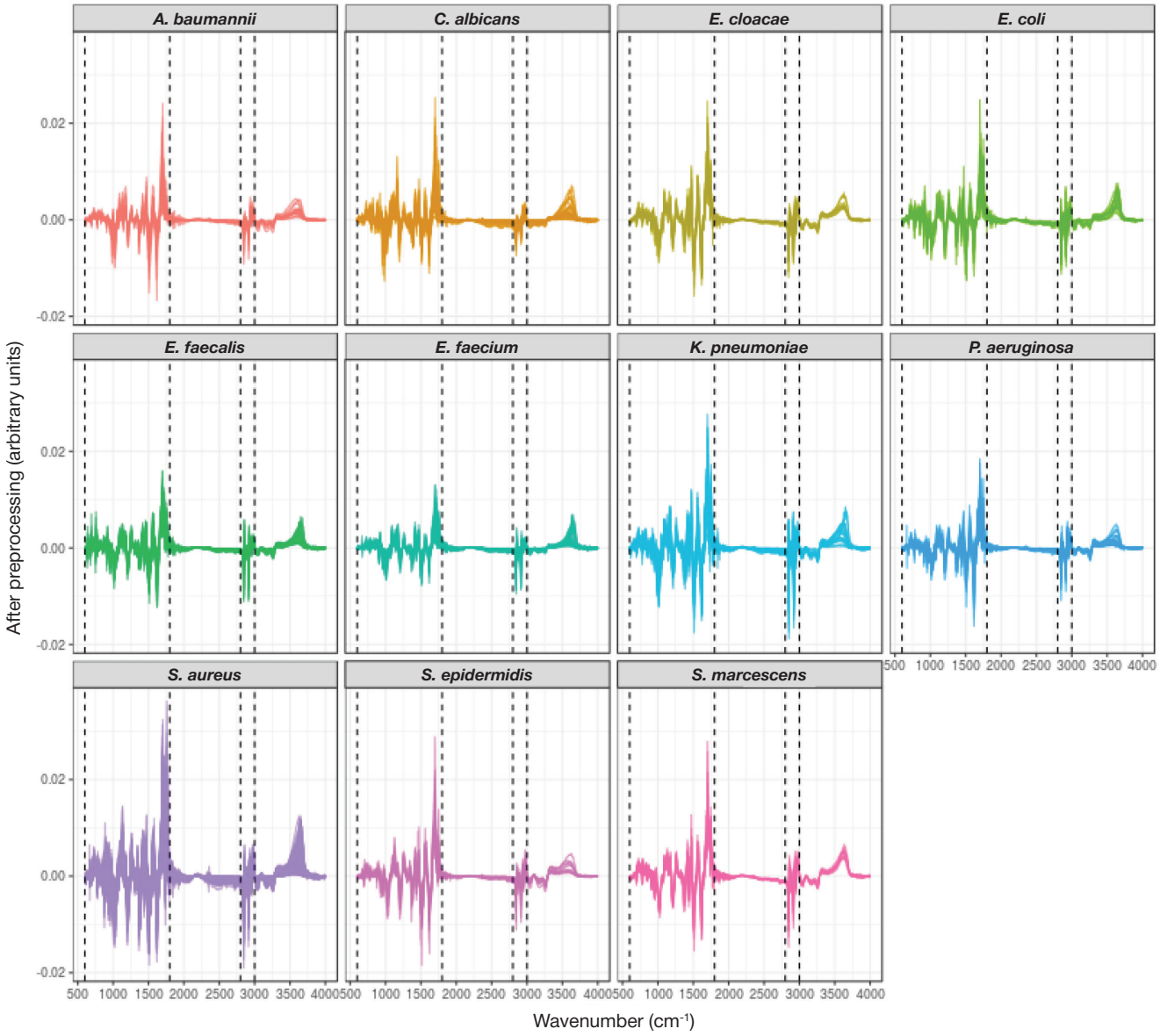

Fig. 2. The Fourier transform infrared spectra after preprocessing: normalization to the average transmission and calculation of the first derivative. Dotted lines show the boundaries of the wavenumber ranges used in the analysis: 600, 1800, 2800, 3000 cm^{-1}

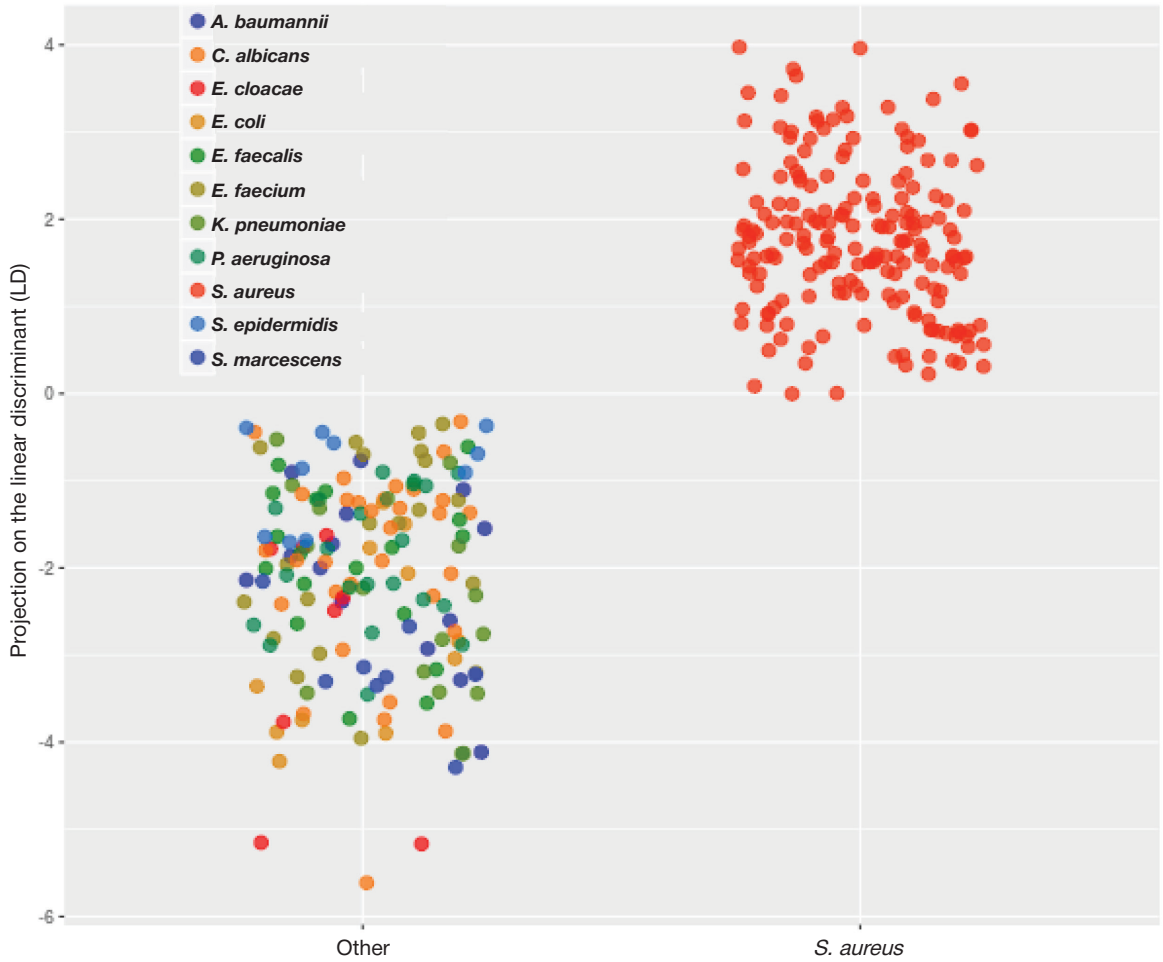

Fig. 3. Projection of the initial data onto the linear discriminant (LD) obtained by PCA-LDA. Pathogens are marked by different colors. For the sake of convenience, the spectra of the target pathogen *S. aureus* are separated from others on X-axis. The groups are well-separated given that LD > 0

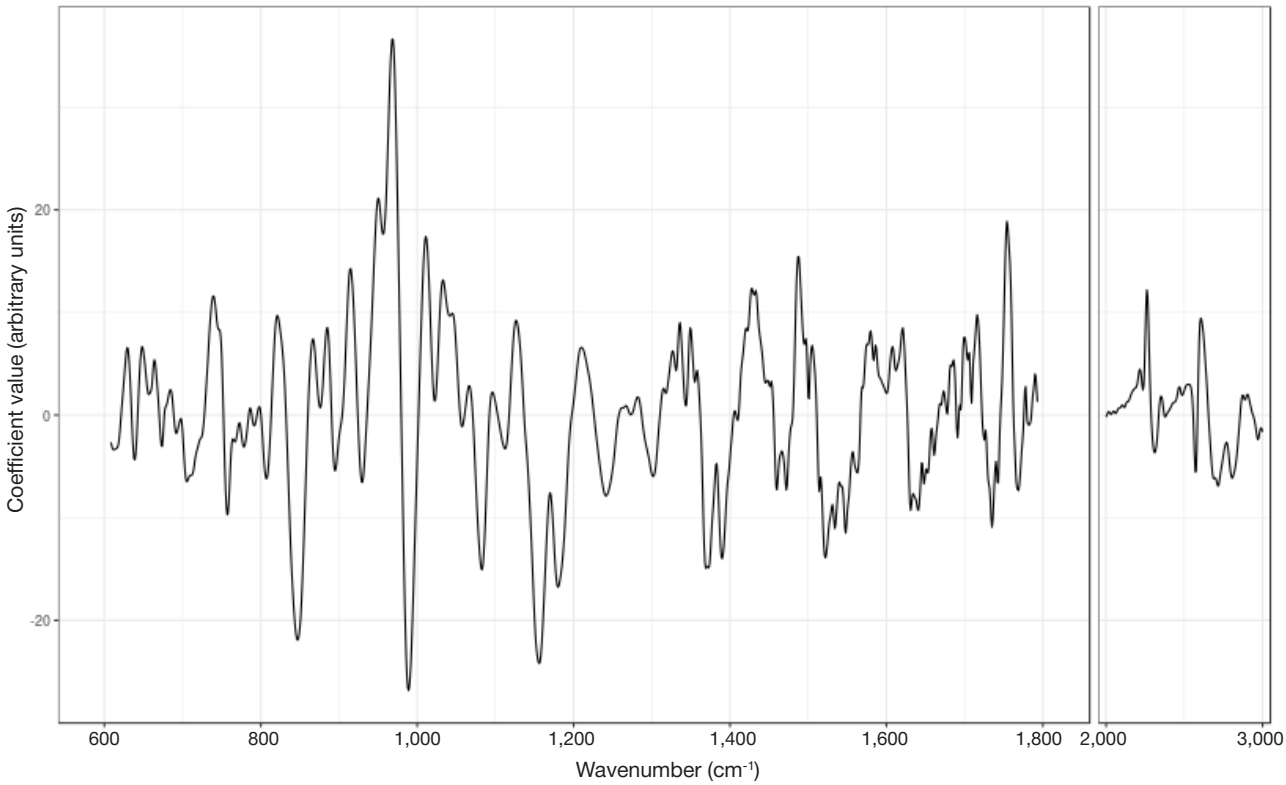

Fig. 4. Linear discriminant coefficients obtained by PCA-LDA. These coefficients were used to obtain the projections in Fig. 3. The coefficients represent the informative value of spectral data. For example, high values of the initial spectrum in the zone of negative coefficients indicate the probability that the studied isolate is not the pathogen of interest

negative coefficients mean that the spectrum is not generated by *S. aureus*, and *vice versa*.

To estimate the feasibility of the proposed approach for clinical microbiology, we studied the ability of our model to identify a target pathogen in mixed cultures. For the analysis, we used 2 methicillin-resistant and 3 methicillin-sensitive *S. aureus* strains. The microorganisms were cultured on blood agar plates for 24 or 48 hours. Then equal volumes of *S. aureus* and gram-negative bacteria (*E. coli*, *K. pneumoniae* or *P. aeruginosa*) cultured on Endo agar were combined. The concentration of bacterial cells per unit volume was not measured. All mixed samples were fixed in alcohol and fed to the final model for identification (see the Table).

In all spectra except 2 representing one and the same sample, the presence of a target pathogen was predicted with high probability, which indicates that the model is reliable and can be used in clinical practice.

Prediction of methicillin-resistance phenotype in *S. aureus* isolates

Prediction of an methicillin-resistance phenotype in ic Staphylococci is a serious challenge faced by clinical microbiology. In this work we attempted to predict the MRSA/MSSA phenotypes in *S. aureus* isolates based on their FTIR spectra. The classification model was constructed in the same fashion, *i.e.* using PCA and LDA in succession followed by cross-validation.

We failed to achieve the same quality of predictions as with *S. aureus*. The accuracy of the model evaluated by cross-validation was 73%. The projection onto the linear discriminant is shown in Fig. 5. Discrimination here was much worse than for *S. aureus*. Still, 80% of the spectra were identified accurately. This observation leads us to hypothesize a larger size of the training sample could raise the reliability of the identification to the acceptable level.

DISCUSSION

The first reports of FTIR application for the identification of microorganisms were published in 1991 [12]. The research works that followed were dedicated to the identification of bacteria, such as lactobacilli and agents of foodborne infections, in the environment [13, 14]. A few studies demonstrated that FTIR can be used to identify Mycobacteria and Listeria [15–17]. In 2011 with the arrival of commercially available spectrometers by Bruker (Germany) and Perkin-Elmer (USA) that reliably identified microorganisms from their FTIR spectra the number of publications on the use of FTIR in microbiology started to grow [18–20]. Research groups were formed outside Germany in Poland [21], the UK [22, 23] and the Netherlands [24]. The Dutch researchers were the first to attempt to identify the causative agents of sepsis in humans and to compare spectral resolutions of different vibrational spectroscopy techniques, including FTIR spectroscopy, Raman spectroscopy, and surface-enhanced Raman spectroscopy (SERS). The authors concluded that FTIR and Raman spectroscopies produced reliable results but were not as sensitive as SERS. In turn, although SERS proved to be a very sensitive technique, its reproducibility was poor.

Recently, a lot of research works have been published on the use of FTIR in clinical microbiology [25–28]. The first work listed here compares spectral resolutions of vibrational spectroscopy techniques, including SERS (accuracy of 74.9%), Raman spectroscopy (accuracy of 97.8%) and FTIR spectroscopy (accuracy of 96.2%), using a number of pathogenic and nonpathogenic bacteria: *P. aeruginosa*, *P. putida*, *E. coli*, *E. faecium*, *Streptomyces lividans*, *B. subtilis*, *B. cereus*, as well as baker's yeast *Saccharomyces cerevisiae*. The last work from the list describes a method for the rapid identification of bacterial microcolonies of 50 to 300 μm in diameter using the state-of-the-art IR-BioTyper spectrometer (Bruker): the colonies are automatically transferred from the agarized culture medium to the CaF_2 surface; the principal component analysis applied to the obtained spectral data is performed by an artificial neural network (ANN) accessible via the Bruker server.

The findings of those studies suggest that FTIR spectra comprehensively describe the chemical composition of cells, including biopolymers that are building blocks for cell walls and membranes, intracellular DNA, phospholipids, sugars, etc. and therefore ensure a) the reliable discrimination between pathogenic bacterial species; b) the accurate identification of microorganisms at the species level; c) the identification of a phylum the studied isolate belongs to using digital libraries of microbial spectra. Platforms for rapid testing based solely on IR spectroscopy data could provide a quick solution to these

Table. Predicted probability of *S. aureus* presence in the sample

Sample ID	Mixt samples	Predicted probability of *S. aureus* presence in the sample
1	MSSA + *K. pneumoniae*	96.8%
1	MSSA + *K. pneumoniae*	95.1%
2	MSSA + *E. coli*	40.0%
2	MSSA + *E. coli*	41.5%
3	MRSA + *K. pneumoniae*	96.4%
3	MRSA + *K. pneumoniae*	97.0%
4	MRSA + *P. aeruginosa*	90.6%
4	MRSA + *P. aeruginosa*	87.7%
5	MRSA + *E. coli*	82.4%
5	MRSA + *E. coli*	73.0%

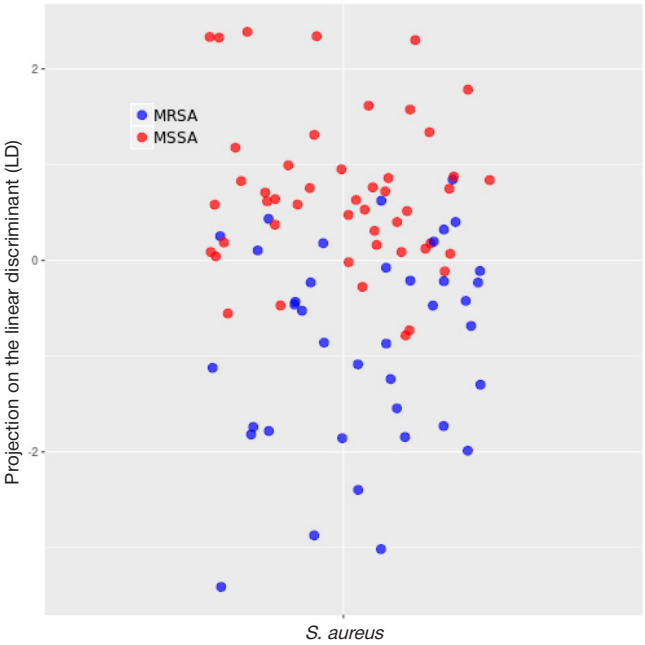

Fig. 5. Projection on the linear discriminant separating phenotypes MSSA and MRSA. Projections of MSSA spectra are shown in red; projections of MRSA spectra are shown in blue. Although 100% classification accuracy was not achieved, it was 80% given that LD > 0

three tasks and assist in optimizing the treatment strategy and adapting it to an individual patient in order to avoid prescription of antibiotics ineffective against the causative pathogen. However, the transition of this approach from the research lab to the clinical setting is obstructed by the absence of an algorithm for automated analysis of microbial FTIR spectra. Such algorithm is expected to identify those components of the spectrum that are determined by the genotype of the strain and not by culturing conditions, such as the growth medium composition, the growth phase, the degree of culture degradation, etc. In all works referred to above the authors sought to standardize culturing conditions, which is quite difficult to achieve in the real clinical setting and is also time consuming.

Such algorithm is proposed in the present work. It allows identification of bacterial species regardless of the growth phase and growth medium composition. We cultured a number of bacterial isolates of *S. aureus*, *E. faecalis*, *E. faecium*, *K. pneumoniae*, *E. coli*, *S. marcescens*, *E. cloacae*, *A. baumannii*, *P. aeruginosa*, *S. epidermidis* and *C. albicans* in different media and for different time periods. Using PCA, we identified the most informative regions of microbial FTIR spectra. The result of the analysis was represented as a system of coefficients that facilitated quick identification of new isolates from their FTIR spectra. The accuracy of the proposed method was assessed by the blind test using pure cultures of *S. aureus* isolates and their paired mixes with *P. aeruginosa*, *E. coli* and *K. pneumoniae.*

The obtained results demonstrate that the proposed algorithm for the analysis of microbial FTIR spectra reliably identifies the presence of *S. aureus* in the culture regardless of the duration of culturing (24 or 48 hours) after being trained on the sample of 11 pathogens representing different phyla (bacteria and ascomycete yeasts). All samples were inactivated in 70% ethanol before their spectra were recorded. This makes manipulations with virulent pathogens safer and stabilizes the samples until further analysis. The presence of whole blood and admixtures of other microorganisms (gram-negative *E. coli*, *K. pneumoniae* and *P. aeruginosa*) in the sample at concentrations more or less equal to the concentration of *S. aureus* does not affect the ability of the proposed algorithm to identify the pathogen of interest. The model predicts the presence of a methicillin-resistant phenotype (MRSA/MSSA) with 80% accuracy. We hope that our algorithm will be capable of identifying any other pathogen cultured in any media after expanding the training set.

CONCLUSIONS

We have described a method for creating a database of microbial FTIR spectra and a comparison algorithm suitable for the identification of pathogenic microorganisms that discriminates between the species regardless of the culture growth phase or medium composition. This algorithm can be used in combination with the standard and affordable spectrometer Spectrum Two (Perkin-Elmer; USA). We have tested out algorithm on the clinical isolates of *S. aureus*, which were reliably discriminated from other causative agents of infections, including *E. faecalis*, *E. faecium*, *K. pneumoniae*, *E. coli*, *S. marcescens*, *E. cloacae*, *A. baumannii*, *P. aeruginosa*, and *C. albicans*, taken as pure cultures and pair mixes.

References

1. Popov DA. Postoperative infectious complications in cardiac surgery. Annaly hirurgii. 2013; (5): 15–21.
2. Priputnevich TV, Ljubasovskaja LA, Dubodelov DV, Melkumjan AR, Igonina EP, Akimkin VG, Degtjarev DN, Suhih GT. Jeffektivnaja profilaktika i lechenie ISMP v rodovspomogatel'nyh uchrezhdenijah Rossijskoj Federacii: nereshennye voprosy organizacii i kontrolja. Vestnik Roszdravnadzora. 2017; (4): 34–41.
3. Popov DA, Nadtochej EA. Algorithm of bacteremia diagnostic in cardiosurgical patients in ICU. Anesteziol Reanimatol. 2017; 62 (5): 382–7.
4. Shlens J. A tutorial on Principal Components Analysis. April 7, 2014; Version 3.02.
5. Fisher RA. The Use of Multiple Measurements in Taxonomic Problems. Annals of Eugenics. 1936; 7 (2): 179–188.
6. Hastie T, Tibshirani R, Friedman J. 4.3 Linear Discriminant Analysis. The Elements of Statistical Learning (2 ed.). New York: Springer; 2009. 763 p.
7. Hastie T, Tibshirani R, Friedman J. 7.10 Cross-Validation. The Elements of Statistical Learning (2 ed.). New York: Springer; 2009.
8. R Core Team. R: A language and environment for statistical computing. R Foundation for Statistical Computing, 2016. Vienna, Austria. URL https://www.R-project.org/
9. Kuhn M. Contributions from Jed Wing, Steve Weston, Andre Williams, Chris Keefer, Allan Engelhardt, Tony Cooper, Zachary Mayer, Brenton Kenkel, the R Core Team, Michael Benesty, Reynald Lescarbeau, Andrew Ziem, Luca Scrucca, Yuan Tang and Can Candan. Caret: Classification and Regression Training. R package version 6.0-71. 2016. https://CRAN.R-project.org/package=caret
10. Venables WN, Ripley BD. Modern Applied Statistics with S. New York: Springer; 2002. 495 p.
11. Wickham H. ggplot2: Elegant Graphics for Data Analysis. New York: Springer; 2009.
12. Naumann D, Helm D, Labischinski H. Microbiological characterizations by FT-IR spectroscopy. Nature. 1991; 351 (6321): 81–2.
13. Oust A, Møretrø T, Kirschner C, Narvhus JA, Kohler A. Evaluation of the robustness of FT-IR spectra of lactobacilli towards changes in the bacterial growth conditions. FEMS Microbiol Lett. 2004 Oct 1; 239 (1): 111–6.
14. Wenning M, Theilmann V, Scherer S. Rapid analysis of two food-borne microbial communities at the species level by Fourier-transform infrared microspectroscopy. Environ Microbiol. 2006 May; 8 (5): 848–57.
15. Miguel Gómez MA, Bratos Pérez MA, Martín Gil FJ, Dueñas Díez A, Martín Rodríguez JF, Gutiérrez Rodríguez P, Orduña Domingo A, Rodríguez Torres A. Identification of species of Brucella using Fourier transform infrared spectroscopy. J Microbiol Methods. 2003 Oct; 55 (1): 121–31.
16. Rebuffo-Scheer CA, Kirschner C, Staemmler M, Naumann D. Rapid species and strain differentiation of non-tuberculous mycobacteria by Fourier-Transform Infrared microspectroscopy. J Microbiol Methods. 2007 Feb; 68 (2): 282–90. Epub 2006 Oct 19.
17. Rebuffo-Scheer CA, Dietrich J, Wenning M, Scherer S. Identification of five Listeria species based on infrared spectra (FTIR) using macrosamples is superior to a microsample approach. Anal Bioanal Chem. 2008 Mar; 390 (6): 1629–35.
18. Schäwe R, Fetzer I, Tönniges A, Härtig C, Geyer W, Harms H, Chatzinotas A. Evaluation of FT-IR spectroscopy as a tool to quantify bacteria in binary mixed cultures. J Microbiol Methods. 2011 Aug; 86 (2): 182–7.
19. Wenning M, Scherer S. Identification of microorganisms by FTIR spectroscopy: perspectives and limitations of the method. Appl Microbiol Biotechnol. 2013 Aug; 97(16): 7111–20.
20. Wenning M, Breitenwieser F, Konrad R, Huber I, Busch U, Scherer S. Identification and differentiation of food-related bacteria: A comparison of FTIR spectroscopy and MALDI-TOF mass

spectrometry. J Microbiol Methods. 2014 Aug; 103: 44–52.
21. Rygula A, Jekiel K, Szostak-Kot J, Wrobel TP, Baranska M. Application of FT-Raman spectroscopy for in situ detection of microorganisms on the surface of textiles. J Environ Monit. 2011 Nov; 13 (11): 2983–7.
22. Driver T, Bajhaiya AK, Allwood JW, Goodacre R, Pittman JK, Dean AP. Metabolic responses of eukaryotic microalgae to environmental stress limit the ability of FT-IR spectroscopy for species identification. Algal Res. 2015 Sep; 11: 148–155.
23. Alvarez-Ordóñez A, Mouwen DJ, López M, Prieto M. Fourier transform infrared spectroscopy as a tool to characterize molecular composition and stress response in foodborne pathogenic bacteria. J Microbiol Methods. 2011 Mar; 84 (3): 369–78.
24. Maquelin K, Kirschner C, Choo-Smith LP, Ngo-Thi NA, van Vreeswijk T, Stämmler M, Endtz HP, Bruining HA, Naumann D, Puppels GJ. Prospective study of the performance of vibrational spectroscopies for rapid identification of bacterial and fungal pathogens recovered from blood cultures. J Clin Microbiol. 2003 Jan; 41 (1): 324–9.
25. Muhamadali H, Subaihi A, Mohammadtaheri M, Xu Y, Ellis DI, Ramanathan R, Bansal V, Goodacre R. Rapid, accurate, and comparative differentiation of clinically and industrially relevant microorganisms via multiple vibrational spectroscopic fingerprinting. Analyst. 2016 Aug 15; 141 (17): 5127–36.
26. Lasch P, Stämmler M, Zhang M, Baranska M, Bosch A, Majzner K. FT-IR Hyperspectral Imaging and Artificial Neural Network Analysis for Identification of Pathogenic Bacteria. Anal Chem. 2018 Jul 11.
27. Bishop CM. Pattern Recognition and Machine Learning. New York: Springer; 2006. ISBN-10: 0-387-31073-8.
28. Beleites C, Sergo V. HyperSpec: a package to handle hyperspectral data sets in R', R package version 0.98-20150304. http://hyperspec.r-forge.r-project.org/

Литература

1. Попов Д. А. Послеоперационные инфекционные осложнения в кардиохирургии. Анналы хирургии. 2013; (5): 15–21.
2. Припутневич Т. В., Любасовская Л. А., Дубоделов Д. В., Мелкумян А. Р., Игонина Е. П., Акимкин В. Г., Дегтярев Д. Н., Сухих Г. Т. Эффективная профилактика и лечение ИСМП в родовспомогательных учреждениях Российской Федерации: нерешенные вопросы организации и контроля. Вестник Росздравнадзора. 2017; (4): 34–41.
3. Попов Д. А., Надточей Е. А. Алгоритм диагностики бактериемии у кардиохирургических больных в орит. Анестезиология и реаниматология. 2017; 62 (5): 382–7.
4. Shlens J. A tutorial on Principal Components Analysis. April 7, 2014; Version 3.02.
5. Fisher RA. The Use of Multiple Measurements in Taxonomic Problems. Annals of Eugenics. 1936; 7 (2): 179–188.
6. Hastie T, Tibshirani R, Friedman J. 4.3 Linear Discriminant Analysis. The Elements of Statistical Learning (2 ed.). New York: Springer; 2009. 763 p.
7. Hastie T, Tibshirani R, Friedman J. 7.10 Cross-Validation. The Elements of Statistical Learning (2 ed.). New York: Springer; 2009.
8. R Core Team. R: A language and environment for statistical computing. R Foundation for Statistical Computing, 2016. Vienna, Austria. URL https://www.R-project.org/
9. Kuhn M. Contributions from Jed Wing, Steve Weston, Andre Williams, Chris Keefer, Allan Engelhardt, Tony Cooper, Zachary Mayer, Brenton Kenkel, the R Core Team, Michael Benesty, Reynald Lescarbeau, Andrew Ziem, Luca Scrucca, Yuan Tang and Can Candan. Caret: Classification and Regression Training. R package version 6.0-71. 2016. https://CRAN.R-project.org/package=caret
10. Venables WN, Ripley BD. Modern Applied Statistics with S. New York: Springer; 2002. 495 p.
11. Wickham H. ggplot2: Elegant Graphics for Data Analysis. New York: Springer; 2009.
12. Naumann D, Helm D, Labischinski H. Microbiological characterizations by FT-IR spectroscopy. Nature. 1991; 351 (6321): 81–2.
13. Oust A, Møretrø T, Kirschner C, Narvhus JA, Kohler A. Evaluation of the robustness of FT-IR spectra of lactobacilli towards changes in the bacterial growth conditions. FEMS Microbiol Lett. 2004 Oct 1; 239 (1): 111–6.
14. Wenning M, Theilmann V, Scherer S. Rapid analysis of two food-borne microbial communities at the species level by Fourier-transform infrared microspectroscopy. Environ Microbiol. 2006 May; 8 (5): 848–57.
15. Miguel Gómez MA, Bratos Pérez MA, Martín Gil FJ, Dueñas Díez A, Martín Rodríguez JF, Gutiérrez Rodríguez P, Orduña Domingo A, Rodríguez Torres A. Identification of species of Brucella using Fourier transform infrared spectroscopy. J Microbiol Methods. 2003 Oct; 55 (1): 121–31.
16. Rebuffo-Scheer CA, Kirschner C, Staemmler M, Naumann D. Rapid species and strain differentiation of non-tubercoulous mycobacteria by Fourier-Transform Infrared microspectroscopy. J Microbiol Methods. 2007 Feb; 68 (2): 282–90. Epub 2006 Oct 19.
17. Rebuffo-Scheer CA, Dietrich J, Wenning M, Scherer S. Identification of five Listeria species based on infrared spectra (FTIR) using macrosamples is superior to a microsample approach. Anal Bioanal Chem. 2008 Mar; 390 (6): 1629–35.
18. Schäwe R, Fetzer I, Tönniges A, Härtig C, Geyer W, Harms H, Chatzinotas A. Evaluation of FT-IR spectroscopy as a tool to quantify bacteria in binary mixed cultures. J Microbiol Methods. 2011 Aug; 86 (2): 182–7.
19. Wenning M, Scherer S. Identification of microorganisms by FTIR spectroscopy: perspectives and limitations of the method. Appl Microbiol Biotechnol. 2013 Aug; 97(16): 7111–20.
20. Wenning M, Breitenwieser F, Konrad R, Huber I, Busch U, Scherer S. Identification and differentiation of food-related bacteria: A comparison of FTIR spectroscopy and MALDI-TOF mass spectrometry. J Microbiol Methods. 2014 Aug; 103: 44–52.
21. Rygula A, Jekiel K, Szostak-Kot J, Wrobel TP, Baranska M. Application of FT-Raman spectroscopy for in situ detection of microorganisms on the surface of textiles. J Environ Monit. 2011 Nov; 13 (11): 2983–7.
22. Driver T, Bajhaiya AK, Allwood JW, Goodacre R, Pittman JK, Dean AP. Metabolic responses of eukaryotic microalgae to environmental stress limit the ability of FT-IR spectroscopy for species identification. Algal Res. 2015 Sep; 11: 148–155.
23. Alvarez-Ordóñez A, Mouwen DJ, López M, Prieto M. Fourier transform infrared spectroscopy as a tool to characterize molecular composition and stress response in foodborne pathogenic bacteria. J Microbiol Methods. 2011 Mar; 84 (3): 369–78.
24. Maquelin K, Kirschner C, Choo-Smith LP, Ngo-Thi NA, van Vreeswijk T, Stämmler M, Endtz HP, Bruining HA, Naumann D, Puppels GJ. Prospective study of the performance of vibrational spectroscopies for rapid identification of bacterial and fungal pathogens recovered from blood cultures. J Clin Microbiol. 2003 Jan; 41 (1): 324–9.
25. Muhamadali H, Subaihi A, Mohammadtaheri M, Xu Y, Ellis DI, Ramanathan R, Bansal V, Goodacre R. Rapid, accurate, and comparative differentiation of clinically and industrially relevant microorganisms via multiple vibrational spectroscopic fingerprinting. Analyst. 2016 Aug 15; 141 (17): 5127–36.
26. Lasch P, Stämmler M, Zhang M, Baranska M, Bosch A, Majzner K. FT-IR Hyperspectral Imaging and Artificial Neural Network Analysis for Identification of Pathogenic Bacteria. Anal Chem. 2018 Jul 11.
27. Bishop CM. Pattern Recognition and Machine Learning. New York: Springer; 2006. ISBN-10: 0-387-31073-8.
28. Beleites C, Sergo V. HyperSpec: a package to handle hyperspectral data sets in R', R package version 0.98-20150304. http://hyperspec.r-forge.r-project.org/

PARAMETERS OF VANCOMYCIN PHARMACOKINETICS IN POSTOPERATIVE PATIENTS WITH RENAL DYSFUNCTION: COMPARING THE RESULTS OF A PHARMACOKINETIC STUDY AND MATHEMATICAL MODELING

Ramenskaya GV[1], Shokhin IE[1], Lukina MV[2] ✉, Andrushchishina TB[2], Chukina MA[2], Tsarev IL[2], Vartanova OA[2], Morozova TE[2]

[1] Department of Pharmaceutical and Toxicological Chemistry, Institute of Pharmacy, Sechenov First Moscow State Medical University (Sechenov University), Moscow

[2] Department of Clinical Pharmacology and Propaedeutics of Internal Diseases, Faculty of General Medicine Sechenov First Moscow State Medical University (Sechenov University), Moscow

Mathematical modeling of pharmacokinetic (PK) and pharmacodynamic (PD) parameters essential for establishing correct dosing regimens is an alternative to pharmacokinetic studies (PKS) adopted in the clinical setting. The aim of this work was to compare the values of PK parameters for vancomycin obtained in an actual PKS and through MM in postoperative patients with kidney injury. Our prospective study included 61 patients (47 males and 14 females aged 60.59 ± 12.23 years). During PKS, drug concentrations at steady state C_{trough} and C_{peak} were measured by high-performance liquid chromatography followed by the calculation of the area under the plasma concentration-time curve AUC_{24}. For mathematical modeling, a single-compartment model was employed; PK parameters were estimated using R 3.4.0. The values of Ctrough measured 48 h after the onset of antibiotic therapy during PKS were significantly lower than those predicted by MM (p = 0.004). In a group of patients with acute kidney injury (AKI), AUC_{24} measured at the end of treatment was significantly higher than its value predicted by MM (p = 0.011). The probability of achieving the target AUC_{24} to MIC ratio of over 400 μg•h /ml is higher in the group of patients with C_{trough} = 10–15 μg /ml. Our findings confirm that the use of MM in postoperative patients with renal dysfunction is limited and therapeutic drug monitoring should be used instead.

Keywords: pharmacokinetic study, vancomycin pharmacokinetics, mathematical modeling, acute kidney injury, surgical patients

Acknowledgements: the authors wish to thank Oleg V. Babenko, Chief Physician of the University Clinical Hospital No.1 of Sechenov First Moscow State Medical University for providing an opportunity to carry out our research

✉ **Correspondence should be addressed:** Maria V. Lukina
Bolshaya Pirogovskaya, 2, bl. 4, Moscow, 119435; mari-luk2010@yandex.ru

Received: 16.05.2018 **Accepted:** 25.08.2018

DOI: 10.24075/brsmu.2018.051

ПАРАМЕТРЫ ФАРМАКОКИНЕТИКИ ВАНКОМИЦИНА У БОЛЬНЫХ С НАРУШЕНИЕМ ФУНКЦИИ ПОЧЕК В ПОСЛЕОПЕРАЦИОННОМ ПЕРИОДЕ: СРАВНЕНИЕ РЕЗУЛЬТАТОВ ФАРМАКОКИНЕТИЧЕСКОГО ИССЛЕДОВАНИЯ И МАТЕМАТИЧЕСКОГО МОДЕЛИРОВАНИЯ

Г. В. Раменская[1], И. Е. Шохин[1], М. В. Лукина[2] ✉, Т. Б. Андрущишина[2], М. А. Чукина[2], И. Л. Царев[2], О. А. Вартанова[2], Т. Е. Морозова[2]

[1] Кафедра фармацевтической и токсикологической химии имени А. П. Арзамасцева, Институт фармации, Первый Московский государственный медицинский университет имени И. М. Сеченова (Сеченовский Университет), Москва

[2] Кафедра клинической фармакологии и пропедевтики внутренних болезней, лечебный факультет, Первый Московский государственный медицинский университет имени И. М. Сеченова (Сеченовский Университет), Москва

В клинической практике возможной альтернативой фармакокинетическим исследованиям (ФКИ) является методика математического моделирования (ММ) фармакокинетических (ФК) и фармакодинамических (ФД) параметров для расчета доз антибактериальных препаратов. Целью исследования было сравнение параметров ФК ванкомицина, полученных на основе ФКИ и ММ, у пациентов с нарушением функции почек в послеоперационном периоде. В проспективное исследование был включен 61 пациент (47 мужчин и 14 женщин, возраст 60,59 ± 12,23 лет). В ходе ФКИ методом высокоэффективной жидкостной хроматографии определяли C_{trough}, C_{peak}, с последующим расчетом площади под фармакокинетической кривой ($ПФК_{24}$). Расчет параметров ФК при ММ проводили с помощью программы R 3.4.0 на основе однокомпартментной модели. По данным ФКИ значения равновесных C_{trough} через 48 ч от начала антибактериальной терапии были достоверно ниже значений, полученных при ММ (p = 0,004). В группе пациентов с острым почечным повреждением (ОПП) на момент завершения терапии значения $ПФК_{24}$ по данным ФКИ были достоверно выше (p = 0,011). Вероятность достижения целевого отношения $ПФК_{24}$ / МПК > 400 мкг•ч /мл выше в группе пациентов, где C_{trough} составляет 10–15 мкг/мл. Таким образом, результаты исследования подтверждают, что у больных с нарушением функции почек в послеоперационном периоде применение ММ имеет ряд ограничений и необходимо проведение терапевтического лекарственного мониторинга (ТЛМ).

Ключевые слова: фармакокинетическое исследование, фармакокинетика ванкомицина, математическое моделирование, острое почечное повреждение, пациенты хирургического профиля

Благодарности: авторы благодарят Бабенко Олега Васильевича, главного врача УКБ № 1 Первого МГМУ им. И. М. Сеченова, за предоставленную возможность проведения фармакокинетического исследования.

✉ **Для корреспонденции:** Мария Владимировна Лукина
ул. Большая Пироговская, 2, стр. 4, Москва, 119435; mari-luk2010@yandex.ru

Статья получена: 16.05.2018 **Статья принята к печати:** 25.08.2018

DOI: 10.24075/vrgmu.2018.051

To deliver safe and effective treatment, a pharmacokinetic study (PKS) or therapeutic drug monitoring (TDM) can be recommended for patients receiving antibacterial drugs with a narrow therapeutic index. According to the international guidelines, vancomycin TDM should include measurements of its trough concentrations (C_{trough}) at steady state, the area under the time-concentration curve (AUC_{24}), and the ratio of AUC_{24} to the minimum inhibitory concentration (MIC) of the prescribed drug. There are a few limitations to the use of TDM in clinical routine often arising from the failure to obtain the sufficient number of blood samples to calculate AUC_{24} [1, 2].

In some clinical circumstances, TDM can be replaced with the mathematical modeling (MM) of drug pharmacokinetics. For a number of antibiotics, including vancomycin, aminoglycosides, and colistin, a starting dosing regimen can be generated by medical calculators exploiting mathematic modeling [3, 4]. The medical calculator for vancomycin is based on a single-compartment pharmacokinetic model and can predict the ratio of pharmacokinetic to pharmacodynamic parameters and the minimum inhibitory concentration (MIC) necessary to calculate an adequate drug dose considering the patient's age, sex, weight, and renal function [5, 6]. The use of different types of mathematical modeling in clinical routine reduces the need for TDM.

There is little information about the use of MM for predicting drug pharmacokinetics in different groups of patients. It is impossible to predict the biotransformation dynamics, the volume of distribution and the elimination rate of antibacterial drugs in patients with acute kidney injury in the early postoperative period. Among other important MM drawbacks are high equipment and software costs [7, 8].

The literature analysis does not allow firm conclusions as to whether MM can be safely used instead of TDM in different clinical circumstances because too few research works have been carried out to compare these two methods.

Therefore, to improve the method of pharmacokinetic MM, pharmacokinetic studies need to be carried out in different groups of patients. The data yielded by such research works will help to improve the efficacy and safety of vancomycin-based therapy.

The aim of this work was to compare the results of a pharmacokinetic study and mathematical modeling of vancomycin pharmacokinetics in surgical patients with acute kidney injury.

METHODS

This prospective observational study was carried out at the facilities of the University Clinical Hospital No. 1 of Sechenov First Moscow State Medical University in September 2016 through January 2018. The study protocol was approved by the local Ethics Committee (Protocol No. 05–16 dated May 18, 2016).

The study included 61 postoperative patients (47 males and 14 females) with septic complications. Their mean age was 60.59 ± 12.23 years. The patients were distributed into two groups depending on the presence of acute kidney injury (AKI) [9]: group 1 included patients with AKI (n = 35; 66.6%), group 2 included patients without AKI (the controls; n = 26; 33.4%). In group 1, mild and moderate kidney injury prevailed: stage 1 AKI was diagnosed in 19 (31.1%) patients; stage 2, in 13 (21.3%) patients; stage 3, in 3 (4.9%) patients. Details are presented in Table 1. The groups were comparable in terms of main clinical characteristics, but the patients representing the group with AKI were significantly older (p = 0.004). In the postoperative period, those patients had higher albumin levels than the controls (p = 0.047).

Vancomycin regimen

All patients with infectious complications received vancomycin (marketed as Edicin by Sandoz; Slovenia). The dosing regimen was 15 to 20 mg per 1 kg of body weight, as recommended by the clinical practice guidelines, with due account of the patients' kidney function as estimated by the Cockroft-Gault equation (creatinine clearance rate Cl_{cr}, ml/min). The maximum

Table 1. Clinical characteristics of patients included in the study

Clinical characteristics	Total n = 61	Without AKI n = 26 (44.8%)	With AKI n = 35 (55.7%)	p
	M ± SD	M ± SD	M ± SD	
Age, years	60.59 ± 12.23	55.46 ± 12.89	64.4 ± 10.33	0.004*
BMI, kg/m^2	27.4 ± 5.2	27.12 ± 6.1	27.29 ± 4.5	0.726
EF_0, %	59.02 ± 7.86	62.53 ± 6.74	56.89 ± 7.83	0.018*
$Cl_{Cr\,0}$, ml/min	96.48 ± 29.01	96.26 ± 24.76	96.64 ± 32.16	0.96
$Cl_{Cr\,1}$, ml/min	61.5 ± 27.2	81.51 ± 23.54	46.64 ± 19.1	< 0.0001*
$Cl_{Cr\,2}$, ml/min	85.98 ± 32.33	87.37 ± 33.52	84.95 ± 31.86	0.776
$Albumin_0$, mg/dl	41.21 ± 4.2	42.46 ± 4.35	40.29 ± 3.97	0.447
$Albumin_1$, mg/dl	33.56 ± 1.52	32.21 ± 2.84	44.57 ± 1.61	0.047*
Hospital stay, days	25.07 ± 15.069	26.77 ± 4.27	23.8 ± 1.17	0.451
MV, days	3.30 ± 1.75	3.00 ± 1.29	3.51 ± 0.887	0.736
Intensive care, days.	6.46 ± 1.187	6.5 ± 2.27	6.43 ± 1.23	0.977
Blood loss, ml	653.44 ± 604.65	512.1 ± 258.8	758.00 ± 754.66	0.118
Mortality, %	11 (18%)	4 (36.4%)	7 (63.6%)	0.454

Note: * significant differences, p_{value} < 0.05; BMI — body mass index; Cl_{Cr} — creatinine clearance rate (Cockroft–Gault equation); $Cl_{Cr\,0}$ — before the surgery; $Cl_{Cr\,1}$ — 2–3 days after the surgery; $Cl_{Cr\,2}$ — 7–10 days after the surgery; MV — mechanical ventilation; EF — ejection fraction.

daily dose of the drug did not exceed 2 g. Vancomycin was administered by intravenous drips for 60 min every 12 h [10]. Dosing adjustments were done 24 to 48 h later based on the estimated Cl_{cr}.

The patients with AKI received significantly lower daily doses of vancomycin in comparison with the patients without kidney disfunction (928.6 ± 275 mg and 1637.9 ± 515.8 mg, respectively; $p < 0.0001$). Therapy duration was 9.61 ± 3.8 days. It depended on the severity and site of infection, results of microbiological tests, and individual patient's tolerability. Therapy duration did not differ significantly between the groups and was 9.17 ± 3.6 and 10.19 ± 4 days for groups 1 and 2, respectively ($p = 0.353$).

Parameters of vancomycin pharmacokinetics measured by high-performance liquid chromatography during the pharmacokinetic study

Blood samples for the PKS were collected from all patients included in the study as recommended by the guidelines for vancomycin TDM [1]. To measure C_{peak} (60 min after the infusion) and C_{trough} (60 min before administering the next dose), blood samples were collected 48 hours after the onset of therapy (1) and upon its completion (2) [11].

Proteins contained in the samples were precipitated using methanol. Quantitative measurements were done on the high-performance liquid chromatography system Agilent 1260 equipped with a gradient pump, a degasser, an autosampler, and the tandem mass spectrometer Agilent 6460 (AgilentTechnologies; USA). For separation, the ZorbaxEclipse Plus-C18 2.1 × 50 mm 1.8 µm column and the Zorbax Eclipse Plus C18 12.5 × 2.1 mm 1.8 µm guard column were used.

AUC_{24} was calculated from the obtained values of C_{peak} and C_{trough} at steady state as a sum of different phases of drug pharmacokinetics using the trapezoidal rule [12]:

$$AUC_{24} = \frac{(Lintrap + Logtrap) \times 24}{\tau};$$

where *Lintrap* is the area under the time-concentration curve during the linear phase of drug infusion:

$$Lintrap = \frac{(C_{trough} + C_{peak}) \times T_{inf}}{2};$$

where T_{inf} is infusion time (h).

Logtrap is the area under the "logarithmic" phase of drug elimination:

$$Logtrap = \frac{(C_{peak} - C_{trough})\ \tau - T_{inf}}{\ln \frac{C_{peak}}{C_{trough}}};$$

where τ is time between the infusions (h).

Method of mathematical modeling

Mathematic modeling was done in R 4.3.0 [12]. We estimated the values of C_{peak}, C_{trough} and AUC_{24} using the equations describing the pharmacokinetic dynamics for the single-compartment model 48 h after the onset of therapy (1) and upon its completion (2) [13]:

$$C_{peak} = \frac{Dose \times 1 - e^{-T_{inf} \times K_{el}}}{T_{inf} \times V_d \times K_{el} \times \left(1 - e^{-\tau \times K_{el}}\right)};$$

$$C_{trough} = C_{peak} \times e^{-K_{el} \times (\tau - T_{inf})};$$

where *Dose* is a single dose of vancomycin (mg), T_{inf} is infusion time (h), τ is time between the infusions (h), K_{el} is the predicted elimination rate (h^{-1}), and V_d is the apparent volume of distribution (l/kg):

$$V_d = 0.7 \times M;$$

where M is the absolute weight of a patient (kg).

To calculate the predicted elimination rate, the following equation was used [14]:

$$K_{el} = 0.00083 \times Cl_{Cr} + 0.0044;$$

where Cl_{Cr} is creatinine clearance (ml/min) determined by the Cockroft-Gault formula:

$$Cl_{Cr} = \frac{[140 - age] \times body\ weight\ (\text{kg}) \times (10.05\ for\ women\ \text{or}\ 10.23\ for\ men)}{blood\ plasma\ creatinine\ \left(\frac{\mu\text{mol}}{\text{l}}\right)}.$$

To calculate AUC_{24}, the trapezoidal rule was applied:

$$AUC_{24} = \frac{(Lintrap + Logtrap) \times 24}{\tau}.$$

Statistical processing was done in IBMSPSS Statistics 18.0. and R 3.4.0. In this work continuous variables with normal distribution are presented as a mean (M) and a mean square deviation (SD). Categorical data are presented as a median (Me) and an interquartile range (IQR). Departure from normality was estimated using the Shapiro–Wilk test. The significance of frequency differences was assessed using Fisher's exact test. The significance of differences in arithmetic means between the groups was tested by ANOVA. Apart from ANOVA, nonparametric tests were applied; differences in mean ranks were compared using the Mann–Whitney–Wilcoxon test. The differences were considered significant at $p < 0.05$. To establish correlations between clinically significant pharmacokinetic parameters C_{trough} and AUC_{24}, Spearman's correlation was applied.

RESULTS

The actual values of K_{el}^1 yielded by the PKS (samples collected 48 h after the onset of therapy and upon its completion) were significantly higher than values predicted by MM (0.109 (0.08–0.15) and 0.06 (0.04–0.072), respectively; $p < 0.0001$). The actual values of C_{trough}^1 at steady state were significantly lower than the values predicted by MM (11.32 (8.1–16.4) and 16.59 (14.03–24.8), respectively; $p = 0.004$). At the same time, the values of C_{trough}^2 measured by HPLC and those predicted by MM did not differ significantly. The actual and predicted values of AUC_{24} did not differ significantly 48 h after the onset of antibacterial therapy ($p = 0.715$). Upon therapy completion, the actual values of AUC_{24}^2 were significantly higher than its predicted values (564.04 (409.5–751.9) and 347.03 (267.43–479.99) respectively; $p = 0.011$) (Table. 2).

Parameters of vancomycin pharmacokinetics measured by HPLC and predicted by MM did not differ significantly between group 1 and group 2, except for the actual values of K_{el}^1 ($p = 0.037$) that was significantly higher in the patients with kidney injury (Table 2).

Parameters of vancomycin pharmacokinetics obtained through real measurements demonstrate the variability of C_{trough} and AUC_{24} both at the onset of therapy and upon its completion (Fig. 1). This can be explained by the specifics of vancomycin pharmacokinetics in the studied sample, given standard dosing regimens. However, the obtained range of PK values predicted by MM and the significant difference from the actual values mean that the use of MM in patients with acute kidney injury is limited.

Table 2. Vancomycin pharmacokinetics evaluated by HPLC and MM in the groups of patients with and without AKI 48 h after the onset of therapy and at the time of its completion

PK parameter	TDM	MM	Mann-Whitney-Wilcoxon test; *p*	TDM (*n* = 61)		Mann-Whitney-Wilcoxon test; *p*	MM (*n* = 61)		Mann-Whitney-Wilcoxon test; *p*
	(*n* = 61)	(*n* = 61)		AKI+ (*n* = 35)	AKI–		AKI+	AKI–	
	Me [IQR]			Me [IQR]			Me [IQR]		
Kel[1] (hour $^{-1}$)	0.109 [0.08–0.15]	0.06 [0.04–0.072]	< 0.0001	0.12 [0.1–0.14]	0.1 [0.06–0.131]	0.037	0.04 [0.04–0.07]	0.06 [0.06–0.077]	0.117
Kel[2] (hour $^{-1}$)	0.08 [0.05–0.14]	0.08 [0.063–0.102]	0.274	0.06 [0.05–0.15]	0.11 [0.07–0.13]	0.412	0.08 [0.05–0.15]	0.09 [0.07–0.11]	0.709
C_{trough}[1] (μg/ml)	11.32 [8.1–16.4]	16.59 [14.03–24.8]	0.004	9.6 [6.9–15.0]	12.08 [8.8–18.27]	0.197	16.2 [14.2–19.7]	14.03 [13.24–18.04]	0.54
C_{trough}[2] (μg/ml)	12.59 [8.5–22.8]	8.65 [5.9–12.06]	0.092	15.7 [6.6–25.8]	12.59 [9.1–21.7]	0.776	8.3 [6.08–11.6]	10.14 [5.7–12.5]	0.765
C_{peak}[1] (μg/ml)	35.6 [31.2-37.2]	27.3 [24.2–32.2]	0.019	35.1 [30.9–37.8]	23.8 [21.3–31.4]	0.502	26.2 [15.8–27.2]	28.2 [26.6–32.8]	0.502
C_{peak}[2] (μg/ml)	22.5 [18.6–30.7]	34.8 [31.7–41.9]	0.002	35.6 [31.9–40.7]	23.8 [21.3–31.4]	0.263	26.23 [24.11–28.1]	34.8 [30.1–43.1]	0.263
AUC_{24}[1] (μg × h/ml)	484.08 [404.5–604.4]	459.72 [433.6–556.01]	0.715	465.7 [399.5–605.3]	530.8 [480.2–603.4]	0.263	462.8 [450.4–548.5]	458.38 [413.8–553.5]	0.709
AUC_{24}[2] (μg × h/ml)	564.04 [409.5–751.9]	347.03 [267.43–479.99]	0.011	551.2 [397.02–786.6]	564.04 [421.9–721.58]	0.765	345.4 [255.5–393.2]	386.8 [273.8–481.5]	0.502

Note: 1 — 48 h after the onset of therapy; 2 — at the time of its completion.

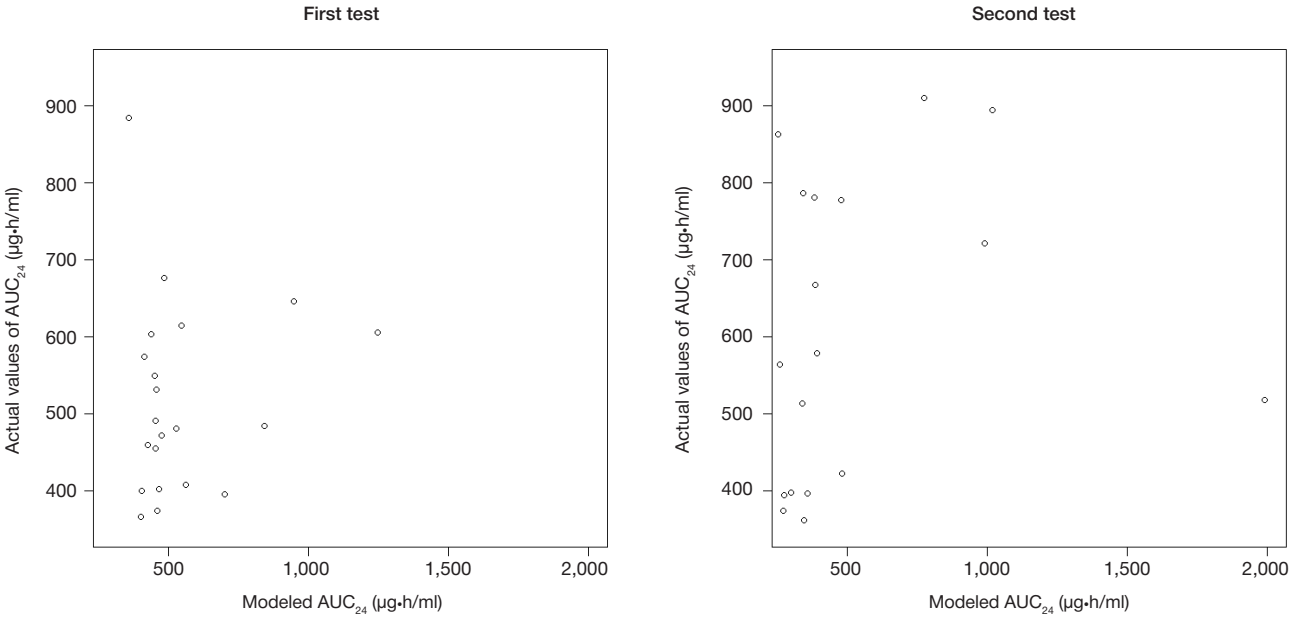

Fig. 1. The range of AUC_{24} values obtained through MM and high-performance liquid chromatography in postoperative patients with acute kidney injury 48 hours after the onset of therapy and upon its completion

In the patients with C_{trough} of 10–15 μg/ml at steady state, AUC_{24} was above 400 μg × h/ml both 48 h after the onset of therapy (Fig. 2) and at the time of its completion (Fig. 3). The correlation analysis revealed a positive correlation between the values of C_{trough} and AUC_{24} at steady state (r = 0.964; p < 0.001).

Predicting the probability of reaching the target PK/PD ratio

The values of AUC_{24} obtained through HPLC suggest that the target PK/PD ratio (AUC_{24}/MIC > 400) is highly probable if MIH equals 1 μg/ml (for *Staphylococcus aureus*). The exception is the group of patients in which C_{trough} is below 10 μg/ml; in this group the target PK/PD ratio was observed in 55% of patients. If MIC increases to 1.5 or 2 μg/ml, the probability of reaching the desired PK/PD ratio in the group of patients with C_{trough} = 10–15 μg/ml is reduced to 30%, and in the group with C_{trough} = 15–20 μg/ml, to 70% (Table 3). Hypothetically, the desired PK/PD ratio can be achieved at MIC = 2 μg/ml only if C_{trough} reaches 20 μg/ml or higher (Table 3).

The analysis of the predicted AUC_{24} to MIC ratio revealed that upon therapy completion the target PK/PD ratio of > 400 was observed mostly in the patients with C_{trough} above 10–15 μg/ml (Table 4).

DISCUSSION

Our study shows that if a standard approach to vancomycin dosing is applied in surgical patients with acute kidney injury, the actual values of C_{trough} measured by HPLC 48 h after the onset of therapy are significantly different from the values predicted by MM (11.32 (8.1–16.4) and 16.59 (14.03–24.8) μg/ml, respectively; $p = 0.004$).

The obtained results are consistent with the findings of other researchers who observed the high variability of pharmacokinetic parameters and the ratio of AUC_{24}/MIC > 400 in the patients of intensive care units treated with standard doses of vancomycin [15, 16].

The differences in the results yielded by PKS and MM can be explained by the drawbacks of the majority of mathematical models. A single-compartment model exploits a fixed mean V_d value of 0.7 l/kg. Pharmacokinetic studies demonstrate that this value can range from 0.2 to 1.25 l/kg and depends on the volume of circulating blood, albumin levels, etc. K_{el} is calculated based on the clearance rate Cl_{cr} estimated by the Cockroft–Gault equation. At present there is no perfect formula for estimating the rate of drug elimination based on the levels of endogenous creatinine [17, 18].

Some authors believe that the use of standard nomograms and MM for predicting drug pharmacokinetics has a number of limitations. First, the majority of these methods were validated on the limited population of healthy volunteers or stable patients. Second, the target values of steady-state C_{trough} were thought to fall within the range of 5–10 μg/ml. At present, the range of these values has risen to 15–20 μg/ml as demonstrated by a number of microbiological studies [19, 20].

It is debatable whether high C_{trough} concentrations and AUC_{24}/MIC of 400 or above really need to be achieved. Local microbiological monitoring demonstrates that at MIC of 1 μg/ml or below C_{trough} does not have to be as high as 15–20 μg/ml [21].

Our retrospective study demonstrates that over 30% of patients reached the target ratio AUC_{24}/MIC of > 400 even at C_{trough} below 15 μg/ml. Regression analysis reveals that

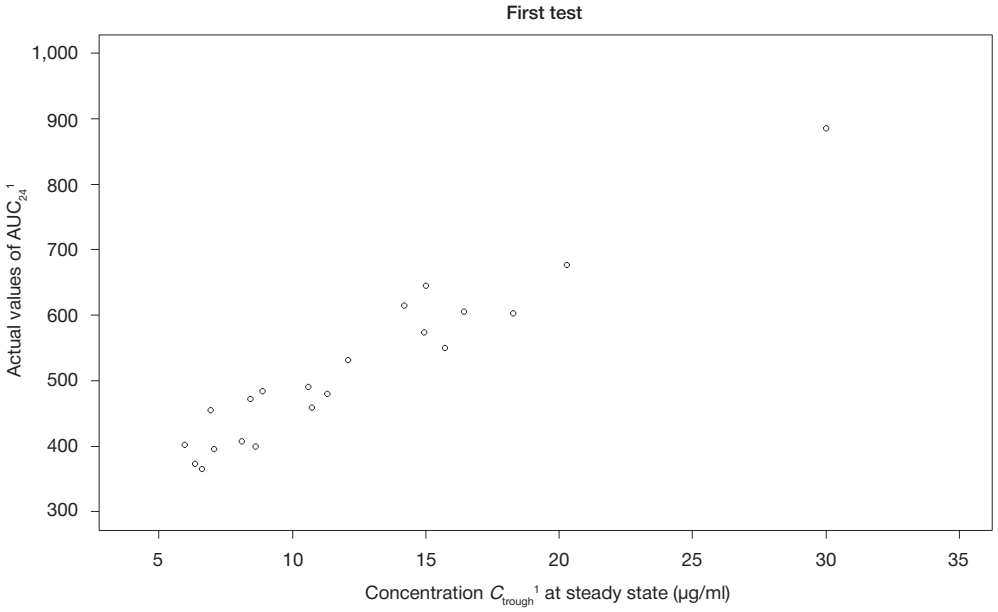

Fig. 2. Dependency of $AUC_{24}{}^1$ on the levels of steady-state $C_{trough}{}^1$ 48 hours after the onset of antibacterial treatment (HPLC)

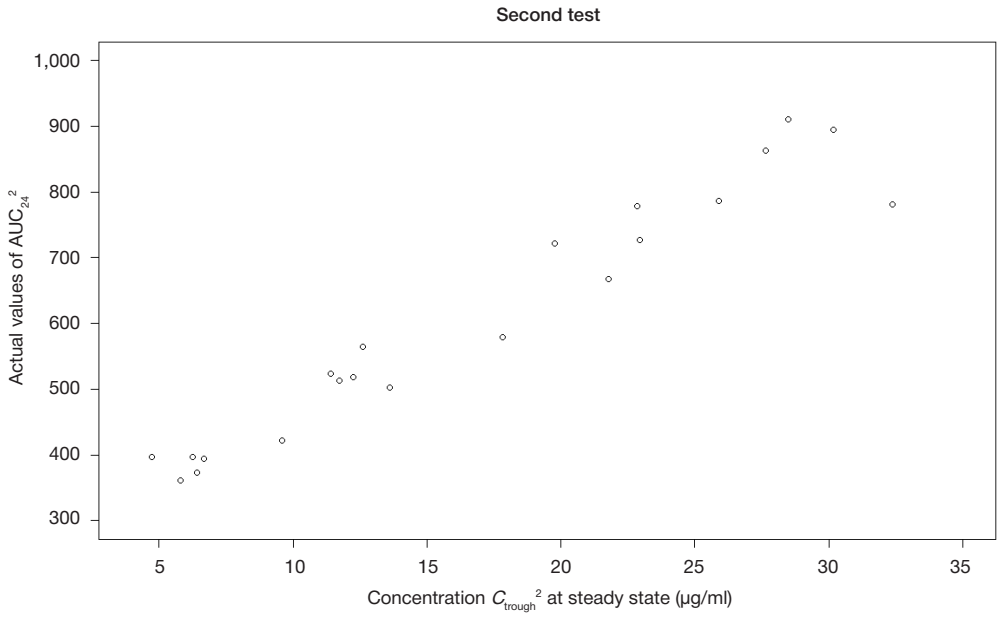

Fig. 3. Dependency of $AUC_{24}{}^2$ on the levels of steady-state $C_{trough}{}^2$ at the time of therapy completion (HLPC)

Table 3. Prediction of the AUC_{24}/ MIC ratio for *Staphylococcus aureus* 48 hours after the onset of vancomycin therapy

Value of C_{trough}, μg/ml	AUC_{24}, μg•h/ml			AUC_{24}/MIC > 400		
	M	min	max	MIC 1 μg/ml (%)	MIC 1.5 μg/ml (%)	MIC 2 μg/ml (%)
< 10	401.9753	365.676	484.0849	55	0	0
10–15	530.8875	459.4124	645.6017	100	30	0
15–20	603.4062	549.4891	605.2955	100	70	0
> 20	780.6152	676.4806	884.7498	100	100	50

Table 4. Prediction of the AUC_{24}/ MIC ratio for *Staphylococcus aureus* at the time of vancomycin therapy completion

Value of C_{trough}, μg/ml	AUC_{24}, μg•h/ml			AUC_{24}/MIC > 400		
	M	min	max	MIC 1 μg/ml (%)	MIC 1.5 μg/ml (%)	MIC 2 μg/ml (%)
< 10	395.1776	361.2053	421.9468	16	0	0
10–15	517.7069	502.5894	564.0411	100	0	0
15–20	650.2483	578.911	721.5856	100	50	0
> 20	783.8409	667.7073	910.8016	100	100	38

C_{trough} = 10.8 μg/ml is a predictor of the target AUC_{24}/MIC value above 400 [22].

In our study the patients treated with standard doses of vancomycin responded positively to treatment although their C_{trough} was 10–15 μg/ml (Table 2). The fact that they reached the target AUC_{24}/MIC ratio of > 400 can be explained by the microbiological monitoring carried out in our hospital (*S. aureus*, MIC of vancomycin < 1 μg/ml in 60–70% cases).

As MIC rises to 1.5 or 2 μg/ml, the efficacy of vancomycin treatment decreases in 30% or 70% of case, respectively.

The obtained data suggest that dosing adjustments aided by MM based on the results of the pharmacokinetic study involving measurements of C_{trough}, C_{peak} and AUC_{24} were more beneficial for the patients than dosing regimens based solely on the monitoring of C_{trough} [23].

Pharmacokinetic studies carried out in specific groups of patients are especially important in the development of a good mathematical model of vancomycin pharmacokinetics and selecting optimal dosing regimens. On a larger scale, the results of such studies can be used to build population models, which in turn requires more pharmacokinetic studies involving different cohorts of patients [24, 25].

CONCLUSIONS

Our study demonstrates that the predicted and actual values of vancomycin pharmacokinetics vary. The differences indicate the necessity of therapeutic drug monitoring in postoperative patients with kidney injury. Information about the actual C_{trough} values ensures better safety of vancomycin-based therapy in patients with acute kidney injury. The efficacy of the antibacterial treatment is constrained by the sensitivity of the infectious agent (MIC). For a better outcome, the AUC_{24}/MIC ratio should be calculated. Further pharmacokinetic studies of vancomycin are necessary to improve the method of mathematical modeling for postoperative patients with acute kidney injury.

References

1. Rybak M, Lomaestro B, Rotschafer JC, Moellering R, Craig W, Billeter M, et al. Therapeutic monitoring of vancomycin in adult patients: a consensus review of the American Society of Health-System Pharmacists, the Infectious Diseases Society of America, and the Society of Infectious Diseases. Am J Health Syst Pharm. 2009 Jan 1; 66 (1): 82–98.
2. Ye ZK, et al. Therapeutic drug monitoring of vancomycin: a guideline of the Division of Therapeutic Drug Monitoring. J Antimicrob Chemother. 2016 Nov 11; 71 (11): 3020–25.
3. Bondareva I. B. Programmnoe obespechenie dlya analiza dannyh FK/FD issledovanij. Klinicheskaya farmakokinetika. 2005; 2 (3): 9–13.
4. Brendel K, Dartois C, Comets E, et al. Are population pharmacokinetic and/or pharmacodynamic models adequately evaluated? A survey of the literature from 2002 to 2004. Clin Pharmacokinet. 2007; 46 (3): 221–34.
5. Clinical Calculators [internet]. Available from: http://clincalc.com/Vancomycin.
6. Lake KD, Peterson CD. A simplified dosing method for initiating vancomycin therapy. Pharmacotherapy. 1985 Nov-Dec; 5 (6): 340–44.
7. Al-Kofide H, Zaghloul I, Al-Naim L. Pharmacokinetics of vancomycin in adult cancer patients. J Oncol Pharm Pract. 2010 Dec 16; 16 (4): 245–250.
8. Burton ME, Gentle DL, Vasko MR. Evaluation of a Bayesian method for predicting vancomycin dosing. DICP. 1989; 23 (4): 294–300.
9. Khwaja A. KDIGO clinical practice guidelines for acute kidney injury. Nephron Clin Pract. 2012; 120 (4): 179–84.
10. Instrukciya po medicinskomu primeneniyu [internet]. Available from: http://grls.rosminzdrav.ru/Grls_View_v2.aspx?routingGuid=80390ff0-c656-4e1b-a33e-a30232cccf1d&t=.
11. Hammett-Stabler CA, Johns T. Laboratory guidelines for monitoring of antimicrobial drugs. Clin Chem. 1998 May; 44 (5): 1129–40.
12. Core Team. R: A language and environment for statistical computing. R Foundation for Statistical Computing, Vienna, Austria. 2017 Available from: https://www.R-project.org.
13. Bauer LA. Applied clinical pharmacokinetics. New York: McGraw-Hill, 2001.p. 26–49.
14. Matzke GR, McGory RW, Halstenson CE, Keane WF. Pharmacokinetics of vancomycin in patients with various degrees of renal function. Antimicrob Agents Chemother. 1984 Apr;25(4):433–7.
15. Patel N, Pai MP, Rodvold KA, Lomaestro B, Drusano GL, Lodise TP. Vancomycin: we can't get there from here. Clin Infect Dis. 2011 Apr 15; 52 (8): 969–74.
16. Bel KA, Bourguignon L, Marcos M, Ducher M, Goutelle S. Is trough concentration of vancomycin predictive of the area under the curve? A clinical study in elderly patients. Ther Drug Monit.

2017 Feb; 39 (1): 83–7.
17. Moise-Broder PA, Forrest A, Birmingham MC, et al. Pharmacodynamics of vancomycin and other antimicrobials in patients with Staphylococcus aureus lower respiratory tract infections. Clin Pharmacokinet. 2004; 43 (13): 925–42.
18. Paglialunga S, Offman E, Ichhpurani N, Marbury TC, Morimoto BH. Update and trends on pharmacokinetic studies in patients with impaired renal function: practical insight into application of the FDA and EMA guidelines. Expert review of clinical pharmacology. 2017; 10 (3): 273–83.
19. Prybylski JP. Vancomycin Trough Concentration as a Predictor of Clinical Outcomes in Patients with Staphylococcus aureus Bacteremia: A Meta-analysis of Observational Studies. Pharmacotherapy. 2015 Oct; 35 (10): 889–98.
20. Murphy JE, Gillespie DE, Bateman CV. Predictability of vancomycin trough concentrations using seven approaches for estimating pharmacokinetic parameters. Am J Health Syst Pharm. 2006 Dec 1; 63 (23): 2365–70.
21. del Mar Fernández de Gatta Garcia M, Revilla N, Calvo MV, Domínguez-Gil A, Sánchez Navarro A. Pharmacokinetic/pharmacodynamic analysis of vancomycin in ICU patients. Intensive Care Med. 2007 Feb; 33 (2): 279-85.
22. Neely MN, Youn G, Jones B, Jelliffe RW, Drusano GL, Rodvold KA, et al. Are vancomycin trough concentrations adequate for optimal dosing? Antimicrob Agents Chemother. 2014; 58 (1): 309–16.
23. Pai MP, Neely M, Rodvold KA, Lodise TP. Innovative approaches to optimizing the delivery of vancomycin in individual patients. Adv Drug Deliv Rev. 2014 Nov 20;77:50–7.
24. Purwonugroho TA, Chulavatnatol S, Preechagoon Y, Chindavijak B, Malathum K, Bunuparadah P. Population pharmacokinetics of vancomycin in Thai patients. The Scientific World Journal. 2012;2012:762649. DOI: 10.1100/2012/762649.
25. Zalloum N, Saleh MI, Al Haj M, Balbisi M, Al-Ghazawi M. Population pharmacokinetics of vancomycin in Jordanian patients Tropical Journal of Pharmaceutical Research. 2018; 17 (2): 351–58.

Литература

1. Rybak M, Lomaestro B, Rotschafer JC, Moellering R, Craig W, Billeter M, et al. Therapeutic monitoring of vancomycin in adult patients: a consensus review of the American Society of Health-System Pharmacists, the Infectious Diseases Society of America, and the Society of Infectious Diseases. Am J Health Syst Pharm. 2009 Jan 1; 66 (1): 82–98.
2. Ye ZK, et al. Therapeutic drug monitoring of vancomycin: a guideline of the Division of Therapeutic Drug Monitoring. J Antimicrob Chemother. 2016 Nov 11; 71 (11): 3020–25.
3. Бондарева И. Б. Программное обеспечение для анализа данных ФК/ФД исследований. Клиническая фармакокинетика. 2005; 2 (3): 9–13.
4. Brendel K, Dartois C, Comets E, et al. Are population pharmacokinetic and/or pharmacodynamic models adequately evaluated? A survey of the literature from 2002 to 2004. Clin Pharmacokinet. 2007; 46 (3): 221–34.
5. Clinical Calculators [интернет]. Available from: http://clincalc.com/Vancomycin
6. Lake KD, Peterson CD. A simplified dosing method for initiating vancomycin therapy. Pharmacotherapy. 1985 Nov-Dec; 5 (6): 340–44.
7. Al-Kofide H, Zaghloul I, Al-Naim L. Pharmacokinetics of vancomycin in adult cancer patients. J Oncol Pharm Pract. 2010 Dec 16; 16(4): 245–250.
8. Burton ME, Gentle DL, Vasko MR. Evaluation of a Bayesian method for predicting vancomycin dosing. DICP. 1989; 23 (4): 294–300.
9. Khwaja A. KDIGO clinical practice guidelines for acute kidney injury. Nephron Clin Pract. 2012; 120 (4): 179–84.
10. Инструкция по медицинскому применению [интернет]. Доступно по ссылке: http://grls.rosminzdrav.ru/Grls_View_v2.aspx?routingGuid=80390ff0-c656-4e1b-a33e-a30232cccf1d&t=
11. Hammett-Stabler CA, Johns T. Laboratory guidelines for monitoring of antimicrobial drugs. Clin Chem. 1998 May; 44 (5): 1129–40.
12. Core Team. R: A language and environment for statistical computing. R Foundation for Statistical Computing, Vienna, Austria. 2017 Available from: https://www.R-project.org
13. Bauer LA. Applied clinical pharmacokinetics. New York: McGraw-Hill, 2001. p. 26–49.
14. Matzke GR, McGory RW, Halstenson CE, Keane WF. Pharmacokinetics of vancomycin in patients with various degrees of renal function. Antimicrob Agents Chemother. 1984 Apr; 25 (4): 433–7.
15. Patel N, Pai MP, Rodvold KA, Lomaestro B, Drusano GL, Lodise TP. Vancomycin: we can't get there from here. Clin Infect Dis. 2011 Apr 15; 52 (8): 969–74.
16. Bel KA, Bourguignon L, Marcos M, Ducher M, Goutelle S. Is trough concentration of vancomycin predictive of the area under the curve? A clinical study in elderly patients. Ther Drug Monit. 2017 Feb; 39 (1): 83–7.
17. Moise-Broder PA, Forrest A, Birmingham MC, et al. Pharmacodynamics of vancomycin and other antimicrobials in patients with Staphylococcus aureus lower respiratory tract infections. Clin Pharmacokinet. 2004; 43 (13): 925–42.
18. Paglialunga S, Offman E, Ichhpurani N, Marbury TC, Morimoto BH. Update and trends on pharmacokinetic studies in patients with impaired renal function: practical insight into application of the FDA and EMA guidelines. Expert review of clinical pharmacology. 2017; 10 (3): 273–83.
19. Prybylski JP. Vancomycin Trough Concentration as a Predictor of Clinical Outcomes in Patients with *Staphylococcus aureus* Bacteremia: A Meta-analysis of Observational Studies. Pharmacotherapy. 2015 Oct; 35 (10): 889–98.
20. Murphy JE, Gillespie DE, Bateman CV. Predictability of vancomycin trough concentrations using seven approaches for estimating pharmacokinetic parameters. Am J Health Syst Pharm. 2006 Dec 1; 63 (23): 2365–70.
21. del Mar Fernández de Gatta Garcia M, Revilla N, Calvo MV, Domínguez-Gil A, Sánchez Navarro A. Pharmacokinetic/pharmacodynamic analysis of vancomycin in ICU patients. Intensive Care Med. 2007 Feb; 33 (2): 279–85.
22. Neely MN, Youn G, Jones B, Jelliffe RW, Drusano GL, Rodvold KA, et al. Are vancomycin trough concentrations adequate for optimal dosing? Antimicrob Agents Chemother. 2014; 58 (1): 309–16.
23. Pai MP, Neely M, Rodvold KA, Lodise TP. Innovative approaches to optimizing the delivery of vancomycin in individual patients. Adv Drug Deliv Rev. 2014 Nov 20; 77: 50–7.
24. Purwonugroho TA, Chulavatnatol S, Preechagoon Y, Chindavijak B, Malathum K, Bunuparadah P. Population pharmacokinetics of vancomycin in Thai patients. The Scientific World Journal. 2012;2012:762649. DOI: 10.1100/2012/762649.
25. Zalloum N, Saleh MI, Al Haj M, Balbisi M, Al-Ghazawi M. Population pharmacokinetics of vancomycin in Jordanian patients Tropical Journal of Pharmaceutical Research. 2018; 17 (2): 351–58.

EVALUATION OF CARDIAC MRI EFFICACY IN THE DIAGNOSIS OF HIBERNATING MYOCARDIUM

Rustamova YK[1] ✉, Imanov GG[2], Azizov VA[1]

[1] Department of Internal Diseases No 2, Azerbaijan Medical University, Baku, Azerbaijan

[2] Department of Internal Diseases No 1, Azerbaijan Medical University, Baku, Azerbaijan

The efficacy of cardiac MRI in the diagnosis of hibernating myocardium remains understudied. The existing body of evidence on this matter comes mainly from observational studies carried out in heterogenous (in terms of cardiac pathology) cohorts of patients, which complicates the interpretation of the results. The aim of our study was to evaluate the efficacy of cardiac imaging techniques in 144 patients with a history of myocardial infarction, multivessel coronary artery disease and a low ejection fraction of the left ventricle. All participants underwent stress echocardiography and cardiac MRI examinations. The following parameters were factored into: a) the number of identified segments with abnormal myocardial contractility; b) the transmurality index (scar thickness); c) the volume of the viable myocardium relative to its total mass. The study revealed that on average there were 2.72 ± 0.82 segments with contractile dysfunction per patient. Cardiac MRI was able to detect significantly more hibernating segments than stress echocardiography. On average, the difference in the number of detected segments was 36 (56; 86) at 95% CI and $p < 0.01$. We established that as the transmurality index increases, the number of hypokinetic segments decreases ($r = –0.78$; $p = 0.0314$) while the number of akinetic segments ($r = –0.84$; $p = 0.0282$) goes up. This needs to be accounted for when selecting a treatment strategy for such patients. We conclude that cardiac MRI is a more effective and sensitive diagnostic technique in patients with hibernating myocardium that allows detecting significantly more cardiac segments with contractile dysfunction than stress echocardiography. Delayed contrast enhancement is instrumental in estimating the thickness and extent of cardiac fibrosis, the parameters that should be accounted for when deciding on the treatment strategy in such patients.

Keywords: hibernating myocardium, cardiac MRI, dobutamine stress echocardiography

✉ **Correspondence should be addressed:** Yasmin K. Rustamova
Bakikhanova 23, Baku, Azerbaijan, AZ1022; yasmin.rst@gmail.com

Received: 16.01.2018 **Accepted:** 20.06.2018

DOI: 10.24075/brsmu.2018.042

ОЦЕНКА ЭФФЕКТИВНОСТИ МЕТОДА МРТ СЕРДЦА В ДИАГНОСТИКЕ ДИСФУНКЦИОНАЛЬНОГО МИОКАРДА

Я. К. Рустамова[1] ✉, Г. Г. Иманов[2], В. А. Азизов[1]

[1] Кафедра внутренних болезней №2, Азербайджанский медицинский университет, Баку, Азербайджан

[2] Кафедра внутренних болезней №1, Азербайджанский медицинский университет, Баку, Азербайджан

Эффективность метода МРТ сердца в диагностике дисфункционального миокарда в настоящее время до конца не изучена. Это обусловлено тем, что доказательная база основана преимущественно на обсервационных исследованиях, которые отличаются разнородностью изучаемых групп по нозологическим формам, что не позволяет убедительно интерпретировать полученные результаты. Целью исследования была оценка эффективности методов визуализации дисфункционального миокарда у 144 пациентов, перенесших инфаркт миокарда и имеющих многососудистое поражение коронарного русла и сниженную фракцию выброса левого желудочка (ФВ ЛЖ). Для визуальной оценки дисфункционального миокарда всем участникам исследования выполняли стресс-эхокардиографию и МРТ сердца. Критерии оценки эффективности диагностических методов включали: а) количество сегментов с нарушенной кинетикой; б) глубину поражения (индекс трансмуральности); в) объем контрастируемого миокарда в пределах сегмента. По результатам исследования, на одного пациента, в среднем, приходилось 2,72 ± 0,82 сегмента с нарушенной кинетикой. При выполнении МРТ сердца выявлялось достоверно большее количество сегментов с нарушенной сократимостью. Средняя разница по количеству сегментов составила 63 сегмента (56; 82) при 95% ДИ, $p < 0,01$. Выявлено, что с увеличением индекса трансмуральности по толщине уменьшается количество сегментов с гипокинезом ($r = –0,78$; $p = 0,0314$) и увеличивается количество сегментов с акинезом ($r = –0,84$; $p = 0,0282$), что особенно важно учитывать при выборе тактики лечения таких пациентов. Можно предположить, что МРТ сердца является более эффективным и чувствительным методом диагностики дисфункционального миокарда и позволяет определять достоверно большее количество сегментов с нарушенной сократимостью, по сравнению с методом стресс-эхокардиографии. Методика отсроченного контрастирования позволяет оценить глубину и распространенность кардиального фиброза, что особенно важно учитывать при выборе стратегии лечения больных с дисфункциональным миокардом.

Ключевые слова: дисфункциональный миокард, МРТ сердца, стресс-эхокардиография с добутамином

✉ **Для корреспонденции:** Ясмин Кямрановна Рустамова
Ул. Бакиханова, д. 23, г. Баку, Азербайджан, AZ1022; yasmin.rst@gmail.com

Статья получена: 16.01.2018 **Статья принята к печати:** 20.06.2018

DOI: 10.24075/vrgmu.2018.042

The prognosis of postinfarction patients with hibernating myocardium largely depends on the timeliness and accuracy of the diagnostic evaluation. Among the diagnostic techniques used to predict the outcomes of this condition are dobutamine stress echocardiography, single-photon emission computed tomography (SPECT), positron emission tomography (PET), and magnetic resonance imaging (MRI) [1].

PET is a reliable prognostic tool in patients with marked heart failure symptoms and a low ejection fraction. Just like SPECT, PET images can be corrected for the attenuation of photons by soft tissues. With these techniques, the turnover of radiolabeled compounds can be easily quantified. In addition, high positron energies generate high-quality images even if patients are obese [2].

However, a wider clinical application of PET is constrained by its high costs and the ultrashort half-life of isotopes. The latter are normally fabricated either on site or close to the facilities where the scan is performed to ensure the quickest shipment possible.

Among the disadvantages of radionuclide-based techniques for the diagnostic evaluation of the myocardium, such as SPECT, is their inability to reliably identify patients with a poor prognosis. No SPECT or PET scanner has been designed yet to have a spatial resolution comparable to that of routinely used ultrasound, X-ray or magnetic resonance imaging machines. Indeed, the 6-mm-resolution scanners are able to identify clinically relevant perfusion and metabolism disturbances. But unlike computed tomography or MRI, these nuclear medicine techniques can “break” the myocardium only into segments but not layers [3]. Besides, currently available radiopharmaceuticals are nonspecific perfusion markers and do not allow discrimination between scars and viable myocardial tissue.

Dobutamine stress echocardiography is a relatively cheap and simple test in comparison with other cardiac imaging techniques. Dobutamine stress echo and SPECT performed after successful revascularization demonstrate similar sensitivity (74–100%); however, the specificity of radionuclide imaging is lower (40–55%) than that of stress echocardiography (77–95%). At the same time, stress echo tends to underestimate the viability of the myocardium, whereas nuclear medicine guarantees more accurate results [4–7].

Because stress echocardiography is used to evaluate myocardial viability while radionuclide cardiac imaging describes the state of cardiomyocyte membranes, these techniques should be regarded as complementary to each other and in some cases are recommended to be used in combination.

The key difference between modern magnetic resonance and radionuclide imaging modalities is that the former is totally safe and provides high spatial resolution [8].

There are two major types of MRI-ECG synchronization protocols; the first type allows visualization of myocardial contraction and relaxation, while the second produces detailed spatial images of myocardial anatomy, its structural layers and morphological components [9]. MRI-ECG synchronization also allows qualitative and quantitative assessment of left/right ventricular regional contractility, providing information on the volume of the intact portion of the cardiac muscle, which is an important factor predicting the course of coronary artery disease (CAD), especially in patients awaiting myocardial revascularization [10, 11].

Delayed contrast-enhanced cardiac MRI with paramagnetic contrast agents helps to identify fibrous tissue and postinfarction myocardial scarring caused by ischemia, inflammation or dystrophy. This technique is suitable for localizing acute myocardial infarction and estimating the size of the lesion; it is also exploited to assess the severity of the postinfarction myocardial fibrosis and to monitor scarring dynamics [12, 13].

Due to its good spatial and temporal resolution, cardiac MRI has become the gold standard in evaluating the global contractility of the left ventricle and detecting regional myocardial contractility abnormalities [14].

Yet the guidelines of the European Society of Cardiology on myocardial revascularization adopted in 2014 recommend high spatial resolution imaging modalities, such as cardiac MRI, only for the purpose of verification of ischemic damage in patients with moderate pretest probability of marked CAD (15–85%) or for the estimation of the volume of scar tissue and contractile reserve. It is emphasized that the diagnostic value of MRI is comparable to that of PET, SPECT and dobutamine stress echocardiography when it comes to estimating myocardial viability and predicting the degree of wall motion recovery [15].

Interestingly, the existing body of evidence on this matter comes from observational studies and meta analyses: randomized trials have solely addressed the efficacy of PET. Besides, clinical trials of MRI efficacy recruit heterogenous (in terms of cardiac pathology) groups of patients, which means that their findings cannot be reliably interpreted.

Considering the abovesaid, there is a need for new research studies aimed to investigate the efficacy of existing techniques for the visualization of hibernating myocardium and to assess their impact on the choice of treatment strategies in a homogenous cohort of patients.

METHODS

The study was conducted at the facilities of the Second Department of Internal Diseases (Azerbaijan Medical University, Baku) and the Department of Hospital Surgery with a course in Pediatric Surgery (Peoples’ Friendship University of Russia, Moscow).

The inclusion criteria were as follows: a history of myocardial infarction; class II–III angina (Canadian Cardiovascular Society grading scale); multivessel coronary artery disease concluded from digital angiography (SYNTAX score of < 32 points); the presence of segments with impaired regional left ventricular contractile function; class I–III heart failure (NYHA classification); the left ventricular ejection fraction (LVEF) < 50%.

Patients with acute coronary syndrome, claustrophobia, implantable cardiac pacemakers or cardioverter defibrillators and those in whom an endovascular intervention was technically impossible were excluded from the study.

Based on the findings of coronary angiography ordered for all the participants, a standard dobutamine stress echo test was recommended to assess myocardial viability in the zones of coronary occlusion.

Regional myocardial contractile function was assessed using a cardiac segmentation model of 17 segments and a 4-point scale; the regional contractility index was calculated as a ratio of the sum scored by each segment of the left ventricle to the total number of analyzed segments. Normal segments scored 1 point; hypokinetic segments, 2 points; akinetic segments, 3 points; dyskinetic ones, 4 points.

The segments were considered viable if their regional contractility improved by 1 or more points. The test was considered negative if no systolic wall thickening was observed following administration of a low dobutamine dose (5–10 mg/kg/min) or if myocardial contractility decreased following administration of a high dobutamine dose (20–40 mg/kg/min).

To visualize myocardial defects, all patients underwent stress echo and cardiac MRI examinations. The obtained images were subsequently analyzed to assess the efficacy of the applied diagnostic techniques.

The following parameters were factored into: a) the number of identified segments with abnormal myocardial contractility; b) the transmurality index (scar thickness); c) the volume of the viable myocardium relative to its total mass.

Cardiac MRI scans were performed on the 1.5 T Magnetom Essenza scanner (Siemens; Germany) synchronized with ECG.

During the scan, the patients were asked to hold their breath on exhale for 6 to 12 s depending on the type of a pulse sequence applied. The contrast agent was injected after precontrast mapping was done and a series of cine, T1- and T2-weighted images was obtained for further cardiac morphology analysis.

Postinfarction fibrosis was estimated by delayed contrast-enhanced MRI using a gadolinium-based paramagnetic agent injected manually.

Ten to fifteen minutes after the contrast agent was injected (2 ml of 0.5 M solution per 10 kg body weight), its accumulation was assessed in a left ventricular segment (corresponding to an ECG segment) with regard to its thickness and volume. The inversion time increment for each successive frame was 10 msec.

The images obtained in the inversion-recovery mode were scrutinized to localize postinfarction fibrosis and gauge its size. Those scars were visualized as hyperintense homogenous areas of delayed washout of the contrast agent, had clear outlines and a typical subendocardial localization.

Using CVI 42 (Circle) and CAAS MRV, the myocardial volume and LF mass were quantified semiautomatically from the short-axis slices of the left ventricle. LF contractility, the amount of scar tissue and the volume of viable myocardial tissue that was not accumulating the contrast agent were also evaluated.

Transmurality of the left ventricle was calculated as a ratio of the maximum wall thickness accumulating the paramagnetic agent to the myocardial thickness in a given segment; we also calculated the volume of the myocardium within the segment (%) accumulating the contrast agent.

Statistical data processing was done in MS Statistica 10.0. We performed dispersion, correlation, regression, discriminant and contingency analyses applying parametric and nonparametric tests. Contingency tables were analyzed using Pearson's χ^2; multiple comparisons were done using the F-test and the Newman–Keuls test. Qualitative parameters were compared by the Mann–Whitney U-test.

RESULTS

Our study recruited a total of 144 patients. The time between infarction and the study was 3 to 18 months (7.7 ± 3.3 months on average).

Clinical, demographic and angiographic characteristics of the patients are presented in Tables 1 and 2.

Table 3 features diagnostic tools used in the study and the number of hibernating segments detected by each tool.

On average, there were 2.72 ± 0.82 hibernating segments per patient. Cardiac MRI was able to detect significantly more segments with contractile dysfunction than stress echocardiography. Specifically, cardiac MRI was more successful in detecting hypo- and akinetic segments than stress echo. On average, the difference in the number of detected segments was 36 (56; 86) at 95% CI and $p < 0.01$.

Images obtained from cardiac MRI with delayed enhancement were analyzed and the transmurality index was calculated, as well as the volume of the myocardial segment accumulating the paramagnetic agent. Based on the transmurality index value, the patients were distributed into a few subgroups: 0.3–0.4, subendocardial accumulation of the paramagnetic agent (n = 25); 0.4–0.5, intramural accumulation (postinfarction fibrosis) (n = 107); over 0.5, transmural accumulation (n = 12). The myocardial volume that actively accumulated the contrast agent in a given segment indicated myocardial fibrosis. Its extent is expressed below as percentage: 20–30% in 54 patients; 30–40% in 52 patients; 40–50% in 23 patients, and over 50% in 12 patients.

We established a negative correlation between the thickness of myocardial scarring and the type of regional contractility dysfunction (Table 4). As the transmurality index increases, the number of hypokinetic segments decreases (r = –0.78; p = 0.0314) while the number of akinetic segments (r = –0.84; p = 0.0282) goes up. This needs to be accounted for when selecting a treatment strategy for such patients.

Interestingly, we did not reveal a correlation between the severity of myocardial fibrosis (the myocardial volume accumulating the contrast agent in a given segment) and global myocardial contractility (Table 5), which leads us to conclude that the severity of myocardial fibrosis has no effect on the global contractility of the myocardium.

Table 1. Clinical and demographic characteristics of patients

Parameter	n = 144	
	Abs.	%
Number of men	96	66.7
Number of women	48	33.3
Mean age	58.4 ± 9.8	
Mean interval post-myocardial infarction	7.7 ± 3.3	
FC 2 angina	52	36.1
FC 3 angina	60	41.7
FC 4 angina	32	22.2
Hypertensive disease	108	75
Type 2 diabetes mellitus	32	22.2
Heart failure (NYHA) FC I FC II FC III	 19 90 35	 13.2 62.5 24.3
Smoking	76	52.8
High cholesterol	98	68.1
History of ACVE	12	8.3
Arrhythmias and conduction disturbances	78	54.2

Note: FC — functional class, ACVE — acute cerebrovascular event.

Table 2. Angiographic characteristics of patients

Type of vascular disorder	n = 144	
	Abs.	%
Double vessel disease	48	33.3
Triple vessel disease	56	38.9
Bifurcation stenosis	28	19.4
Ostial stenosis	12	8.3
Arteries involved		
ADA stenosis	70	48.6
CA stenosis	32	22.2
RCA stenosis	42	29.2

Note: ADA — anterior descending artery; CA — circumflex artery; RCA — right coronary artery.

Table 3. The number of cardiac segments with impaired regional contractility

Contractile dysfunction	Number of segments		Number of discrepancies	*p*
	Cardiac MRI	Stress echocardiography		
Hypokinesis	224	186	38	0.002
Akinesis	175	154	21	0.024
Dyskinesis	6	8	2	0.322
Total	405	348	61	0.017

Note: $p < 0.05$ indicates statistical significance of differences.

Table 4. The correlation analysis of scar thickness and regional contractility

Contractile dysfunction	Transmurality index (scar thickness)			*p*
	0.3–0.4 (*n* = 25)	0.4–0.5 (*n* = 107)	over 0.5 (*n* = 12)	
Hypokinesis[1]	65	142	17	0.0314
Akinesis[2]	8	169	28	0.0282

Note: $r^1 = -0.78$; $r^2 = -0.84$.

Table 5. The correlation analysis of fibrosis extent (%) and global myocardial contractility parameters

Global myocardial contractility parameters	Volume of the myocardial segment accumulating the contrast agent (%)				*p*
	20–30 (*n* = 54)	30–40 (*n* = 52)	40–50 (*n* = 23)	over 50 (*n* = 12)	
EDV (ml)	149.2 ± 3.7	146.4 ± 3.2	150.8 ± 3.3	154.2 ± 3.8	0.632
ESV (ml)	71.4 ± 0.9	68.2 ± 0.7	68.8 ± 0.8	64.8 ± 0.8	0.824

Note: for EVD $r = 0.01$; for ESV $r = 0.01$.

DISCUSSION

The extent of myocardial fibrosis in patients with a history of myocardial infarction is an objective prognostic criterion in patients awaiting surgical revascularization that can predict its outcome [10].

The technique planned for surgical revascularization should account for post-infarction structural changes in the myocardium such as ventricular aneurisms or mural thrombi. These sequelae of infarction determine the necessity of surgery on the coronary arteries or the lack of thereof. There is no point in recovering the blood flow in the area of extensive unviable postinfarction fibrosis. But it is necessary to measure the volume of the myocardium that has a potential to restore its contractility after revascularization [13, 15].

Despite relative safety and high informative value of cardiac MRI performed to assess heart morphology, function and structural changes, this modality does not enjoy wide application and is considered an ancillary technique that helps to decide on the strategy of revascularization in difficult cases.

In the course of our study we analyzed the findings of stress echocardiography and MRI in a cohort of postinfarction patients with hibernating myocardium who had not received a timely revascularization surgery on the involved artery and developed multivessel coronary artery disease in the background of reduced global myocardial contractility.

The obtained data were analyzed in an attempt to find correlations between the depth and extent of postinfarction fibrosis and the types of contractility defects, as well as global contractility of the myocardium. These parameters are crucial and should be estimated prior to surgical revascularization as they help to optimize the treatment strategy in patients with hibernating myocardium.

CONCLUSIONS

Cardiac MRI is an effective and sensitive diagnostic technique in patients with hibernating myocardium that reliably detects more segments with contractile dysfunction that stress echocardiography. Delayed contrast enhancement allows assessment of scar thickness and is instrumental in visualizing subendocardial nontransmural myocardial lesions as small as 2–3 mm in size, which is an impossible ask for echocardiography. The established negative correlation between the thickness of myocardial scarring and the type of regional contractility dysfunction demonstrates that as the transmural index grows, the number of hypokinetic segments goes up, while the number of akinetic segments decreases. No correlation was found between the severity of myocardial fibrosis (the myocardial volume accumulating the contrast agent in a given segment) and global myocardial contractility (end-diastolic and end-systolic volumes).

References

1. Kwon DH, Hachamocitch R, Popovic ZB. et al. Survival in patients with severe ischemic cardiomyopathy undergoing revascularization versus medical therapy: association with end-systolic volume and viability. Circulation. 2012; (126): 3–8.
2. Ryzhkova DV, Kostina IS. Magnitno-rezonansnaja i pozitronno-jemissionnaja tomografija serdca v prognozirovanii obratimosti lokal'noj funkcii levogo zheludochka u bol'nyh s hronicheskimi okkljuzijami koronarnyh arterij. Rossijskij kardiologicheskij zhurnal. 2014; 2 (106): 72–8.
3. Camici PG, Kumak SP, Rimoldi OE. Stunning, Hybernating and Assesment of Myocardial Viability. Circulation. 2008; (117): 103–14.
4. Nagel E, Schuster A. Shortening without contraction: new insights into hibernating myocardium. J Am Coll Cardiol Img. 2010; (3): 731–33.

5. Alehin MN, Bozhev AM, Morozova JuA i dr. Stress-jehokardiografija s dobutaminom v diagnostike zhiznesposobnosti u bol'nyh s revaskuljarizaciej miokarda. Kardiologija. 2000; (12): 44–9.
6. Ling LH, Marvick TH, Flores DR, et al. Identification of therapeutic benefit from revascularization in patients with left ventricular systolic dysfunction: inducible ischemia versus hibernating myocardium. Circ Cardiovasc Imaging. 2013; (6): 363–72.
7. Hickman M, Chelliah R, Burden L, Senior R. Resting myocardial blood flow, coronary flow reserve, and contractile reserve in hibernating myocardium: implications for using resting myocardial contrast echocardiography vs. dobutamine echocardiography for the detection of hibernating myocardium. Eur J Echocardiogr. 2010; (119): 756–62.
8. Usov VJu, Arhangelskij VA, Fedorenko EV. Ocenka zhiznesposobnosti povrezhdennogo miokarda u kardiohirurgicheskih bol'nyh: sravnenie vozmozhnostej magnitno-rezonansnoj i jemissionnoj tomografii. Kompleksnye problemy serdechno – sosudistyh zabolevanij. 2014; (3): 124–33.
9. Arai AE. The cardiac magnetic resonance approach to assessing myocardial viability. J Nucl Cardiol. 2011; 18 (6): 1095–102.
10. Trufanov GE, Rud SD, Zheleznjak SE. MRT v diagnostike ishemicheskoj bolezni serdca: uchebnoe posobie. SPb.: ELBI-SPb; 2012. 63 s.
11. Kokov A. N., Masenko V. L., Semenov S. E., Barbarash O. L MRT serdca v ocenke postinfarktnyh izmenenij i ee rol' v opredelenii taktiki revaskuljarizacii miokarda. Kompleksnye problemy serdechno-sosudistyh zabolevanij. 2014; (3): 97–102.
12. Pennell DJ. Cardiovascular magnetic resonance. Circulation. 2010; (121): 692–705.
13. West AM, Kramer CM. Cardiovascular magnetic resonance imaging of myocardial infarction, viability and cardiomyopathies. Curr Probl Cardiol. 2010; (35): 176–220.
14. Windecker S, Kolh P, Alfonso F, et al. 2014 ESC/EACTS Guidelines on myocardial revascularization. Eur Heart J. 2014; (35): 2541–619.
15. Kramer CM, Schulz-Menger J, Bluemke DA. et al. Standardized cardiovascular magnetic resonance imaging (CMR) protocols, society for cardiovascular magnetic resonance: board of trustee's task force on standardized protocols. J Cardiovasc Magn Reson. 2013; 15 (1): 35.

Литература

1. Kwon DH, Hachamocitch R, Popovic ZB. et al. Survival in patients with severe ischemic cardiomyopathy undergoing revascularization versus medical therapy: association with end-systolic volume and viability. Circulation. 2012; (126): 3–8.
2. Рыжкова Д. В., Костина И. С. Магнитно-резонансная и позитронно-эмиссионная томография сердца в прогнозировании обратимости локальной функции левого желудочка у больных с хроническими окклюзиями коронарных артерий. Российский кардиологический журнал. 2014; 2 (106): 72–8.
3. Camici PG, Kumak SP, Rimoldi OE. Stunning, Hybernating and Assesment of Myocardial Viability. Circulation. 2008; (117): 103–14.
4. Nagel E, Schuster A. Shortening without contraction: new insights into hibernating myocardium. J Am Coll Cardiol Img. 2010; (3): 731–33.
5. Алехин М. Н., Божьев А. М., Морозова Ю. А. и др. Стресс-эхокардиография с добутамином в диагностике жизнеспособности у больных с реваскуляризацией миокарда. Кардиология. 2000; (12): 44–9.
6. Ling LH, Marvick TH, Flores DR, et al. Identification of therapeutic benefit from revascularization in patients with left ventricular systolic dysfunction: inducible ischemia versus hibernating myocardium. Circ Cardiovasc Imaging. 2013; (6): 363–72.
7. Hickman M, Chelliah R, Burden L, Senior R. Resting myocardial blood flow, coronary flow reserve, and contractile reserve in hibernating myocardium: implications for using resting myocardial contrast echocardiography vs. dobutamine echocardiography for the detection of hibernating myocardium. Eur J Echocardiogr. 2010; 11 (9): 756–62.
8. Усов В. Ю., Архангельский В. А., Федоренко Е. В. Оценка жизнеспособности поврежденного миокарда у кардиохирургических больных: сравнение возможностей магнитно-резонансной и эмиссионной томографии. Комплексные проблемы сердечно – сосудистых заболеваний. 2014; (3): 124–33.
9. Arai AE. The cardiac magnetic resonance approach to assessing myocardial viability. J Nucl Cardiol. 2011; 18 (6): 1095–102.
10. Труфанов Г. Е., Рудь С. Д., Железняк С. Е. МРТ в диагностике ишемической болезни сердца: учебное пособие. СПб.: ЭЛБИ-СПб; 2012. 63 с.
11. Коков А. Н., Масенко В. Л., Семенов С. Е., Барбараш О. Л МРТ сердца в оценке постинфарктных изменений и ее роль в определении тактики реваскуляризации миокарда. Комплексные проблемы сердечно-сосудистых заболеваний. 2014; (3): 97–102.
12. Pennell DJ. Cardiovascular magnetic resonance. Circulation. 2010; (121): 692–705.
13. West AM, Kramer CM. Cardiovascular magnetic resonance imaging of myocardial infarction, viability and cardiomyopathies. Curr Probl Cardiol. 2010; (35): 176–220.
14. Windecker S, Kolh P, Alfonso F, et al. 2014 ESC/EACTS Guidelines on myocardial revascularization. Eur Heart J. 2014; (35): 2541–619.
15. Kramer CM, Schulz-Menger J, Bluemke DA. et al. Standardized cardiovascular magnetic resonance imaging (CMR) protocols, society for cardiovascular magnetic resonance: board of trustee's task force on standardized protocols. J Cardiovasc Magn Reson. 2013; 15 (1): 35.

THE EFFICACY OF CRISPR-CAS9-MEDIATED INDUCTION OF THE CCR5DELTA32 MUTATION IN THE HUMAN EMBRYO

Kodyleva TA[1], Kirillova AO[1], Tyschik EA[1], Makarov VV[2], Khromov AV[2], Gushchin VA[2], Abubakirov AN[1], Rebrikov DV[1,3] ✉, Sukhikh GT[1]

[1] Kulakov National Medical Research Center for Obstetrics, Gynecology and Perinatology, Moscow

[2] Lomonosov Moscow State University, Moscow

[3] Pirogov Russian National Research Medical University, Moscow

The editing of the CCR5 gene in the CD4+ T cell genome is an effective way of preventing HIV-1 proliferation. Very similar strategies can be used to protect the fetus of an HIV-infected female showing a weak response to antiretroviral therapy. Inducing the "natural" CCR5delta32 mutation in a zygote may guard the fetus against HIV infection both in utero and at birth. In this study, we optimize the CRISPR-Cas9 system to induce a homozygous 32-nt deletion similar to the naturally occurring CCR5delta32 allele in the human zygote at the S-phase. Edits were done in the abnormal tripronuclear zygotes unsuitable for IVF. Sixteen tripronuclear zygotes in the S-phase obtained from WT CCR5 donors were injected with an original CRISPR-Cas9 system designed by the authors. Upon injection, the zygotes were transferred into the Blastocyst (COOK) embryo culture medium and cultured for 5 days in a CO_2 incubator until blastocysts were formed (approximately 250 cells). Eight zygotes that successfully developed into blastocysts were PCR-genotyped to analyze the efficacy of genome editing. Of 16 zygotes injected with CRISPR-Cas9, only 8 reached the blastocyst stage. PCR genotyping revealed the absence of the initial WT CCR5 variant in 5 of 8 blastocysts (100% CCR5delta32 homozygous). Two had about 3% and one about 20% of WT CCR5 mosaicism. This leads us to conclude that the efficacy of the proposed CRISPR-Cas9 system for the induction of the CCR5delta32 mutation in human embryos is very high producing more than 50% of completely modified embryos.

Keywords: CRISPR-Cas9, genome editing, human embryo, CCR5, CCR5delta32, HIV resistance

✉ **Correspondence should be addressed:** Denis V. Rebrikov
Ostrovityanova 1, Moscow, 117997; drebrikov@gmail.com

Received: 26.09.2018 **Accepted:** 09.10.2018

DOI: 10.24075/brsmu.2018.052

ЭФФЕКТИВНОСТЬ СОЗДАНИЯ ДЕЛЕЦИИ CCR5DELTA32 МЕТОДОМ CRISPR-CAS9 В ЭМБРИОНАХ ЧЕЛОВЕКА

Т. А. Кодылева[1], А. О. Кириллова[1], Е. А. Тыщик[1], В. В. Макаров[2], А. В. Хромов[2], В. А. Гущин[2], А. Н. Абубакиров[1], Д. В. Ребриков[1,3] ✉, Г. Т. Сухих[1]

[1] Национальный медицинский исследовательский центр акушерства, гинекологии и перинатологии имени В. И. Кулакова, Москва

[2] Московский государственный университет имени М. В. Ломоносова, Москва

[3] Российский национальный исследовательский медицинский университет имени Н. И. Пирогова, Москва

Изменение гена CCR5 путем редактирования генома CD4+-Т-клеток является одним из способов предотвращения распространения ВИЧ-1-инфекции. Однако похожая стратегия защиты от ВИЧ может быть использована и для защиты плода ВИЧ-инфицированных женщин со слабым ответом на антиретровирусную терапию. Создание «естественного» аллеля CCR5delta32 на стадии зиготы может защитить плод от ВИЧ-инфекции во время внутриутробного развития и родов. Целью данного исследования была оптимизация системы CRISPR-Cas9 под создание гомозиготной 32-нуклеотидной делеции (аналогичной природному варианту CCR5delta32) в S-фазе зиготы человека. Для редактирования генома были использованы зиготы с аномальным числом пронуклеусов (более двух), непригодные для ЭКО. 16 аномальных зигот от доноров с WT CCR5 были инъецированы разработанной системой CRISPR-Cas9 в S-фазе. После инъекции зиготы помещали в культуральную среду Blastocyst (COOK) и культивировали в течение 5 дней в CO_2-инкубаторе до стадии бластоцисты (приблизительно 250 клеток). Для анализа эффективности редактирования генома 8 успешно развивавшихся эмбрионов были генотипированы методом полимеразной цепной реакции (ПЦР). Из 16 зигот, инъецированных системой CRISPR-Cas9, лишь 8 достигли стадии бластоцисты. ПЦР-генотипирование показало отсутствие исходного варианта WT CCR5 в 5 из 8 бластоцист (100% гомозиготы по CCR5delta32). Два эмбриона продемонстрировали около 3% и один — около 20% мозаицизма по WT CCR5. Таким образом, эффективность разработанной CRISPR-Cas9 системы для создания аллеля CCR5delta32 в эмбрионах человека довольно высока: более половины эмбрионов оказываются полностью модифицированными.

Ключевые слова: CRISPR-Cas9, редактирование генома, эмбрион человека, CCR5, CCR5delta32, устойчивость к ВИЧ

✉ **Для корреспонденции:** Денис Владимирович Ребриков
ул. Островитянова, д. 1, г. Москва, 117997; drebrikov@gmail.com

Статья получена: 26.09.2018 **Статья принята к печати:** 09.10.2018

DOI: 10.24075/vrgmu.2018.052

In the past few years the rapid evolution of CRISPR-based technologies has expanded their application scope and paved their way to preclinical trails. The successful editing of the CD4+ T cell genome by either knocking out or modifying the gene encoding the chemokine receptor CCR5 has raised new hope for the true functional cure of HIV-1 infection [1–5].

Apart from the edits in the CCR5-encoding gene of T cells that block the development of AIDS in HIV-infected patients, genome editing techniques can be used to induce the CCR5delta32 mutation in the egg as part of *in vitro* fertilization (IVF) procedures to protect the fetus of an HIV-infected female showing a weak response to antiretroviral therapy [6, 7].

Injecting CRISPR-Cas9 components into the zygote will entail genome modifications in almost all cells of the organism, which has already been demonstrated for a few deleterious hereditary mutations [8–12]. Importantly, the edited genome will be passed on to subsequent generations.

A modification identical to the naturally occurring mutant allele CCR5delta32 can be expected to protect the fetus from HIV infection in utero and at childbirth. Another beneficial effect of this edit is a potential lifelong immunity to HIV.

In this study we optimize the CRISPR-Cas9 system to induce a homozygous 32-nt deletion similar to the mutant CCR5delta32 allele in the human zygote during the S-phase. Editing was performed on the abnormal tripronuclear zygotes unsuitable for IVF.

METHODS

Ethical approval and consent to participate

The study protocol was reviewed and approved by the Ethics Committee of Kulakov National Medical Research Center for Obstetrics, Gynecology and Perinatology (Approval Reference: No.2017/45). The study complied with the international guidelines for human embryo research. Written informed consent was obtained from each couple before they could donate tripronuclear zygotes. Only homozygous wild-type CCR5 pairs were included in the study.

Zygote collection procedures

Tripronuclear zygotes were donated by patients undergoing IVF treatment from September 2017 through April 2018 at Kulakov National Medical Research Center for Obstetrics, Gynecology and Perinatology (Moscow, Russia). In total, 21 tripronuclear zygotes were obtained from 11 couples, of which 16 were injected with CRISPR-Cas9 and 5 were used as a control.

Design, synthesis and *in vitro* activity of gRNAs

Guide RNAs (gRNAs) were designed to match the target locus of wild-type (WT) CCR5 and CCR5delta32 alleles from the National Center for Biotechnology Information database (USA) were used to design guide RNAs (gRNAs). A 200 bp-long DNA sequence was picked for further editing in which the sites for base pairing between gRNA and target DNA were selected adjacent to the PAM sequence (Fig. 1). In total, 9 gRNAs were designed to target the sites convenient for the subsequent homologous repair of double-stranded breaks (Table 1).

The transcription template was generated by pairwise annealing of primers (Evrogen; Russia) and PCR-amplified by Taq polymerase (Evrogen; Russia). Guide RNA was synthesized from the template using T7 RNA polymerase (SybEnzyme; Russia).

The activity of the resulting gRNAs was studied using a test plasmid coding for the wild-type CCR5 sequence. *In vitro*

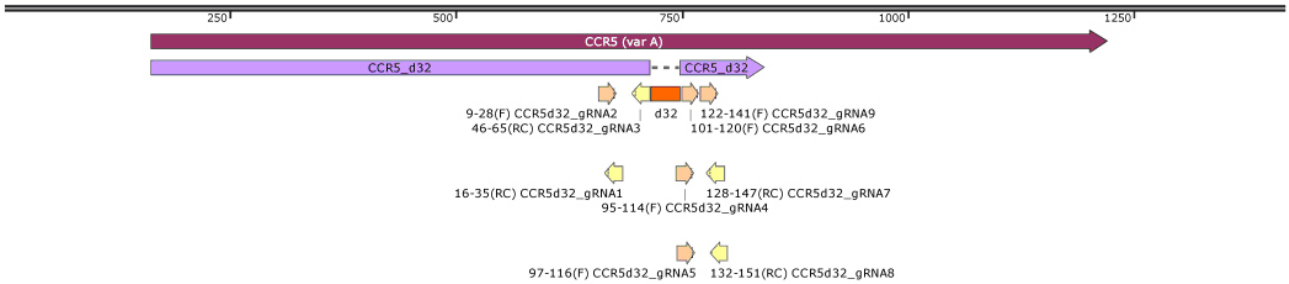

Fig. 1. gRNAs layout inside the human CCR5 gene

Table 1. Oligos for gRNA and DNA patches

CCR5_BamHI_F	GGATCCTAGGTACCTGGCTGTCGTCCATG
CCR5_XbaI_R	TCTAGAATGCAGCAGTGCGTCATCC
CCR5d32_gRNA1	TAATACGACTCACTATAGGAAGACCTTCTTTTTGAGATCGTTTTAGAGCTAGAAATAGCAAG
CCR5d32_gRNA2	TAATACGACTCACTATAGGTTTACCAGATCTCAAAAAGAGTTTTAGAGCTAGAAATAGCAAG
CCR5d32_gRNA3	TAATACGACTCACTATAGGGTATGGAAAATGAGAGCTGCGTTTTAGAGCTAGAAATAGCAAG
CCR5d32_gRNA4	TAATACGACTCACTATAGGGACATTAAAGATAGTCATCTGTTTTAGAGCTAGAAATAGCAAG
CCR5d32_gRNA5	TAATACGACTCACTATAGGACATTAAAGATAGTCATCTTGTTTTAGAGCTAGAAATAGCAAG
CCR5d32_gRNA6	TAATACGACTCACTATAGGAAAGATAGTCATCTTGGGGCGTTTTAGAGCTAGAAATAGCAAG
CCR5d32_gRNA7	TAATACGACTCACTATAGGTGACCATGACAAGCAGCGGCGTTTTAGAGCTAGAAATAGCAAG
CCR5d32_gRNA8	TAATACGACTCACTATAGGCAGATGACCATGACAAGCAGGTTTTAGAGCTAGAAATAGCAAG
CCR5d32_gRNA9	TAATACGACTCACTATAGGGGTCCTGCCGCTGCTTGTCAGTTTTAGAGCTAGAAATAGCAAG
CCR5_big_leftpart_F	CAACTCTTGACAGGGCTCTATTTTATAGGC
CCR5_big_leftpart_R	GGACCAGCCCCAAGATGACTATCTTTAATGTATGGAAAATGAGAGCTGCAGGTGTAA
CCR5_big_rightpart_R	GCATAGCTTGGTCCAACCTGTTAG
CCR5_gib_rightpart_F	TTAAAGATAGTCATCTTGGGGCTGGTCC
CCR5_small_F	GTGATCACTTGGGTGGTGGC
CCR5_small_R	TTAGGATTCCCGAGTAGCAGATGAC
CCR5_small_hairpin_R	GCTAAGCGGGTGGGACTTCCTAGTCCCACCCGCTTAGGATTCCCGAGTAGCAGATGAC

DNA cleavage by the complex formed by RNA and EnGen® Cas9 NLS (New England Biolabs; USA) was performed as recommended by the manufacturer of the enzyme. The best results were shown by gRNAs #1 and #5, which were subsequently used for *in vivo* experiments mixed at a 1:1 ratio.

DNA patch

A standard overlap extension PCR technique was used to obtain a DNA patch. After the construct was assembled, a shorter single-stranded DNA product (perfect for promoting recombination over non-homologous end joining NHEJ) was amplified by asymmetric PCR with one of the primers (index F) used in excess. The resulting fragment reads as follows: GTGATCACTTGGGTGGTGGCTGTGTTTGCGTCTCT CCCAGGAATCATCTTTACCAGATCTCAAAAAGAAGGTCTTC ATTACACCTGCAGCTCTCATTTTCCATACATTAAAGATAGTCA TCTTGGGGCTGGTCCTGCCGCTGCTTGTCATGGTCATCTG CTACTCGGGAATCCTAA

Preparation of RNP complexes

The following components were used to prepare RNP complexes: Cas9 (20 μM), a mix of gRNA#1 and gRNA#5 at a ratio of 1:1 (30 ng/μl), ssDNA (100 ng/μl), a dilution buffer (0.25 mM EDTA/10 mM TrisHCl, pH 7.4).

The injectable solution was prepared by mixing 0.5 μl of Cas9 (20 μM) with 4.5 μl of the dilution buffer. Then, 1.56 μl of Cas9 (2 μM), 0.6 μl of the gRNA mix (30 ng/μl) and 2.5 μl ssDNA (100 ng/μl) were combined with 5.34 μl of the dilution buffer. The mix was incubated at 37 °C for 10 min and immediately used for injecting.

Injection of CRISPR-Cas9

The CRISPR-Cas9 complex was injected into tripronuclear zygotes in the S-phase according to the standard Intracytoplasmic Sperm Injection (ICSI) protocol [13]. The injection volume was 1 nl. After the injection, the zygotes were washed twice in the Sydney IVF Cleavage Medium (COOK Medical LLC; USA), then moved into the Sydney IVF Blastocyst Medium (COOK Medical LLC; USA) and incubated in the EmbryoPlan CO_2 Incubator (West trade LLC; Russia) under standard conditions for 5 days until blastocysts were formed (about 250 cells). Upon incubation each blastocyst was transferred into 12 μl of the dilution buffer and immediately analyzed by PCR.

PCR genotyping and data analysis

Genotyping by double-tube PCR was performed in the DTprime Real-Time PCR Cycler (DNA-Technology, Russia) as described in [14], but to exclude the gRNA region, another universal primer CCR5_check2_R was used with the following sequence: TCATTTCGACACCGAAGCAGA. PCR data were analyzed in the DTprime Real-Time PCR Cycler Software v.7.7 (DNA-Technology; Russia).

RESULTS

Of 16 zygotes injected with the CRISPR-Cas9 complex only 8 reached the blastocyst stage, whereas of 5 control zygotes injected with the dilution buffer 3 developed into a blastocyst. This is the standard rate of blastocyst formation for abnormal zygotes, meaning that the injection did not increase the risk of aborted development. PCR genotyping revealed the absence of the initial WT CCR5 variant in 5 of 8 blastocysts, so those embryos were 100% CCR5delta32- homozygous. Two embryos demonstrated about 3% and one about 20% of WT CCR5 mosaicism (Fig. 2). Cp values for each embryo are presented in Table 2. For each negative control sample (dilution buffer) each PCR was performed in two replicates. The reaction yielded no PCR products.

DISCUSSION

CRISPR-Cas9-mediated editing of the human zygote is an effective method for intracellular DNA modification capable of eliminating nearly 100% of the initial sequence in more than half of embryos

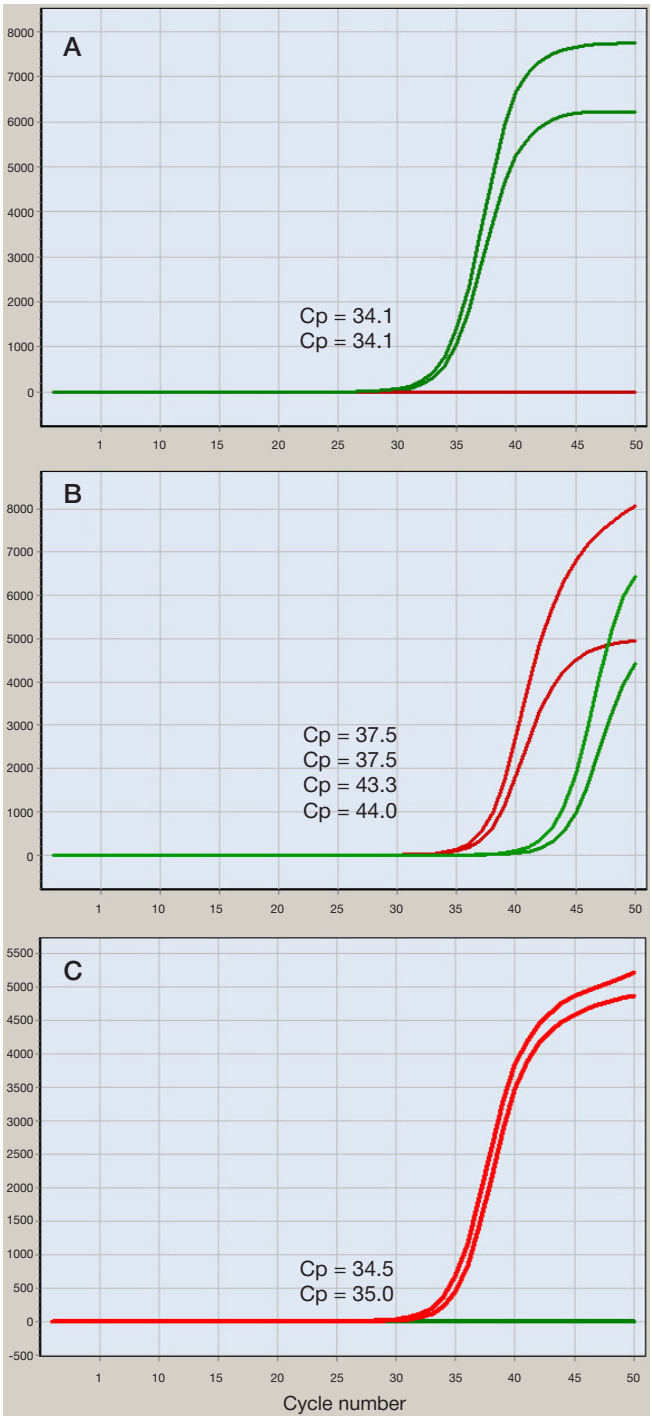

Fig. 2. Examples of real-time PCR curves for different genotypes: **A** — two control embryos, **B** — two mosaic embryos with about 3% of WT CCR5, **C** — two CCR5delta32 homozygous embryos

Table 2. Real-time PCR Cp values for each embryo

Embryo №	Cp WT	Cp del
Control 1	34.1	–
Control 2	34.1	–
Control 3	36.0	–
Exp 1	–	38.1
Exp 2	40.8	38.1
Exp 3		37.8
Exp 4	44.0	37.5
Exp 5	–	37.3
Exp 6	43.3	37.5
Exp 7	–	34.5
Exp 8	–	35.0

Note: – no PCR products.

[9, 10, 12, 15]. Our results are well correlated with those yielded by other GE-system models demonstrating very high efficacy.

In the past few years we have witnessed the rapid evolution of GE-systems. However, the off-target activity of such GE-systems still remains a challenge. Genome editing techniques can be introduced into clinical practice only if they have been proved to be safe for the patient.

CONCLUSIONS

This is the first study demonstrating the efficacy of CRISPR-Cas9-mediated induction of the CCR5delta32 mutation in the human embryo. Its efficacy is very high producing more than 50% of completely modified embryos.

References

1. Yu S, Yao Y, Xiao H, Li J, Liu Q, Yang Y, et al. Simultaneous Knockout of CXCR4 and CCR5 Genes in CD4+ T Cells via CRISPR-Cas9 Confers Resistance to Both X4- and R5-Tropic Human Immunodeficiency Virus Type 1 Infection. Hum Gene Ther. 2018 Jan; 29 (1): 51–67. DOI: 10.1089/hum.2017.032.
2. Xu L, Yang H, Gao Y, Chen Z, Xie L, et al. CRISPR-Cas9-Mediated CCR5 Ablation in Human Hematopoietic Stem/Progenitor Cells Confers HIV-1 Resistance In Vivo. Mol Ther. 2017 Aug 2; 25 (8): 1782–9. DOI: 10.1016/j.ymthe.2017.04.027.
3. Haworth KG, Peterson CW, Kiem HP. CCR5-edited gene therapies for HIV cure: Closing the door to viral entry. Cytotherapy. 2017 Nov; 19 (11): 1325–38. DOI: 10.1016/j.jcyt.2017.05.013.
4. Liu Z, Chen S, Jin X, Wang Q, Yang K, Li C, et al. Genome editing of the HIV co-receptors CCR5 and CXCR4 by CRISPR-Cas9 protects CD4+ T cells from HIV-1 infection. Cell Biosci. 2017 Sep 9; (7): 47. DOI: 10.1186/s13578-017-0174-2.
5. Nerys-Junior A, Braga-Dias LP, Pezzuto P, Cotta-de-Almeida V, Tanuri A. Comparison of the editing patterns and editing efficiencies of TALEN and CRISPR-Cas9 when targeting the human CCR5 gene. Genet Mol Biol. 2018 Jan-Mar; 41 (1): 167–79. DOI: 10.1590/1678-4685-GMB-2017-0065.
6. Makokha EP, Songok EM, Orago AA, Koech DK, Chemtai AK, Kobayashi N, et al. Maternal immune responses and risk of infant infection with HIV-1 after a short course Zidovudine in a cohort of HIV-1 infected pregnant women in rural Kenya. East Afr Med J. 2002 Nov; 79 (11): 567–73.
7. French CE, Tookey PA, Cortina-Borja M, de Ruiter A, Townsend CL, Thorne C. Influence of short-course antenatal antiretroviral therapy on viral load and mother-to-child transmission in subsequent pregnancies among HIV-infected women. Antivir Ther. 2013; 18 (2): 183–92. DOI: 10.3851/IMP2327.
8. Liang P, Xu Y, Zhang X, Ding C, Huang R, Zhang Z, et al. CRISPR-Cas9-mediated gene editing in human tripronuclear zygotes. Protein Cell. 2015 May; 6 (5): 363–72. DOI: 10.1007/s13238-015-0153-5. Epub 2015 Apr 18.
9. Tang L, Zeng Y, Du H, Gong M, Peng J, Zhang B, et al. CRISPR-Cas9-mediated gene editing in human zygotes using Cas9 protein. Mol Genet Genomics. 2017 Jun; 292 (3): 525–33. DOI: 10.1007/s00438-017-1299-z.
10. Ma H, Marti-Gutierrez N, Park SW, Wu J, Lee Y, Suzuki K, et al. Correction of a pathogenic gene mutation in human embryos. Nature. 2017 Aug 24; 548 (7668): 413–19. DOI: 10.1038/nature23305.
11. Fogarty NME, McCarthy A, Snijders KE, Powell BE, Kubikova N, Blakeley P, et al. Genome editing reveals a role for OCT4 in human embryogenesis. Nature. 2017 Oct 5; 550 (7674): 67–73. DOI: 10.1038/nature24033.
12. Liang P, Ding C, Sun H, Xie X, Xu Y, Zhang X, et al. Correction of β-thalassemia mutant by base editor in human embryos. Protein Cell. 2017 Nov; 8 (11): 811–22. DOI: 10.1007/s13238-017-0475-6.
13. Joris H, Nagy Z, Van de Velde H, De Vos A, Van Steirteghem A. Intracytoplasmic sperm injection: laboratory set-up and injection procedure. Hum Reprod. 1998 Apr; 13 Suppl 1: 76–86.
14. Kofiadi IA, Rebrikov DV, Trofimov DY, Alexeev LP, Khaitov RM. Allelic distribution of the CCR5, CCR2, and SDF1 gene polymorphisms associated with HIV-1/AIDS resistance in Russian populations. Dokl Biol Sci. 2007 Jul-Aug; (415): 320–3.
15. Kang X, He W, Huang Y, Yu Q, Chen Y, Gao X, Sun X, Fan Y. Introducing precise genetic modifications into human 3PN embryos by CRISPR/Cas-mediated genome editing. J Assist Reprod Genet. 2016 May; 33 (5): 581–588. DOI: 10.1007/s10815-016-0710-8.

Литература

1. Yu S, Yao Y, Xiao H, Li J, Liu Q, Yang Y, et al. Simultaneous Knockout of CXCR4 and CCR5 Genes in CD4+ T Cells via CRISPR-Cas9 Confers Resistance to Both X4- and R5-Tropic Human Immunodeficiency Virus Type 1 Infection. Hum Gene Ther.

2018 Jan; 29 (1): 51–67. DOI: 10.1089/hum.2017.032.
2. Xu L, Yang H, Gao Y, Chen Z, Xie L, et al. CRISPR-Cas9-Mediated CCR5 Ablation in Human Hematopoietic Stem/Progenitor Cells Confers HIV-1 Resistance In Vivo. Mol Ther. 2017 Aug 2; 25 (8): 1782–9. DOI: 10.1016/j.ymthe.2017.04.027.
3. Haworth KG, Peterson CW, Kiem HP. CCR5-edited gene therapies for HIV cure: Closing the door to viral entry. Cytotherapy. 2017 Nov; 19 (11): 1325–38. DOI: 10.1016/j.jcyt.2017.05.013.
4. Liu Z, Chen S, Jin X, Wang Q, Yang K, Li C, et al. Genome editing of the HIV co-receptors CCR5 and CXCR4 by CRISPR-Cas9 protects CD4+ T cells from HIV-1 infection. Cell Biosci. 2017 Sep 9; (7): 47. DOI: 10.1186/s13578-017-0174-2.
5. Nerys-Junior A, Braga-Dias LP, Pezzuto P, Cotta-de-Almeida V, Tanuri A. Comparison of the editing patterns and editing efficiencies of TALEN and CRISPR-Cas9 when targeting the human CCR5 gene. Genet Mol Biol. 2018 Jan-Mar; 41 (1): 167–79. DOI: 10.1590/1678-4685-GMB-2017-0065.
6. Makokha EP, Songok EM, Orago AA, Koech DK, Chemtai AK, Kobayashi N, et al. Maternal immune responses and risk of infant infection with HIV-1 after a short course Zidovudine in a cohort of HIV-1 infected pregnant women in rural Kenya. East Afr Med J. 2002 Nov; 79 (11): 567–73.
7. French CE, Tookey PA, Cortina-Borja M, de Ruiter A, Townsend CL, Thorne C. Influence of short-course antenatal antiretroviral therapy on viral load and mother-to-child transmission in subsequent pregnancies among HIV-infected women. Antivir Ther. 2013; 18 (2): 183–92. DOI: 10.3851/IMP2327.
8. Liang P, Xu Y, Zhang X, Ding C, Huang R, Zhang Z, et al. CRISPR-Cas9-mediated gene editing in human tripronuclear zygotes. Protein Cell. 2015 May; 6 (5): 363–72. DOI: 10.1007/s13238-015-0153-5. Epub 2015 Apr 18.
9. Tang L, Zeng Y, Du H, Gong M, Peng J, Zhang B, et al. CRISPR-Cas9-mediated gene editing in human zygotes using Cas9 protein. Mol Genet Genomics. 2017 Jun; 292 (3): 525–33. DOI: 10.1007/s00438-017-1299-z.
10. Ma H, Marti-Gutierrez N, Park SW, Wu J, Lee Y, Suzuki K, et al. Correction of a pathogenic gene mutation in human embryos. Nature. 2017 Aug 24; 548 (7668): 413–19. DOI: 10.1038/nature23305.
11. Fogarty NME, McCarthy A, Snijders KE, Powell BE, Kubikova N, Blakeley P, et al. Genome editing reveals a role for OCT4 in human embryogenesis. Nature. 2017 Oct 5; 550 (7674): 67–73. DOI: 10.1038/nature24033.
12. Liang P, Ding C, Sun H, Xie X, Xu Y, Zhang X, et al. Correction of β-thalassemia mutant by base editor in human embryos. Protein Cell. 2017 Nov; 8 (11): 811–22. DOI: 10.1007/s13238-017-0475-6.
13. Joris H, Nagy Z, Van de Velde H, De Vos A, Van Steirteghem A. Intracytoplasmic sperm injection: laboratory set-up and injection procedure. Hum Reprod. 1998 Apr; 13 Suppl 1: 76–86.
14. Kofiadi IA, Rebrikov DV, Trofimov DY, Alexeev LP, Khaitov RM. Allelic distribution of the CCR5, CCR2, and SDF1 gene polymorphisms associated with HIV-1/AIDS resistance in Russian populations. Dokl Biol Sci. 2007 Jul-Aug; (415): 320–3.
15. Kang X, He W, Huang Y, Yu Q, Chen Y, Gao X, Sun X, Fan Y. Introducing precise genetic modifications into human 3PN embryos by CRISPR/Cas-mediated genome editing. J Assist Reprod Genet. 2016 May; 33 (5): 581–588. DOI: 10.1007/s10815-016-0710-8.

LEVELS OF CELL-FREE DNA AND DNASE I ACTIVITY IN COMPLICATED AND NORMAL PREGNANCIES

Avetisova KG[1] ✉, Kostyuk SV[2], Kostyuk EV[2], Ershova ES[2], Shmarina GV[2], Veiko NN[2], Spiridonov DS[1], Klimenko PA[1], Kurtser MA[1]

[1] Department of Obstetrics and Gynecology, Faculty of Pediatrics, Pirogov Russian National Research Medical University, Moscow

[2] Laboratory of Molecular Biology, Research Centre for Medical Genetics, Moscow

Placental pathology is accompanied by the activation of apoptosis in the trophoblast and the subsequent increase in the concentrations of microvesicles containing placental (or fetal) DNA accumulating in the maternal blood. Fragments of fetal DNA stimulate the release of nuclear and/or mitochondrial DNA fragments by neutrophils. Therefore, one can expect that complicated pregnancies will be characterized by the dramatic elevation of total cell-free DNA (cfDNA) levels in maternal plasma. The aim of this work was to study the dynamics of plasma cfDNA concentrations and the activity of DNase I, an enzyme involved in the elimination of cfDNA from the bloodstream, in nonpregnant and pregnant women. Our study recruited 40 healthy nonpregnant women, 40 women with uncomplicated pregnancies and 35 women with the intrauterine growth restriction (IUGR) of the fetus. We did not observe the elevation of the total cfDNA concentrations in the patients with complicated pregnancies. Moreover, cfDNA concentrations in their plasma were even lower (though this difference was statistically insignificant) than in healthy pregnant and nonpregnant women. The median values of cfDNA concentrations in the group of healthy nonpregnant women were 75.5 ng/ml; in the group of healthy pregnant women, 78.0 ng/ml; and in the patients with IUGR, 42.1 ng/ml. At the same time, we observed a significant increase in DNase I activity in the plasma of women with IUGR. The median DNase I activity in the groups of healthy pregnant and nonpregnant women was 3.0 and 3.4 IU/ml, respectively. In patients with different grades IUGR of the fetus this parameter was as high as 6.3 IU/ml ($p < 0.001$). Increased DNase I activity in the plasma of women with complicated pregnancies indirectly suggests a transient elevation of circulating cfDNA levels. Our study shows that the high level of activity exhibited by the cfDNA elimination system impedes the analysis of cfDNA concentrations in complicated pregnancies and skews its results. However, if cfDNA, DNase I activity and the cfDNA/DNase I ratio were all taken into account, it could be possible to develop a tool for the monitoring of cell death in the mother throughout the entire pregnancy.

Keywords: cfDNA, DNase I, pregnancy, preeclampsia, IUGR

✉ **Correspondence should be addressed:** Kristina G. Avetisova
Sevastopolsky prospect, 24a, Moscow, 117209; c.avetisova2016@yandex.ru

Received: 15.03.18 **Accepted:** 27.06.18

DOI: 10.24075/brsmu.2018.041

УРОВЕНЬ ВНЕКЛЕТОЧНОЙ ДНК И АКТИВНОСТЬ ДНКАЗЫ I ПРИ НОРМАЛЬНОЙ И ОСЛОЖНЕННОЙ БЕРЕМЕННОСТИ

К. Г. Аветисова[1] ✉, С. В. Костюк[2], Э. В. Костюк[2], Е. С. Ершова[2], Г. В. Шмарина[2], Н. Н. Вейко[2], Д. С. Спиридонов[1], П. А. Клименко[1], М. А. Курцер[1]

[1] Кафедра акушерства и гинекологии, педиатрический факультет, Российский национальный исследовательский медицинский университет имени Н. И. Пирогова, Москва

[2] Лаборатория молекулярной биологии, Медико-генетический научный центр, Москва

При патологии плаценты происходит активация апоптотических процессов в трофобласте, что сопровождается повышением в кровотоке матери концентрации микровезикул, содержащих плацентарную ДНК (или ДНК плода). Фрагменты ДНК плода стимулируют выброс нейтрофилами участков ядерной и/или митохондриальной ДНК. Таким образом, при осложненной беременности следует ожидать значительного увеличения общей концентрации внутриклеточной ДНК (вкДНК) в плазме матери. Целью работы было исследование совместных изменений концентрации вкДНК и активности одного из компонентов системы элиминации вкДНК из кровотока — фермента ДНКазы I в плазме небеременных и беременных женщин. В исследовании принимали участие 40 здоровых небеременных женщин, 40 беременных женщин с нормально протекающей беременностью и 35 пациенток с внутриутробной задержкой роста плода (ВЗРП). Мы не обнаружили повышения уровня суммарной вкДНК у пациенток с осложненной беременностью. Более того, концентрация вкДНК в плазме пациенток была даже ниже (статистически незначимо), чем соответствующие показатели в плазме здоровых беременных и небеременных женщин. Так, значение медианы концентрации вкДНК в группе здоровых небеременных женщин составило 75,5 нг/мл, в группе здоровых беременных женщин этот показатель достигал 78,0 нг/мл, у пациенток с ВЗРП он был равен 42,1 нг/мл. В то же время мы обнаружили достоверное повышение активности ДНКазы I в плазме женщин с ВЗРП. Медиана активности ДНКазы в группах здоровых беременных и небеременных женщин составила соответственно 3,0 и 3,4 IU/мл. У пациенток с ВЗРП различной степени тяжести этот показатель достигал 6,3 IU/мл ($p < 0,001$). Повышенная активность ДНКазы I в плазме женщин с патологией беременности косвенно свидетельствует о транзиторном повышении у них уровня циркулирующей вкДНК. Полученные результаты показывают, что высокий уровень активности системы элиминации вкДНК затрудняет и искажает результаты анализа концентрации вкДНК при беременности, особенно при патологии. Однако если учитывать три показателя — концентрацию вкДНК, активность ДНКазы I и отношение вкДНК/ДНКаза I, то в перспективе можно разработать систему мониторинга уровня гибели клеток в организме матери на протяжении всего периода беременности.

Ключевые слова: вкДНК, ДНКаза I, беременность, преэклампсия, ВЗРП

✉ **Для корреспонденции:** Кристина Григорьевна Аветисова
Севастопольский проспект, д. 24а, г. Москва, 117209; c.avetisova2016@yandex.ru

Статья получена: 15.03.18 **Статья принята к печати:** 27.06.18

DOI: 10.24075/vrgmu.2018.041

The presence of DNA in human blood plasma and serum was discovered as early as 1948, a few years before the structure of this molecule was figured out [1]. This type of DNA went by the name of circulating or cell-free DNA (cfDNA) [2]. In 1997 fetal cfDNA was detected in the blood plasma of a pregnant woman [3]. The discovery of fetal cfDNA in maternal plasma and serum inspired the development of noninvasive methods of prenatal screening for genetic abnormalities in the fetus [4]. Today, it has become possible to sequence the entire fetal genome from cfDNA circulating in the maternal blood [5].

Cell-free DNA analysis is not solely used to screen for genetic defects in the fetus; among its other applications is monitoring for pregnancy complications, such as preeclampsia and miscarriage [6–8]. Here, the idea is not to look for an individual mutant gene but to measure total cfDNA concentrations in maternal blood or the concentration of fetal cfDNA alone. The primary source of fetal cfDNA in maternal blood is thought to be necrosis and/or apoptosis of placental cells [9].

It is important to note that while taking these measurements, researchers tend to ignore the regulatory processes causing cfDNA concentrations to decline. Growing cfDNA levels associated with increased cell death signal the cfDNA elimination system to activate and clear excess cfDNA from the bloodstream. Dropping cfDNA concentrations are observed in patients with chronic conditions accompanied by increased cell death, such as cardiovascular disorders [10] and occupational exposure to radiation [11].

Previously, we investigated the dynamics of cfDNA concentrations and the activity of DNase I, an enzyme involved in the elimination of cfDNA from the bloodstream, in the plasma of nonpregnant women and women with normal and complicated pregnancies [12] Our findings were not consistent with the literature. Firstly, cfDNA levels in the women with normal and complicated pregnancies did not exceed the values demonstrated by the controls (according to the literature, in both healthy and complicated pregnancies cfDNA concentrations are expected to surge [13]). Secondly, the level of DNase I activity was twice as high in the participants with complicated pregnancies. This phenomenon had not been described previously by other researchers. Considering the obtained results, we decided to conduct another research study with a special focus on the clinical characteristics of healthy nonpregnant and pregnant women.

METHODS

The study recruited 1175 women aged 22 to 40 (the mean age was 32 ± 4 years) residing in Moscow, Russia, and coming from the same social stratum. Inclusion criteria varied depending on the group: group 1 included healthy nonpregnant female volunteers (medical students and clinical residents; n = 40); group 2 consisted of healthy women > 37 weeks of uncomplicated pregnancy (n = 40) who had previously given birth to healthy children with no signs of hypoxia or underweight; group 3 consisted of women with complicated pregnancies, miscarriages, placental insufficiency, intrauterine growth restriction of the fetus (IUGR), chronic hypoxia of the fetus, or thin uterine scars (> 30 weeks of gestation, n = 35). Exclusion criteria were not applied. Blood samples of healthy nonpregnant women were collected between days 10 and 15 of their menstrual cycles. This study was part of the PhD dissertation and was approved by the Ethics Committee of Pirogov Russian National Medical Research University (Protocol 159 dated November 21, 2016). The recruited women gave informed consent to participate.

Fetal development

Fetal development was evaluated by ultrasonography: a few biometric measurements were taken, including the biparietal diameter, thoracic and abdominal circumferences, and femur length. If the measured sizes were showing a 2-week lag behind the population average [14], the patient was diagnosed with grade I IUGR; a 2–4-week lag, grade II IUGR; more than a 4-week lag, grade III IUGR. The final diagnosis was established postpartum based on the newborn's weight. The reference interval lay between the 75th and 25th percentiles; grade I IUGR corresponded to the 2th–10th percentiles; grade II, to the 10th–3th percentiles; grade III was below the 3th percentile [15]. We also calculated the weight-to-height ratio: the value of >60 suggested normal growth; grade I IUGR corresponded to the range from 55 to 60; grade II IUGR, to 50–55; grade III IUGR was below 50. Fetal cardiac function was evaluated by cardiotocography (CTG) and Doppler ultrasonography of the uterine, umbilical and fetal blood flows. Ultrasonography was performed on Voluson 530 MT (Kretztechnik; Austria) and Voluson E8 (General Electric; USA) equipped with three different transducers: RIC 5–9 D (4–9 MHz), C1–5D (2–5 MHz), and RAB 4–8 D (2–8 MHz). CTG was done using the GE Corometrics (250CX) fetal monitor (USA).

Special assays

Fragments of circulating cfDNA were isolated from 1 ml of heparinized blood plasma samples by phenol extraction. Blood cells were pelleted by centrifugation at 400 g for 10 min. The obtained plasma was mixed with 10% sodium lauroyl sarcosinate, 0.2 M EDTA and a standard 0.075 mg/ml RNase solution (Sigma; USA) and incubated for 45 min. Then it was treated with a standard 0.2 mg/ml proteinase K solution (Promega; USA) and left to sit for 24 h at 37 °C. Following 2 cycles of washing with a saturated phenol solution, the DNA fragments were pelleted by adding two volumes of ethanol and 2 M ammonium acetate. Then the pellet was washed twice with 75% ethanol, dried and dissolved in water. CfDNA concentrations were measured by fluorescence on LS-55 (Perkin Elmer; USA) using the Pico Green fluorescent probe (Sigma; USA).

DNase I activity in blood plasma was measured using a technique proposed in [16]. Briefly, the substrate for DNase I (Sintol, Russia) is a 30 b.p. long double-stranded oligodeoxyribonucleotide described by the formula R6G - ACC CCC AGC GAT TAT CCA AGC GGG - BHQ1. The sequence of a model substrate is not critical. On its 5′-end the oligonucleotide is tagged with fluorescent 5(6)-carboxyrhodamine; on its 3′-end it contains the fluorescence quencher BHQ1. As the endonuclease continues to hydrolyze phosphodiester bonds, the emitted fluorescent signal intensifies. In our experiment, we added 10 µl of blood plasma to 90 µl of the solution for DNase I containing 10 mM HEPES, pH 7.5, 20 mM $MgCl_2$, 5 mM $CaCl_2$, and 3 pM of the oligonucleotide. The reaction went on for 1 h at 37 °C. Fluorescence was recorded using a plate reader (EnSpire; Finland). DNase I activity was calculated from a calibration curve showing a correlation between fluorescence enhancement and the concentration of a standard DNase I sample (Sigma; USA) in the solution. DNase I activity was expressed in arbitrary units: 1 unit = 1 ng/ml, i.e. it shows an increase in the substrate fluorescence resulting from the activity of DNase I taken at a concentration of 1 ng/ml (1 h 37 °C). At least three parallel measurements were taken for each sample. The relative standard error of measurement was 5%.

The data were processed in StatPlus 2007 (Statistical Graphics Corp.; USA); the Mann–Whitney U-test was applied.

RESULTS

In group 2 consisting of women with uncomplicated pregnancies fetal cardiac function scored from 7 to 10 points on the Fisher scale; the aortic blood flow was 180 to 260 ml/min; the umbilical blood flow was 86 to 140 ml/min per 1 kg of the fetus's weight. In group 3, 28 of 35 women demonstrated poorer fetal cardiac function (4 to 7 points on the Fisher scale); the aortic blood flow was 120 to 174 ml/min; the umbilical blood flow was 60 to 86 ml/min per 1 kg of the fetus's weight. The data obtained from the patients with grades I, II and III IUGR are presented in Table 1. The most pronounced impairment of fetal cardiac function was observed in the patients with grades II and III IUGR. In the participants with grades II IUGR, circulation disorders manifested as uteroplacental and fetoplacental blood flow abnormalities. Grade III IUGR was characterized by fetoplacental blood flow disorders, such as the absent or reversed diastolic flow in the umbilical artery or aorta, and the abnormal uterine blood flow. In the patients with grades II and III IUGR fetal cardiac function scored less than 7 points on the Fisher scale; their diastolic flow in the umbilical artery or aorta was either reversed or absent and the uterine blood flow was abnormal.

Concentrations of cfDNA in the healthy nonpregnant participants (Table 2) varied from 11 to 123 ng/ml (the median value was 75.5 ng/ml); in uncomplicated pregnancies the figures ranged from 2 to 347 ng/ml (the median value was 78 ng/ml), and in IUGR this interval was from 1.2 to 595.7 ng/ml (the median value was 42.1 ng/ml). The Mann–Whitney U-test did not reveal significant differences between the groups ($p > 0.05$). Nine samples (22.5%) representing groups 2 and 3 had cfDNA concentrations falling above the reference interval established for nonpregnant women (123 ng/ml). Interestingly, unlike the nonpregnant participants, the pregnant women demonstrated a wider variability of cfDNA concentrations. The variation coefficient was 0.42 for group 1, 0.87 for group 2, and 1.37 for group 3.

Perhaps, a decline in cfDNA concentrations was largely caused by the increased activity of the components constituting the system of cfDNA elimination from the bloodstream. One of the factors affecting cfDNA elimination is the activity of DNase I in blood plasma, an enzyme responsible for cfDNA hydrolysis. In our study the activity of this enzyme (Table 2) in the nonpregnant participants varied from 1.1 to 5.9 IU/ml (the median value was 3 IU/ml); in normal pregnancies, between 0.6 and 14.8 IU/ml (the median value was 3.4 IU/ml); in IUGR, between 3.9 and 14.3 IU/ml (the median value was 6.3 IU/ml). The Mann–Whitney U-test did not reveal any significant differences between groups 1 and 2 ($p > 0.05$). However, the group of patients with complicated pregnancies significantly differed from the group of healthy nonpregnant ($p < 10^{-7}$) and healthy pregnant women ($p < 10^{-5}$) in terms of DNase I activity in blood plasma. So, the blood plasma of pregnant women with IUGR shows higher levels of DNase I activity in comparison with healthy pregnant and nonpregnant women. In 18 (51.4%) of 35 pregnant women from group 3 DNase I activity was high; in contrast, high DNase I activity is not typical for nonpregnant

Table 1. Characteristics of patients with IUGR of the fetus

	Patients with grade I IUGR $n = 11$	Patients with grade II IUGR $n = 13$		Patients with grade III IUGR $n = 11$		
Blood flow in the aorta	220 (154; 254)	150 (126; 180)	$p1$ 0.0002	122 (120; 142)	$p1$ 0.0001	$p2$ 0.0005
Blood flow in the umbilical vein	110 (82; 120)	80 (64; 86)	0.0001	64 (60; 68)	0.0001	0.0002
Reversed diastolic flow in the umbilical artery or aorta	–	1 (7.7%)	1	6 (54.5%)	0.0124	0.0233
Preterm labor	–	3 (23.1%)	0.2228	4 (36.3%)	0.0902	0.6591
Preeclampsia	–	3 (23.1%)	0.2228	7 (63.6%)	0.0039	0.0953
Scores on Fisher scale	8 (7; 9)	6.5 (6; 7)	0.0001	5 (4.5; 6)	0.0001	0.0002
Gestatinoal age, weeks	40 (38; 41)	38 (36; 41)	0.0397	37 (30; 40)	0.0008	0.0084
Weight of the fetus, g	2,790 (2,630; 3,030)	2,520 (2,350; 2,650)	0.0001	1,720 (600; 2,270)	0.0001	< 0.0001
Height of the fetus, cm	48 (47; 51)	47 (46; 50)	0.0221	43 (29; 47)	0.0002	0.001

Note: results are presented as median values (the maximum value ÷ the minimum value); $p1$ is the p value indicating the difference from the group of pregnant patients with grade I IUGR; $p2$ is the p value indicating the difference from the group of pregnant patients with grade II IUGR.

Table 2. Concentrations of plasma cfDNA and the activity of DNase I in healthy nonpregnant women and women with normal and complicated pregnancies

	Healthy nonpregnant women $n = 40$	Healthy pregnant women $n = 40$		Pregnant women with IUGR of the fetus $n = 35$		
Concentration of cfDNA, ng/ml	75.5 (11.0; 123.0)	78 (2.0; 347.0)	$p1$ 0.59	42.1 (1.2; 595.7)	$p1$ 0.316	$p2$ 0.258
DNase I activity, IU/ml	3 (1.1; 5.9)	3.4 (0.6; 14.8)	0.088	6.3 (3.9; 14.3)	< 0.001	< 0.001
cfDNA/DNase I ratio	20.5 (6.5; 101.8)	25.9 (0.3; 112.4)	0.889	8.4 (0.1; 152.7)	< 0.001	0.002

Note: results are presented as median values (the maximum value ÷ the minimum value); $p1$ is the p value indicating the difference from the group of healthy nonpregnant women $p2$ is the p value indicating the difference from the group of healthy pregnant women.

healthy women. In group 2 increased DNase I activity was observed for only 4 (10%) of 40 pregnant women ($p = 0.0002$; Fisher's exact test applied).

Table 3 shows the correlation between cfDNA concentrations and the level of DNase I activity. The group of healthy nonpregnant women demonstrated a moderate but statistically significant negative correlation between these two parameters ($R = 0.37$; $p < 0.05$). The pregnant women, especially those with complicated pregnancies, demonstrated a weak correlation between cfDNA levels and DNase I activity.

The subgroups of patients with different grades IUGR did not differ significantly in terms of the studied parameters. However, cfDNA concentrations and the ratio of cfDNA to DNase I activity strongly tended to grow with the severity of IUGR (Table 4). The analysis revealed that only 4 (16.7%) of 24 patients with grades I and II IUGR had high cfDNA concentrations not observed in nonpregnant women, whereas there were as many as 6 women (54.5%; $p = 0.041$, Fisher's exact test applied) in the subgroup of 11 patients with grade III IUGR who had elevated cfDNA levels. Moreover, when comparing the cfDNA/DNase I ratio between the patients with different grades IUGR and the controls, significant differences were observed only for the patients with grades I and II IUGR ($p < 0.001$). The patients with grade III IUGR had the same cfDNA/DNase I ratio as the healthy pregnant and nonpregnant participants (Tables 2, 4).

DISCUSSION

Concentrations of maternal cfDNA strongly correlate with the amount of placental cfDNA [17]. It is known that only a small fraction of maternal cfDNA circulating in blood comes from solid organs such as the liver or kidneys; the rest originates from hematopoietic cells. For example, differentiating erythroblasts are a stable source of low molecular weight cfDNA fragments. Rapid elevation of cfDNA levels in the circulation in pathology or following physical effort is caused by the activation of neutrophils that release extracellular traps containing nuclear and/or mitochondrial DNA [18].

CfDNA has an impact on many cells in the body. Circulating DNA can contribute to oxidative stress, stimulate the synthesis of anti-inflammatory cytokines and induce aseptic inflammation [19]. CfDNA-containing extracellular traps released by activated neutrophils attract platelets and significantly increase the risk of thrombosis [18]. The body defends itself against the negative impact of excess cfDNA by activating the system of its elimination from the bloodstream. A part of this system is the activity of endonucleases present in human blood. DNase I is the main blood endonuclease that hydrolyzes phosphodiester bonds in DNA strands. Accumulation of single-strand breaks entails double-strand breaks, thus producing low molecular weight cfDNA fragments. These fragments can be easily eliminated through the kidneys. Healthy nonpregnant women participating in our study demonstrated a moderate but statistically significant negative correlation between the amount of cfDNA in blood plasma and the activity of DNase I. It looks like this activity is the major factor responsible for the elimination of cfDNA fragments from the bloodstream. Women with uncomplicated pregnancies and patients with IUGR showed no correlation between DNase I activity and cfDNA levels.

Placental pathology is accompanied by apoptosis in the trophoblast with the subsequent increase in the concentration of microvesicles with placental cfDNA in the maternal blood stream. Trophoblast microvesicles, in turn, stimulate the release of web-like nuclear and mitochondrial DNA strands (netosis) by neutrophils. Therefore, one can expect that complicated pregnancies will be characterized by the dramatic elevation of total cfDNA levels in maternal plasma. However, in the course of this work we did not observe an increase in total cfDNA concentrations in pregnant women with IUGR. Moreover, plasma cfDNA concentrations were lower (insignificantly, though) in complicated pregnancies than in healthy pregnant and nonpregnant women. At the same time, we observed a statistically significant increase in DNase I activity exerted in the plasma of pregnant women with IUGR, which indirectly suggests a transient elevation of circulating cfDNA levels in patients with complicated pregnancies. Perhaps, a substantial increase in total cfDNA levels circulating in the plasma of pregnant women with IUGR triggers the activation of protective mechanisms, of which DNase I is particularly important, promoting elimination of excess cfDNA from the bloodstream. The majority of our patients with grades I and II IUGR had moderate placental flow defects (Table 1) that led to a moderate and possibly transient increase in cfDNA levels rapidly eliminated from the blood stream by activated DNase I. Those patients had low cfDNA concentrations, highly active DNase I and a low cfDNA/DNase I ratio. The majority of patients with grade III IUGR underwent rapid accumulation of cfDNA in plasma which the elimination mechanisms failed to handle. Those patients had increased cfDNA concentrations, highly active DNase I and a high cfDNA/DNase I ratio. Besides, excess cfDNA in the circulation

Table 3. Spearman's correlation between cfDNA concentrations and DNase I activity

	R	*p*
Healthy nonpregnant women	–0.39	< 0.05
Healthy pregnant women	–0.28	> 0.05
Women with complicated pregnancies	–0.18	> 0.05

Table 4. Levels of cfDNA and DNase I activity in patients with different grades IUGR

	Patients with grade I IUGR *n* = 11	Patients with grade II IUGR *n* = 13		Patients with grade III IUGR *n* = 11		
Concentration of cfDNA, ng/ml	34.7 (8.0; 160.7)	76 (7.8; 251.1)	*p*1 0.817	103.5 (1.2; 595.7)	*p*1 0.212	*p*2 0.354
DNase I activity, IU/ml	5.7* (4.1; 13.1)	7.5* (3.9; 14.3)	0.183	5.2* (3.9; 10.0)	0.793	0.271
cfDNA/DNase I ratio	5.2* (0.6; 28.2)	10.1* (0.8; 36.4)	0.817	18.5 (0.1; 152.7)	0.325	0.271

Note: results are presented as median values (the maximum value ÷ the minimum value; *p*1 is the *p* value indicating the difference from the group of patients with grade I IUGR; *p*2 is the p value indicating the difference from the group of patients with grade II IUGR; * represents $p < 0.01$ indicating the difference from the groups of healthy nonpregnant and pregnant women.

aggravates placental flow defects and increases the risk of poor pregnancy outcomes.

Our study demonstrates that high activity of the cfDNA elimination system impedes the analysis of cfDNA concentrations in pregnancy, especially if the latter is complicated, and skews results. This could be the reason why the literature is very controversial on the dynamics of cfDNA concentrations in pregnancy. However, if all of the three parameters (cfDNA concentrations, DNase 1 activity and the cfDNA/DNase I ratio) are taken into account, the development of a tool for cell death monitoring throughout the entire pregnancy becomes possible (such tests could be done once in a trimester, for instance). These parameters provide information on cell death and the performance of the cfDNA elimination system composed of DNase I and other components that have a role in pregnancy. If such tests revealed increased DNase I activity during a certain week of pregnancy plus elevated cfDNA levels, one could infer the increased rates of cell (specifically, placental) death. High cfDNA concentrations in combination with increased DNase I activity indicate insufficient clearance of cfDNA from the body and, therefore, pathology in the stages when ultrasonography is unable to detect IUGR due to the lack of visible signs.

CONCLUSIONS

We have studied the dynamics of cfDNA concentrations and the activity of DNase I in the blood plasma of healthy nonpregnant women and women with normal and complicated pregnancies. We have shown that plasma cfDNA concentrations alone are not a reliable marker of IUGR in the last trimester. However, if cfDNA levels and DNase I activity are measured in combination, they can offer valuable information on the development of IUGR.

References

1. Mandel P, Metais P. Les acides nucléiques du plasma sanguin chezl'homme. C R Acad Sci Paris 1948; 142: 241–3.
2. Fleischhacker M, Schmidt B. Circulating nucleic acids (CNAs) and cancer — a survey. Biochimica et biophysica acta. 2007; 1775 (1): 181–232. DOI: 10.1016/j.bbcan.2006.10.001.
3. Urbanova M, Plzak J, Strnad H, Betka J. Circulating nucleic acids as a new diagnostic tool. Cell Mol Biol Lett. 2010 Jun; 15 (2): 242–59. DOI: 10.2478/s11658-010-0004-6.
4. Lo YM, Chiu RW. Genomic analysis of fetal nucleic acids in maternal blood. Annu Rev Genomics Hum Genet. 2012; 13: 285–306. DOI: 10.1146/annurev-genom-090711-163806.
5. Lo YM. Non-invasive prenatal testing using massively parallel sequencing of maternal plasma DNA: from molecular karyotyping to fetal whole-genome sequencing. Reprod Biomed Online. 2013 Dec; 27 (6): 593–8. DOI: 10.1016/j.rbmo.2013.08.008.
6. Bauer M, Hutterer G, Eder M, Majer S, Leshane E, Johnson KL, et al. A prospective analysis of cell-free fetal DNA concentration in maternal plasma as an indicator for adverse pregnancy outcome. Prenat Diagn, 2006; 26: 831–36. DOI: 10.1002/pd.1513.
7. Zhong XY, Laivuori H, Livingston JC, Ylikorkala O, Sibai BM, Holzgreve W, et al. Elevation of both maternal and fetal extracellular circulating deoxyribonucleic acid concentrations in the plasma of pregnant women with preeclampsia. Am J Obstet Gynecol, 2001; 184 (3), 414–9. DOI: 10.1067/mob.2001.109594.
8. Hahn S, Rusterholz C, Hösli I, Lapaire O. Cell-free nucleic acids as potential markers for preeclampsia. Placenta. 2011 Feb; 32 Suppl: 17–20. DOI: 10.1016/j.placenta.2010.06.018.
9. Al Nakib M, Desbrière R, Bonello N, Bretelle F, Boubli L, Gabert J, et. al. Total and fetal cell-free DNA analysis in maternal blood as markers of placental insufficiency in intrauterine growth restriction. Fetal Diagn Ther. 2009; 26 (1): 24–8. DOI: 10.1159/000236355.
10. Vejko NN, Bulycheva NV, Roginko OA, Vejko RV, Ershova ES, Kozdoba OA, i dr. Fragmenty transkribiruemoj oblasti ribosomnogo povtora v sostave vnekletochnoj dnk — marker gibeli kletok organizma. Biomedicinskaja himija. 2008; 54 (1): 78–93.
11. Korzeneva IB, Kostuyk SV, Ershova LS, Osipov AN, Zhuravleva VF, Pankratova GV, et. al. Human circulating plasma DNA significantly decreases while lymphocyte DNA damage increases under chronic occupational exposure to low-dose gamma-neutron and tritium β-radiation. Mutat Res. 2015 Sep; 779: 1–15. DOI: 10.1016/j.mrfmmm.2015.05.004.
12. Ershova E, Sergeeva V, Klimenko M, Avetisova K, Klimenko P, Kostyuk E, Veiko N, Veiko R, Izevskaya V, Kutsev S, Kostyuk S. Circulating cell-free DNA concentration and DNase I activity of peripheral blood plasma change in case of pregnancy with intrauterine growth restriction compared to normal pregnancy. Biomed Rep. 2017 Oct; 7 (4): 319–24. DOI: 10.3892/br.2017.968.
13. Sur Chowdhury C, Hahn S, Hasler P, Hoesli I, Lapaire O, Giaglis S. Elevated Levels of Total Cell-Free DNA in Maternal Serum Samples Arise from the Generation of Neutrophil Extracellular Traps. Fetal Diagn Ther. 2016; 40 (4): 263–7. DOI: 10.1159/000444853.
14. Demidov VN, Bychkov PA, Logvinenko AV, Voevodin SM. Ul'trazvukovaja biometrija. Spravochnye tablicy i uravnenija. V knige: Medvedeva M. V., Zykina B. I., redaktory. Klinicheskie lekcii po UZ-diagnostike v perinatologii. M., 1990; 83–92.
15. Dement'eva G. M. Ocenka fizicheskogo razvitija novorozhdennyh: posobie dlja vrachej. M., 2000. 25 s.
16. Ermakov AV, SV Kostyuk, MS Konkova, NA Egolina, EM Malinovskaya, NN Veiko. Extracellular DNA fragments. Annals of the New York Academy of Sciences. 1137 (1): 41–6.
17. Muñoz-Hernández R, Medrano-Campillo P, Miranda ML, Macher HC, Praena-Fernández JM, Vallejo-Vaz AJ, et. al. Total and Fetal Circulating Cell-Free DNA, Angiogenic, and Antiangiogenic Factors in Preeclampsia and HELLP Syndrome. Am J Hypertens. 2017 Jul 1; 30 (7): 673–82. DOI: 10.1093/ajh/hpx024.
18. Hahn S, Giaglis S, Buser A, Hoesli I, Lapaire O, Hasler P. Cell-free nucleic acids in (maternal) blood: any relevance to (reproductive) immunologists? J Reprod Immunol. 2014 Oct; 104–105: 26–31. DOI: 10.1016/j.jri.2014.03.007.
19. Nadeau-Vallée M, Obari D, Palacios J, Brien MÈ, Duval C, Chemtob S, et. al. Sterile inflammation and pregnancy complications: a review. Reproduction. 2016 Dec; 152 (6): R277–R292. Epub 2016 Sep 27.

Литература

1. Mandel P, Metais P. Les acides nucléiques du plasma sanguin chezl'homme. C R Acad Sci Paris 1948; 142: 241–3.
2. Fleischhacker M, Schmidt B. Circulating nucleic acids (CNAs) and cancer — a survey. Biochimica et biophysica acta. 2007; 1775 (1): 181–232. DOI: 10.1016/j.bbcan.2006.10.001.
3. Urbanova M, Plzak J, Strnad H, Betka J. Circulating nucleic acids as a new diagnostic tool. Cell Mol Biol Lett. 2010 Jun; 15 (2): 242–59. DOI: 10.2478/s11658-010-0004-6.
4. Lo YM, Chiu RW. Genomic analysis of fetal nucleic acids in maternal blood. Annu Rev Genomics Hum Genet. 2012; 13: 285–306. DOI: 10.1146/annurev-genom-090711-163806.
5. Lo YM. Non-invasive prenatal testing using massively parallel sequencing of maternal plasma DNA: from molecular karyotyping to fetal whole-genome sequencing. Reprod Biomed Online. 2013

Dec; 27 (6): 593–8. DOI: 10.1016/j.rbmo.2013.08.008.
6. Bauer M, Hutterer G, Eder M, Majer S, Leshane E, Johnson KL, et al. A prospective analysis of cell-free fetal DNA concentration in maternal plasma as an indicator for adverse pregnancy outcome. Prenat Diagn, 2006; 26: 831–36. DOI: 10.1002/pd.1513.
7. Zhong XY, Laivuori H, Livingston JC, Ylikorkala O, Sibai BM, Holzgreve W, et al. Elevation of both maternal and fetal extracellular circulating deoxyribonucleic acid concentrations in the plasma of pregnant women with preeclampsia. Am J Obstet Gynecol, 2001; 184 (3), 414–9. DOI: 10.1067/mob.2001.109594.
8. Hahn S, Rusterholz C, Hösli I, Lapaire O. Cell-free nucleic acids as potential markers for preeclampsia. Placenta. 2011 Feb; 32 Suppl: 17–20. DOI: 10.1016/j.placenta.2010.06.018.
9. Al Nakib M, Desbrière R, Bonello N, Bretelle F, Boubli L, Gabert J, et. al. Total and fetal cell-free DNA analysis in maternal blood as markers of placental insufficiency in intrauterine growth restriction. Fetal Diagn Ther. 2009; 26 (1): 24–8. DOI: 10.1159/000236355.
10. Вейко Н. Н., Булычева Н. В., Рогинко О. А., Вейко Р. В., Ершова Е. С., Коздоба О. А. и др. Фрагменты транскрибируемой области рибосомного повтора в составе внеклеточной днк — маркер гибели клеток организма. Биомедицинская химия. 2008; 54 (1): 78–93.
11. Korzeneva IB, Kostuyk SV, Ershova LS, Osipov AN, Zhuravleva VF, Pankratova GV, et. al. Human circulating plasma DNA significantly decreases while lymphocyte DNA damage increases under chronic occupational exposure to low-dose gamma-neutron and tritium β-radiation. Mutat Res. 2015 Sep; 779: 1–15. DOI: 10.1016/j.mrfmmm.2015.05.004.
12. Ershova E, Sergeeva V, Klimenko M, Avetisova K, Klimenko P, Kostyuk E, Veiko N, Veiko R, Izevskaya V, Kutsev S, Kostyuk S. Circulating cell-free DNA concentration and DNase I activity of peripheral blood plasma change in case of pregnancy with intrauterine growth restriction compared to normal pregnancy. Biomed Rep. 2017 Oct; 7 (4): 319–24. DOI: 10.3892/br.2017.968.
13. Sur Chowdhury C, Hahn S, Hasler P, Hoesli I, Lapaire O, Giaglis S. Elevated Levels of Total Cell-Free DNA in Maternal Serum Samples Arise from the Generation of Neutrophil Extracellular Traps. Fetal Diagn Ther. 2016; 40 (4): 263–7. DOI: 10.1159/000444853.
14. Демидов В. Н., Бычков П. А., Логвиненко А. В., Воеводин С. М. Ультразвуковая биометрия. Справочные таблицы и уравнения. В книге: Медведева М. В., Зыкина Б. И., редакторы. Клинические лекции по УЗ-диагностике в перинатологии. М., 1990; 83–92.
15. Дементьева Г. М. Оценка физического развития новорожденных: пособие для врачей. М., 2000. 25 с.
16. Ermakov AV, SV Kostyuk, MS Konkova, NA Egolina, EM Malinovskaya, NN Veiko. Extracellular DNA fragments. Annals of the New York Academy of Sciences. 1137 (1): 41–6.
17. Muñoz-Hernández R, Medrano-Campillo P, Miranda ML, Macher HC, Praena-Fernández JM, Vallejo-Vaz AJ, et. al. Total and Fetal Circulating Cell-Free DNA, Angiogenic, and Antiangiogenic Factors in Preeclampsia and HELLP Syndrome. Am J Hypertens. 2017 Jul 1; 30 (7): 673–82. DOI: 10.1093/ajh/hpx024.
18. Hahn S, Giaglis S, Buser A, Hoesli I, Lapaire O, Hasler P. Cell-free nucleic acids in (maternal) blood: any relevance to (reproductive) immunologists? J Reprod Immunol. 2014 Oct; 104–105: 26–31. DOI: 10.1016/j.jri.2014.03.007.
19. Nadeau-Vallée M, Obari D, Palacios J, Brien MÈ, Duval C, Chemtob S, et. al. Sterile inflammation and pregnancy complications: a review. Reproduction. 2016 Dec; 152 (6): R277–R292. Epub 2016 Sep 27.

COMPARATIVE ASSESSMENT OF STILLBIRTH RATE IN BRYANSK REGION, EU AND CIS COUNTRIES (1995–2014)

Korsakov AV[1] ✉, Hoffmann V[2], Pugach LI[1], Lagerev DG[1], Korolik VV[3], Bulatseva MB[3]

[1] Bryansk State Technical University, Bryansk

[2] University of Greifswald, Institute for Community Medicine, Section Epidemiology of Health Care and Community Health, Greifswald, Germany

[3] Hygiene Department, Pediatric Faculty, Pirogov Russian National Research Medical University, Moscow

Stillbirth rate is one of the most important indicators allowing assessment of the population's living standards and forecasting its growth rate. This study aimed to compare the frequency of stillbirths in the Bryansk region, EU and CIS countries based on the official statistical data covering the period from 1995 to 2014. It was established that male stillbirth rate is greater than female stillbirth rate both in the Bryansk region and the Russian Federation (by 14.2% and 9%, respectively), which is consistent with the worldwide trend that has the male stillbirth risk 10% higher than that for girls. Provided the dynamics remain the same, 2016 to 2021 the share of stillbirths in the Bryansk region will continue to grow and reach 28.8% by 2021, which is greater than nationwide. The gender distribution will also grow to 32.6% (male stillbirths more common than female) by 2021.

Keywords: stillbirths, boys, girls, Bryansk region, Russian Federation, European Union, Commonwealth of Independent States, World Health Organization.

Funding: the study is a deliverable *under the state assignment 19.9992.2017/5.2* in the context of the international research and educational cooperation between the Ministry of Education and Science and DAAD, part of the Mikhail Lomonosov program.

✉ **Correspondence should be addressed:** Anton V. Korsakov
Boulevard 50-let Oktyabrya, 7, Bryansk, 241035; korsakov_anton@mail.ru

Received: 15.06.2018 **Accepted:** 21.07.2018

DOI: 10.24075/brsmu.2018.048

СРАВНИТЕЛЬНАЯ ОЦЕНКА ЧАСТОТЫ МЕРТВОРОЖДАЕМОСТИ В БРЯНСКОЙ ОБЛАСТИ, СТРАНАХ ЕВРОПЕЙСКОГО СОЮЗА И СОДРУЖЕСТВА НЕЗАВИСИМЫХ ГОСУДАРСТВ (1995–2014 ГГ.)

А. В. Корсаков[1]✉, В. Хоффманн[2], Л. И. Пугач[1], Д. Г. Лагерев[1], В. В. Королик[3], М. Б. Булацева[3]

[1] Брянский государственный технический университет, Брянск

[2] Институт общественной медицины Университета Грайфсвальда, секция эпидемиологии и общественного здравоохранения, Грайфсвальд, Германия

[3] Кафедра гигиены, педиатрический факультет, Российский национальный исследовательский медицинский университет имени Н. И. Пирогова, Москва

Одним из важнейших показателей, позволяющих оценить уровень жизни населения и спрогнозировать рост его численности, служит частота случаев мертворождения детей. Целью работы было на основании официальных статистических данных за 1995–2014 гг. провести сравнительную оценку частоты мертворождаемости мальчиков и девочек в Брянской области, странах ЕС и СНГ. Установлено превышение частоты мертворожденных мальчиков над девочками, как по Брянской области (на 14,2%), так и по Российской Федерации в целом (на 9%), что подтверждает общемировые тенденции, выявившие повышенный риск мертворождения плодов мужского пола примерно на 10%. При сохранении существующих тенденций динамики мертворождаемости в Брянской области коэффициент мертворождений будет увеличиваться относительно общероссийских значений в период 2016–2021 гг. и достигнет 28,8% к 2021 г., причем разрыв между мальчиками и девочками будет возрастать и составит 32,6% к 2021 г.

Ключевые слова: мертворождаемость, мальчики, девочки, Брянская область, Российская Федерация, Европейский союз, Содружество Независимых Государств, Всемирная организация здравоохранения

Финансирование: работа выполнена *в рамках государственного задания 19.9992.2017/5.2.* В рамках международного научно-образовательного сотрудничества Минобрнауки и DAAD по программе «Михаил Ломоносов».

✉ **Для корреспонденции:** Антон Вячеславович Корсаков
Бульвар 50-лет Октября, д. 7, г. Брянск, 241035; korsakov_anton@mail.ru

Статья получена: 15.06.2018 **Статья принята к печати:** 21.07.2018

DOI: 10.24075/vrgmu.2018.048

According to the World Health Organization [1], there were about 2.6 million stillbirths registered worldwide in 2009. Every day, over 7,200 children are born dead; 98% of these stillbirths occur in countries with low and mid-level standards of living. The same WHO report [1] states that 1995 to 2009 the rate of stillbirths decreased by just 1.1%, from 3,000,000 cases in 1995 to 2,600,000 cases in 2009. Finland is the country with the lowest number of stillbirths (2 dead-born in every 1,000 newborns), Nigeria and Pakistan are the nations where the rate of stillbirths is the highest (40 out of 1,000 births) [1]. In 2011, Nepal had the stillbirth rate of 22.4 per 1,000, with 80% of these deaths occurring during the pregnancy period [2]. The largest absolute number of stillbirths in the world was recorded in India — about 590,000 in 2015 [3].

It was also established that gender of the child matters. A group of researchers from the Exeter University (UK) has analyzed over 30,000,000 cases of stillbirth worldwide [4] and found that boys run an approximately 10% greater risk than girls, which translates into about 100,000 more stillborn males a year. The reasons for such a difference are yet unknown; it may be defined, for example, by the peculiarities of placenta development and functions, or the greater sensitivity of male fetuses to harmful environmental factors. China and India were the exceptions to the rule: there, the percentage of stillborn boys and girls did not differ. This may be due to the selective abortions, which are common in these countries: when the US scan shows the fetus is female, abortion is the option of choice in many cases. Overall, the rate of stillbirths in China and India was slightly higher than the global average [4].

There is a number of factors that up the risk of bearing a dead child, including complications during childbirth, maternal age over 35, preeclampsia, placental abruption, chronic infections in mother during pregnancy (brucellosis, toxoplasmosis, listeriosis, tuberculosis, syphilis, etc.), acute infections (angina, influenza, pneumonia etc.), high blood pressure, diabetes, diseases of the heart, lungs, kidneys and other internal organs, drug abuse [5–7], socioeconomic problems, poor educational status [8], as well as polluted environment, intrauterine growth retardation and congenital malformations (FCA) [9]. Refusal to visit antenatal clinics and/or lack of antenatal aid is a major factor affecting the risk of stillbirth; unlike many other factors, this one is can be influenced [10].

Almost half of all stillbirths (1,200,000 cases) occur during childbirth. These deaths are the result of mothers and children not having any help from qualified specialists in this critical process. Two-thirds of the cases belong to rural areas, where obstetricians — midwives and doctors aiding childbirth — are not always available, same as assistance in emergency situations that require interventions like cesarean section [1]. In the countries where the standards of living (and level of income) are high, the share of stillbirths occurring during childbearing was decreased significantly through better obsteric care; in the contrary, the number of stillbirths did not go down significantly [11]. This fact proves that even in the richer countries, stillbirth prevention strategies based on the detection of high-risk pregnancies were unsuccessful.

Approximately in a quarter of cases the causes of stillbirth remain unclear; this is one of the priority problems for the modern medicine [4]. A very important step on the way to its solution is the discovery of a new factor reducing the risk of stillbirth, the detection of which requires gathering special statistical data [4]. Large FCA may be such a factor, those rendering living impossible and leading to both spontaneous abortions (miscarriages) [9] and abortions for medical reasons; such FCA are detected more often in pregnancies carried by women residing in areas contaminated by the Chernobyl meltdown [12].

Thus, the primary mission of healthcare professionals is timely arrest of pathological processes in pregnant women both during pregnancy (including early FCA diagnosing) and in the process of delivery.

It should be noted that in 2015, Bryansk region ranked 16 out of 18 regions belonging to the Central Federal District in terms of quality of life, while in the national rating its position was 52 (out of 85); as for the health of its population, the region is 67th nationwide [13].

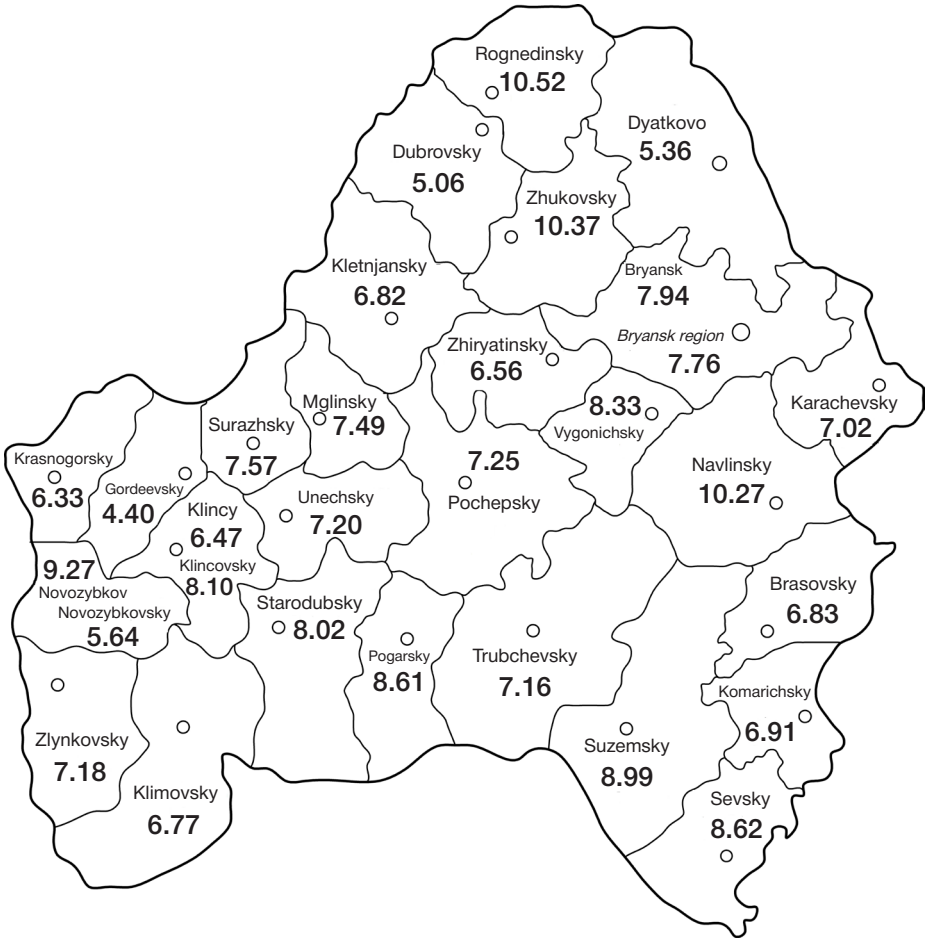

Fig. 1. Stillbirth rate in Bryansk Region, boys, 1995 to 2015 (per 1,000 births, ‰)

In this connection, a long-term observation and analysis of the dynamics of stillbirth rate (overall and by gender) in Bryansk region, EU and CIS countries is an extremely important and urgent task.

METHODS

Source of the statistical data covering the period from 1995 to 2015 and describing the rate of stillbirths (by gender) in Bryansk region and in Russia — official materials issued by Bryanskstat, territorial body of the Federal State Statistics Service in Bryansk region [14]. Source of the data describing stillbirth rate registered in the EU and CIS countries in 1995 to 2014 — reports published to the official website of WHO [15].

Stata SE 14 software was used to perform statistical analysis of the data obtained. Sample mean was taken as the average value. Student's *t*-test helped determine statistical significance of deviations.

Using the data available, we forecast the stillbirth rate for the Bryansk region and the Russian Federation, overall and by gender. To this effect, we applied the least squares method to find the $y = ax + b$ linear function that approximates the statistical data for each of these categories most accurately. Data analyzed covered the period from 2009 to 2015 for Bryansk region and from 2009 to 2014 for the Russian Federation (data covering 2015 are not yet available for the Russian Federation). Using the aforementioned linear function, we forecast the dynamics for the two three-year periods from 2016 to 2021.

RESULTS

Figures 1 through 3 depict the data describing stillbirth rate in the Bryansk region (years 1995 through 2015): boys, girls, overall and by districts.

Most often, boys are stillborn in Rognedinsky district (10.52 stillbirths per 1,000 births), followed by Zhukovsky (10.37), Navlinsky (10.27) and Suzemsky (8.99) districts (Figure 1); on the other side of the range are Gordeevsky (4.40), Dubrovsky (5.06), Dyatkovo (5.36) and Novozybkovsky (5.64) districts. The stillbirth rate in the region ranges from 4.40 to 10.52. In Rognedinsky district, the incidence is 2.4 times as frequent as in Gordeevsky district. Stillbirth rate registered in the city of Bryansk is 7.94.

As for the female stillbirths, they are most common in Zhiryatinsky district (12.80 girls born dead out of every 1,000 born), Pogarsky (9.57), Dubrovsky (8.77) and Klimovsky (8.59) districts; the lowest rates are in Zlynkovsky (3.80), Gordeevsky 4,02), Karachevsky (4,20) and Krasnogorsky districts (5,27). The highest rate in the region, which was registered in Zhiryatinsky district, is 3.4 times greater than the lowest rate, registered in Zlynkovsky district. In Bryansk, the average female stillbirth rate is 6.35, which is 20% less than male still births (Fig. 2).

Overall, the districts with the most stillbirths (both boys and girls) registered within the period considered are Zhiryatinsky (9.68), Rognedinsky (9.09), Pogarsky (9.09) and Zhukovsky (8.53); those with the lowest stillbirth rate are Gordeyevsky (4.21), Novozybkovsky (5.36), Zlynkovsky (5.49) and Karachevsky (5.61) (Figure 3). The stillbirth rate in the region

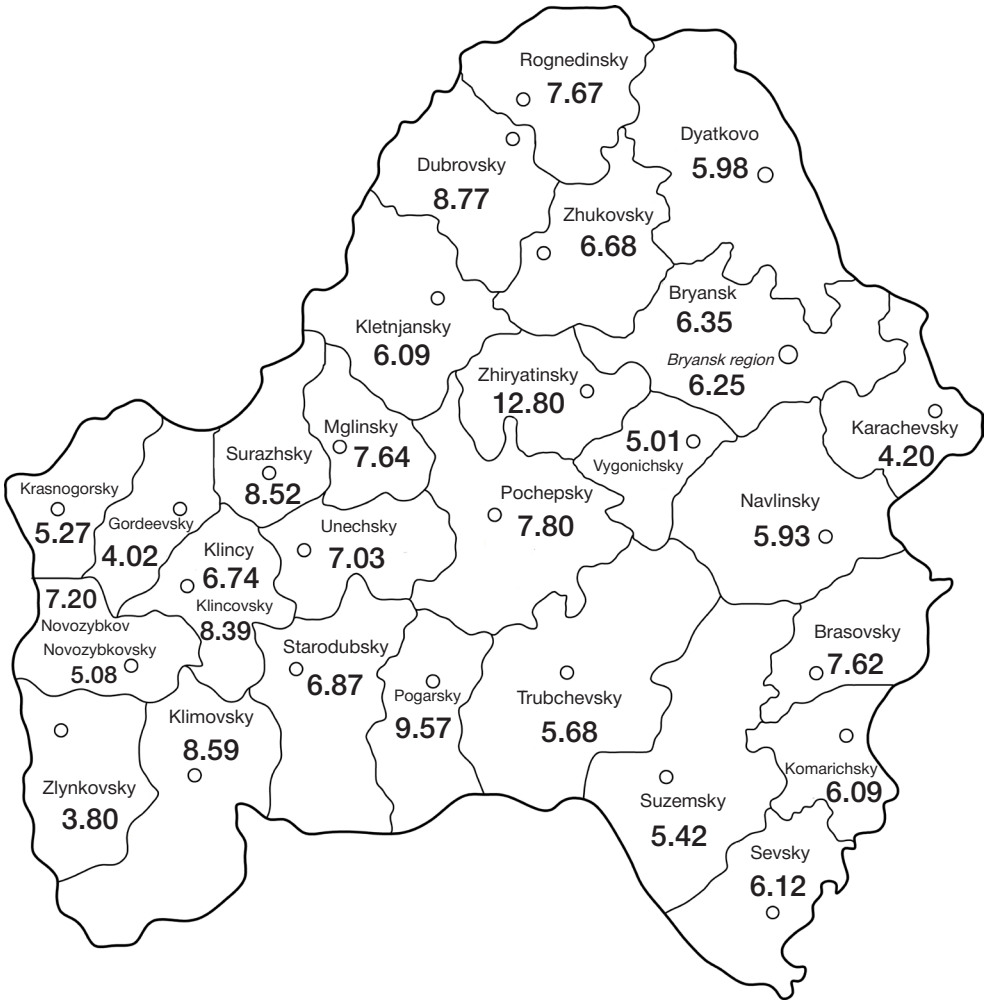

Fig. 2. Stillbirth rate in Bryansk Region, girls, 1995 to 2015 (per 1,000 births, ‰)

ranges from 4.21 to 9.09 deaths in a 1,000 born. The highest rate was registered in Zhiryatinsky district (2.2 greater than in Gordeyevsky district). The rate registered in the city of Bryansk is 7.15.

As shown in Table 1, the average percentage of stillborn boys in Bryansk region (years 1995 to 2014) is 16.5% greater than the national average: 7.49 against 6.43 ($p < 0.05$); as for girls, the rate is 11.2% greater than the national average, 6.56 against 5.90 ($p > 0.05$). The overall stillbirth rate registered in the Bryansk region is 13.8% ($p < 0.05$) greater than the national average: 7.02 (boys) and 6.17 (girls). Male stillbirths are 14.2% more common than female stillbirths in the Bryansk region (7.49 and 6.56 deaths per 1,000 births, respectively); compared to the national indicators, it is 9.0% greater (6.43 and 5.90, respectively) although the differences do not reach the level of significance ($p > 0.05$).

Table 2 shows that the average stillbirth rate in the years from 1995 to 2014 in the EU countries was less than in the CIS countries by 2.47 times ($p < 0.001$). The highest rates are recorded in Armenia (15.74), Ukraine (15.36), Georgia (14.30), Azerbaijan (11.67), Tajikistan (10.99) and in the CIS countries on the whole (12.17); the lowest rates are seen in the Czech Republic (2.98), Italy (3.10), Spain (3.43), Finland (3.47), Sweden (3.55) and the EU countries on the whole (4.93). In the EU, the highest stillbirth rate is registered in France (8.00), Bulgaria (7.49), Latvia (6.91) and the Netherlands (5.96). In the CIS countries, the stillbirth rate ranges from 4.90 to 15.74, while in the EU countries the range is from 2.98 to 8.00. In the Russian Federation, the stillbirth rate is 6.17 ± 0.23, which is 1.25 times higher than in the EU but 1.97 times lower than in the other CIS countries (differences being statistically significant, $p < 0.001$). It should be noted that only three EU countries — France, Bulgaria and Latvia, — have stillbirth rates higher than in the Russian Federation (8.0, 7.49 and 6.91, respectively). In the Republic of Belarus, the stillbirth rate is 1.26 times lower than in the Russian Federation and 2.48 times lower than in the CIS countries (4.90); it is almost the same as in the EU (4.93).

Dynamics of the stillbirth rate in Bryansk region, Russian Federation, EU countries and CIS countries in 1995–2014 (Fig. 4) confirm the data provided in Table 2 and show that in the CIS countries the stillbirth rate is the highest; it reached the maximum in 1997–1998 (17.1), then from 1999 it was gradually decreasing, reaching the minimum in 2011–2014 (8.9). Unlike CIS countries, EU has not seen sharp fluctuations of stillbirth rate over the considered 20-year period (1995–2014): the

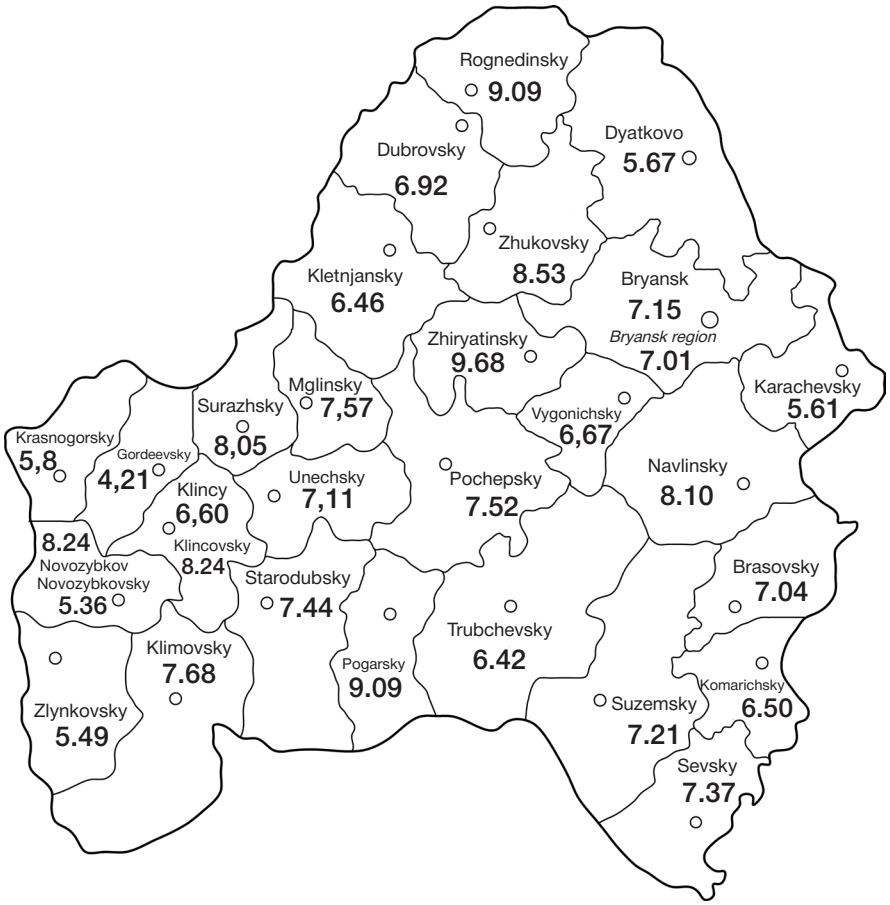

Fig. 3. Stillbirth rate in Bryansk Region, boys and girls, 1995 to 2015 (per 1,000 births, ‰)

Table 1. Stillbirth rate in Bryansk region and the Russian Federation, 1995–2014, boys and girls, per 1,000 births, M ± *m*

Country, region	Stillbirth rate, boys, ‰	Stillbirth rate, girls, ‰	Stillbirth rate, boys and girls combined, ‰
Bryansk region	7.49 ± 0.41	6.56 ± 0.27	7.02 ± 0.32
Russian Federation	6.43 ± 0.25	5.90 ± 0.22	6.17 ± 0.23

Note: difference between male and female stillbirth rate in Bryansk region and in the Russian Federation, $p > 0.05$;
difference between male stillbirth rate in Bryansk region and in the Russian Federation, $p < 0.05$;
difference between female stillbirth rate in Bryansk region and in the Russian Federation, $p > 0.05$;
difference between overall stillbirth rate (boys and girls combined) in Bryansk region and in the Russian Federation, $p < 0.05$.

Table 2. Stillbirth rate in the EU and CIS countries, 1995–2014, boys and girls combined, per 1,000 births, M ± *m*

Country, region	Stillbirth rate (1995–2014), ‰	Significance of differences with the EU, *p*
Commonwealth of Independent States	*12.17 ± 0.69*	*p < 0.001*
European Union	*4.93 ± 0.03*	–
Armenia	15.74 ± 0.55	*p* < 0.001
Ukraine	15.36 ± 1.46	*p* < 0.001
Georgia	14.30 ± 0.78	*p* < 0.001
Azerbaijan	11.67 ± 0.30	*p* < 0.001
Tajikistan	10.99 ± 0.24	*p* < 0.001
Kyrgyzstan	9.94 ± 0.76	*p* < 0.001
Moldova	9.38 ± 0.51	*p* < 0.001
Turkmenistan	9.20 ± 1.01	*p* < 0.001
Kazakhstan	8.64 ± 0.30	*p* < 0.001
Uzbekistan	8.06 ± 0.82	*p* < 0.001
France	8.00 ± 0.55	*p* < 0.001
Bulgaria	7.49 ± 0.09	*p* < 0.001
Latvia	6.91 ± 0.34	*p* < 0.001
Russian Federation	6.17 ± 0.23	*p* < 0.001
Netherlands	5.96 ± 0.12	*p* < 0.001
Serbia	5.42 ± 0.12	*p* < 0.001
Lithuania	5.41 ± 0.18	*p* < 0.05
Ireland	5.34 ± 0.20	*p* > 0.05
Romania	5.25 ± 0.22	*p* > 0.05
UK	5.25 ± 0.07	*p* < 0.001
Estonia	5.21 ± 0.36	*p* > 0.05
Poland	5.08 ± 0.23	*p* > 0.05
Slovenia	5.00 ± 0.15	*p* > 0.05
Republic of Belarus	4.90 ± 0.42	*p* > 0.05
Hungary	4.82 ± 0.14	*p* > 0.05
Greece	4.74 ± 0.21	*p* > 0.05
Malta	4.63 ± 0.31	*p* > 0.05
Denmark	4.63 ± 0.13	*p* < 0.05
Luxembourg	4.59 ± 0.30	*p* > 0.05
Belgium	4.48 ± 0.08	*p* < 0.001
Portugal	4.43 ± 0.26	*p* > 0.05
Croatia	4.27 ± 0.12	*p* < 0.001
Switzerland	4.09 ± 0.08	*p* < 0.001
Austria	3.88 ± 0.08	*p* < 0.001
Germany	3.81 ± 0.07	*p* < 0.001
Slovakia	3.79 ± 0.11	*p* < 0.001
Sweden	3.55 ± 0.08	*p* < 0.001
Finland	3.47 ± 0.13	*p* < 0.001
Spain	3.43 ± 0.07	*p* < 0.001
Italy	3.10 ± 0.13	*p* < 0.001
Czech Republic	2.98 ± 0.08	*p* < 0.001

range was from 4.6 to 5.1. In Bryansk region, stillbirth rate ranged from 4.3 to 9.9, the curve depicting its dynamics featuring a number of humps: the rate was in line with the national average in 1995 and 1996 (7.4), increased in 1997 to 9.9, then decreased and stabilized in 1998–2005 (7.2–8.5). In 2006–2010, the rate went down to the country average level (4.3–5.2), and in 2011–2014 it grew up again (5.8–7.9). As for the Russian Federation in general, in 1995–1997 the stillbirth rate was almost unchanged (7.4–8.0), then, 1998 to 2011, it decreased gradually and reached 4.5 in 2011, but within the last three years the rate has grown to 6.2.

In the Czech Republic, Finland and Germany, the stillbirth rate ranges from 2.3 to 4.8 ans does not exceed the EU average (Fig. 5). Unlike the Czech Republic, Finland and Germany, France has had a stillbirth rate surge registered in 2002: it increased 1.7 times, from the stable EU average of 4.6–5. (seen 1995 through 2001) to 8.2. The rate peaked at 11.7 in 2009 and remained relatively high and stable in 2010–2014 (9.6–10.2).

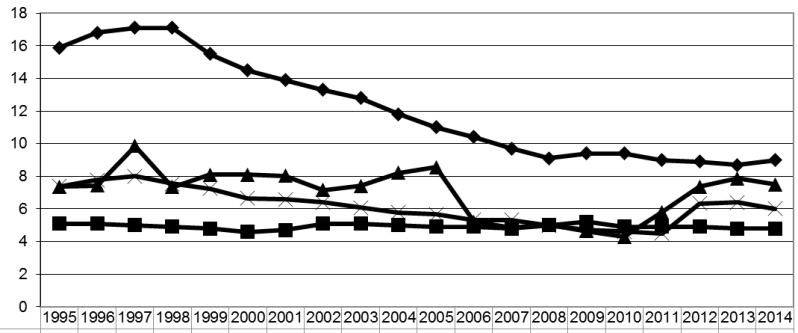

	1995	1996	1997	1998	1999	2000	2001	2002	2003	2004	2005	2006	2007	2008	2009	2010	2011	2012	2013	2014
CIS countries	15,9	16,8	17,1	17,1	15,5	14,5	13,9	13,3	12,8	11,8	11	10,4	9,7	9,1	9,4	9,4	9	8,9	8,7	9
EU	5,1	5,1	5	4,9	4,8	4,6	4,7	5,1	5,1	5	4,9	4,9	4,8	5	5,2	4,9	4,9	4,9	4,8	4,8
Bryansk region	7,4	7,4	9,9	7,3	8,1	8,1	8,0	7,2	7,4	8,2	8,5	5,2	4,8	5,0	4,6	4,3	5,8	7,4	7,9	7,5
Russia	7,4	7,8	8,0	7,5	7,2	6,7	6,6	6,4	6,1	5,8	5,7	5,3	5,3	5,0	4,7	4,6	4,5	6,3	6,4	6,0

Fig. 4. Stillbirth rate, dynamics, boys and girls combined, Bryansk region, Russian Federation, EU and CIS countries, 1995 to 2015 (per 1,000 births, ‰)

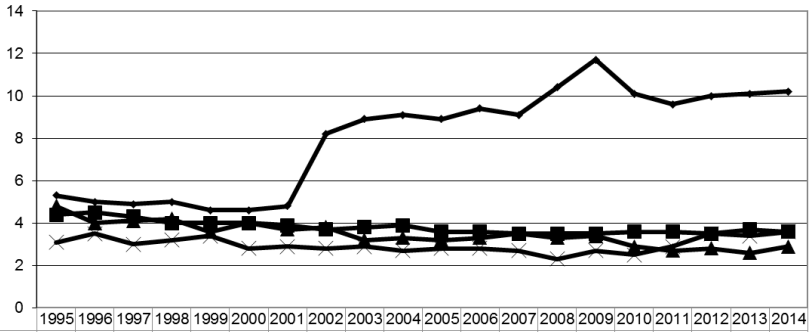

	1995	1996	1997	1998	1999	2000	2001	2002	2003	2004	2005	2006	2007	2008	2009	2010	2011	2012	2013	2014
France	5,3	5	4,9	5	4,6	4,6	4,8	8,2	8,9	9,1	8,9	9,4	9,1	10,4	11,7	10,1	9,6	10	10,1	10,2
Germany	4,4	4,5	4,3	4	4	4	3,9	3,7	3,8	3,9	3,6	3,6	3,5	3,5	3,5	3,6	3,6	3,5	3,7	3,6
Finland	4,8	4	4,1	4,2	3,6	4	3,7	3,8	3,2	3,3	3,2	3,3	3,5	3,3	3,4	2,9	2,7	2,8	2,6	2,9
Czech	3,1	3,5	3	3,2	3,4	2,8	2,9	2,8	2,9	2,7	2,8	2,8	2,7	2,3	2,7	2,5	2,9	3,5	3,4	3,6

Fig. 5. Stillbirth rate in France, Germany, Finland and the Czech Republic, boys and girls combined, 1995 to 2014 (per 1,000 births, ‰)

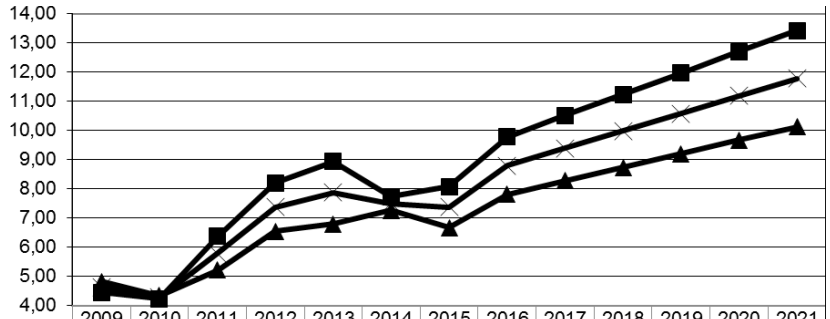

	2009	2010	2011	2012	2013	2014	2015	2016	2017	2018	2019	2020	2021
Boys	4,45	4,23	6,38	8,20	8,93	7,73	8,08	9,78	10,51	11,23	11,96	12,69	13,42
Girls	4,82	4,34	5,21	6,55	6,80	7,27	6,67	7,81	8,27	8,73	9,20	9,66	10,13
Total	4,64	4,28	5,80	7,37	7,86	7,50	7,37	8,79	9,39	9,98	10,58	11,18	11,78

Fig. 6. Stillbirth rate, dynamics, boys and girls, Bryansk region, 2009–2015 and 2016–2021 linear forecast (per 1,000 births, ‰)

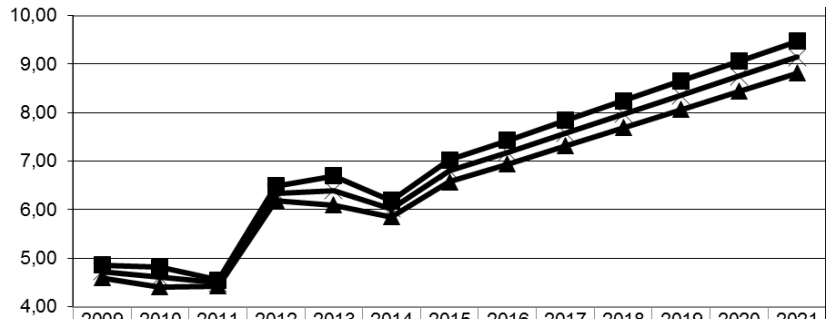

	2009	2010	2011	2012	2013	2014	2015	2016	2017	2018	2019	2020	2021
Boys	4,86	4,81	4,55	6,49	6,70	6,19	7,03	7,43	7,84	8,25	8,66	9,06	9,47
Girls	4,60	4,41	4,43	6,19	6,10	5,85	6,57	6,95	7,32	7,69	8,07	8,44	8,81
Total	4,73	4,61	4,49	6,34	6,4	6,02	6,80	7,19	7,58	7,97	8,36	8,75	9,14

Fig. 7. Stillbirth rate, dynamics, boys and girls, Russian Federation, 2009–2014 and 2016–2021 linear forecast (per 1,000 births, ‰)

We applied the following method to forecast the stillbirth rate for 2017–2021: a) calculated the linear regression $y = ax + b$ based on the data covering 1986 to 2016, with y being the stillbirth rate, x — year (short format, e.g., 9 or 16); b) found y in this formula for $x = 17, ..., 21$. The results filled the table and allowed plotting a graph.

Bryansk region, boys: $y = 0.730x - 1.901$.

Bryansk region, girls: $y = 0.464x + 0.379$.

Bryansk region, boys and girls combined: $y = 0.597x - 0.761$.

Russian Federation, boys: $y = 0.407x + 0.915$.

Russian Federation, girls: $y = 0.374x + 0.966$.

Russian Federation, boys and girls combined: $y = 0.391x + 0.940$.

According to our calculations, if the current trend persists the stillbirth rate in Bryansk region will continue to grow, and the gap between stillborn boys and girls will reach 32.6% by 2021 (Fig. 6 and 7).

The forecast has the gap between stillbirth rate in Bryansk region and the Russian Federation on the whole reaching 28.8% by 2021.

DISCUSSION

Evaluating the data above, it should first of all be noted that the male stillbirth rate calculated for the 20-year period (1995–2014) is greater than the female rate by 14.2% in Bryansk region and 9.0% in the Russian Federation. The results are consistent with the global trends, which have the risk for boys approximately 10% higher than for girls [4].

In 2015 Bryansk occupied the 16 position in the Central Federal District's living standards rating (18 regions all in all) and 52 in the same national rating (85 regions all in all), and its population's health puts the region on the 67 place in the appropriate rating of the Russian regions [13]; the data we received are consistent with the ratings: through the 20 years considered (1995–2014), Bryansk region has the stillbirth rates 16.5% (boys) and 11.2% (girls) greater than the national average.

The stillbirth rates calculated for the EU and CIS countries (1995–2014) align with the WHO report that puts 98% of stillbirths to countries with low-to-medium living standards (levels of income) [1], and the average stillbirth rate in the CIS countries is 2.5 times higher than that in the EU countries ($p < 0.001$).

Overall, EU countries have shown a stable stillbirth rate throughout the 20 years considered (1995–2014): it never exceeded 10.9% (4.6–5.1); in the CIS countries and, the rate was surging and dropping, fluctuations equaling 92.1% (8.9–17.1) and 122.0% (4.2–9.1).

In France, Latvia and Bulgaria, all of which are EU countries, stillbirth rate is higher than in the Russian Federation, although Russia ranks 58 in the worldwide living standards rating (out of 142 countries) while France, Latvia and Bulgaria rank 22, 40 and 51, which is closer to the top of the list [16].

Unexpectedly, France had a stillbirth rate surge in 2002, when it increased 1.7 times from 4.6–5.3 deaths per 1,000 births (average European values in 1995–2001) to 8.2 stillbirths, then peaked in 2009 at 11.7 and remained relatively high and stable in 2010–2014 (9.6–10.2). A number of factors, including migration, could have affected the data, which translates into the need for further research.

It should be noted that the Republic of Belarus has the lowest stillbirth rate among the CIS countries, 4.90; it is 25.9% lower than the Russian Federation's rate and almost the same as in the EU (4.93).

Since about a quarter of stillbirths remain unexplained [4], and one of the major factors contributing to the growth of the stillbirth rate is FCA, it would be interesting to compare stillbirth rates peculiar to Bryansk region and other regions of Russia, Ukraine and Belarus that suffered the consequences of the Chernobyl meltdown while taking into account the degree of radioactive contamination of the areas (long-lived radionuclides), as well as chemical pollution of the environment resulting from operation of factories, plants, vehicles.

Our 2016–2021 forecast, which projects the stillbirth rate for Bryansk region in particular and the Russian Federation in general, has revealed alarming trends and should not only be analyzed by the scientific community but taken as a decision-making factor by the healthcare authorities of the region: if the situation develops as it does, the stillbirth rate in Bryansk region will reach 28.8% by 2021, which is considerably greater than the national average, and the gap between male and female stillbirth rates will be 32.6%.

CONCLUSIONS

Over the 20-year period (1995–2014), male stillbirth rate in both Bryansk region and the Russian Federation exceeds female stillbirth rate by 14.2% (Bryansk) and 9.0% (Russia), which is consistent with the world statistics that have the stillbirth risk about 10% higher for boys. In Bryansk region, the rates for boys and girls are higher than the national average by 16.5% and 11.2%, respectively. CIS countries have the stillbirth rate 2.5 times higher than the EU countries; in Russia, the rate is 1.3 times higher than in the EU countries ($p < 0.001$).

The highest stillbirth rate among CIS countries is registered in Armenia (15.7), the lowest in Belarus (4.9); as for the EU, the highest stillbirth rate was registered in in France (8.0), the lowest — in the Czech Republic (3.0).

Provided the dynamics remain the same, 2016 to 2021 the share of stillbirths in the Bryansk region will continue to grow and reach 28.8% by 2021, and the gender gap will grow to 32.6% (male stillbirths more common than female) by 2021.

References

1. Statisticheskie dannye VOZ po chislu mertvorozhdenij v mire v 2009. Dostupno po ssylke: http://www.who.int/reproductivehealth/topics/maternal_perinatal/stillbirth/Press_release_stillbirths_2011/ru/
2. Lawn JE, Blencowe H, Oza S, You D, Lee AC, Waiswa P, et al. Lancet Every Newborn Study Group: Every Newborn: progress, priorities, and potential beyond survival. Lancet. 2014; 384 (9938): 189–205. DOI: 10.1016/S0140-6736(14)60496-7.
3. Blencowe H, Cousens S, Jassir FB, Say L, Chou D, Mathers C, et al. National, regional, and worldwide estimates of stillbirth rates in 2015, with trends from 2000: a systematic analysis. The Lancet Global health. 2016; 4 (2): e98–e108. Epub 2016/01/23. DOI: 10.1016/S2214-109X(15)00275-2 .
4. Mondal D, Galloway T, Bailey T, et al. Elevated risk of stillbirth in males: systematic review and meta-analysis of more than 30 million births. BMC Medicine. 2014. Available from: http://bmcmedicine.biomedcentral.com/articles/10.1186/s12916-014-0220-4
5. Getahun D, Ananth CV, Kinzler WL. Risk factors for antepartum and intrapartum stillbirth: a population-based study. Am J

Obstet Gynecol. 2007; 196 (6): 499–507. DOI: 10.1016/j.ajog.2006.09.017.
6. Salihu HM, Wilson RE, Alio AP, Kirby RS. Advanced maternal age and risk of antepartum and intrapartum stillbirth. J ObstetGynaecol Res. 2008; 34 (5): 843–50. DOI: 10.1111/j.1447-0756.2008.00855.x.
7. Facchinetti F, Alberico S, Benedetto C, Cetin I, Cozzolino S, Di Renzo GC, et al. Italian Stillbirth Study Group: a multicenter, case-control study on risk factors for antepartum stillbirth. J Matern Fetal Neonatal Med. 2011; 24 (3): 407–10. DOI: 10.3109/14767058.2010.496880.
8. Ghimire PR, Agho KE, Renzaho A, Christou A, Nisha MK, Dibley M, et al. Socio-economic predictors of stillbirths in Nepal (2001–2011). PLoS One. 2017 Jul 13; 12 (7): e0181332. DOI: 10.1371/journal.pone.0181332. eCollection 2017.
9. Korsakov A. V., Jablokov A. V., Troshin V. P., Pugach L. I., Sidorov I. V., Zhilin A. V. i dr. Dinamika chastoty vrozhdennyh porokov razvitija u detskogo naselenija Brjanskoj oblasti, prozhivajushhego v uslovijah radiacionnogo zagrjaznenija (1991–2012). Zdravoohranenie Rossijskoj Federacii. 2014; (6): 49–53.
10. Ashish KC, Nelin V, Wrammert J, Ewald U, Vitrakoti R, Baral GN, et al. Risk factors for antepartum stillbirth: a case-control study in Nepal. BMC Pregnancy Childbirth. 2015 Jul 5; 15: 146. DOI: 10.1186/s12884-015-0567-3.
11. Goldenberg RL, McClure EM, Bann CM. The relationship of intrapartum and antepartum stillbirth rates to measures of obstetric care in developed and developing countries. ActaObstetGynecol Scand. 2007; 86 (11): 1303–9. DOI: 10.1080/00016340701644876.
12. Korsakov A. V., Jablokov A. V., Geger' Je. V., Pugach L. I. Dinamika chastoty polidaktilii, redukcionnyh porokov konechnostej i mnozhestvennyh vrozhdennyh porokov razvitija u novorozhdennyh radioaktivno zagrjaznennyh territorij Brjanskoj oblasti (1999–2014). Radiacionnaja biologija. Radiojekologija. 2016; 56 (4): 397–404.
13. Rejting rossijskih regionov po kachestvu zhizni – 2015. M.: OOO Rejtingovoe agentstvo RIA Rejting; 2016. 62 s.
14. Informacionnaja spravka po urovnju mertvorozhdenij po Brjanskoj oblasti i Rossijskoj Federacii s 1995 po 2015 gg. (dogovor # 65-ARM). Brjansk: upravlenie Federal'noj sluzhby gosudarstvennoj statistiki po Brjanskoj oblasti; 2016. 21 s.
15. Chastota mertvorozhdenij v 1970–2014 gg. v raznyh stranah mira po dannym VOZ. Dostupno po ssylke: http://gateway.euro.who.int/ru/visualizations/choropleth-map-charts/hfa_82-fetal-deaths-per-1000-births/#table
16. Tablica urovnja zhizni 142 stran mira v 2015. http://gotoroad.ru/best/indexlife

Литература

1. Статистические данные ВОЗ по числу мертворождений в мире в 2009. Доступно по ссылке: http://www.who.int/reproductivehealth/topics/maternal_perinatal/stillbirth/Press_release_stillbirths_2011/ru/
2. Lawn JE, Blencowe H, Oza S, You D, Lee AC, Waiswa P, et al. Lancet Every Newborn Study Group: Every Newborn: progress, priorities, and potential beyond survival. Lancet. 2014; 384 (9938): 189–205. DOI: 10.1016/S0140-6736(14)60496-7.
3. Blencowe H, Cousens S, Jassir FB, Say L, Chou D, Mathers C, et al. National, regional, and worldwide estimates of stillbirth rates in 2015, with trends from 2000: a systematic analysis. The Lancet Global health. 2016; 4 (2): e98–e108. Epub 2016/01/23. DOI: 10.1016/S2214-109X(15)00275-2 .
4. Mondal D, Galloway T, Bailey T, et al. Elevated risk of stillbirth in males: systematic review and meta-analysis of more than 30 million births. BMC Medicine. 2014. Available from: http://bmcmedicine.biomedcentral.com/articles/10.1186/s12916-014-0220-4
5. Getahun D, Ananth CV, Kinzler WL. Risk factors for antepartum and intrapartum stillbirth: a population-based study. Am J Obstet Gynecol. 2007; 196 (6): 499–507. DOI: 10.1016/j.ajog.2006.09.017.
6. Salihu HM, Wilson RE, Alio AP, Kirby RS. Advanced maternal age and risk of antepartum and intrapartum stillbirth. J ObstetGynaecol Res. 2008; 34 (5): 843–50. DOI: 10.1111/j.1447-0756.2008.00855.x.
7. Facchinetti F, Alberico S, Benedetto C, Cetin I, Cozzolino S, Di Renzo GC, et al. Italian Stillbirth Study Group: a multicenter, case-control study on risk factors for antepartum stillbirth. J Matern Fetal Neonatal Med. 2011; 24 (3): 407–10. DOI: 10.3109/14767058.2010.496880.
8. Ghimire PR, Agho KE, Renzaho A, Christou A, Nisha MK, Dibley M, et al. Socio-economic predictors of stillbirths in Nepal (2001–2011). PLoS One. 2017 Jul 13; 12 (7): e0181332. DOI: 10.1371/journal.pone.0181332. eCollection 2017.
9. Корсаков А. В., Яблоков А. В., Трошин В. П., Пугач Л. И., Сидоров И. В., Жилин А. В. и др. Динамика частоты врожденных пороков развития у детского населения Брянской области, проживающего в условиях радиационного загрязнения (1991–2012). Здравоохранение Российской Федерации. 2014; (6): 49–53.
10. Ashish KC, Nelin V, Wrammert J, Ewald U, Vitrakoti R, Baral GN, et al. Risk factors for antepartum stillbirth: a case-control study in Nepal. BMC Pregnancy Childbirth. 2015 Jul 5; 15: 146. DOI: 10.1186/s12884-015-0567-3.
11. Goldenberg RL, McClure EM, Bann CM. The relationship of intrapartum and antepartum stillbirth rates to measures of obstetric care in developed and developing countries. ActaObstetGynecol Scand. 2007; 86 (11): 1303–9. DOI: 10.1080/00016340701644876.
12. Корсаков А. В., Яблоков А. В., Гегерь Э. В., Пугач Л. И. Динамика частоты полидактилии, редукционных пороков конечностей и множественных врожденных пороков развития у новорожденных радиоактивно загрязненных территорий Брянской области (1999–2014). Радиационная биология. Радиоэкология. 2016; 56 (4): 397–404.
13. Рейтинг российских регионов по качеству жизни – 2015. М.: ООО Рейтинговое агентство РИА Рейтинг; 2016. 62 с.
14. Информационная справка по уровню мертворождений по Брянской области и Российской Федерации с 1995 по 2015 гг. (договор № 65-АРМ). Брянск: управление Федеральной службы государственной статистики по Брянской области; 2016. 21 с.
15. Частота мертворождений в 1970–2014 гг. в разных странах мира по данным ВОЗ. Доступно по ссылке: http://gateway.euro.who.int/ru/visualizations/choropleth-map-charts/hfa_82-fetal-deaths-per-1000-births/#table
16. Таблица уровня жизни 142 стран мира в 2015. http://gotoroad.ru/best/indexlife

PREVALENCE OF TOXOCARA INFECTION IN DOMESTIC DOGS AND CATS IN URBAN ENVIRONMENT

Kurnosova OP[1], Odoevskaya IM[1]✉, Petkova S[2], Dilcheva V[2]

[1] Skryabin All-Russian Scientific Research Institute of Fundamental and Applied Parasitology of Animals and Plants, Moscow

[2] Department of Experimental Parasitology,
Institute of experimental morphology, pathology and anthropology with museum, Bulgarian Academy of Sciences, Sofia, Bulgaria

Toxocariasis is the type of helminthic infection found in dogs and cats most often. It is a zoonotic disease that presents a serious threat to the national public health. Urban environment favors transmission of toxocara from animals to people; soil is the key element of such transmission. To learn the degree of toxocara invasion in domestic cats and dogs living in Moscow, we studied their feces for 7 years applying the flotation method. We found that in domestic dogs the intensity of toxocara invasion was 2.43%, but there is a big difference between puppies and adult animals: 5.53% of the former, twice as much as the latter, suffered from the invasion. The intensity of infection in adult cats was 3.97%; kittens, same as puppies, were more prone to host toxocara: 10.44% of those examined did. In general, 5.75% of cats had toxacara, which is twice as much compared to dogs; the figure applies to all ages. Stable infestation of domestic animals with this species of helminths makes them a constant source of toxocara eggs contamination in urban environments, which ups the risk of larvae toxocariasis for people.

Keywords: prevalence of toxocariasis, toxocara, domestic dogs, domestic cats

Funding: this work was supported by the Russian Science Fund, Project #14-1600026.

✉ **Correspondence should be addressed:** Irina M. Odoevskaya
Bolshaya Cheremushkinskaya 28, Moscow, 117218; odoevskayaim@rambler.ru

Recieved: 16.06.18 **Accepted:** 10.08.18

DOI: 10.24075/brsmu.2018.044

РАСПРОСТРАНЕНИЕ ТОКСОКАРОЗНОЙ ИНВАЗИИ У ДОМАШНИХ СОБАК И КОШЕК В ГОРОДСКИХ УСЛОВИЯХ

О. П. Курносова[1], И. М. Одоевская[1]✉, С. Петкова[2], В. Дильчева[2]

[1] Всероссийский научно-исследовательский институт экспериментальной и прикладной паразитологии животных и растений имени К. И. Скрябина, Москва

[2] Кафедра экспериментальной паразитологии,
Институт экспериментальной морфологии, патологии и антропологии с музеем, Болгарская академия наук, София, Болгария

Токсокароз — один из самых распространенных гельминтозов собак и кошек. Заболевание является зоонозом и представляет серьезную проблему для отечественного здравоохранения. В городской среде создаются благоприятные условия для передачи токсокар от домашних животных к человеку, при этом почва играет ведущую роль в распространении данной инвазии. С целью изучения интенсивности инвазии токсокарами домашних собак и кошек, проживающих на территории г. Москвы, в течение 7 лет проводили исследование фекалий флотационным методом. Показано, что в среднем интенсивность инвазии токсокарами у домашних собак составляет 2,43%, но при этом зараженность щенков в 2 раза выше, чем взрослых особей и составляет 5,53%. Средняя интенсивность инвазии у взрослых кошек составляет 3,97%, а у котят — 10,44%. В целом зараженность кошек токсокарами составляет 5,75%. Исследования показали, что в целом зараженность кошек токсокарозом в 2 раза выше, чем у собак, во всех возрастных группах. Стабильная зараженность домашних животных данным видом гельминтов делает их постоянным источником обсеменения городской среды яйцами токсокар, что создает напряженную эпидемическую обстановку в плане возможности заражения людей ларвальной формой токсокароза.

Ключевые слова: распространенность токсокар, токсокароз, собаки, кошки

Финансирование: работа выполнена при финансовой поддержке гранта РНФ 14-16-00026.

✉ **Для корреспонденции:** Ирина Михайловна Одоевская
ул. Большая Черемушкинская, д. 28, Москва, 117218; odoevskayaim@rambler.ru

Статья получена: 16.06.18 **Статья принята к печати:** 10.08.18

DOI: 10.24075/vrgmu.2018.044

Toxocariasis is a parasitic disease caused by *Toxocara* nematodes that affects dogs and cats. Mature helminth worms concentrate in the small intestine of carnivores; reaching soil with the excrements of infected animals, toxocara eggs remain alive and capable to invade a host for a long period of time. Toxocariasis in dogs and cats is one of the most common helminth infections in the city of Moscow. Some reports claim that 11.9% to 18.1% of all domestic dogs living in the city suffer from this disease; as for the stray dogs of Moscow, the infection rate is up to 55% [1, 2]. The share of domestic cats hosting toxocara is 11.1%. Prenatal and transmammary mechanisms of disease transmission makes youngest animals especially susceptible to the invasion of *Toxocara* nematodes [3]: all (100%) stray puppies and over a half (57.1%) of stray kittens host the worms [4, 5].

Soil is the key media where the larvae survive and through which toxocariasis spreads [6]. The main source of contamination and subsequent invasion is the feces of infected animals; toxocara eggs, especially those capable of infecting animals, are very resistant to the adverse factors of the environment [7]. Analysis of the soil collected in Moscow revealed that the average content of toxocara eggs is 13.5%

(range — from 1.1% to 46.9%); at the playgrounds adjacent to residential housing the figure was 14.8% [8, 9]. One study put the number of toxocara eggs found in 1 kg of the Moscow's soil at 25 to 500 pieces [1]. Contamination was the highest in the areas where people walk their dogs.

Human toxocariasis is primarily a chronic disease. After infection, toxocara larvae migrate through the human organism carried by lymph and blood flow, which results in damage to various tissues and organs and sensitization by the parasite's metabolism byproducts. Clinical manifestations of human toxocariasis are varied, but generally they translate into damage to internal organs, liver and lungs for the most part, but also eyes and the central nervous system. Cutaneous toxocariasis causes changes peculiar to *larva migrans*. There is a number of factors that define the severity of the disease, including the number of infectious eggs swallowed, frequency of reinvasion, response of the organism to the damage done and antigenic effect produced by migrating larvae, their concentration site. Combined, such factors shape the development of pathological changes and the disease prognosis in general [10].

Most often, *Toxocara* nematodes invade adults who often contact animals and/or contaminated soil (occupational hazard) and children whose personal hygiene skills are yet insufficient. Infection occurs more often in rural areas, where contact with soil is more common and domestic animals are not subjected to preventive dehelmintization [11]. However, the well-developed social infrastructure in big cities does not eliminate the threat of contracting toxocariasis [12]. The number of domestic dogs grows, and stray dogs and cats migrate freely, which translates into the growing number of toxocara infested sites in the cities and ensures continued activity of those that already exist. Quite often, numerous owners of domestic dogs walk their pets in small parks and squares and do not pick the excrements their animals leave there. As a rule, dogs and cats enter playgrounds freely, and sandboxes have no lids or tarpaulins. Stray cats cover their excrements with sand or loose earth, which turns playground sandboxes into toxocariasis infection reservoirs dangerous to children.

Throughout the country, researchers analyze the spread of human toxocariasis, as well as the degree of the population's seropositivity to the antigens of these nematodes. The figures received are various. Overall, the occurrence of human toxocariasis in Russia doubled from 2003 to 2007 [12]. For example, in Tula the level of seropositivity is 19.3%, in Ekaterinburg — 2%, in Vladivostok — 8.6%, up to 20.8% in the Altai Republic, in Moscow — up to 17%. In the south of Russia the infection rate is 14.6 to 36.4%, which is 2–3 times higher than in other parts of the country [5, 12–15].

The role *T. canis* and *T. cati* nematodes play in the current situation is yet to be established. Single cases of feline toxocara infection in human beings were registered (damage to eyes and internal organs reported) [16]. Current examination methods, serological identification of toxocara do not allow establishing the type of nematodes the patient is infected with.

The purpose of our research was to investigate the prevalence of toxocara invasion of gastrointestinal tract of domestic dogs and cats in Moscow.

METHODS

The study lasted 7 years, from 2011 to 2017. *Pasteur* veterinary lab and the K. I. Skryabin All-Russian Scientific Research Institute of Fundamental and Applied Parasitology of Animals and Plants were the facilities where we analyzed 1632 samples of feces of domestic dogs and 1146 sample of feces of domestic cats. The samples were delivered to the laboratory in the special plastic or glass containers.

The feces were examined using ammonium nitrate (density of 1.24), flotation method. Biological microscope *Biolam* (LOMO; Russia) was used to study the samples, magnification ×10, ×40. After examination, samples were decontaminated through autoclaving.

Table 1. Indices of infection by Toxocara of domestic dogs

Year	Puppies, total	Infected, of them	EI (%)	Adult dogs	Infected, of them	EI (%)	Total	Infected, of them	EI (%)
2011	13	1	7.69	35	1	2.85	48	2	4.16
2012	83	2	2.4	225	3	1.33	308	5	1.62
2013	74	8	10.8	219	3	1.36	293	11	3.75
2014	64	3	4.68	195	3	1.53	259	6	2.31
2015	97	4	4.12	201	2	14.3	298	6	2.01
2016	75	3	4	185	2	1.08	260	5	1.92
2017	46	4	8.6	120	1	0.83	166	5	3.01
Total	452	25	5.53	1180	15	1.27	1,632	40	2.45

Note: EI — the extensity of infestation.

Table 2. Indices of infection by Toxocara in domestic cats

Year	Kittens, total	Infected, of them	EI (%)	Adult cats	Infected, of them	EI (%)	Total	Infected, of them	EI (%)
2011	19	1	5.26	57	1	1.75	76	2	2.63
2012	51	6	11.76	151	1	0.66	202	7	3.46
2013	56	7	12.5	147	6	4.08	203	13	6.4
2014	57	6	10.5	127	4	3.14	184	10	5.43
2015	56	5	8.92	140	4	2.85	196	9	4.59
2016	51	5	9.1	121	7	5.78	172	12	6.97
2017	26	3	11.53	87	10	11.49	113	13	11.5
Total	316	33	10.44	830	33	3.97	1,146	66	5.75

Note: EI — the extensity of infestation.

RESULTS

The average rate of toxocara infestation in domestic dogs is 2.45% (Table 1). Throughout the term of the research, we have witnessed various degree of infection: in adult animals it ranged from 0.83 to 2.85%, in puppies from 2.4 to 10.8%. On the whole, the prevalence on the parasite infection in puppies is two times higher than in adult dogs, reaching an average of 5.53% (Fig. 1).

Table 2 shows the data on toxocara infestation in domestic cats: the average rate for adult animals is 3.97%, minimum registered in 2012 (0.66%) and maximum in 2017 (11.49%). Same as puppies, kittens suffer infestations more often than adult cats (10.44%). Overall, 5.75% of cats host toxocara. Figure 2 and Figure 3 show the results of studies reporting that cats are infested with such nematodes twice as often as dogs (both adult and young animals).

DISCUSSION

Analysis of literature describing the like research efforts has shown that toxocara infestation in dogs and cats is the one diagnosed more often than other intestinal helminthiases, but the rates of infestation vary [4, 18–20]. The studies report that up to 7.3% of adult domestic dogs suffer the infection, while the share of toxocara nematodes hosts among puppies is 30.2%; the figures for cats are 11.1% (adult animals) and up to 33.3% (kittens) [4]. Researchers that studied stray dogs and cats have registered the maximum infestation rate in puppies (100%) and kittens (57.1%) [4]. Such differences in research depend on the category of animals selected. For example, the data we have outlined above describes domestic cats and dogs and shows that the toxocara infection rate among them is quite low. This may be due to the specifics of parasitological research in a commercial laboratory, which is the destination veterinarians send their patients to for analysis when there is a suspected case of toxocariasis or owners of domestic dogs and cats wish to subject their pets to examination.

Nonintensive invasions without clinical symptoms peculiar to toxocariasis often cancel the need to suspect that the animal suffers this type of helminthiasis. There is no doubt that a general screening of all domestic dogs and cats would produce higher infestation rates.

CONCLUSIONS

The study conducted has shown that there is a functioning site of toxocara infestation within the boundaries of the megalopolis of Moscow. This nature of this disease is zoonotic; it poses serious social and medical dangers since the infection can be contracted by people via the components of their environment contaminated with invasive toxocara eggs.

Thus, timely and regular laboratory examinations, treatment and preventive dehelmintization of pets would allow reducing the risk of contamination of urbanized territory with toxocara eggs. Stray animals have not been subjected to such activities for a long period of time, which made them a source of infestation targeting both other dogs and cats and human beings. Epidemiologists need to regularly examine soil and samples from sandboxes in search for toxocara eggs, as well as recommend property managing companies to fence playgrounds in order to prevent neglected stray animals from entering them.

Fig. 1. *T. canis* eggs

Fig. 2. *T. cati* egg

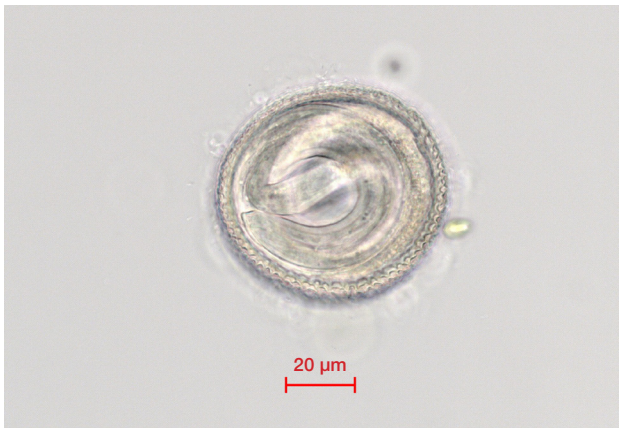

Fig. 3. *T. cati* invasive egg

References

1. Peshkov RA. Jepizootologicheskaja situacija po toksokarozu u plotojadnyh i gel'mintologicheskaja ocenka vneshnej sredy v megapolise Moskva [dissertacija]. M.: 2010.
2. Peshkov RA. Gel'mintofauna sobak i koshek v uslovijah g. Moskvy. V sbornike: Teorija i praktika bor'by s parazitarnymi boleznjami: materialy dokladov nauchnoj konferencii VIGIS. 2007; (8): 277–8.
3. Gorohov VV, Peshkova RA, Gorohova EV. Toksokaroz kak jekologicheskaja problema. Veterinarnaja patologija. 2009; (1): 10–12.
4. Panova OA. Toksokaroz plotojadnyh: metody diagnostiki i biojekologicheskie aspekty razvitija vozbuditelej v uslovijah megapolisa [dissertacija]. M.: 2011.
5. Pautova EA, Dovgalev AS, Astanina SJu. Toksokaroz u detej i podrostkov s allergicheskimi i bronholegochnymi zabolevanijami, grupp riska po VICh-infekcii, gepatitam V i S (rezul'taty serologicheskogo skrininga. Med. parazitol. 2013; (2): 13–17.
6. Zaichenko IV. Gel'mintozy plotojadnyh gorodskoj populjacii (rasprostranenie, diagnostika, lechenie) [dissertacija]. Stavropol': 2012.
7. Masalkova JuJu. Osobennosti vozdejstvija ul'trazvuka na jajca Toxocara canis. Rossijskij parazitologicheskij zhurnal. 2014; (1): 52–56.
8. Guzeeva MV. Sovremennaja situacija po toksokarozu v Moskve. Med. parazitol. 2009; (1): 49–51.
9. Uspenskij AV, Peshkov RA, Gorohov VV, Gorohova EV. Toksokaroz v sovremennyh uslovijah. Med. parazitol. 2011; (2): 3–6.
10. Sergiev VP, Lobzin JuV, Kozlova SS, redaktory. Parazitarnye bolezni cheloveka. SPb.: Foliant; 2006. 592 s.
11. Slobodenjuk AV, Kosova AA, Rukoleeva SI. Osobennosti rasprostranenija toksokaroza na territorii sel'skogo i gorodskogo tipa. Med. parazitol. 2005; (3): 36–8.
12. Guzeeva MV. Sovremennaja situacija po toksokarozu v Moskve. Med. parazitol. 2009; (1): 49–51.
13. Derzhavina TJu. Monitoring za geogel'mintozami u ljudej v Tul'skoj oblasti. Med. parazitol. 2010; (30): 42–4.
14. Ermolenko AV, Rumjanceva EE, Bartkova AD, Voronok VM, Poljakova LF. Nematodozy u ljudej v Primorskom krae. Med. parazitol. 2013; (1): 31–5.
15. Espinoza Y. A., Huapaya P. E., Roldan W. HSeroprevalence of human toxocariasis in Andean communities from the Northeast of Lima. Rev Inst Med Trop Sau Paulo. 2010; 52 (1): 31–36. DOI: 10.1590/S0036-46652010000100006.
16. Fogt-Wyrwas R, Jarosz W, Mizgajska-Wiktor H. Utilizing a polymerase chain reaction method for the detection of Toxocara canis and T. cati eggs in soil. J Helminthol. 2007; 81(1): 75–8. DOI:10.1017/S0022149X07241872.
17. Kotelnikov GA. Diagnostika gel'mintozov zhivotnyh. M.: Kolos; 1974. 240 s.
18. Kurnosova OP. Rasprostranenie prostejshih Lamblia (Giardia) sp. sredi sobak i koshek goroda Moskvy. Med. parazitol. 2014; (3): 23–5.
19. Skripova LV. Parazitologicheskaja situacija na ob"ektah dlja pit'evogo i hozjajstvenno-bytovogo vodosnabzhenija. Zdravoohranenie. 2010; (6): 22–3.
20. Shishkanova LV. Toksokaroz na juge Rossii (jepizootologicheskaja, sanitarno-parazitologicheskaja i serojepidemiologicheskaja harakteristika) [disertacija]. M.: 2011.

Литература

1. Пешков Р. А. Эпизоотологическая ситуация по токсокарозу у плотоядных и гельминтологическая оценка внешней среды в мегаполисе Москва [диссертация]. М.: 2010.
2. Пешков Р. А. Гельминтофауна собак и кошек в условиях г. Москвы. В сборнике: Теория и практика борьбы с паразитарными болезнями: материалы докладов научной конференции ВИГИС. 2007; (8): 277–8.
3. Горохов В. В., Пешкова Р. А., Горохова Е. В. Токсокароз как экологическая проблема. Ветеринарная патология. 2009; (1): 10–12.
4. Панова О. А. Токсокароз плотоядных: методы диагностики и биоэкологические аспекты развития возбудителей в условиях мегаполиса [диссертация]. М.: 2011.
5. Паутова Е. А., Довгалев А. С., Астанина С. Ю. Токсокароз у детей и подростков с аллергическими и бронхолегочными заболеваниями, групп риска по ВИЧ-инфекции, гепатитам В и С (результаты серологического скрининга. Мед. паразитол. 2013; (2): 13–17.
6. Заиченко И. В. Гельминтозы плотоядных городской популяции (распространение, диагностика, лечение) [диссертация]. Ставрополь: 2012.
7. Масалкова Ю. Ю. Особенности воздействия ультразвука на яйца Toxocara canis. Российский паразитологический журнал. 2014; (1): 52–56.
8. Гузеева М. В. Современная ситуация по токсокарозу в Москве. Мед. паразитол. 2009; (1): 49–51.
9. Успенский А. В., Пешков Р. А., Горохов В. В., Горохова Е. В. Токсокароз в современных условиях. Мед. паразитол. 2011; (2): 3–6.
10. Сергиев В. П., Лобзин Ю. В., Козлова С. С., редакторы. Паразитарные болезни человека. СПб.: Фолиант; 2006. 592 с.
11. Слободенюк А. В., Косова А. А., Руколеева С. И. Особенности распространения токсокароза на территории сельского и городского типа. Мед. паразитол. 2005; (3): 36–8.
12. Гузеева М. В. Современная ситуация по токсокарозу в Москве. Мед. паразитол. 2009; (1): 49–51.
13. Державина Т. Ю. Мониторинг за геогельминтозами у людей в Тульской области. Мед. паразитол. 2010; (30): 42–4.
14. Ермоленко А. В., Румянцева Е. Е., Барткова А. Д., Воронок В. М., Полякова Л. Ф. Нематодозы у людей в Приморском крае. Мед. паразитол. 2013; (1): 31–5.
15. Espinoza Y. A., Huapaya P. E., Roldan W. HSeroprevalence of human toxocariasis in Andean communities from the Northeast of Lima. Rev Inst Med Trop Sau Paulo. 2010; 52 (1): 31–36. DOI: 10.1590/S0036-46652010000100006.
16. Fogt-Wyrwas R, Jarosz W, Mizgajska-Wiktor H. Utilizing a polymerase chain reaction method for the detection of Toxocara canis and T. cati eggs in soil. J Helminthol. 2007; 81(1): 75–8. DOI:10.1017/S0022149X07241872.
17. Котельников Г. А. Диагностика гельминтозов животных. М.: Колос; 1974. 240 с.
18. Курносова О. П. Распространение простейших Lamblia (Giardia) sp. среди собак и кошек города Москвы. Мед. паразитол. 2014; (3): 23–5.
19. Скрипова Л. В. Паразитологическая ситуация на объектах для питьевого и хозяйственно-бытового водоснабжения. Здравоохранение. 2010; (6): 22–3.
20. Шишканова Л. В. Токсокароз на юге России (эпизоотологическая, санитарно-паразитологическая и сероэпидемиологическая характеристика) [дисертация]. М.: 2011.